Spring 11-9-2016

Characterizing Responses of Primary Biological Aerosols to Oxidative Atmospheric Conditions

Odessa Mason Gomez
University of Colorado at Boulder, odessa.gomez@colorado.edu

Characterizing Responses of Primary Biological Aerosols to Oxidative Atmospheric Conditions

by

ODESSA MASON GOMEZ

B.S., Rensselaer Polytechnic Institute

M.S., University of Colorado

A thesis submitted to the
Faculty of the Graduate School of the
University of Colorado in partial fulfillment
of the requirement for the degree of
Doctor of Philosophy
Department of Civil, Architectural and
Environmental Engineering
2016

This thesis entitled:

Characterizing Responses of Primary Biological Aerosols to Oxidative Atmospheric Conditions

written by Odessa Mason Gomez

has been approved for the Department of Civil, Architectural and Environmental Engineering

Examination Committee:

Dr. Mark Hernandez, University of Colorado Boulder (Chair)

Dr. Anne Perring, University of Colorado Boulder/NOAA

Date _____

The final copy of this thesis has been examined by the signatories, and we find that both the content and the form meet acceptable presentation standards of scholarly work in the above mentioned discipline.

Gomez, Odessa Mason (Ph.D., Environmental Engineering)
Characterizing Responses of Primary Biological Aerosols to Oxidative Atmospheric Conditions
Thesis directed by Professor Mark T. Hernandez

ABSTRACT

Biological aerosols (bioaerosols) constitute a significant portion of airborne particulate matter, both indoors and outdoors; however, the extent to which anthropogenic oxidative air pollutants can modify bioaerosols remains unclear. This work isolated the potential for atmospheric ozone to modify important biopolymers in ubiquitous types of bioaerosols. Independent lines of evidence for ozone-mediated modifications of bioaerosols were obtained from environmentally controlled chamber studies designed to challenge bioaerosols with ozone and humidity conditions relevant to the current US EPA NAAQ standards. Before and during different ozone exposures, intrinsic bioaerosol fluorescence was monitored concurrently with the quantity and activity of significant allergens and enzymes present in pure bioaerosols. Results indicate significant decreases in fluorescence intensity, enzyme activity and specific allergen content with ozone exposure, while liberated water soluble organic carbon (WSOC) concomitantly increased over time in all environmental conditions tested.

As judged by real-time intrinsic fluorescence measurements of whole bioaerosols (airborne sporulated *Aspergillus spp*. and *Bacillus subtilis*), and the intrinsic fluorescence properties of the liberated bioaerosol WSOC fraction, differences in specific fluorescence began to appear within an hour of bioaerosol exposures to ozone and high humidity. Significant decreases in measureable airborne fungal enzyme activity (beta-N-acetylhexosaminidase) and allergen (Aspf1) content were encountered in response to ozone exposures. On time scales relevant for lower atmosphere environmental ozone bioaerosol exposures, these are the first

observations implicating ozone inhibition of key enzymes responsible for fungal spore germination, and antigenic modification of the *Aspergillus* allergen Asp f 1.

Results from these controlled bioaerosol exposure chamber studies were related to actual environmental aerosol samples that had experienced extreme oxidative stress during a local wildfire. The carbon content and intrinsic fluorescence profiles of WSOC from collected wildfire aerosols indicate that distinct fluorescence patterns from the WSOC present in wildfire emissions changed over the course of the wildfire event in both indoor and outdoor locations, further demonstrating the infiltration potential of wildfire emissions into the indoor environment. Results from this work contribute to a limited body of existing observations documenting the potential impacts of oxidative air pollutants on bioaerosols present in both outdoor and indoor environments.

DEDICATION

I am the luckiest 'kid in the world' to have such supportive parents, family and friends! We have all gone through some amazing obstacles over the last decade(s), but through these I think we have all seen what we can endure and achieve, so dedicate this to you all. Mom you are my biggest cheerleader with amazing support and encouragement through times both rough and shining. Dad you will never stop helping your kids with their homework – your support through this process has been amazing! Brother and sister from the same mister, you guys are such talented and supportive smarty pants – Nick don't send the check! Joo-ju-be – are you for real? Not many guys put up with these kind shenanigans from their ladies. To the Gomez and Mason families, your continued encouragement and love through the years has been wonderful – though I am finally graduating, I will never stop being a 'perma-student'.

To every single one of my past and present teachers, professors, academic and research advisors (27 years as a student generates a big list!). Incredible lessons have been learned and opportunities gained at each step of the way. I am appreciative for each rung on this mental and emotional ladder I have climbed. Mark, I am truly grateful for the life preserver you extended, twice, as I contemplated leaving graduate school waters. This could not have happened without your belief, understanding, and support. Third time's the charm!

This was not a solo journey. This was not a solo struggle. This was not a solo victory.

This is where I spread the wealth and praise my champions.

ACKNOWLEDGEMENTS

Odessa Gomez was supported from an EPA STAR Graduate Fellowship (2012-2015); NSF Alliances for Graduate Education and Professoriate funding (AGEP); and the Department of Civil, Environmental and Architectural Engineering Dissertation Completion Fellowship (2015). The following are also acknowledged for their kind and generous research support: DetectionTek; Droplet Measurement Technologies; Aerosol Devices, Inc.; Indoor Biotechnologies; Carrier; Mycometer, Inc.; the Summers, Rosario, and Linden Research Labs; and the United States Geological Survey.

Dr. Mark Hernandez "El Jefe", your mentorship, energy and guidance through this process has been incredible! I truly appreciate all of the amazing opportunities (local to international) to participate in exciting projects. Hernandez Lab members (Hernandoids and Hernanditos), past and present. Dr. Alina Handorean, you will always be our 'lab mom'. Dr. Joan Marcano, for taking the protein journey from Ferrari to Corolla. Jordan Jimenez and Scott Cusack, sorry about the electrical mishaps-a learning experience for us all! Alex and Ismael for your incredible lab support, positive energy and entertainment en español. Dr. Jane Turner, we have gone through the academic ringer together and you are still there for amazing support and I'm glad to be your Air Sister! Carleigh Samson, continual friend with the current brain of a former math teacher and late night co-creator of the "DiF Measure" :) Dr. Sara Beck, your support, resilience and drive are constantly inspiring me! Dr. Camilo Gomez, 'Dad' and 'Matlab Guru', your analytical talents have helped bring these analyses to a whole new level! Dr. Anne Perring, fellow volcano hiker and incredible research mentor, I really appreciate your insight and analysis support. Dr. Darin Toohey, I appreciate your dedication to mentorship and attention to detail.

Finally, I am thankful for the guidance, flexibility, support, patience, and feedback from all of my doctoral thesis committee members: Dr. Mark Hernandez, Dr. Anne Perring, Dr. Fernando Rosario-Ortiz, Dr. Zhiyong (Jason) Ren, Dr. Michael Hannigan, and Dr. Darin Toohey.

TABLE OF CONTENTS

LIST OF TABLES

LIST OF FIGURES

GLOSSARY

Term	Definition
Aged	Biological aerosols not exposed to ozone, but have similar suspension times as those exposed to ozone (i.e. baseline results)
Asp f 1	Known allergen present on *Aspergillus fumigatus*
Bioaerosol	Biological aerosol, including airborne viable and nonviable microorganisms whole and fragmented
Biopolymer	Including total proteins, allergenic proteins, enzymes (consist of proteins), chitin, sporopollenin, melanin, etc.
EC	Elemental aerosol carbon
EEM	Excitation-emission matrix
EOD	Equivalent optical diameter of bioaerosol
DOC	Dissolved organic carbon
Fresh	Freshly aerosolized bioaerosols, not yet aged or exposed to ozone (i.e. initial measurements)
FI	Fluorescence Index
FrI	Freshness Index
HIX	Humification Index
MARIA	Mulitplex Array for Indoor Allergens, here measuring Asp f 1
NAHA	β-N-acetylhexosiminidase
OC	Organic aerosol carbon
Old	Mature microbial cultures used to produce bioaerosols
Ozone exposure	Integral of ozone concentration (ppb) over the time bioaerosols are in contact with ozone (hr), reported as 'ppb-hr'
PAH	Polyaromatic hydrocarbon
PM	Particulate matter
pQY	Psuedo-quantum yield
pWIBS	Portable Wideband Integrated Bioaerosol Spectrometer, also known as InstaScope
RH	Relative humidity (%)
$SUVA_{254}$	Specific UV absorbance at 254nm
WSOC	Water soluble organic carbon
Young	Young microbial cultures used to produce bioaerosols

CHAPTER 1. **INTRODUCTION**

1.1. Rationale: "Take a breath, and you sample the world" – Nathan Wolf

A single cubic meter of outdoor air can contain up to 10^6 microorganisms, including airborne bacteria, pollen, and fungal spores [1]. A significant portion of these primary biological aerosols (bioaerosols) may have traveled vast distances [2] and undergone a great deal of atmospheric processing (aging), including but not limited to interactions with various oxidants. Bioaerosols, including whole microorganisms regardless of viability, microbial fragments, detritus and plant/animal debris, can significantly to the mass of atmospheric PM [1] and indoor PM mass [3]. The source and presence of bioaerosols, the extent of their aging, and their impact on environmental and human health have become a growing concern among the research community and the general public. Bioaerosol can range in size from 20 nm to >100 μm, and represent a significant portion of the inhalable fraction of particulate matter (PM) [4]. Urban air pollution can modify the surface composition of pollen, and subsequently their bioactivity, leading to increases in immunological responses from pollen exposed to urban air [5] and anthropogenically sourced oxidative pollutants [6]. Decreases in pollen viability [7] and crop yields [8] have also been cited with increased oxidative pollutant exposures, raising an increased awareness on the indirect effects of air pollutants on ecology. One of the main pollutants responsible for the oxidation of organic substances in the atmosphere includes ozone (O_3), either directly emitted from anthropogenic activity (vehicle emissions) or indirectly formed through photo-oxidation processes [9]. The US EPA recently reduced ground-level standards for ozone, one of six principle pollutants listed in the National Ambient Air Quality Standards (NAAQS), to

70ppb over an 8 hour period; and reflecting a broader concern on the impact of ozone on public health, welfare, and the environment.

In addition to the context of oxidative bioaerosol modification on public health, there has been an increasing body of work dedicated to the relevance of bioaerosols in cloud formation and precipitation by serving as nucleation sites for water droplets and ice crystals [10], citing that atmospheric processes can also be influenced by the surface properties of bioaerosols [11]. Methods for bioaerosol detection, quantification and characterization are numerous [1]; however, environmental factors, such as the presence of other air pollutants (ozone) and relative humidity (RH), can influence the biopolymer composition of these bioaerosols [12-14]. In response to the demand for real-time bioaerosol measurements, in-situ, or on-line, fluorescence particle monitors have been developed to aid in enumeration, and to some extent classification, of bioaerosols based on their intrinsic fluorescence of proteins and other biopolymers [1, 15]. Recent studies indicated that changes in the fluorescence intensity of aged aerosolized proteins and whole bacteria can be detected using an on-line bioaerosol monitor [14, 16].

Aerosol intrinsic fluorescence is also beginning to be utilized in post-sampling characterization by evaluating the fluorescent excitation-mission matrices (EEMs) of aerosol aqueous extracts [17, 18]. In water quality research, EEMs have been extensively used for characterizing dissolved organic matter [19, 20] and it has become clear that oxidation processes can influence the intrinsic fluorescence profiles of dissolved organic matter [21]. Ozone disinfection processes for water treatment have initiated numerous studies on the surface oxidation processes of different microorganisms in aqueous environments [22]. This research provides valuable insight on the mechanisms of oxidation. However, to determine oxidation

events unique to different classes of bioaerosols and their effect on characterization, quantification methods of biopolymer modification must be extended from the aqueous environment to the atmospheric environment. Further, research focus needs to be shifted beyond gas-phase oxidation mechanisms of isolated biopolymers to that of whole airborne cells (bioaerosols). In response to these current research gaps, controlled environmental chamber studies were conducted to evaluate the impact of varying RH levels and ozone exposures, on whole-cell biopolymer content (and their biologically active fractions) and intrinsic-fluorescent signatures of model bioaerosols.

1.2. Formal Hypotheses

The following hypotheses were developed and challenged to investigate the overarching hypothesis driving this research that biopolymers present in and on whole airborne microorganisms can be modified by ozone in environmentally relevant concentrations and time frames:

Hypothesis I. *Oxidative aging processes, by environmentally relevant ozone and relative humidity levels, will significantly reduce the intrinsic fluorescence signatures of biopolymers present in whole-cell bioaerosols models.*

> ***Hypothesis Ia.*** *Real-time fluorescent measurements will detect a decrease in intrinsic fluorescence intensities of model bioaerosols during exposure.*
>
> ***Hypothesis Ib.*** *Changes in intrinsic fluorescence intensities of exposed bioaerosol aqueous extracts, over those of fresh bioaerosols, can be characterized by excitation-emission matrices.*

Hypothesis II. *Bioaerosol exposure to gas-phase ozone, under environmentally relevant conditions, will modify biopolymers on the surface of common airborne pollens, fungi, and bacterial spores.*

1.3. Dissertation Guideline

This thesis has been designed such that each chapter can be read independently, while also addressing the outlined hypotheses. General environmental chamber characteristics and microbial culturing techniques are covered in Chapter 2. Chapters 3 through 5 directly address the outlined hypotheses as they relate to intrinsic fluorescence or biochemical analysis. Specific methods (for example, protein quantitation or real-time bioaerosol fluorescence measurements) will be covered in their respective chapters. Chapter 6 covers application to practice by characterizing the water soluble organic carbon content and intrinsic fluorescence properties of environmental aerosol samples collected during a local wildfire event.

CHAPTER 2. **METHODS OF BIOAEROSOL CULTURING AND EXPOSURES**

2.1. Introduction

The following methods outline the environmental bioaerosol exposure chamber design and operation, fungal and bacterial spore culturing and aerosolization techniques, as well as bioaerosol sampling and enumeration details. Methods specific to certain analyses and characterizations can be found in their respective chapters.

2.2. Environmental Bioaerosol Exposure Chamber

For these bioaerosol oxidation studies, an environmental chamber (11.4 m^3) was designed and built to conduct controlled bioaerosol exposure studies for extended periods of time (>4 hours) in environmentally-relevant conditions. The basic design and function of the exposure chamber was similar to studies conducted by Peccia et al. 2001 [23]. For this work, the environmentally-relevant conditions tested included low RH (20-30%) and high RH (85%), with and without the presence of ozone. The completely isolated 11.4 m^3 chamber was design to be operated in batch reactor mode, where relative humidity (RH), light, and concentrations of ozone and bioaerosols were tightly controlled and monitored. Figure 2-1 indicates the bioaerosol inlet and sampling locations, as well as basic functional components of the environmental exposure chamber.

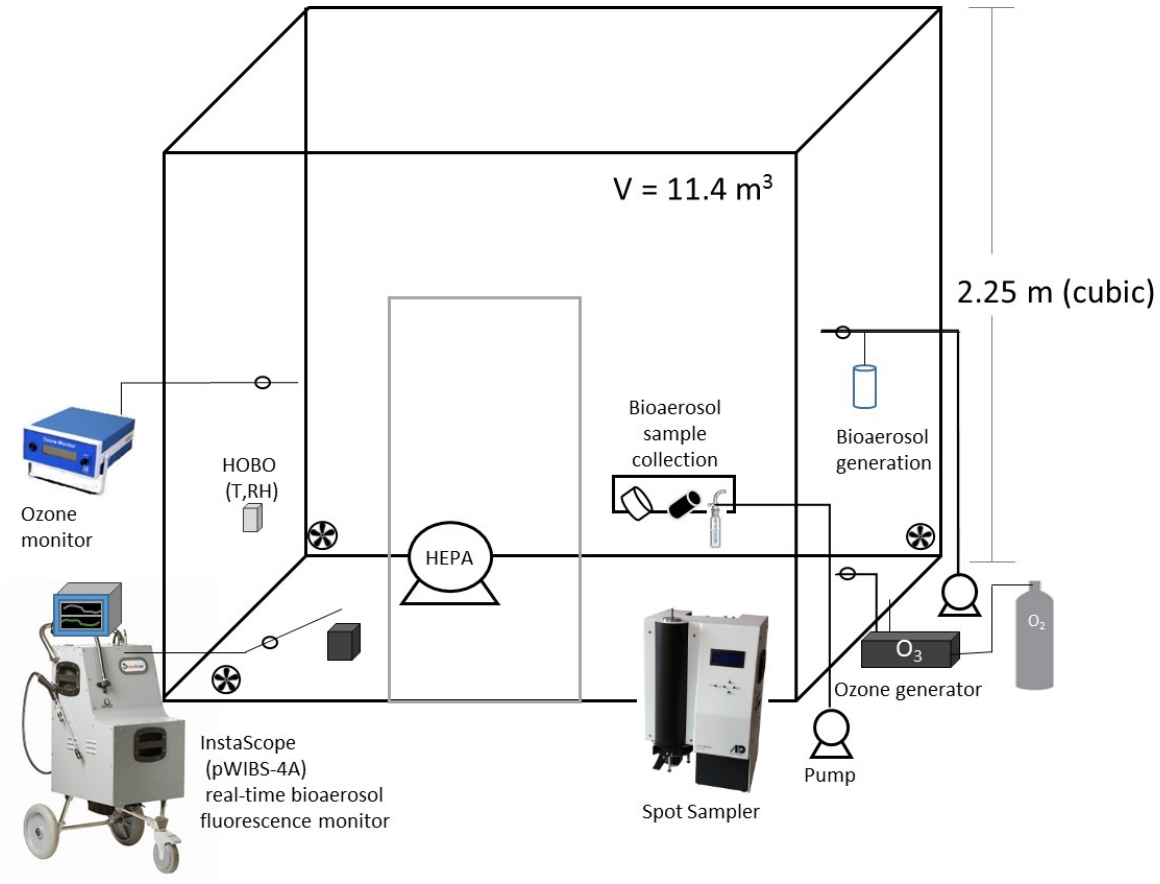

Figure 2-1. Schematic of environmental chamber and sampling equipment used for bioaerosol oxidation studies.

Three 10-inch portable fans were implemented radially to ensure complete mixing within the chamber. Gaseous ozone was generated via corona discharge (A2Z Ozone MP 1000) with pure oxygen as the source gas to avoid additional introduction of oxidizing ozone generation byproducts such as NO_x [24]. The ozone concentration inside the camber was continuously monitored and logged using a Model 202 Ozone Monitor (2B Technologies). A carbon ozone scrubber and high volume HEPA filter were present inside the chamber (controlled from the outside) to facilitate quick removal ozone and bioaerosols from the air after bioaerosol exposure

experiments. The relative humidity inside the chamber was controlled and monitored by an IMAGE Digital Air Humidity Controler Sensor (WH8040). The accuracy of the IMAGE humidity sensor measurements was verified within +/- 5% RH (RH ranging from 15% - 85%) of by a Picarro Cavity Ring-Down Spectroscopy (CRDS) analyzer. Bioaerosol was generated using either a Collision six-jet nebulizer (BGI Inc.) at an operation pressure of 20 psi for bacterial spore aerosolization, or by using dry pressurized HEPA filtered air passing over pure sporulated fungal cultures. Specific bioaerosol collection techniques are described below and in their relevant chapters.

2.2.1. Condensing Particle Capture Sampling Method

The Spot Sampler Airborne Particle Collector (Aerosol Devices Inc.) was used to concentrate aerosolized fungal spores during chamber studies where impingers could not achieve the desired final collected sample mass (ie for allergen testing). The Spot Sampler provided a high particle collection efficiency (>95% for particles 5nm - 2.5 μm) with a continuous sample stream (~1.5 lpm) that passed through a three-stage condensation growth chamber and deposited high concentrations of spores in a 75μl sample wells, see Figure 2-2.

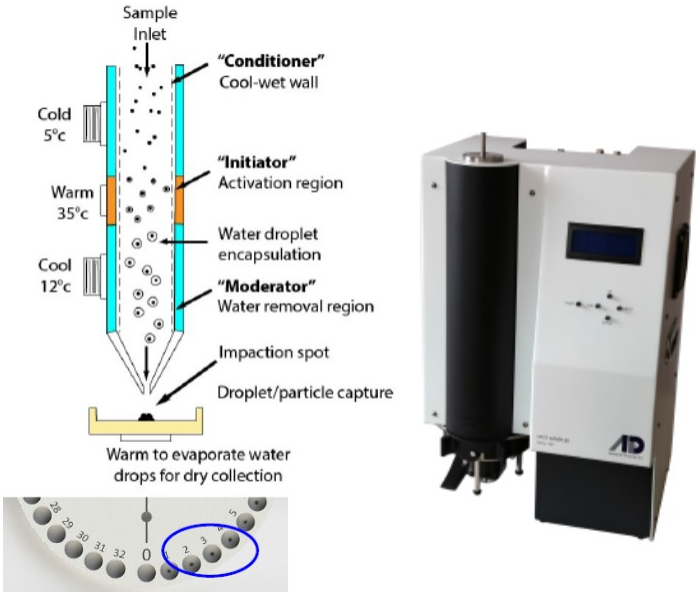

Figure 2-2. Schematic of the Spot Sampler Airborne Particle Collector with the condensation growth chamber and particle sampling tray.

Estimations of the Spot Sampler sampling time required to collect enough airborne fungal biomass to safely exceed the lower limit of detection for allergen and protein are displayed in Table 2-1. These required *Aspergillus fumigatus* biomass estimations are based on preliminary fungal biomass protein and allergen range finding studies using ATCC *A. fumigatus* source material and estimated spore mass. Estimations of *A. fumigatus* spore mass were determined from a *Bacillus subtilis* spore density of 1.335 g/cm3 [25], mean *A. fumigatus* spore diameter of 2.2 μm [current work], and bioaerosol concentration in the chamber determined from optical particle counts (InstaScope). Samples collected for biopolymer characterization (protein and allergen content), were collected at high spore concentrations (> $7x10^4$ spores/L), while most real-time fluorescence studies were conducted at lower aerosolized spore concentrations

($5x10^3$ – $1.5x10^4$ spores/L) to eliminate potential aerosol concentration influence on the fluorescence intensity detectors.

Table 2-1. *Aspergillus fumigatus* sampling time look-up table

Spores/ L air	Sampling Time (min)	InstaScope (spore counts per sec)	Biomass (mg)
1.8E+05	6.0	2500	0.035
1.4E+05	7.5	2000	0.028
1.2E+05	8.5	1750	0.024
1.1E+05	10.0	1500	0.021
8.9E+04	12.0	1250	0.017
7.1E+04	15.0	1000	0.014
5.4E+04	19.9	750	0.010
3.6E+04	29.9	500	0.007
2.9E+04	37.4	400	0.006
2.5E+04	42.7	350	0.005
2.4E+04	44.0	340	0.005
2.4E+04	45.3	330	0.005
2.3E+04	46.7	320	0.004
2.2E+04	48.2	310	0.004
2.1E+04	49.8	300	0.004

Specific methods related to sample processing for protein and allergen quantitation of samples collected with the Spot Sampler can be found in Chapter 5.

2.3. Bioaerosol Microscope Counting Techniques with a Hemocytometer

All bioaerosol enumeration of Spot Sampler and impinger samples were conducted by direct microscopy counts using a hemocytometer (model and 1mm x 1mm). The hemocytometer was soaked in water/soap from 10 minutes, thoroughly washed with ethanol and dried with

filtered air between each use to ensure all residual spores had been removed. Each sample was thoroughly vortexed and diluted with 0.05% Tween/DI water solution to ensure accurate counts with an average target grid average sum (here a grid is defined as a corner square consisting of 16 smaller squares, where grid dimensions are 1mm x 1mm x 0.1mm) of roughly 60 or less spores per grid. Ten microliters of diluted sample was added to each side of the hemocytometer slide allowing for 8 grid sums to be averaged and used in the final count estimates. Microscopy counts (with phase contrast) were performed at 20X (2,000) magnification.

2.4. *Aspergillus spp.* Culturing Techniques

Aspergillus cultures were grown at room temperature on 10 ml of potato dextrose agar coated on the bottom of 475 ml sterile glass jars, and fit with 100 mm petri dish lids to allow for ventilation of condensation when needed. During growth, the culture jars were sealed with parafilm. Cultures were grown until spores developed (2-4 weeks from inoculation). To remove residual condensation on the walls of the culture jars, and allow the cultures to equilibrate with ambient RH, the parafilm was removed 24 hours before aerosolization into the chamber. To aerosolize the cultured *Aspergillus* spores, each jar was fitted with custom made stainless steel lid attachments consisting of two - ¼" diameter stainless steel tubes to allow for dry HEPA filtered house air to enter one tube, pass over the culture and carry spores out through the other tube and into the chamber.

2.5. *Bacillus subtilis* Culture and Sporulation

Bacillus subtilis spores were cultured and harvested with the same method as Dow et al. [26]. Pure cultures of vegetative *B. subtilis* were grown in Tryptic Soy Broth at 37°C for 24 hours. Sporulation was induced with a 1:100 dilution of culture to 20mg/L MnCL2 in phosphate buffer. The inoculum (1ml) was spread onto R2 Agar plates for 14 day incubation at 37°C, enough time to ensure a 95% spore to vegetative cell ratio. Either immunofluorescence microscopy or phase-contrast microscopy confirmed the presence of spores. Figure 2-3, shows an example of a 100x magnification of a sporulated *B. subtilis* culture tagged with fluorescent antibodies, where the bright blue spots indicate the spores.

Figure 2-3. Immunofluorescent microscope image of *B. subtilis* spores at 100x magnification.

CHAPTER 3. **REAL-TIME BIOAEROSOL FLUORESCENCE**

3.1. Introduction

This chapter presents results from experiments that were designed to challenge *Hypothesis Ia* as it pertains to *Hypothesis I*, previously presented in Chapter 1:

> ***Hypothesis I.*** *Oxidative aging processes, by pollutant and RH exposure, can significantly change intrinsic fluorescence properties of whole cell bioaerosols.*
>
> ***Hypothesis Ia.*** *On-line fluorescent measurements can detect changes in intrinsic fluorescence properties of bioaerosols during aging.*

For context, a brief review of relevant literature pertaining to the scope of these specific bioaerosol aging experiments will be covered, along with details of the experimental methods, results and discussion.

3.2. Previous Work on Real-Time Bioaerosol Fluorescence

Bioaerosols have intrinsic fluoresce properties which have been leveraged to size, enumerate, classify airborne microorganisms in the atmospheric environment [27-30]. Fluorescence has been used to describe bioaerosol response to atmospheric processes [1], bioaerosol occurrence in health care settings [31, 32], and in the context of classifying biological warfare agents of national security concern [33, 34]. Advances in real-time bioaerosol fluorescence measurements have improved resolution and discrimination capabilities by

incorporating real-time, single-particle fluorescence monitors with multiple excitation and emission channels [35-41].

The ability to classify bioaerosols based on their size and fluorescence behavior (excitation-emission wavelengths and intensity) using multi-channel bioaerosol fluorescence monitors has been of growing interest because of the potential to determine interferences by non-biological particles (i.e combustion particles) and establishing methods for bioaerosol identification [37, 40-42]. For example, Sivaprakasam et al. 2011 [37] were able to improve discrimination between bioaerosols and diesel exhaust particles with the addition of a 350nm excitation wavelength, where these aerosol fluorescence profiles would have overlapped with 266nm excitation alone. Robinson et al. 2013 [43] leveraged cluster analysis techniques for interpreting single-particle bioaerosol fluorescence data to classify bioaerosol types, reporting that algorithms used to interpret fluorescence spectra could be adjusted to confidently separate bacteria and fungi into unambiguous particle groups.

In this context, cluster analysis is based on the assumption that the fluorescence properties are constant; however, perspectives are emerging that question the influences atmospheric aging and/or oxidative exposures may have on the chemical and optical properties of bioaerosols. It is evident that aging influences viability as defined by the ability to be recovered by culturing techniques; thus, it follows that the changes of intracellular biopolymers which accompany the loss of viability would likely affect the detectable properties of bioaerosols, including intrinsic fluorescence properties. Because of the optical properties of bioaerosols, many of the biopolymers and enzymatic energy carriers which make up microbial cells are candidates for real-time fluorescence characterization—based on the quantum yield

from unique combinations of excitation and emission wavelengths [4, 39]. Table 3-1, adapted from Pöhlker et al. [15], outlines the more common biological fluorophores thought to contribute to this bioaerosol detection approach.

Table 3-1.Summary of relevant fluorophores reported in bioaerosol detection

Bioaerosol Fluorophore	Function/Remarks (possible WIBS-4 Channel)	Excitation Wavelength (nm)	Emission Wavelength (nm)	Study*
Tryptophan (Trp)	Amino acid, responsible for ~90% of signal from native proteins (FL1)	280 – 295, 286	340 - 353	1, 2-6
Tyrosine (Tyr)	Amino acid, responsible for ~10% of signal from native proteins (FL1)	275, 280	300 - 304	1, 2-6
NADH and NADPH	Coenzymatic redox carrier (indicator of viability) – (FL3)	290 – 295, 340 - 366	440 - 470	1, 2-5, 8, 9
Flavins (riboflavin and FMN)	Coenzymatic redox carrier and photoreceptor (indicator for cell metabolism) – (FL3)	380, 450-488, 280, 373, 445	520-560, 523	1, 4, 5, 8, 12, 13
Chitin	Fungal cell wall component (FL2 & FL3)	335, 254, 373	413, 452 - 458	1, 28-30
Sporopollenin	Pollen and fungal spore cell wall component (FL2 & FL3)	300-550	400-650	35-37
Carotenoids	Accessory pigment in photosynthesis and UV protection (FL3)	400-500	520-560	36, 50

Emerging studies of particulate matter using on-line fluorescence measurement techniques have largely focused on discriminating between biological and non-biological aerosols [39], and more recently have leveraged the ability of fluorescence-based bioaerosol detectors to discriminate between classes of bioaerosols. For example, O'Connor et al. [42] used

principal component analysis (PCA) to evaluate fluorescent emission properties of thirteen types of pollen and fungal spores at a single excitation wavelength of 370 nm. They determined that grass pollens had the most intense and distinct emission spectra when compared with the other common pollen grains and fungal spores. This marked intensity made grass pollen easier to discriminate from other pollens and fungal spores with fluorescent methods. Baumgardner et al. 2013 [44] reported that distinct groupings of fluorescence spectra corresponded to phenotypic groupings of bioaerosols, and that comparing the ratio of emission between 420-650 nm when challenged with excitation of 280 or 370 nm, was able to resolve fungal spores from some similar sized pollens (or their fragments). A classification method for discriminating between bioaerosol types based on fluorescence bandwidth, or the combinations of bandwidths, was successfully developed and applied by Perring et al. 2015, to investigate variations in bioaerosol types across the United States [40]. Perring and coworkers reported that size segregated fluorescent aerosol detected in the lower atmosphere (c.a. < 1000 ft.) across the Southeast United States, was consistent with the sizes and fluorescence patterns of fungal spores observed in a laboratory setting [41], while a shift to larger fluorescent particle sizes, with markedly different fluorescence patterns, was more commonly observed across the Southwest U.S.

In a series of controlled environmental chamber studies, size (optical diameter), particle fluorescence and intensity distributions were catalogued from a collection of more than 50 aerosolized pure cultures of fungi and bacteria [41]. When aerosolized, the size-normalized fluorescence type distributions of whole microbial cells, as well as pollen grains and their fragments, clustered into obvious patterns which could be associated with their major phenotypic classes. This library approach was used as a reference to implicate fluorescence signatures

(within the relevant size range) in patient rooms and soiled textile storage rooms in a modern hospital; fluorescence spectra were in agreement with co-located molecular profiles of airborne bacterial genes recovered from the same locations [31].

Kanaani et al. [45] found that on-line fluorescence measurements can discriminate between two types of fungal spores (*Aspergillus spp.* and *Penicillium spp.*); but, as the spores were exposed to air, the fluorescence intensities for both genera decreased with exposure time. Further, vegetative bacterial cells (*E.coli and B. subtilis*) exposed to elevated temperatures (20 ˚C – 200 ˚C) also exhibited marked decreases in fluorescence intensity with an inverse trend between fluorescence and temperature beyond 40 ˚C [46]. Creating baseline libraries of bioaerosol response with different instruments is important, but there are few reports which characterize the fluorescence properties of bioaerosols as they age and experience changes in environmental variables - temperature, humidity and redox condition.

Recent studies indicate that changes in the fluorescence intensities of octapeptide and whole bacteria could be detected using an on-line bioaerosol monitor [14, 16]. These studies provided some of the earliest indications that common gas-phase oxidants (such as ozone), at different RH levels, may impact the surface of commonly occurring bioaerosols. A laboratory chamber study conducted by Santarpia at el. [16] aerosolized both *Yersinia rohdei* bacteria and MS2 bacteriophage in a rotating drum containing ozone, and detected a decrease in on-line fluorescence emission spectra in the near UV region (263 nm excitation / 330 nm emission). In this same experimental series, aerosolized MS2 particles were challenged with ozone as humidity varied from low RH to high RH, which was reported to have a significant impact on specific fluorescence intensity. A recent study by Pan et al. [14] reported changes in fluorescence

spectra of aerosolized octapeptides exposed to environmentally relevant ozone concentrations at varying RH levels, with higher RH levels associating with the greatest spectral response (decline) when challenged with ozone. Further, the emission spectra from immobilized octapeptide experienced a blue-shift as ozone concentrations increased, indicating ozone-induced modifications to these fluorescing compounds. This same study reported an increase in fluorescence particle intensity in response to ozone exposure. The authors suggest this increase was associated with the formation of kynurenine and/or its oxidized conjugate, ozonide N-formyl kynurenine, from the oxidation of specific tryptophan residues in this octapeptide. However, no analytical chemistry measurements confirmed the decay of octapeptide, its integrated tryptophan residues, nor measurements reporting the concomitant appearance of kynurenine containing compounds.

The current aerobiology literature concerning particle aging remains limited and tenuous, particularly where fluorescence properties are concerned. Controlled observations of airborne microbe interactions with common air pollutants, and whole cell bioaerosols, have yet to be comprehensively explored.

3.3. Experiment Specific Methods and Materials

The methods presented in this chapter are specific to the experiments conducted by individual particle interrogation and real-time fluorescence bioaerosol measurements. For general methods related to analytical techniques, or other sample collection and processing, and chamber design, refer to Chapter 2.

3.3.1. Overview of Instrumentation

A high-throughput aerosol monitor, which concurrently reports the optical diameters and selected fluorescence properties of airborne particles (InstaScope, Detectiontek, Inc, Boulder, CO) was used for this research. This instrument is a portable variant of the Wideband Integrated Bioaerosol Spectrometer – Model 4 (WIBS4, Droplet Measurement Technologies), which has been seeing increased use for ambient aerosol characterization [39, 47]. The InstaScope (referred to hereafter as a portable WIBS, or pWIBS) is a single particle interrogation device designed to measure and record total particle concentrations, their equivalent optical diameter (EOD), and associated fluorescence properties (if any) as outlined below in Table 3-2:

Table 3-2. InstaScope (pWIBS) fluorescent detection channel assignments

Channel ID	Excitation Wavelengths (nm)	Emission Wavelengths (nm)	Potential Corresponding Biological Fluorophore
A (FL1_280)	280	310 - 400	Tryptophan (protein)
B (FL2_280)	280	420 - 650	Sporopollenin/chitin
C (FL2_370)	370	420 - 650	Nicotinamide adenine dinucleotide, reduced (NADH)

Common biological fluorophores, which are germane to the detection of whole microbial cells, are included with their correspondence to each of three different fluorescent channels which are detected by the pWIBS as listed above. Channels are defined here as specific emission bandwidths, which correspond specific excitation wavelengths. It should be noted that many other fluorophores can be measured in these channels, including non-biological particles which may present interference (false positives) [48]. In this work, a series of controlled environmental chamber experiments provided conditions for those potential interferences to be controlled (eliminated).

Single-particle size and associated fluorescence data are electronically stored in an archive, which can provide population data from between 3,000 to 30,000 single-particle measurements from a predetermined time frame (in consecutive 10 minute intervals), over the course of aerosol chamber experiments. Real-time fluorescence and particle concentration data were archived while other bioaerosol samples were concurrently collected from the chamber air (filters, impingers, etc.) for subsequent microscopic and biochemical analyses. The pWIBS sample flow rate was 14 mL/s (0.84 L/min), where all inlet flow passed through HEPA filters after measurements were conducted and before being discharged. A schematic of the p-WIBS instrument and direction of particle flow during measurements, adapted from the Droplet Measurement Technologies instrument manual [40], is shown in Figure 3-1

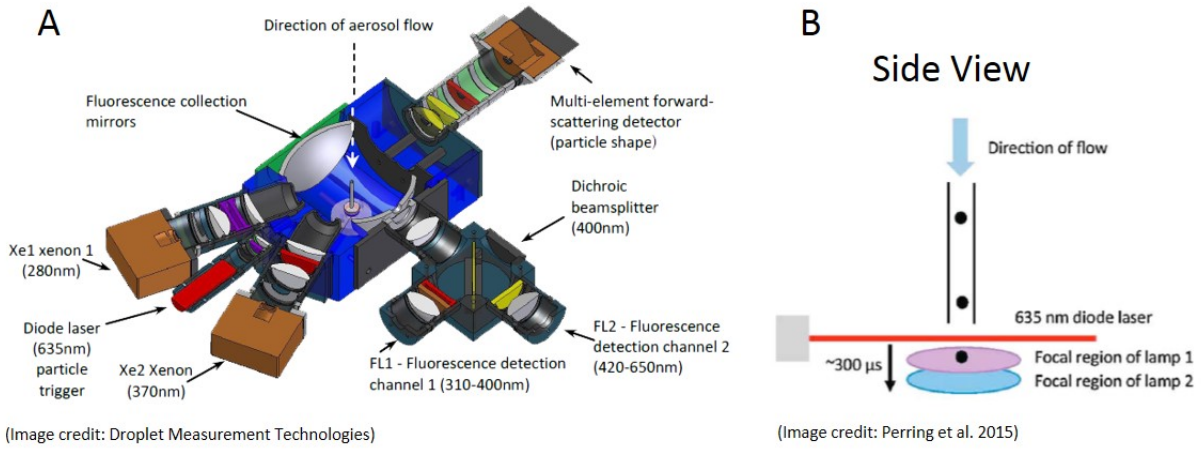

Figure 3-1. Schematic of the pWIBS4 particle detection cell as viewed from above (A) and from the side (B).

3.3.2. Discussion of Calibrations and Data Analysis Methods

In order to best determine particle fluorescence properties above background, an analytical threshold was determined for each channel by forcing the instrument to acquire signal in the absence of particles. This approach was used to determine the "background" fluorescence associated with the instrument electronics under any operating condition, and is simply referred to as a "forced trigger". This background was removed from each particle's fluorescence spectra across all channels. Figure 3-2 illustrates the background fluorescence for each detector channel at different gain settings, where gain is the electronic signal sensitivity of the fluorescent light detectors. Detector gain settings only impacted the FL1 channel as shown in Figure 3-2-A. Examples of the potential influence on uncorrected fluorescence data for each channel are shown in Figure 3-2-D-F for *Aspergillus fumigatus* spores recovered from a high humidity atmosphere. In this case, it is clear that background fluorescence is significant and could skew analysis of

actual particle fluorescence; therefore, it is simply determined by running a forced trigger protocol immediately before sampling, and subtracted from particle fluorescence observations. For each experiment reported here, a background fluorescence intensity histogram was fit with a lognormal curve, placing the background threshold value at +/- 3σ from the max peak location. Maximum background fluorescence intensity values were 128 for higher gain settings and 87 for lower gain settings in the FL1 channel respectively; an intensity of 68 for the FL2 channel; and, an intensity of 4 for the FL3 channel.

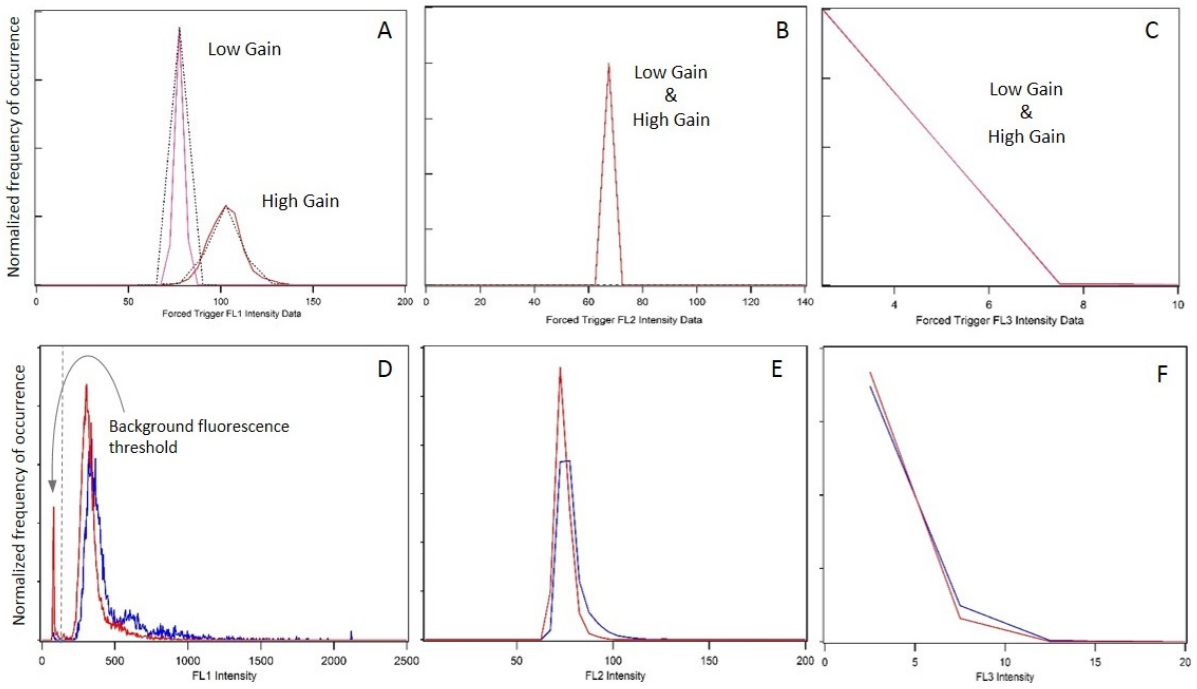

Figure 3-2. Background fluorescence (forced trigger) response from pWIBS at high and low gain detector settings. Examples of probability densities determined from normalized fluorescence histograms without background correction (plots A – C). Probability density plots compiled from observations of airborne *Aspergillus fumigatus* spores before ozone exposure (blue), and after 3 hour 200ppb ozone exposure (red), at 85% RH: FL1 channel (Channel A), the FL2 channel (Channel B), and the FL3 channel (Channel C) (plots D-F).

The pWIBS was regularly calibrated with green and yellow polystyrene latex (PSL) microspheres to verify that the excitation and detection channels were operating correctly. The single-particle optical diameters for all bioaerosols measured are reported here as equivalent optical diameter (EOD), and determined from measuring elastically scattered light of each bioaerosol after passing through a 635nm continuous laser beam. The scattered light from all particles are then compared to EOD "look-up tables" constructed based on observed scattered light intensity from non-fluorescent polystyrene latex spheres (PSLs) of known diameters (0.85um, 1um, 1.3um, and 3um) and refractive index of 1.59 (Fisher Scientific). The optical scatter data was fit with the Bohren and Huffman (1983) [49] treatment of the Mie Theory calculations. Particle size distributions were constructed for each bioaerosol, in each chamber experiment, using log-normal particle size distributions [50], widely utilized in aerosol research. In many cases the diameter determined from elastic scattered light (optical diameter) is different from the aerodynamic diameter depending on the particle shape and surface characteristics, and light refractive indices. Here, scanning electrograph microscopy (SEM) images of *Aspergillus fumigatus* spores were taken for size verification and particle surface characteristics. The EOD and measured physical diameter for *A. fumigatus* spores were in good agreement, therefore using the calculated EOD in these studies provided a reasonable estimate of particle diameter.

All data were compiled in a dataset compatible for graphical and statistical analyses using IGOR Pro (Wavemetrics) and Matlab (Mathworks). Fluorescence data were gated to use those values which corresponded with particle sizes in the EOD range of whole microbial cells, as verified by direct microscopy. Fluorescence, size and intensity data for each channel (FL1, FL2, and FL3) were analyzed, in part, by comparing three-dimensional histograms (heat maps) which

facilitated the comparison of analytical centroids with accepted statistical tests. Size (EOD) and intensity frequency distributions for each bioaerosol population, in each channel, for each experimental condition were compiled. To minimize the influence of kurtosis introduced by the disproportional fluorescence of sub-cellular size particles (i.e. fractions of cells) or particle clusters, while accounting for instrument gain, approximately 75% of all the optical data collected were used for fluorescence analyses after being gated for the EOD size range corresponding to individual whole microbial cells. These gated data were used to compile size-segregated intensity (frequency) distributions from the raw optical data sets. Particle sizes (EOD) and associated fluorescence intensity, with their respective variance, were compared with gated mean fluorescence in each channel using lognormal data transforms into standard, multivariate Gaussian distributions. Using fluorescence spectra and size, airborne cellular response to ozone could then be judged by shifts in the centroids of these size-segregated fluorescence intensity distributions in two dimensions, as a standard Euclidean distance. These spectral shifts are defined here as a "Difference in Fluorescence (DiF)" determined from their Euclidean distance normalized by particle size (EOD), according to the following analytical geometry:

$$DiF\ Measure = \frac{\left(\sqrt{\left(\ln\left(D_{post}\right) - \ln\left(D_{pre}\right)\right)^2 + \left(\ln\left(FI_{post}\right) - \ln\left(FI_{pre}\right)\right)^2}\right)}{\left(\ln\left(D_{post}\right) - \ln\left(D_{pre}\right)\right)}$$

Where in the DiF Measure equation,

D is the mean fluorescence corresponding to the equivalent optical diameter before (*pre*), and after (*post*) ozone exposure; and,

FI is the corresponding mean fluorescence intensity in a given channel before (pre), and after (post) ozone exposure.

A concern for measuring bioaerosol fluorescence with instruments that have operator-determined gain settings (i.e. detector sensitivity) is the ability to saturate the electronic signal range of the respective detectors under different conditions. This can result in a reduced ability to characterize the full range of the intensity spectrum associated with microbiological fluorophores, especially where associated with larger particles. Fluorescence data obtained by the pWIBS at the low and high gain settings were analyzed for the fraction of particles saturating the detector. For bioaerosol fluorescence measurements below the saturating range, power-law, linear, and multivariate Gaussian models were fit to log-normal transformed fluorescence data detected in each fluorescence channel. Bioaerosol fluorescence and size (EOD) data under these low gain conditions were not normally distributed; thus, determining significant differences between the cumulative frequency distributions (CFDs) before and after ozone exposure, were conducted with the non-parametric Kolmogorov-Smirnov (KS) test. As previously described, these data were size gated to the following ranges to eliminate variation introduced by cell fragments and cell clusters: fungal spores, 0.85 μm < EOD < 4 μm; bacterial spores, 0.5 μm < EOD < 2.5 μm.

3.4. Results

3.4.1. Bioaerosol size distributions

Bioaerosol size distributions (equivalent optical diameter (EOD)) for each experiment were determined for initial conditions (pre-ozone exposure) and final measurements (following 3 hours of exposure, t=3hrs). In each case, normalized particle number distributions were fit with log-normal functions to determine the mean particle EOD and their associated standard deviations (as referenced by its centroid). EOD data sets, before and after ozone exposure, were trimmed to remove cell fragments and clusters, which then included the optical data corresponding to only those particles with EOD between ± 3σ of the mean. Significance of differences in optical properties in response to ozone exposure, was then assessed using the Kolmogorov-Smirnov test of cumulative frequency distribution (CFD).

Figure 3-3-A-E shows example of the log-normal EOD number distributions for each type of microbe challenged with ozone at high RH and low RH. Figure 3-3-F includes an electron micrograph (magnification 6,520x), showing a morphology typical of that of *Aspergillus fumigatus* spores collected during these experiments with a copper impactor: the mean optical diameter was approximately 2 μm, as judged by a reticule installed on a scanning electron microscope (SEM), where gold coating is used to enhance resolution. More than 20 SEM images of *A. fumigatus* spores were acquired from samples collected to represent all the bioaerosol chamber conditions tested in the presence and absence of ozone. Careful inspection of the *A. fumigatus* spores in all SEM images did not provide any visual evidence to suggest structural

degradation of the spores' coats in response to ozone, regardless of environmental condition, ozone concentration or residence time.

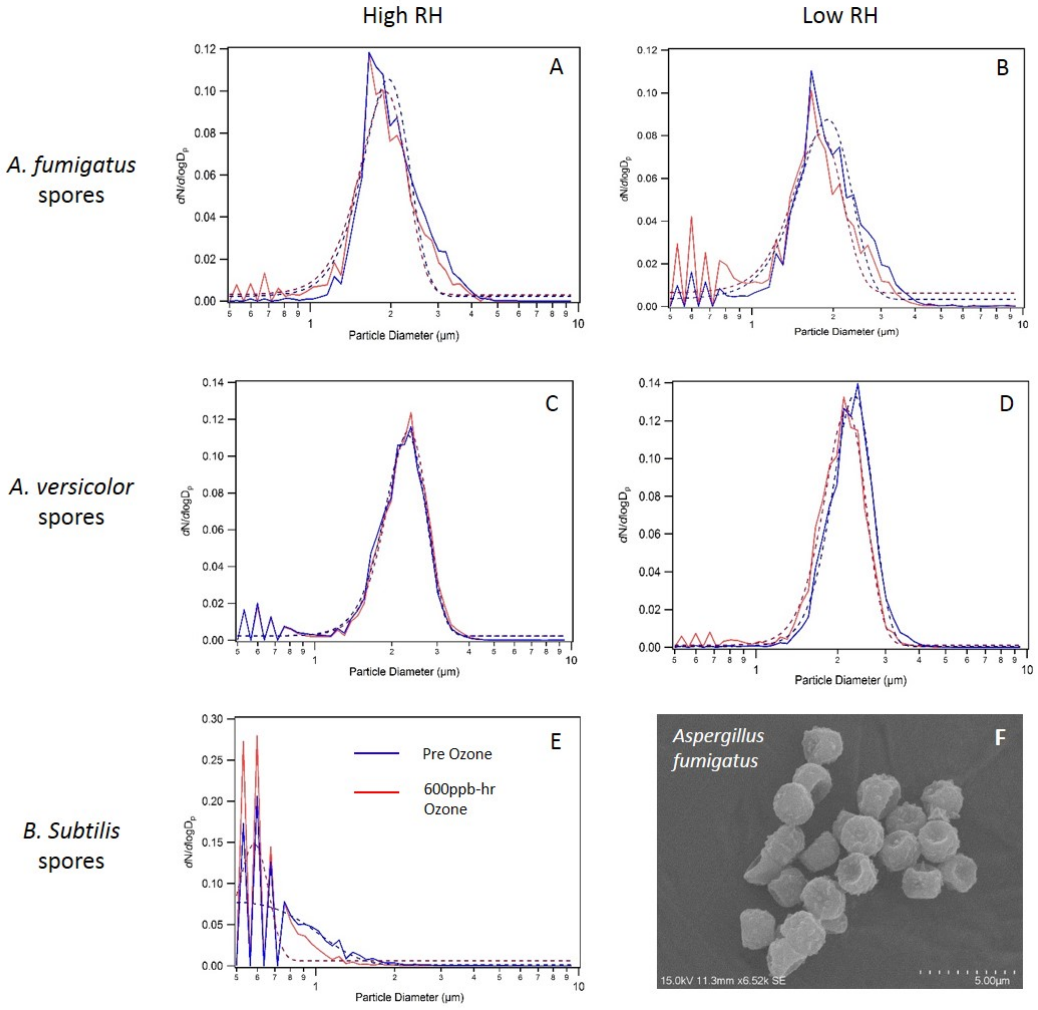

Figure 3-3. Normalized log normal number distributions of airborne *A. fumigatus* spores at 85% RH (A) and 30% RH (B); for airborne *A. versicolor* spores at 85% RH (C) and 20% RH (D); and, for airborne *B. subtilis* spores at 85% RH (E). Distributions corresponding to bioaerosol collected prior to ozone exposure are shown in blue (—), and distributions following 3 hours of ozone exposure are shown in red (—). Log normal fit of aeorsol data prior to ozone exposure, are shown by the blue dotted line (- - -), and log normal fit following ozone exposure are shown by the red dotted *line (- - -)*. True optical diameter of aerosolized A. fumigatus spores are shown at 6,520X magnification, in SEM image (F).

The mean EOD for each bioaerosol case did not significantly change in response to any ozone exposure scenario, as indicated by insignificant shift of the EOD distribution centroid. While the bacterial spores show average EOD decreases in response to increasing residence time, it should be noted that these measurements are approaching the lower calibrated limit of detection of this instrument of 0.85μm. As with their fungal counterparts, significant differences between the cumulative frequency distribution (CFDs), as well as their median values, were determined by the KS test previously described. The resulting CFDs including ozone challenges of *B. subtilis* spores are shown in Figure 3-3-E.

The KS statistic is a measure of the maximum difference (%) between the two distributions (seen as red vertical line in Figure 3-4) and the median values (at 0.5 on the cumulative distributions) are depicted as the green horizontal line. These data suggest that RH, not ozone exposure, played a large role in the differences found between the cumulative EOD distributions of fungal spores at the beginning and end of each chamber experiment. Lower RH levels (< 30%) were associated with greater median decreases in spore EOD than the same conditions at high RH (85%). The EOD log-normal means, standard deviations, CFD median values, KS statistics and associated significance thresholds (p-values) for every condition tested are presented in Table 3-3.

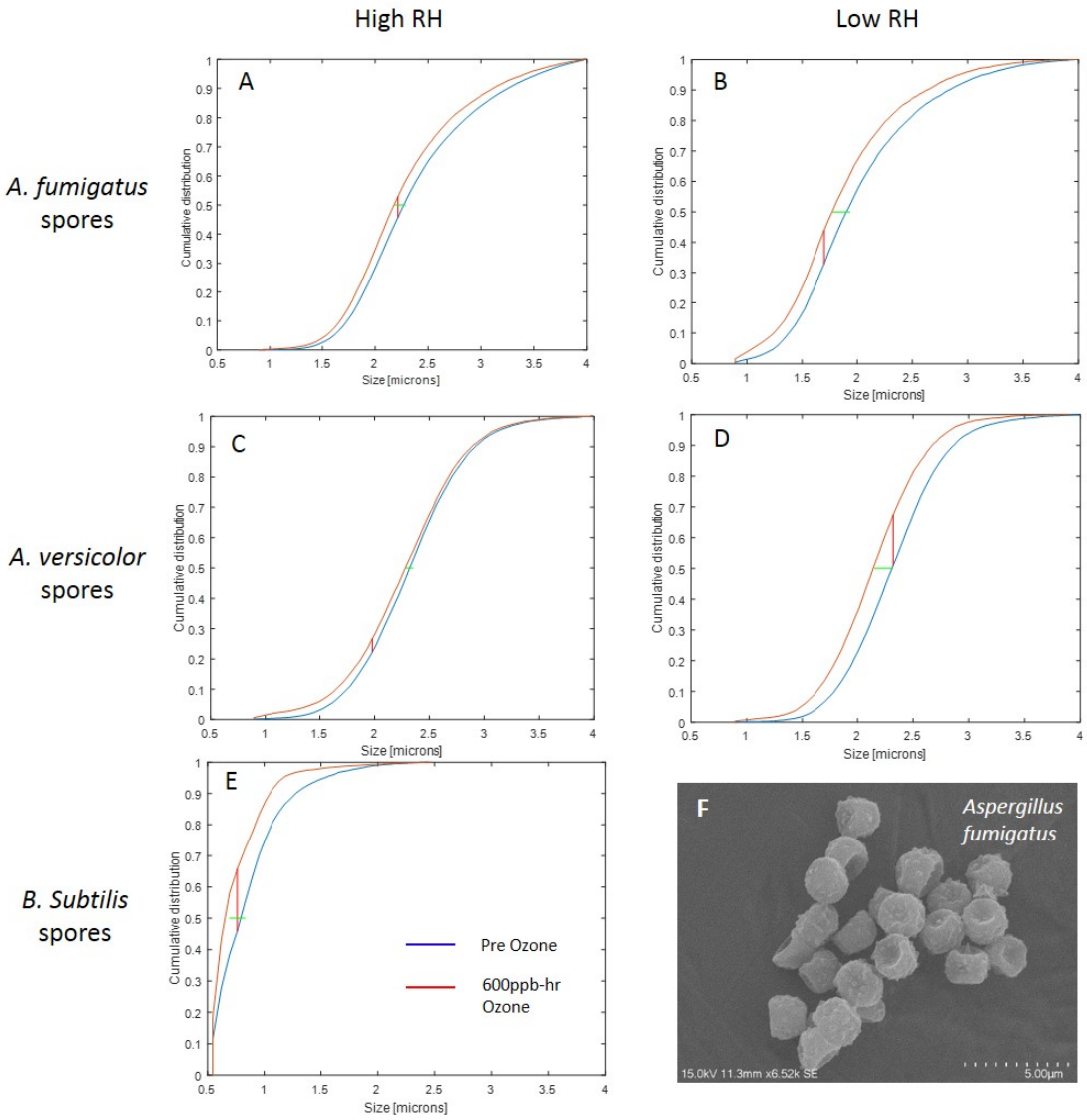

Figure 3-4. Cumulative distributions (CFD) of EOD for airborne *A. fumigatus* spores at 85% RH (A) and 30% RH (B); for airborne *A. versicolor* spores at 85% RH (C) and 20% RH (D); and, for airborne *B. subtilis* spores at 85% RH (E). Distributions corresponding to bioaerosols collected prior to ozone exposure are shown in blue (—), and distributions following 3 hours of ozone exposure are shown in red (—). The KS statistic is shown as the red vertical line (|) between the pre and post-exposure CFDs. The respective median is shown as the green horizontal line (|) between distributions. Physical diameter of aerosolized *A. fumigatus* spores is shown at 6,520X magnification in SEM image for comparison (F).

Table 3-3. Bioaerosol EOD log normal and CFD descriptive statistics

Culture	Culture Age (Days)	RH(%)	Ozone (ppb-hr)	EOD Log Normal max (mm)	EOD Log Normal SD	CFD Median EOD (mm)	KS Statistic (%)	KS p-value
A. versicolor	39	85	0	2.29	0.46	2.35	4.5	4.8E-28
A. versicolor	39	85	600	2.35	0.43	2.28		
A. versicolor	38	85	0	2.41	0.47	2.38	15.8	1.9E-64
A. versicolor	38	85	0	2.25	0.44	2.19		
A. versicolor	36	30	0	2.27	0.35	2.32	26.5	8.7E-104
A. versicolor	36	30	600	2.1	0.32	2.01		
A. versicolor	35	30	0	2.3	0.39	2.32	16.4	4.3E-89
A. versicolor	35	30	0	2.16	0.38	2.15		
A. fumigatus	78	85	0	2.28	0.49	2.29	7.1	2.34E-85
A. fumigatus	78	85	600	2.12	0.23	2.19		
A. fumigatus	15	85	0	2.02	0.38	2.04	6.3	3.68E-06
A. fumigatus	15	85	0	1.97	0.37	2.01		
A. fumigatus	11	85	0	1.91	0.38	2.01	7.7	3.06E-07
A. fumigatus	11	85	600	1.96	0.39	1.94		
A. fumigatus	18	20	0	1.91	0.43	1.94	11.0	2.99E-41
A. fumigatus	18	20	600	1.79	0.37	1.78		
A. fumigatus	24	20	0	1.84	0.33	1.9	12.3	3.15E-49
A. fumigatus	24	20	0	1.79	0.29	1.78		
A. fumigatus	18	20	0	1.99	0.43	2.01	3.2	0.1
A. fumigatus	18	20	1000	1.98	0.40	2.01		
A. fumigatus	15	20	0	1.93	0.37	1.9	5.2	0.0001
A. fumigatus	15	20	1200	1.84	0.31	1.94		
A. fumigatus	15	20	0	1.97	0.36	1.97	3.2	0.11
A. fumigatus	15	20	7500	1.92	0.34	2.01		
B. subtilis	14	85	0	0.775	0.32	0.83	19.8	5.8E-152
B. subtilis	14	85	600	0.576	0.06	0.69		
B. subtilis	14	85	0	0.49	0.45	0.69	18.9	7.3E-134
B. subtilis	14	85	0	0.58	0.08	0.62		

3.4.2. Fluorescence Channel Distributions

Theoretically, the intensity measured from a fluorescing particle should be a function of its size (cross section) and fluorophore composition; for spherical particles, this can be modeled by a power-law function. Previous studies of bioaerosol fluorescence have attempted to normalize emission intensity by size-apportioned exponents or other constants [14, 16, 33, 37, 51, 52]. Because of the heterogeneous physiological composition of microbial cells and spores in the environment, and the fact that biopolymers in microbial cells change in response to growth and environmental conditions, modeling bioaerosol fluorescence intensity presents an analytical and mathematical challenge. In this context, normalizing what is likely a dynamic fluorescence response for many different types of microbial cells in the environment (determined under a broad range of conditions) introduces the potential for a broad range of uncertainties. In response to this challenge, the next section introduces new analytical methods that can support a more robust statistical approach for describing and modeling size dependent fluorescence spectra of bioaerosols.

The following suite of experimental results include the airborne particles exhibiting fluorescence above the pWIBS background in the following channels: FL1 (‘Channel A’, ex/em: 280nm/310-420nm), FL2 (‘Channel B’, ex/em: 280nm/420-650nm), FL3 (‘Channel C’, ex/em: 370nm/420-650nm). These are compared to non-fluorescing particles (below background) in chamber studies where *Aspergillus versicolor* spores (Figure 4.#), *Aspergillus fumigatus* spores (Figure 4.# and Figure 4.#), and *Bacillus subtilis* spores (Figure 4.#) are aerosolized under various exposure conditions. All fluorescence distribution data were corrected for background

fluorescence (forced trigger data, see Figure 3-2), and gated for EO diameters between ± 3 standard deviations of the mean, as previously described, in the following ranges:

1.5 μm < EOD < 3.5 μm, for both species of fungal spores, *A. fumigatus* and *A. versicolor*

0.5 μm < EOD < 1.5 μm, for *Bacillus subtilis* spores

Given the background corrections, the pWIBS gain setting (high or low) did not have an impact on fluorescence intensity detection (quantitation) of these bioaerosols in a given fluorescence channel; however, gain settings did have an impact on of the fraction of *A. fumigatus* spores that saturated the FL1 (Channel A) detector.

The influence of ozone exposure on the distribution of *A. versicolor* (35 days < spore culture age < 39 days) across the different fluorescent channels in the pWIBS was most apparent after 600ppb-hr ozone exposure at 85% RH (Figure 3-5-A), where the following changes were detected: Channel C decreased from 18% to 10%, while a slight increase in non-fluorescing spores was measured 0.8% to 2.4%. Under otherwise identical exposure conditions at low RH (Figure 3-5-C), a significant decrease in Channel A (98% to 90%) and Channel B (63% to 53%) was observed with a concomitant increase in the percentage of non-fluorescing spores (1% to 6%). Under the lowest RH conditions (RH < 30%), airborne *A. versicolor* spores that had been aged in the absence of ozone as well as exposed to ozone for up to 3 hours, had higher percentages of the spores detected by Channel B (~60%) than at high RH (~50%). The RH level also had an impact on the percentage of *A. fumigatus* spores detected in each channel, as well as the fraction of airborne spores that saturated the Channel A detector, as shown in Figure 3-6.

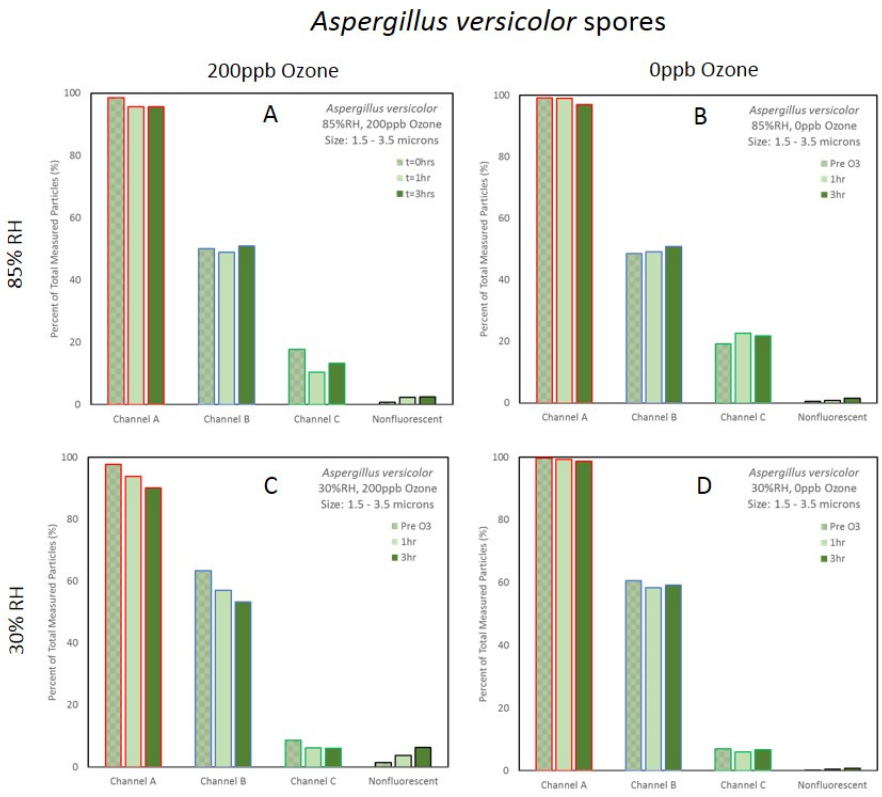

Figure 3-5. Percentage of total airborne *Aspergillus versicolor* spores exhibiting fluorescence above background in Channel A ('FL1', red outline (□)), Channel B ('FL2', blue outline (□)), Channel C ('FL3', green outline (□)), and non-fluorescent (below FT background threshold, black outline (□)) observations prior ozone exposure are represented by pattern filled bars (▒). The extent of ozone exposure response is represented by the darkness of solid green shading: following 1 hour of exposure/aging (light green (▉); and following 3 hours exposure/aging (dark green (▉)). All *A. versicolor* cultures were between 35 and 39 days old immediately prior to their aerosolization. The following conditions are described for individual experiments: 200ppb ozone @ 85% RH (**A**); No ozone @ 85% RH (**B**); 200ppb ozone @ 30% RH (C); and, No ozone @ 30% RH (**D**).

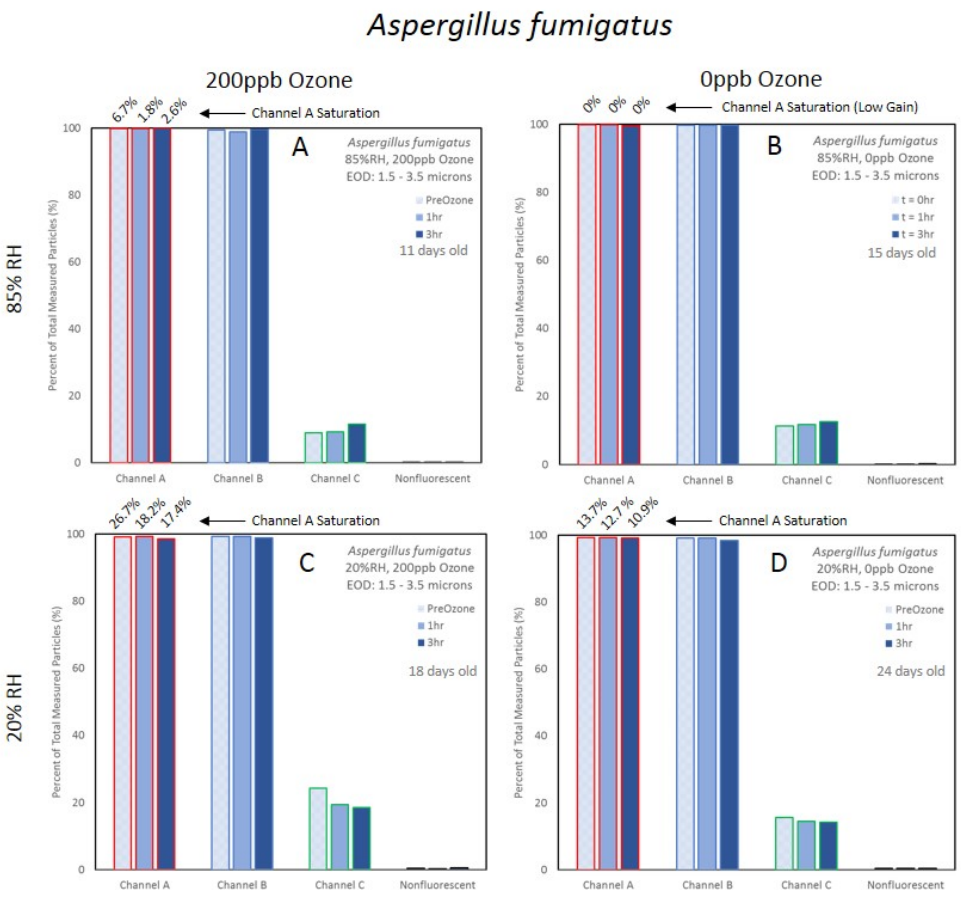

Figure 3-6. Percentage of total airborne *Aspergillus fumigatus* spores exhibiting fluorescence above background in Channel A ('FL1', red outline (□)), Channel B ('FL2', blue outline (□)), Channel C ('FL3', green outline (□)), and non-fluorescent (below FT background threshold, black outline (□)) observations prior ozone exposure are represented by pattern filled bars (▒). The extent of ozone exposure response is represented by the darkness of solid green shading: following 1 hour of exposure/aging (light blue (▒); and following 3 hours exposure/aging (dark blue (▒)). All A. fumigatus cultures were between 11 and 24 days old immediately prior to their aerosolization. The following conditions are described: 200ppb ozone @ 85% RH (**A**): No ozone @ 85% RH (**B**), 200ppb ozone @ 20% RH (C), and No ozone @ 20% RH (**D**). Where the channel A detector was saturated, the fraction of particles at or above this fluorescence intensity is presented at a percentage of that channel's total spore count, presented above each plot.

The influence of ozone exposure on the distribution of *A. fumigatus* spores (11 days < spore culture age < 24 days) across the different fluorescent channels in the pWIBS, was most apparent after 600ppb-hr ozone exposure (Figure 3-6-A), where the following changes were detected: a decrease in the saturated fraction detected in Channel A (27% to 17%) with 600ppb-hr exposure ozone under low RH conditions (20% < RH) concomitant with a decrease in Channel C (24% to 18%). Unlike *A. versicolor*, the non-fluorescent fraction was consistently below 1% of these airborne spores observed in all cases. Further, low RH conditions appeared to influence the magnitude of the increased fraction of *A. fumigatus* spores detected in Channel C in response to ozone exposure at high RH (~10% and ~20%, respectively), opposite the behavior in Channel C of *A. versicolor* spores at low and high RH. Additionally, almost all of the *A. fumigatus* spores consistently were detected in both Channels A and B, where all *A. versicolor* spores are detected in Channel A, but only approximately half were also detected by Channel B. The effects of fungal spore maturity on fluorescence response to ozone exposure within a species (A. fumigates) and addressed later in this chapter.

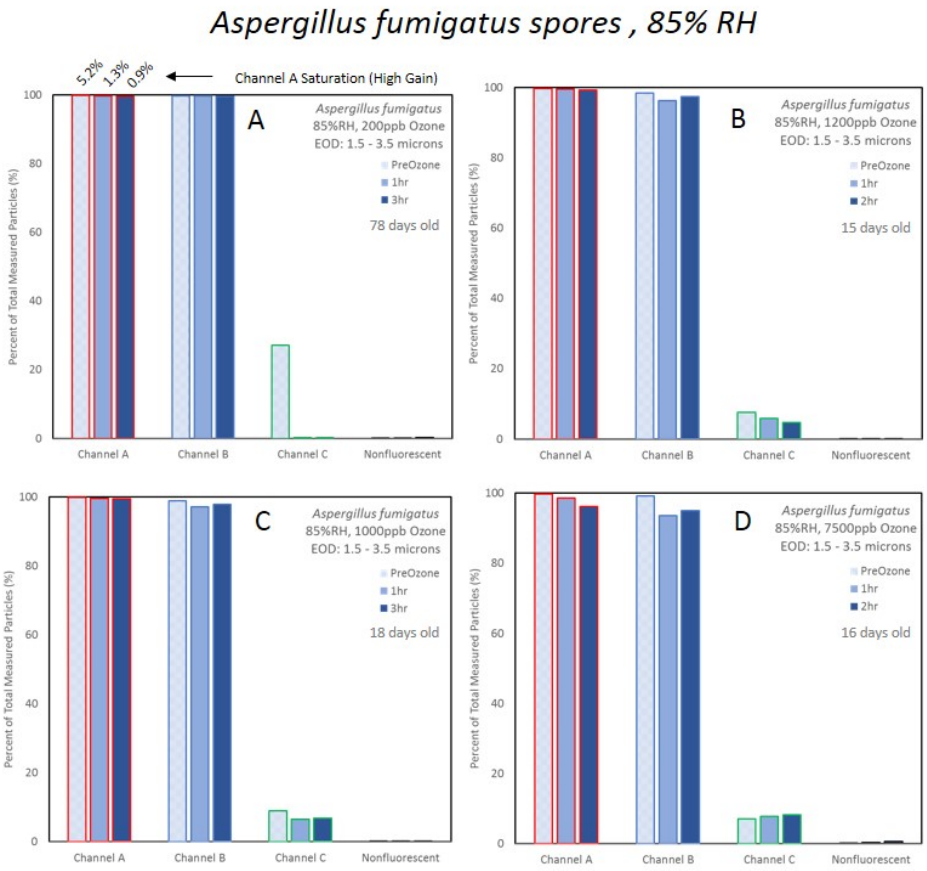

Figure 3-7. Percentage of total airborne Aspergillus fumigatus spores exhibiting fluorescence above background in Channel A ('FL1', red outline (□)), Channel B ('FL2', blue outline (□)), Channel C ('FL3', green outline (□)), and non-fluorescent (below FT background threshold, black outline (□)). Observations prior ozone exposure are represented by pattern filled bars (▒). The extent of ozone exposure response is represented by the darkness of solid green shading: following 1 hour of exposure/aging (light blue (▒); and following 3 hours exposure/aging (dark blue (▒)). All A. fumigatus cultures were between 11 and 24 days old immediately prior to their aerosolization. The following conditions are described, all of which were executed at RH = 85%: 200 ppb ozone w/ spore age = 78 d (**A**); 1200 ppb ozone w/ spore age 15d (**B**); 1000 ppb ozone w/ spore age 18d (**C**); and, 7500 ppb ozone w/ spore age 16 (**D**). Where the channel A detector was saturated, the fraction of particles at or above this fluorescence intensity threshold is presented as a percentage of that channel's total spore count, presented above the plot.

The oldest (most mature) cultures tested were *A. fumigatus* spores that had been aged 78 days prior to their aerosolization; this mature culture displayed a higher fraction of spores initially in Channel C, than any other *A. fumigatus* condition/spore age tested. In the case of these mature spores, the fraction of the airborne population reporting above the detection limit in Channel C, decreased from 27% to less than 1% of the total spores after a 600 ppb-hr ozone exposure at 85% RH. Increases in ozone levels resulted in small decreases in the percentage of spores reported in Channel B, where 1000 ppb-hr ozone exposure decreased the channel B count from 99% to 97% of the total spores; 1200ppb-hr ozone exposure decreased 99% to 96%, and 7500ppb-hr ozone decreased from 99% to 93%; there were no changes in the percentage of particles detected by Channel B at 85% RH at or below ozone exposures 600 ppb-hr. The profile of bacterial spores from *Bacillus subtilis* show a markedly different pattern in percent of particles detected in all channels, as shown in Figure 3-8.

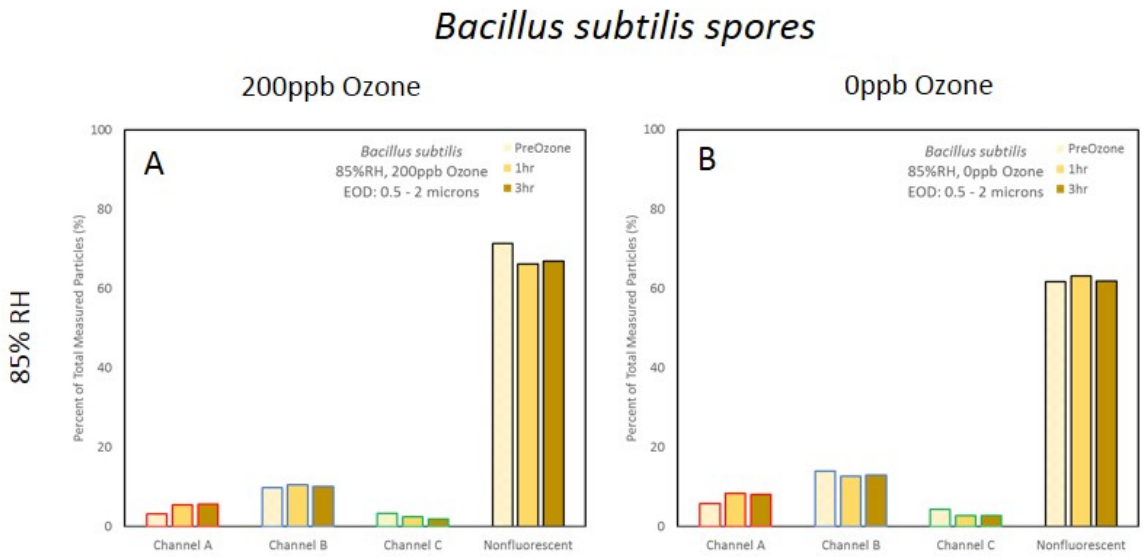

Figure 3-8. Percentage of total airborne *Bacillus subtilis* spores exhibiting fluorescence above background in Channel A ('FL1', red outline (□)), Channel B ('FL2', blue outline (□)), Channel C ('FL3', green outline (□)), and non-fluorescent (below FT background threshold, black outline (□)). Observations prior to ozone exposure are represented by pattern filled bars (▒). The extent of ozone exposure response is represented by the darkness of solid gold shading: following 1 hour of exposure/aging (light gold (▒); and following 3 hours exposure/aging (dark gold (▒)). All *B. subtilis* cultures were between 35 and 39 days old immediately prior to their aerosolization. The following conditions are described for individual experiments: 200ppb ozone @ 85% RH (**A**); No ozone @ 85% RH (**B**).

The percentage of *B. subtilis* spores detected in any channel was significantly lower than for *Aspergillus spp.* spores, with a much larger contribution of non-fluorescent particles. Because of the EOD size range investigated, the larger contribution of non-fluorescent particles may be due to the phosphate buffered saline (PBS) solution the spores were washed with to remove their growth and sporulation media. Unlike their fungal counterparts, these bioaerosols were generated from liquid suspension via nebulization, where all fungal spores were dry aerosolized directly from their cultures thereby eliminating this issue. In general, ozone exposure does not impact the percentage of total bioaerosols detected in each fluorescent channel. A summary of

the percentages of particles detected across the fluorescence channels A, B, and C each pure culture bioaerosol and set of atmospheric exposure conditions is outlined in Table 3-4.

Table 3-4. Percentage of bioaerosols detected in fluorescent Channels A, B, C, and the non-fluorescent fraction

Bioaerosol Spore Type	Channel A (FL1) Ex: 280 nm Em: 310-420 nm	Channel B (FL2) Ex: 280 nm Em: 420-650 nm	Channel C (FL3) Ex: 370 nm Em: 420-650 nm	Non-Fluorescing
Aspergillus versicolor	High RH: 95-99% Low RH: 90-99%	High RH: 48-50% Low RH: 53-60%	High RH: 11-22% Low RH: 6-9%	High RH: 0.6-2.5% Low RH: 0.3-6%
Aspergillus fumigatus	High RH: 99% Low RH: 98-99%	High RH: 99% Low RH: 98-99%	High RH: 9-13% Low RH: 19-24%	High RH: <1% Low RH: <1%
Bacillus subtilis	High RH: 3-9%	High RH: 9-14%	High RH: 2-4%	High RH: 62-71%

These results report the spores counted above background and the fractions thereof which saturated Channel A, or were otherwise below the detection limit in any channel. Though ozone exposures induced some changes in distributions reported by each fluorescence channel, this does not include the extent to which the fluorescence intensity in each channel is influenced by ozone exposure. Characterization of fluorescence intensity, with and without respect to their corresponding EOD is discussed in the following section.

3.4.3. Characterization of Bioaerosol Fluorescence Intensity with Exposure Conditions

The fluorescence present in the FL1 channel (referred to as Channel A in the previous section for comparison to literature) has been typically associated with the protein content of bioaerosols - specifically tryptophan and tyrosine residues. When these amino acids are pure in

aqueous solution, they fluoresce when excited at 280 nm and the resulting emission can be detected by the pWIBS between 310 nm and 420 nm (measured as a cumulative intensity across this region). Fluorescence intensity at a given excitation has been used in a limited context to discriminate between bioaerosol types and gauge changes in biopolymer properties in other oxidative aging studies. In this work, fluorescence intensity distributions measured by the FL1 channel where characterized by a gated EOD range using bulk intensity histograms and CFD distributions (with KS test for significant differences). Two dimensional histograms were then constructed which report fluorescence intensity with respect to EOD; these were log-normal transformed and fit with multivariate Gaussian distributions. The bioaerosol fluorescence intensity distributions in the FL2 and FL3 channels were also evaluated for differences before and after atmospheric aging, in the presences and absence of ozone, and at different relative humidity conditions. These differences were judged for statistical significance the KS and multivariate Gaussian metrics previously introduced, for which a comprehensive compilation of these values can be found in the Appendix. Figure 3-1 shows examples of bulk FL1 intensity histogram data for fungal and bacterial spores before and after ozone exposures.

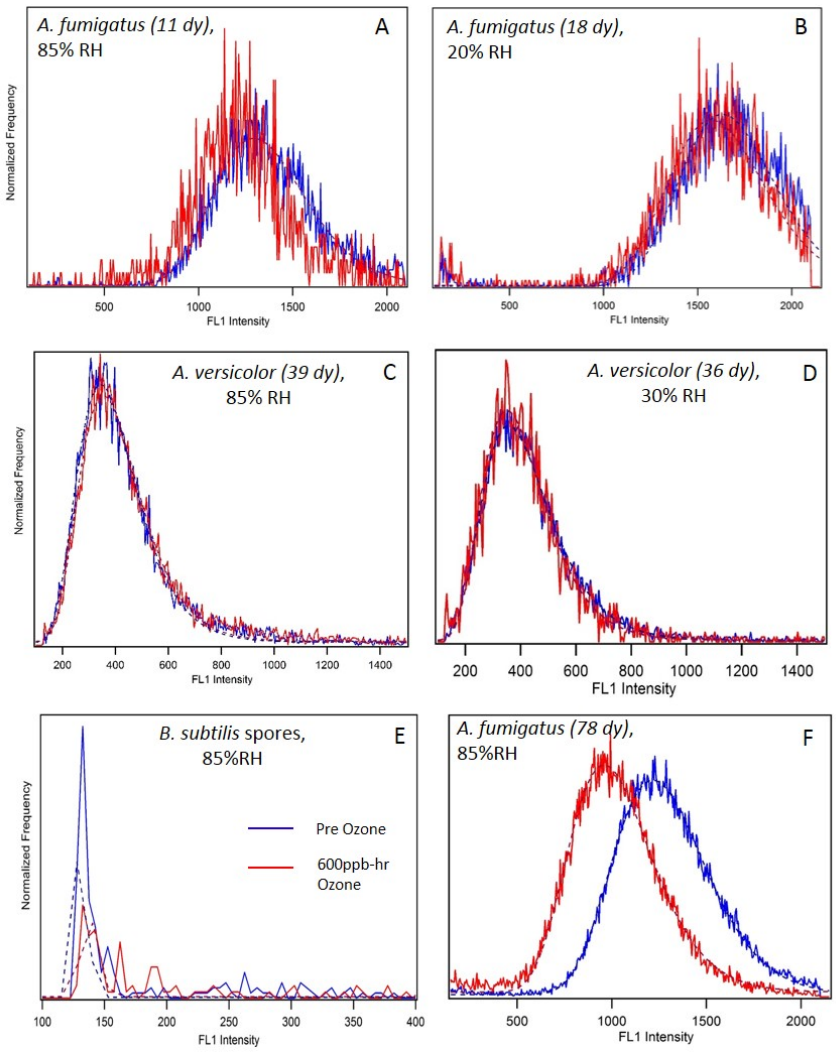

Figure 3-9. Normalized frequency histograms of fluorescence intensity associated with pure cultures of aerosolized spores before and after 600ppb-hr ozone exposure. Fluorescence was measured in the FL channel between 310nm – 420nm (excitation at 280nm). Spore diameters were gated to ranges between 0.85 um < EOD < 4 um for *Aspergillus spp.*; and, 0.5 um < EOD < 1.5 um for *Bacillus subtilis*. Frequency distributions are shown by blue lines prior to ozone exposure (—), and red lines following 600 ppb-hr ozone exposure (—). Panels describe the culture maturity and ozone exposure condition: *A. fumigatus* 11days old @ 85% RH (**A**); *A. fumigatus* 18 days old @ 20 % RH (**B**); *A. versicolor*, 39 days old @ 85% RH (**C**); *A. versicolor*, 36 days old @ 30 % RH (**D**); *B. subtilis* 14 days old @ 85% RH (**E**); and, *A. fumigatus* 78 days old @ 85% RH (**F**).

As judged by fluorescence, single channel intensity histograms (gated, but not normalized by size) can give some indication of the influence culture age can have on the potential for ozone modification during exposure experiments; however, this type of analysis cannot elucidate shifts in fluorescence intensity due to changes in spore volume (as indicated by EOD) or modifications to biogenic fluorophores. In Figure 3-9, the most extreme shifts in FL1 fluorescence intensity (at high gain) was typically found at high RH conditions, increasing spore age, and increased ozone levels (not shown, see Appendix for all FL1 histogram data). Determinate differences between FL1 distributions are illustrated in the CFDs shown in Figure 3-10 below, using non-parametric methods previously described. Median FL1 values are denoted by the green line, and the KS statistic values show by the red vertical lines.

Differences between fluorescence intensity distributions for each fluorescence channel are summarized in Table 3-5, where the largest differences in response to ozone exposure expressed in the format of CFD distribution manifest in significant reductions in specific FL1 and FL3 intensities, which are most extreme in cases with the older fungal spore cultures tested, (*A. fumigatus*, 78 days old, 600 ppb O_3 - hr), or at elevated exposure levels (*A. fumigatus*, 15 days old, 7500 ppb O_3 – hr).

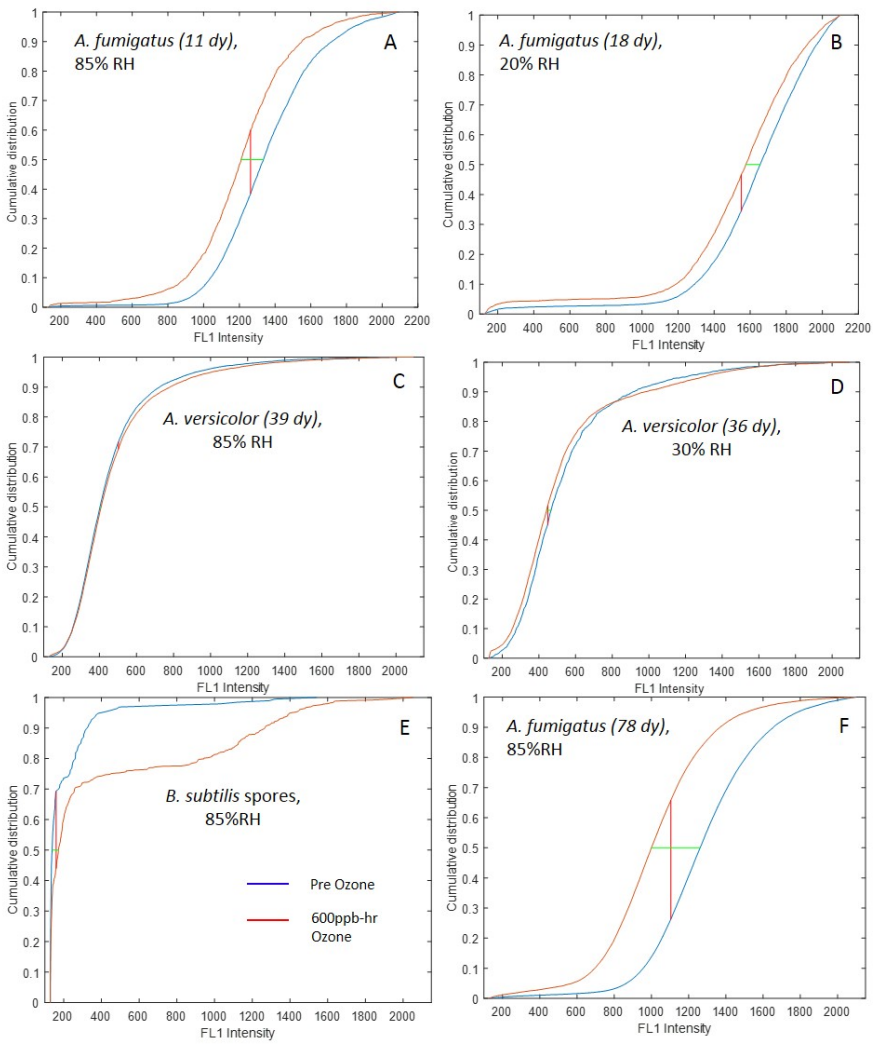

Figure 3-10. Cumulative frequency distributions of fluorescence intensity associated with pure cultures of aerosolized spores before and after 600ppb-hr ozone exposure. Fluorescence was measured between 310nm – 420nm (excitation at 280nm, FL1 channel). Spore diameters were gated to ranges between 0.85 um < EOD < 4 um for Aspergillus spp.; and, 0.5 um < EOD < 1.5 um for *Bacillus subtilis*. Cumulative distributions prior to ozone exposure are shown by blue lines (—), and following 600 ppb-hr ozone exposure, shown by red lines (—). Median values are indicated by green horizontal line (—), and KS statistic value indicated by red vertical line (|). Panels describe the culture maturity and ozone exposure condition: *A. fumigatus* 11days old @ 85% RH (**A**); *A. fumigatus* 18 days old @ 20 % RH (**B**); *A. versicolor*, 39 days old @ 85% RH (**C**); *A. versicolor*, 36 days old @ 30 % RH (**D**); *B. subtilis* 14 days old @ 85% RH (**E**); and, *A. fumigatus* 78 days old @ 85% RH (**F**).

Table 3-5. Overview of KS statistics for CFDs of fluorescence intensity for FL1, FL2, and FL3 channels

Culture	Culture Age (Days)	RH (%)	Ozone (ppb-hr)	KS FL1 Statistic (%)	KS FL2 Statistic (%)	KS FL3 Statistic (%)
A. versicolor	39	85	0	2.3	3.5	3.1
A. versicolor	39	85	600			
A. versicolor	38	85	0	6.1	3.3	1.8
A. versicolor	38	85	0			
A. versicolor	36	30	0	6.4	7.1	5.7
A. versicolor	36	30	600			
A. versicolor	35	30	0	6.3	4.5	9.2
A. versicolor	35	30	0			
A. fumigatus	78	85	0	39.5	3.7	48.8
A. fumigatus	78	85	600			
A. fumigatus	15	85	0	5.8	4.7	3.1
A. fumigatus	15	85	0			
A. fumigatus	11	85	0	21.5	4.9	4.1
A. fumigatus	11	85	600			
A. fumigatus	18	20	0	12.2	26.6	7.8
A. fumigatus	18	20	600			
A. fumigatus	24	20	0	10.9	15.7	4.3
A. fumigatus	24	20	0			
A. fumigatus	18	85	0	18.8	10.1	11.9
A. fumigatus	18	85	1000			
A. fumigatus	15	85	0	16.9	9.4	24.3
A. fumigatus	15	85	1200			
A. fumigatus	15	20	0	44.9	13.3	51.0
A. fumigatus	15	20	7500			
A. fumigatus	28	85	0	13.5	2.2	5.6
A. fumigatus	28	85	600			
B. subtilis	14	85	0	25.5	7.8	13.0
B. subtilis	14	85	600			
B. subtilis	14	85	0	4.3	6.4	10.3
B. subtilis	14	85	0			

The KS statistic and CFD plots give a good indication of bulk fluorescence behavior of a population of particles in a certain size range; however, they cannot indicate specific particle fluorescence with respect to bioaerosol size. Thus, heat maps were constructed with these histogram data to illustrate fluorescence intensity across the EOD ranges observed in all fluorescence channels. The lightest colors in the plots that follow, Figure 3-11, indicate the highest frequencies of fluorescence intensities for a given EOD. As judged by a composite metric of size-normalized fluorescence intensity in any channel or combinations of channels, the effect of ozone exposure was most pronounced on the decrease in FL1 intensity emitted from older *A. fumigatus* spores following their exposure to 600 ppb-hr; this was accompanied by a significant decrease in particles with FL3 fluorescence above the detection limit.

To qualify significant differences in fluoresce intensity responses, the EOD and magnitude of peak frequency (the location of lightest region on the respective histograms) were adjusted to remove the influence of fluorescence from cellular fragments or cellular clusters. The density of the resulting adjusted volumes, compiled from intensity maxima in each channel, and the intensity distribution across the EOD range, could be assigned a mean and two dimensional variance with a multivariate Gaussian fit of lognormal transformed data. An example of this approach, as applied to all ozone exposure experiments, is shown in Figure 3-12 where *A. fumigatus* exposed to 7500 ppb-hr ozone at 85% RH.

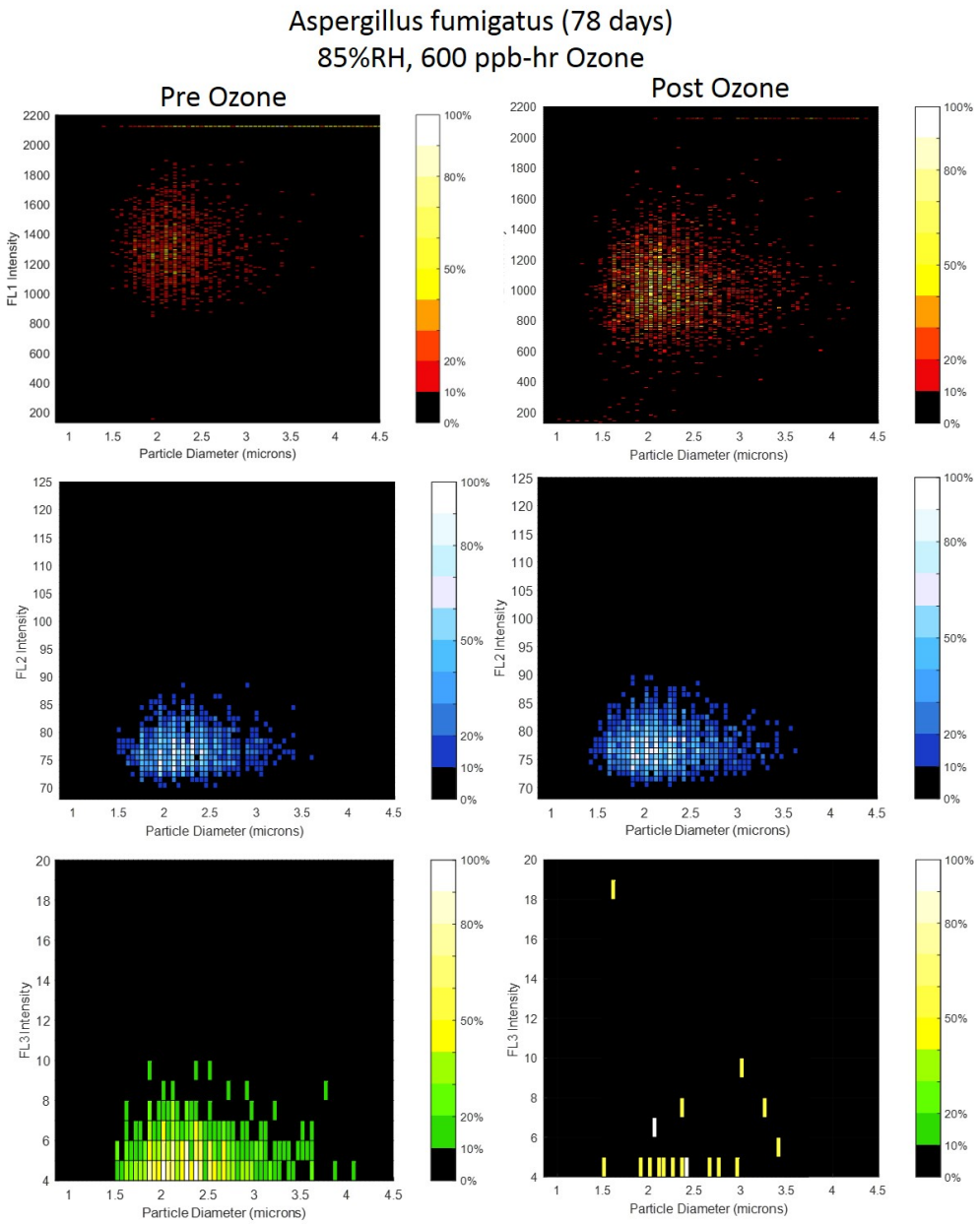

Figure 3-11. Heat maps of fluorescence intensity from an individual experiment is shown across the EOD range observed for aerosolized *Aspergillus fumigatus* spores (78 days old) prior to ozone exposure (**left panels**); and, following 600 ppb O_3- hr exposure (**right panels**). FL1 response is represented by the red-based heat map (**top panels**), FL2 by the blue-based heat map (**central panels**); and, FL3 response represented by green-based heat map (**bottom panels**). The color scales on the respective heat maps are apportioned to their maximum intensity frequency where darker shades correspond to lesser frequency, and lighter shades correspond to increasing frequency.

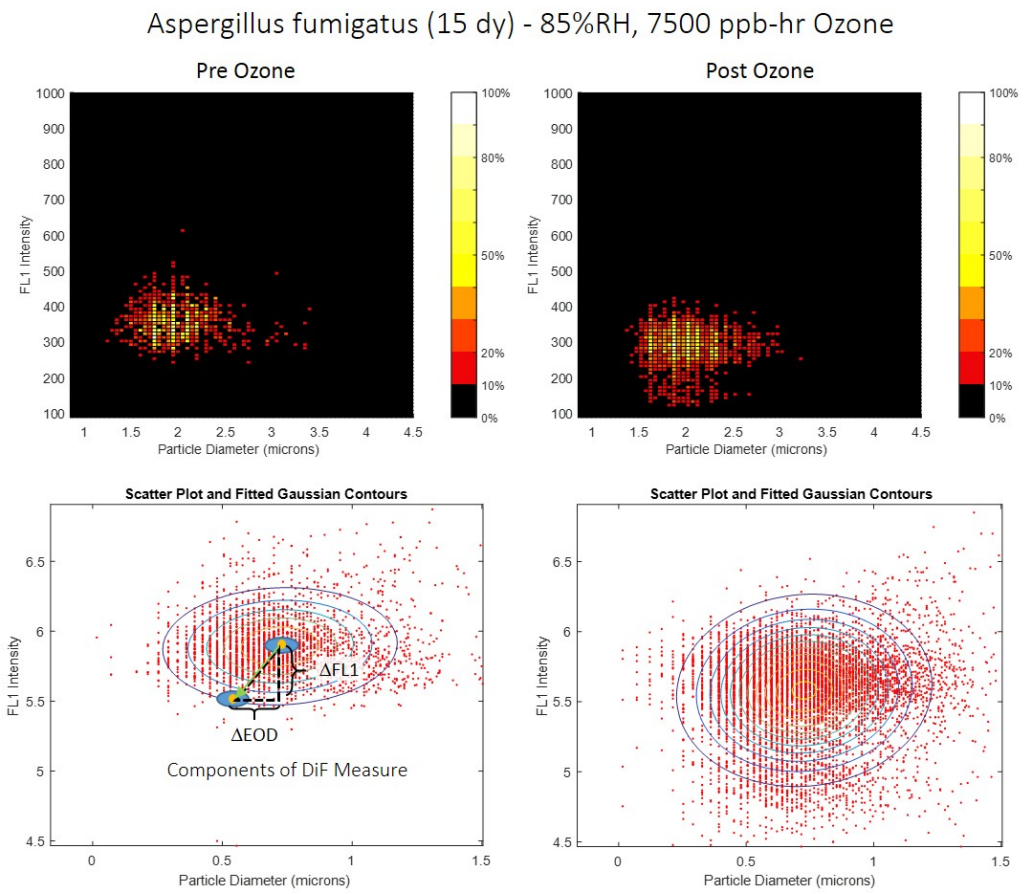

Figure 3-12. Frequency heat maps (**top**) and Gaussian contour maps of log-normal data (**bottom**) of fluorescence intensity and EOD prior to ozone exposure (**left**), and following the 7500 ppb– hr ozone exposure of airborne *Aspergillus fumigatus* spores (15 days old) (**right**). The vector components used to calculate the the DiF Measure are indicated in the lower left plot.

Changes in fluorescence intensity considering both EOD decrease with time and ozone exposure are accounted for by a normalizing Euclidian distance expressed the DiF Measure by the change in EOD with time. Figure 3-13 illustrates different ozone exposure scenarios of *A. fumigatus* presenting changes in mean FL1 fluorescence intensity (at 85%RH, measured at low gain) and EOD for ozone exposures of 0 ppb-hr, 1000ppb-hr, 1200ppb-hr, and 7500ppb-hr. The effect of decreasing EOD on FL1 intensity is accounted for by the DiF Measure, where

increasing DiF values indicate the increasing influence of ozone on FL1. The values of the DiF Measure are relative, and can serve useful only where comparison of similar bioaerosol physiology are the goal. Decreases in mean FL1 intensity were associated with increases in ozone exposure, as expressed by larger DiF values relative to baseline conditions.

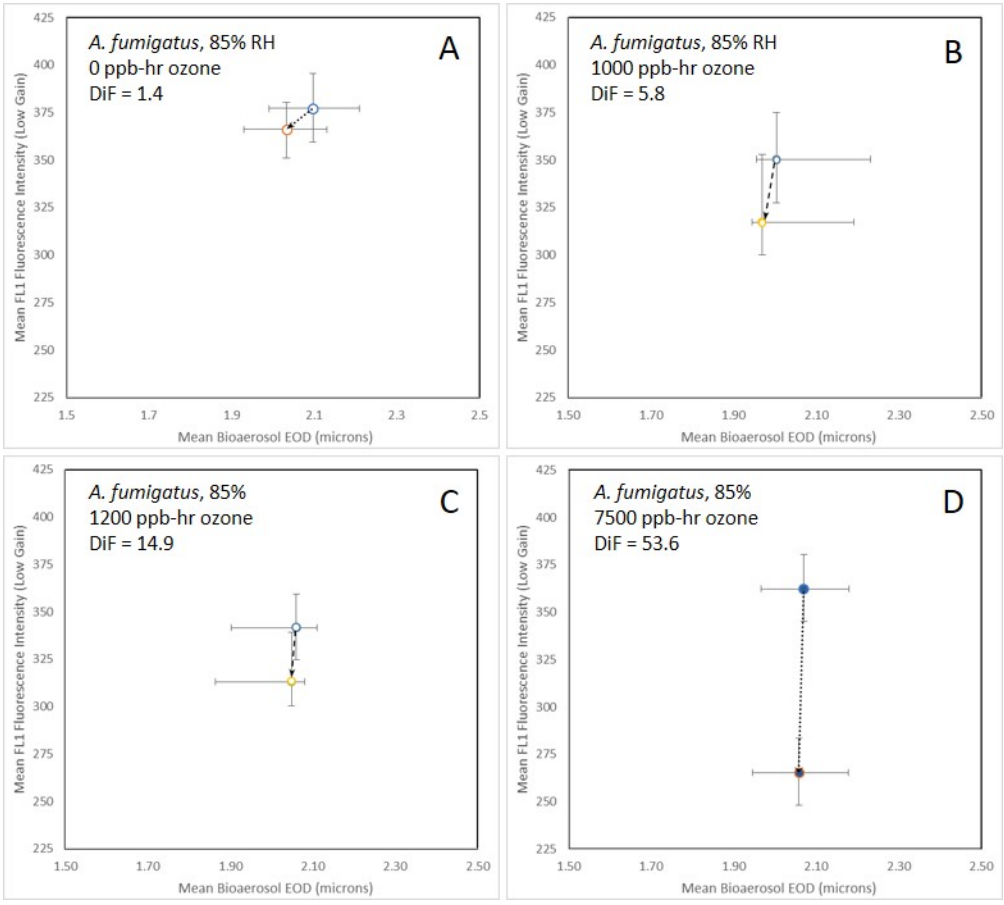

Figure 3-13. Means of peak fluorescence intensity across the EOD ranges tested, prior to and following ozone exposure of *A. fumigatus* spores at 85%RH. Expressed as normalized vectors (---->), the magnitude of the DiF Measure indicates significant shifts in size-normalized mean fluorescence intensity considering the variance of each exposure scenario: (**A**) control, no ozone exposure; (**B**)1000 ppb-hr; (**C**) 1200 ppb-hr, and (**D**) 7500ppb-hr.

FL1 fluorescence intensity is specific to species and pWIBS detector gain. However, this DiF measure provides a systematic basis for intra-experimental comparisons to isolate the potential for ozone (or any other physical or chemical challenge) to modify fluorescence properties. With increasing ozone exposures (0, 1000, 1200, 7500 ppb-hr) to otherwise identical airborne *A. fumigatus* spores (Figure 3-13) the DiF values were 1.4, 5.8, 14.9 and 53.8, respectively. A more complete overview of other case comparisons of Mean FL1 and DiF Measures are outlined in Table 3-6. This analytical approach was applied to each pure culture *A. fumigatus, A. versicolor*, and *B. subtilis*, and noting the culture age for each ozone exposure scenario at each RH condition tested.

Table 3-6. Multivariate Gaussian mean size, FL1 location and DiF Measures for various bioaerosol and exposure conditions

Culture	Culture Age (Days)	RH(%)	Ozone (ppb-hr)	Gain	EOD Mean	FL1 Mean	Dif Measure
A. versicolor	39	85	0	High	2.34	429	1.1
A. versicolor	39	85	600	High	2.30	426	
A. versicolor	38	85	0	High	2.43	429	1.3
A. versicolor	38	85	0	High	2.21	397	
A. versicolor	36	30	0	High	2.41	499	1.2
A. versicolor	36	30	600	High	2.15	460	
A. versicolor	35	30	0	High	2.31	451	1.3
A. versicolor	35	30	0	High	2.15	482	
A. fumigatus	78	85	0	High	2.40	1322	5.0
A. fumigatus	78	85	600	High	2.26	981	
A. fumigatus	28	85	0	High	2.10	1297	4.1
A. fumigatus	28	85	600	High	2.04	1156	
A. fumigatus	11	85	0	High	2.10	1364	3.2
A. fumigatus	11	85	600	High	2.00	1179	
A. fumigatus	15	85	0	Low	2.10	377	1.4
A. fumigatus	15	85	0	Low	2.03	366	
A. fumigatus	18	85	0	Low	2.00	350	5.8
A. fumigatus	18	85	1000	Low	1.97	317	
A. fumigatus	15	85	0	Low	2.06	342	14.9
A. fumigatus	15	85	1200	Low	2.05	313	
A. fumigatus	15	85	0	Low	2.07	362	53.6
A. fumigatus	15	85	7500	Low	2.06	265	
B. subtilis	14	85	0	High	1.00	162	1.0
B. subtilis	14	85	600	High	0.87	160	
B. subtilis	14	85	0	High	0.96	176	1.0
B. subtilis	14	85	0	High	0.78	175	

3.5. Discussion

A limited, but increasing number of studies are attempting to characterize the impact environmental conditions on bioaerosol fluorescence including, but not limited to, ozone. Bioaerosols can travel vast distances and encounter a broad range of oxidative atmospheric environments during their atmospheric transport. Therefore, characterizing the potential these environments have on real-time bioaerosol fluorescence may aid in efforts utilizing fluorescence measurement techniques for bioaerosol characterization and discrimination, and further improve the current understanding on the impact of air pollutants on bioaerosols in our environment. The ozone levels selected for these studies were based on the USA EPA National Ambient Air Quality Standards for ozone of 70 ppb given an 8 hour exposure horizon, recognizing this is an average threshold and that ozone levels vary widely. This research employed the Ct concept which is widely used in disinfection studies, to control and quantify ozone exposure. Here ozone exposure is defined as the integrated ozone concentration (ppb) over the bioaerosol contact time with ozone (hours), resulting in ozone exposure expressed in ppb-hrs. An ozone exposure of 600 ppb-hr is reflective of the EPA standard outlined above. Higher ozone exposures were also evaluated in these experiments (1000 ppb-hr, 1200 ppb-hr and 7500ppb-hr) and reflect exposure conditions during multi-day transport conditions experienced by bioaerosols in the lower atmosphere during summer months.

In order to determine the impact of the ozone exposure on bioaerosol fluorescence, an average optical diameter (EOD) of the bioaerosol population during these measurements was systematically accounted for, as measured fluorescence intensity has been noted to be

proportional to particle diameter [37, 47, 53]. Methods for assessing the relationships between fluorescence intensity and bioaerosol size in this work will be discussed. In general, changes in size (EOD) distributions over time frames these experiments were not substantial, and in most cases not significant, as illustrated in Figure 3-3and Figure 3-4, and evaluated with the KS statistic.

The largest changes in bioaerosol EOD distributions over the duration of 3 to 4 hours of suspension time were encountered at lower RH conditions (20% < RH < 30%). This decrease in EOD under the lower RH conditions observed was likely due to desiccation, where this would be less likely to occur at high RH. Though spores walls are considered rigid, like many dense structural proteins they are susceptible to changes in water sorption potential that dictate the hydration of these biopolymers. Not all bioaerosol (spore) response to changing RH conditions are the same, and have been suggested to be species and age dependent. In some cases humidity has been to shown to have a negligible effect on cell size on the time frame of hours (e.g. *Mycobacteria spp.*) [23], while others report a notable effect on bioaerosol size under similar time frames [16, 54].

Though particle fluorescence has been reported to be proportional to particle size, this relationship seems to be inconsistent with some bioaerosol including those observed here. A number of attempts have been made to model particle fluorescence intensity as a function of particle size with varying levels of success where compared to polystyrene latex spheres (PSLs) [47]; some report linear dependence of fluorescence intensity on the size of vegetative bacterial cells [53], while others report an exponential dependence of fluorescence intensity of various PSLs and bioaerosols [37]. What is clear from this and other studies is that modeling

fluorescence intensity using only one characteristic dimension of fungal spores, bacterial spores or vegetative cells cannot be applied across the diversity of whole cell bioaerosols, and certainly not to their fragments or clusters. Indeed no microbe is perfectly spherical and was confirmed by inspection with SEM in this and other studies. Indeed bioaerosol intrinsic fluorescence is dependent not only on geometry, but also the type and composition of their biochemical fluorophores.

In attempting to normalize fluorescence intensity measured in this work by the optical diameter, it became clear that this characteristic dimension may not be appropriate for every exposure condition tested (ultimately relating to environmental conditions). A select number of cases were fit with liner and exponential relationships, resulting in variable results between chamber runs (comparing initial results), and between exposure conditions for the same bioaerosol type. Understandably, attempts have been made to normalize bioaerosol fluorescence by some relationship with diameter; however, these types of normalization approaches incorporate a constant derived from an ideal case or condition, which is extrapolated to conditions which render these relationships poorly predictive [14, 16, 51]. Normalizing the bioaerosol fluorescence by any constant that has the potential to vary unpredictably with environmental conditions and species, may not be appropriate for most bioaerosol cases given the morphological diversity of the microbial world. In response to these limitations, bulk (population) fluorescence characterization, required size gating based on the location of a log-normal maxima; this gating was applied between 3σ of the mean particle size (EOD) distributions.

A small, but growing number of studies are demonstrating the utility of individual particle interrogation and bioaerosol fluorescent as a method for characterizing and identifying types of bioaerosols based on their fluorescence profiles [31, 40, 41]. The three fluorescence detection channels used in this work, overlap with the fluorescence of tryptophan (FL1/Channel A), sporopollenin or chitin (FL2/Channel B), and selected metabolites, vitamins, and electron carriers (e.g. flavins) (FL3/Channel C). Changes in bioaerosol detection sensitivity by combinations of responses from these respective fluorescence channels had yet to be investigated until now, particularly in respect to oxidation potential. This work presented evidence for the discrimination between bioaerosol types, challenged with zone, from the differences in the percentage of total particles found in each fluorescence channel. At both high and low RH, the majority of *Aspergillus* spores from both species were detected in FL1, suggesting a fairly uniform presence of protein-like compounds on the spore walls. However, further investigation of the fluorescence intensity distributions between the species yielded a lower mean intensity for *A.versicolor* than for *A. fumigatus*, either an indicator of the presentation or concentration of this or other similarly behaving fluorophore on the spore surface. Half the number of *A.versicolor* spores were detected in the FL2 channel when compared to it close microbial relative, *A. fumigatus*, probably due to more variability in the presence or presentation of their common fluorophore (if in fact it is common).

Humidity had an inverse effect on the number of spores detected in FL3 for both *Aspergillus* species observed, where high RH decreased the percentage of spores detected in FL3 for *A. versicolor* and increased the percentage in FL3 for *A. fumigatus*. Ozone exposure effects were minimal on these distributions, but seem to play a role in slightly decreasing the percentage

of total particles detected in FL1. *Bacillus subtilis* spores did not respond with significant shifts in fluorescence channel distributions when exposed to ozone under these conditions, but this observation was complicated by the fact that there were relatively large fractions of non-fluorescent particles present during these ozone challenge studies (probably from nebulized PBS in which B. subtilis was aerosolized). In relative order, the larger factors in influencing changes in fluorescence contribution from any individual channel, or combination thereof was bioaerosol type; this followed by relative humidity; followed by ozone exposure.

The literature in this arena is new and tenuous. The difficulty in comparing fluorescence responses to ozone exposure of the bioaerosols tested here, to those reported in the literature, is that many (if not all) of those reports include data which are normalized by some function of cellular or spore diameter. Bioaerosol size and fluorescence data in this work was also modeled with exponential functions under these conditions to compare responses prior to, and following ozone exposure. In most cases any constants used to describe this relationship decreased with ozone exposure, and resulted in very different results where any characteristic length (diameter) was used for normalization—in some cases dramatically increasing the normalized fluorescence intensity with ozone exposure. To avoid the limitations of the approach, two dimensional histograms (heat plots) were constructed to track the changes in fluorescence at different bioaerosol sizes, as judged by EOD. Data was analyzed to track the maximum occurrence of fluorescence intensity and its corresponding sizes; data from these plots were analyzed both to isolate the spread from the bottom quartile of the max intensity frequency (i.e. corresponding to the peak or hot region), and data was log normally transformed and analyzed with multivariate Gaussian distributions to incorporate the maximum density of the data adjusted to minimize the

influence of kurtosis. By analyzing data both ways, the changes in the most frequent intensity occurrences was tracked, as well as how the rest of the bioaerosol population behaves with response to ozone exposure. A normalized Euclidian distance was developed as a size sensitive metric (DiF) to track changes in the densest regions (mean) of the sample population fluorescence in response to ozone exposure, but specifically to indicate whether the components of fluorescence changes were more or less influenced by bioaerosol diameter or by the impacts of ozone. When comparing similar experiments (i.e. bioaerosol type and detector gain) with the Dif Measure, higher values indicate changes in mean fluorescence intensity are more influenced by environmental conditions than by diameter. With *A. fumigatus* spores, accounts of progressively increasing DiF values corresponded with increasing ozone exposures, indicating a primary effect of ozone interacting with spores to decreasing fluorescence intensity independent of their size.

Greater decreases in fluorescence intensity have been noted with ozone exposures at higher RH conditions [14, 16], as well as changes in allergenic content and gross protein content (water soluble or solvent extractable). The influence of RH on biochemical activities (enzymatic activity, as well as allergen and protein content) was also suggested by the data resulting from this work and is discussed in detail in Chapter 6

Humidity had no consistent effect on fluorescence properties. At higher RH, more water can and sorbed or otherwise associates with the biopolymers present on and in bioaerosols—in some cases introducing elasticity in the biopolymers present (i.e decreasing viscosity noted with protein), and increasing the potential for oxidant diffusivity. Shiraiwa et al. [55] demonstrated diffusion –limited ozone uptake by a model of amorphous, semisolid protein, where a steep

ozone concentration gradient occurred near the surface, assuming reactions with select amino acids occurred. They noted with increasing RH, an extended ozone uptake into the bulk protein matrix, where it was assumed additional amino acid oxidation could occur. Whether this type of selective heterogeneous diffusive can be extended to the behavior of bioaerosols used in this work, could not be determined, but this theory is not consistent with the RH responses observed here. Changes in surface composition most like explain the variable responses of RH on the extent of fluorescence (and biochemical changes) seen in different types of bioaerosols.

CHAPTER 4. **BIOAEROSOL EXCITATION EMISSION MATRICES**

4.1. Introduction

This chapter will detail the results from experiments that challenge *Hypothesis Ib,* as it pertains to *Hypothesis I*, previously presented in Chapter 1:

> ***Hypothesis I.*** *Oxidative aging processes, associated with ozone exposure at different RH levels, can significantly change the intrinsic fluorescence spectra of pure cultures of whole-cell bioaerosol models.*
>
> ***Hypothesis Ib.*** *Compared to their fresh counterparts, changes in intrinsic fluorescence properties of water soluble organic carbon liberated from aged bioaerosols, or those exposed to ozone, can be determined from analyses of excitation-emission matrices.*

For context, a brief overview of relevant literature pertaining to fluorescence characterization of water soluble bioaerosol components is outlined below, and details of the experimental methods, results and discussion are presented in subsequent sections. For bioaerosol culture, aerosolization, and enumeration techniques, refer to Chapter 2.

4.1.1. Microbial Characterization by Excitation-Emission Matrices (EEMs)

Characterization of the water soluble organic carbon (WSOC) fraction of airborne PM has been receiving increased attention in broad atmospheric contexts due to its the potential impact on climate (cloud nucleation and radiative balance) [56], visibility [57], and public health

[58]. Recent reports suggest that the WSOC portion atmospheric PM can range between 20-70% of the total carbon content [1]; however, the literature suggests that much of the organic compounds present in this water soluble fraction have yet to be resolved [59]. A limited, but growing body of work has focused on the fluorescence properties of aerosol WSOC as a means to characterize sources of, and contributions to, the total aerosol load [17, 18, 59, 60]. Many primary and secondary organic aerosols from biological, terrestrial, and anthropogenic sources contain a number of fluorophores in the water soluble fraction that can be characterized by three dimensional fluorescence excitation-emission matrices (EEMs). Each peak appearing on the EEMs defines a fluorescence intensity volume that corresponds to a given region of excitation and emission wavelengths characteristic a known fluorophore or combination of fluorophores. EEMs have been widely utilized for characterizing dissolved organic matter in the context of drinking water treatment and pollution control, but are now also emerging as a characterization tool for aerosol studies [17, 18, 61, 62]. The sensitivity of EEMs allow compounds present in WSOC to be characterized in a way that could otherwise be missed by classical methods for analyzing the bulk total organic carbon (OC) and WSOC content, refer to Chapter 6 for an environmental application of this approach as it applies wildfire aerosol characterization.

A number of spectroscopic indices have been developed to characterize the sources and nature of fluorophores present in the complex heterogeneous mixtures of aquatic dissolved organic matter (DOM) as captured and described by EEMs [63]. Previously developed indices implemented through this work as it relates to bioaerosol fluorescence include the following: (i) specific UV absorbance at 254nm (SUVA 254 - indication of aromaticity [64]); (ii) the fluorescence index (FI), indication of aromaticity [19]); (iii) the humification index (HIX –

contribution of humic-like compounds [65]); (iv) the freshness index (FRI – indication of freshly produced microbial products [66]), and (v) comparisons of whole protein fluorescence, with respect to the region corresponding to tryptophan (P/Po) [67]; and (vi) Tyr/P – indicates changes in the nature of protein fluorescence with oxidation. An example EEM adapted from Gabor et al. 2014 [63], Figure 4-1, indicates and summarizes the fluorescence regions used to calculate the indices described above. The boundaries of the excitation and emission regions described above, will be numerically defined in the Methods section.

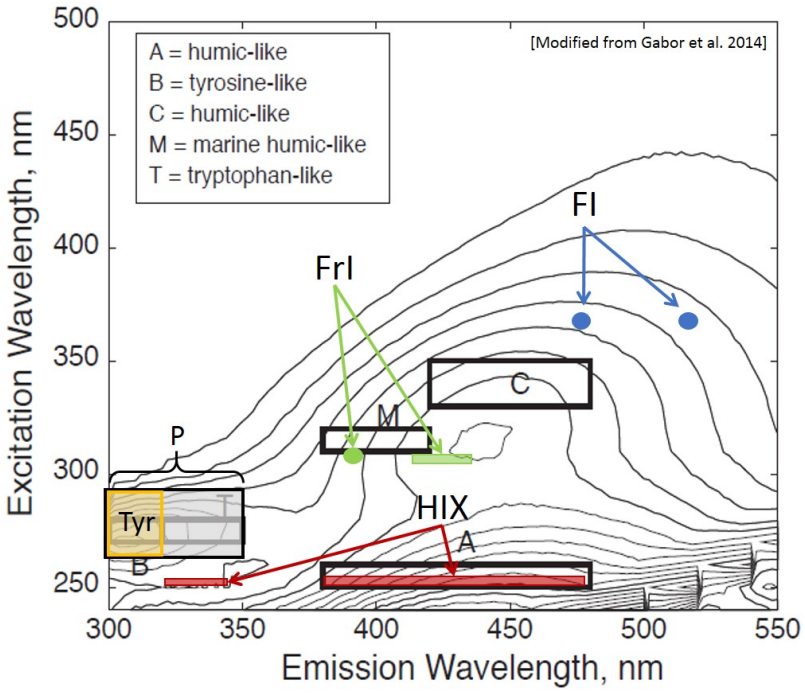

Figure 4-1. Boundaries of regions within EEMs, used to define analytical indices or otherwise identified with known fluorophores, as adapted from Gabor et al. 2014. Protein fluorescence regions and associated blue shifted region often associated with oxidized protein are indicated by 'P' and 'Tyr' respectively. The humification index 'HIX', the freshness index 'FrI', and the fluorescence index 'FI' are identified on the EEM.

Previous work leveraging EEM analysis for aerosol studies have highlighted a number of fluorophores, postulated to be similar to those found in water and soil research, including terrestrial and marine humic-like substances and protein-like fluorophores [17, 18, 59-61]. Along with terrestrial and biogenic-sourced organic fluorophores, the atmospheric environment also contains anthropogenic fluorescent compounds that can appear in the same EEM regions associated with terrestrial and microbially produced organic matter [18, 48, 62]. Mladenov et al. [18] demonstrated that EEMs from diesel exhaust exhibit potential interference in regions of EEMs associated with protein-like peaks. Pohlker et al. [48] cited fluorescent properties of naphthalene, a petroleum derived polyaromatic hydrocarbon used in fumigation, can overlap with the marine derived humic-like region in EEMs. To account for these potential anthropogenic interferences, a study utilizing EEMs analysis to characterize aerosols collected in the Canadian Arctic compared protein-like fluorescence with concurrent measurements of elevated pollen and fungal tracers (mannitol and sucrose, respectively) and decreased PAH levels to demonstrate the presence of long-range transported bioaerosols during late spring [59]. More recently, bioaerosols have been show to transport vast distances, while encountering a number of oxidating environments in the atmosphere [1]. In an effort to resolve oxidative effects on biogenic aerosols, Lee et al. [62] conducted controlled laboratory studies of O_3 and OH aged biogenic secondary organic aerosols (SOA), and demonstrated significant overlap in terrestrial and marine humic-like regions in EEM profiles; further pointing out potential interference in excitation-emission channels used in real-time fluorescence detection of bioaerosols.

Table 4-1, adapted from Pohlker et al. [48], outlines the fluorescent properties of a number of common fluorophores present in bioaerosols.

Table 4-1. Summary of relevant fungal spore fluorophores reported for bioaerosol detection

Bioaerosol Fluorophore	**Function/Remarks (level of fluorescence detection)**	**Excitation Wavelength (nm)**	**Emission Wavelength (nm)**
Tryptophan (Trp)	Amino acid, responsible for ~90% of signal from native proteins (high)	280 – 295	340 - 353
Tyrosine (Tyr)	Amino acid, responsible for ~10% of signal from native proteins (medium)	280	300 - 304
Flavins (riboflavin and FMN)	Coenzymatic redox carrier and photoreceptor, indicator for cell metabolism (high)	280, 373, 450-488	520-560
Vitamin D compounds (ergosterol)	UV-protective fungal cell wall component (medium)	290 -360	360 - 460
Lignin	Fungal cell wall component (medium)	240-320, 331-345	470-510, 419-458
Chitin	Fungal cell wall component (high)	254, 335, 373	413, 452 - 458
Sporopollenin	Pollen and fungal cell wall component (high)	300-550	400-650
Carotenoids	Accessory pigment in photosynthesis and UV protection (high)	400-500	520-560
Phenolics	Defense agent in fungi (medium-high)	300-380	400-500
Terpenoids	Pigment, toxins (medium)	250 - 395	400-725

EEMs have been extensively used for characterizing fluorescence properties of natural organic matter in aqueous systems [19, 20], and have demonstrated that oxidation processes can influence the fluorescence characteristics of dissolved natural organic matter (DOM) [21, 67]. Ozone disinfection processes for water treatment have initiated numerous studies on the impact oxidation processes on different microorganisms in water systems [22]. Zhang et al. [21] demonstrated an enhancement of fluorescence intensity in the EEM regions associated with proteinaceous materials and a decrease in a number of humic-like fluorescent regions after ozonation of dissolved organic matter. Increases in protein-like fluorophores were reportedly

associated with the breakdown of large proteinaceous material during ozonation, thus increasing the amount of smaller protein molecules with exposed fluorescent amino acid residues. The reduction of fluorescence intensity in the humic-like regions were cited to result from significant decreases in the aromaticity and molecular weight of humic-like structures that occurr from the destruction of highly polycyclic aromatic structures by ozone.

After ozonating water containing *Escherichia coli* with a 30 minute exposure of 600ppm ozone, Komanapalli et al. [68] reported an increase in total protein liberation, with a corresponding 75% reduction of bacterially associated protein fluorescence. The increase in aqueous protein content was attributed to the release of intracellular material, while the decrease in the total protein-like fluorescence intensity was posited as tryptophan oxidation. Korak et al. 2015 [67] oxidized intracellular organic material from cyanobacteria isolates with 80ppm ozone in water for 30 minutes and found decreases in protein fluorescence with oxidation and increases in fluorescence index (suggesting a decrease in aromaticity) [67]. It should be noted that the later cited oxidation study was conducted directly on intracellular material present as dissolved organic matter and not the whole microbial cells themselves, probably explaining the differences reported between studies examining protein-like fluorescence with ozone exposure.

These studies provide valuable insight on how ozone oxidation can influence the fluorescence properties of biogenic secondary organic aerosols, as well as natural organic matter and microorganisms in aqueous systems. Optical methods for characterizing changes in primary bioaerosol WSOC fluorescence as a result of atmospheric processing will be extended from the aqueous environment to the bioaerosol environment using traditionally defined spectroscopic measures, as well as some novel approaches. Though a few aerosol studies have successfully

demonstrated how EEMs analysis can be used for describing primary biological materials, biopolymer modification during controlled atmospheric oxidation studies have yet to be characterized using EEMs. Fluorescence profiles of bioaerosol derived WSOC will be presented here to describe the response of aerosolized *Aspergillus* spores at different RH levels to the presence and absence of ozone.

4.2. Chapter Specific Methods and Materials

4.2.1. Overview of Aerosol Sample Collection and Processing

To control the potential for culture age dependent variations on spore fluorescence [45], ozone exposure studies were conducted with fungal cultures of similar maturity (<5 days apart). Specific *Aspergillus fumigatus* and *Aspergillus versicolor* culture techniques are outlined in Chapter 2. Fungal cultures were grown in sterile glass jars fit with stainless steel lids specifically designed for HEPA filtered air to pass over the culture in one port, and carry air-entrained spores out the other port and into the well mixed chamber. Sterile borosilicate glass impingers (SKC Biosamplers) were filled with 20 ml cold sterile filtered DI water for sample collection at 12.5 lpm for 15 minutes. Sequential replicate samples were taken for each exposure condition per chamber experiment.

4.2.2. Quantification and Characterization of WSOC and Characterization

Characterization of WSOC and its fluorescence properties was conducted both on whole spore extract and lysed spore extracts for aerosolized spore samples and spores harvested directly from their source fungal cultures. Aliquots of each sample were also retained for spore enumeration using a widely accepted hemocytometer method for counting cells with phase-contrast microscopy at 40X magnification. Aqueous extracts of collected impinger samples were produced using an established glass bead beating cell lysis method [69]. Briefly, 1.7 ml of well mixed impinger samples were added to 2ml sterile polypropylene screw cap tubes containing 0.3g of 100 μm (diameter) and 0.1g 500μm borosilicate glass beads (previously baked at 550°C) [70] and lysed by bead beating (BioSpec Mini-Beadbeater) for 30 seconds at 2500rpm. Whole spore samples (WSOC eluted from the spore wall) were also taken from the impingers and centrifuged at 4°C for 2 minutes at 10,000g to ensure cellular material was removed from the bulk liquid sample. All lysed and whole spore samples were centrifuged for 2 minutes at 4C at 10,000g to remove spore debris. Spore lysate and whole spore extracts were stored at -20°C (for consistency) until thawed in preparation for WSOC and fluorescence measurements.

Water soluble organic carbon (WSOC) content was determined from the aqueous extracts using a Sievers Laboratory TOC Analyzer (Model 5310 GE), with accuracy of +/- 0.5 ppb TOC. The relatively low WSOC (TOC) levels in the samples (<1ppm) required instrument settings to include 2.0 ml/min acid and 0.7 ml/min of oxidizer. All samples were diluted with sterile DI water to a final volume of 20 ml and measured in sterile glass vials. Water blanks were measured every fourth sample to flush the instrument and ensure accuracy of the readings. Bead-beated water blanks were read in triplicate to establish background WSOC content for each sample.

Fluorescence spectra of the aqueous extracts were measured using a Fluoromax-4 spectrofluorometer (Horiba), where the emission intensity was measured in 2 nm wavelength increments between 300nm and 550nm, in response to excitation in 10nm increments in the range between 240nm and 500nm. The excitation and emission ranges were selected based on the F4 instrument specific limitations of the upper and lower ranges of light emitted from the xenon lamp and capabilities of the detecting photomultiplier tubes. The bandpass was 5 nm for both excitation and emission monochromators, with a 0.25 second integration time. Prior to fluorescence measurements, UV-Vis absorption spectra were measured between 200nm and 800nm for all samples, where the optical density (OD) at 254nm was less than 0.1, ensuring a dilute enough sample for accurate fluorescence readings. The EEMs were constructed and adjusted with MATLAB software (MathWorks). Instrument and inner-filter corrections, as well as Raman normalization and bead beated blank subtractions, were applied to all EEMs [18]. It should be noted that the sample bead beating process liberated some background WSOC, which was accounted for, and blank subtracted where appropriate. Normalization of fluorescence signal by the Raman area of sterile filtered MiliQ water excited at 350nm allowed for comparison of specific fluorescence between samples, reported as Raman Units (RU) [71]. All EEM spectra were smoothed with standard splines, and had their primary and secondary scattering removed, where the spectra in those regions were interpolated for presentation (i.e. interpolated areas were not included in the index calculations). Corrected and normalized EEMs are presented in Raman Units per microgram WSOC (RU/μg WSOC).

Fluorescence characterization of dissolved organic matter present in aquatic systems has been widely conducted with EEMs in the context of source apportionment and water quality

[20]. It has become clear that oxidation processes can influence fluorescence properties of dissolved organic matter [21, 67]. To assess changes in fluorescence profiles between samples of freshly aerosolized spores and aerosolized spores in the presence or absence of ozone (suspended for 3 hours), regions affiliated with protein fluorescence were integrated to determine peak volumes, and a number of previously adopted indices were utilized to compare the ratios of protein peak regions, as well as other noted fluorophores associated with fungi [48]. The following table outlines the indices and regions that were examined for changes with respect to ozone oxidation. Some fluorescence indices (i.e. HIX, FRI (BIX), FI and SUVA 254) have traditionally been applied to water samples from aqueous environments influenced by both terrestrial and microbial sources. Here, these indices have been shown to be a useful tool in characterizing airborne microbial oxidation and their water soluble fluorescence components. Additionally, these results show the extent that airborne microbial oxidation can influence regions associated with these indices.

Table 4-2. Overview of EEM indices and their fluorescence regions

Index	Indication/ Use in This Work	Excitation-Emission Ranges	Reference Studies
SUVA 254	Aromaticity, greater SUVA, greater degree of aromaticity	Absorbance at 254nm	Westerhoff 1999 [72]
Fluorescence Index (FI)	Aromaticity/organic matter source – FI closer to 1.2 - higher aromaticity/terrestrial source; FI close to 1.8 lower – lower aromaticity /microbial source	(Em:470 nm @ Ex:370 nm) / (Em: 520 nm @ Ex: 370 nm)	Cory 2010 [73]
Humification Index (HIX)	Here, an indication of extent fungal cell components contribute to humic-like region with respect to smaller microbial products	(Em:435-480 nm @ Ex:254 nm) / (Em: 330-345 nm @ Ex: 370 nm)	Zsolnay 1999[65]

Tyr/P	Fraction of tyrosine-like fluorescent volume of total protein region fluorescence	(Em:300-320nm @ Ex:260-290nm) / (Em: 300-350nm @ Ex:260-290nm)	Adapted from reported protein regions [67]
P:Po	Percent volume change in protein-like peak region after exposure	(Em:300-350nm @ Ex:260-290nm) / (Em: 300-350nm @ Ex:260-290nm)	Korak et al. 2015[67]

The 'Tyr/P' index was developed here to track the blue shift in the protein-like fluorescence region encountered after aerosolization and gas phase ozone oxidation. This protein-like peak blue-shifting was encountered in aerosolized spores from both *Aspergillus* species used in these studies, but not in their freshly cultured counterparts (where tryptophan-like fluorescence dominated). The humification index (HIX) assesses the degree of humification of natural organic matter by comparing the fluorescence region of higher weight humic-like compounds (typically associated with terrestrial sources) to those of a lower weight compounds (originally associated with intracellular material) [65]. The greater the HIX value, the greater contribution to the longer wavelength region, thus the degree of humification (i.e. increased polycondensation/lower H:C ratios). The freshness index (more commonly known as BIX, but referred to here as 'FrI') traditionally indicates a measure of freshly produced microbial dissolved organic matter compared with aged or marine humic-like substances found in aqueous environments [66].

The fluorescence index (FI) was developed as an indication of organic matter origin in certain water systems and an indication of aromaticity [19, 73]. Fulvic acids derived from microbially dominated aqueous environments display a narrow fluorescence peak between 450nm and 520nm, when excited at 370nm, yielding higher FI values (1.7 - 2.0) than the broader

peak displayed by terrestrially derived fulvic acids (FI values 1.3 – 1.4). In this context, FI also has been reported as an indication of aromaticity, where microbially-derived fulvic acids contain less of an aromatic carbon (12%-17%) content than terrestrially-derived fulvic acids (25%-30%)[19]. It follows that microbially-derived fulvic acid absorb less UV and visible light than its more aromatic terrestrial counterparts. In addition to FI for a qualitative assessment of aromaticity, lower specific UV absorption at 254nm (SUVA 254) is also presented [64]. Results from changes in EEM peak fluorescence regions and indices will be outlined and discussed below.

4.3. Results

4.3.1. Bioaerosol EEMs

All fluorescence intensities (reported as Raman Units, RU) in the EEMs presented here, and their associated absorbance data, were normalized by their respective sample WSOC (μg/ml) content in order to compare fluorescence intensity characteristics across species and experimental conditions. The WSOC content increased per aerosolized spore in response to suspension time during ozone exposure as well as ozone free aerosol aging conditions. It should be noted that visual inspection of collected spore samples via SEM images and phase contrast microscope enumeration indicated that the spores remained intact over the course of the chamber experiments, even in the presence of ozone, so increases in WSOC per spore are likely from changes to the spore coat. These results will be discussed in more detail in Chapter 5 as they

relate to water soluble protein and allergen content; however, Figure 4-2 is shown here to illustrate the increase in liberated WSOC content over the *Aspergillus versicolor* spore remain in an aerosol phase.

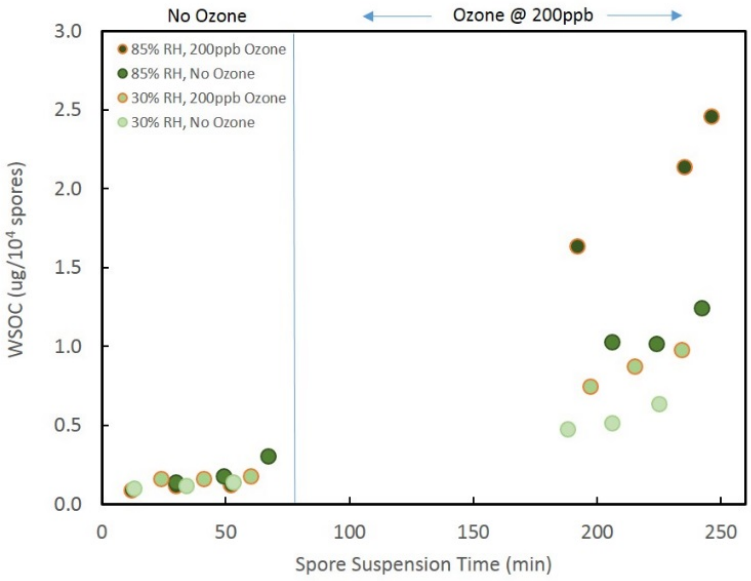

Figure 4-2. Water soluble organic carbon content of aerosolized *A. versicolor* spore lysates measured in sequential replicate before and during ozone exposure, or aerosol aging under otherwise identical conditions in the absence of ozone. Where exposed, ozone was introduced after 70 minutes of aerosol suspension time. Low RH conditions are represented by light green circles (●); high RH conditions are represented by dark green (●) circles. Exposure to 200 ppb ozone is denoted by an orange ring around the symbol (**O**).

High RH (85%) and 600ppb-hr ozone exposure (200ppb ozone for 3 hours) conditions had the greatest impact on increasing the WSOC content of these spores during their suspension time. Even small increases in WSOC content were realized at low RH during relatively short suspension times with no ozone present. The absorbance spectra of each WSOC sample was measured to ensure the samples were dilute enough to measure fluorescence, and to determine the $SUVA_{254}$ values. Figure 4-3 illustrates the difference (decrease) in WSOC normalized

absorbance before and after airborne *A. versicolor* spore ozone exposure (600ppb-hr) at 85%RH.

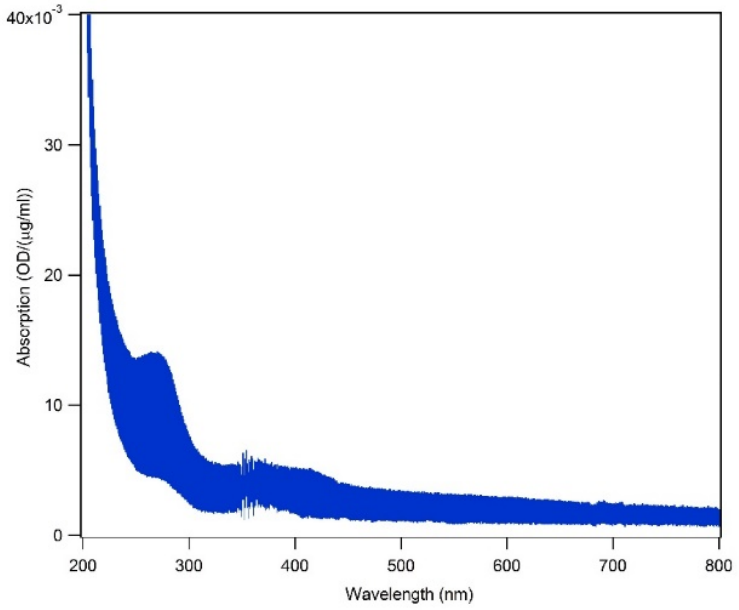

Figure 4-3. Differences in absorption spectra for WSOC extracts of lysed aerosolized *A. versicolor* spores are displayed in the blue area region, where the top outline corresponds to the pre ozone WSOC absorption spectra, and the bottom outline is the post-ozone (600 ppb-hr) exposure WSOC absorption spectra. All absorption is reported here as optical density normalized to WSOC (ug/ml).

EEMs were constructed from the fluorescence spectra collected from *A. versicolor* and *A. fumigatus* spores. The fluorescence spectra presented for these bioaerosols may deviate from conventional EEMs for many environmental water and aerosol extract samples, so the dominant fluorescent peaks shown on EEMs constructed for *A. versicolor* and *A. fumigatus* spore lysates and from controlled fungal cultures (grown under standardized conditions), are overlaid with potential fungal fluorophore candidates cited from the literature [48]. Cited excitation and

emission wavelength ranges for the fungal fluorophore candidates listed for Regions A – I can be found on

Table 4-1 in the introductory section. Identified fluorescence regions affiliated with the fungal spore EEMs presented in this work will be referred to by their letter assignments shown in Figure 4-4.

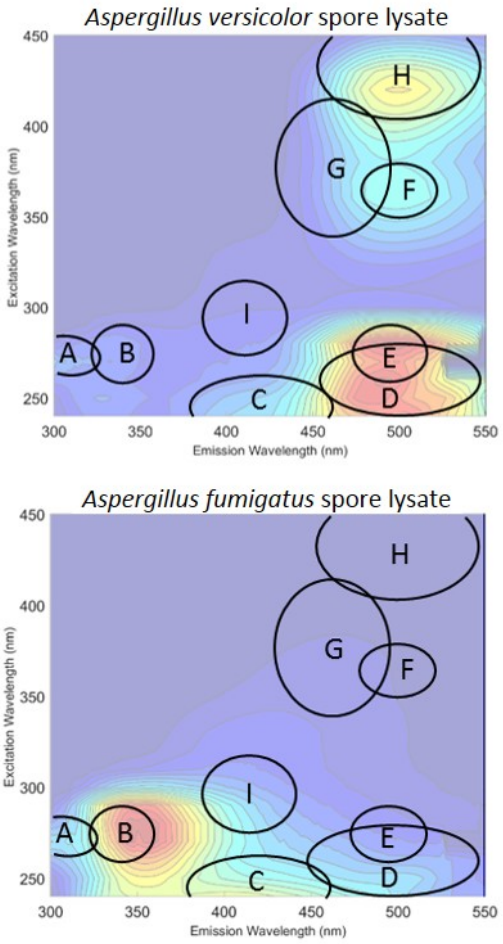

EEM Peak ID	Potential Fungal Fluorophore
A	Tyrosine
B	Tryptophan
C	Metabolites, Lignin, Terpenoids
D	Chitin, Lignin, Terpenoids
E	Riboflavin, Terpenoids
F	Riboflavin, Flavins, Sporopollenin
G	Sporopollenin, Chitin, Lignin
H	Riboflavin, Sporopollenin, Carotenoids
I	Ergosterol, Sporopollenin, Phenolics, Terpenoids

Figure 4-4. EEMs of fungal culture spore lysates from *A. versicolor* (**top**) and *A. fumigatus* (**bottom**), with WSOC normalized fluorescence intensity scale removed for clarity of

presentation. The regions defined by the respective ellipses, are adapted as published by Pohlker et al. 2012.

The following consecutive EEMs panels include fluorescence profiles of WSOC from lysed *A. versicolor* spore immediately harvested from culture as compared with these same spores following their aerosolization. This includes extracts of aerosolized spores (whole spore and lysed) collected immediately before and after 600ppb-hr ozone exposure at 85%RH, as well as spores in the absence of ozone (3hr suspension) at 85%RH, Figure 4-5. The same spore scenario for Figure 4-5 is shown for *A. versicolor* spores, in the chamber atmosphere of 30% RH, Figure 4-6.

Finally, fluorescence EEM profiles of WSOC from lysed *A. fumigatus* spores, immediately following their harvest from culture, are compared with aerosolized spore samples (both whole and lysed, shown in Figure 4-7) from the same culture cohort, and collected immediately before and after 600ppb-hr ozone exposure at 85% RH, as well as aerosol aged spores in the absence of ozone (3hr suspension) at 85% RH. This same sampling scenario was repeated at experimental conditions of 20% RH with the presence and absence of ozone.

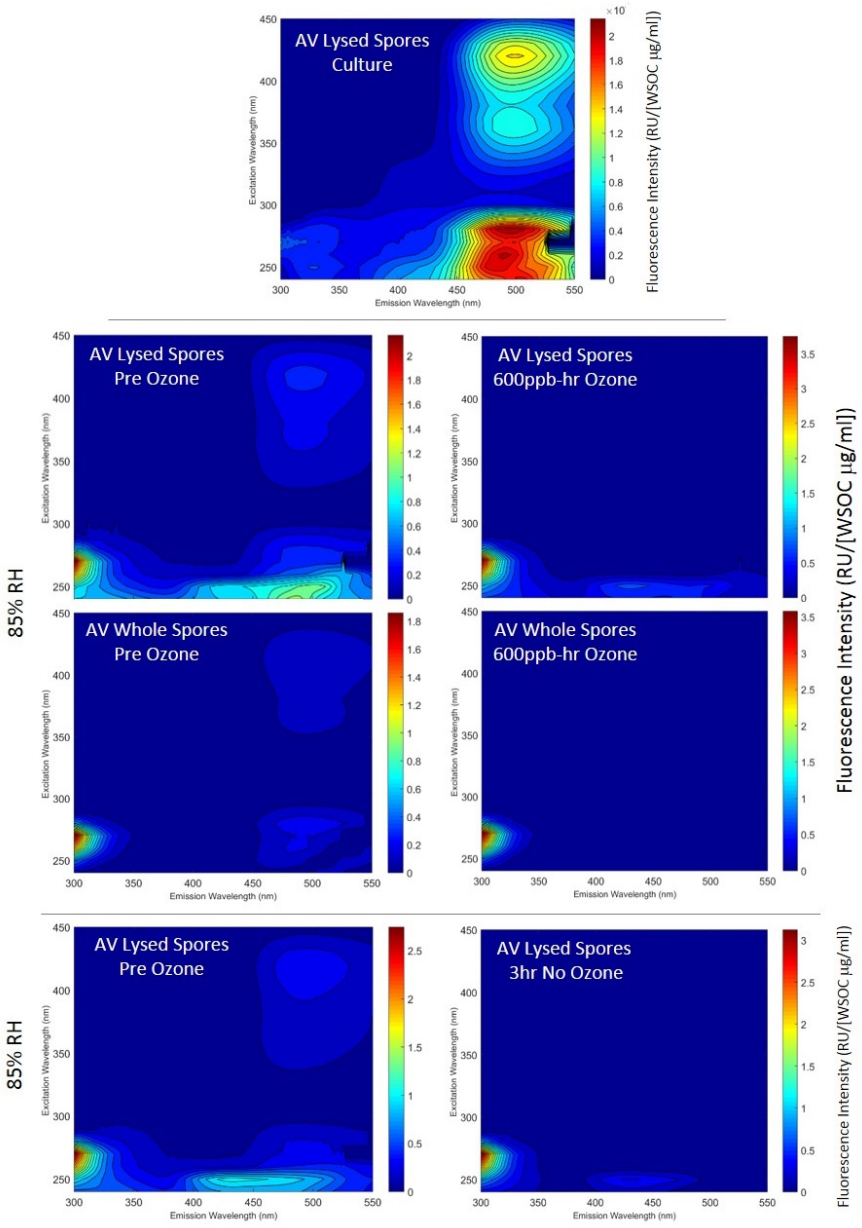

Figure 4-5. EEMs of WSOC recovered from *A. versicolor* spores immediately harvested from controlled fungal culture (**center, top**). **Left panels**, represent WSOC recovered from airborne *A. versicolor* spores following an hour of aerosol aging in the absence of ozone where (**left, top**) is from spore lysate; (**left, center**) is from whole spores; and (**left, bottom**) is from spore lysate. **Right panels**, with exception to bottom right (an aerosol aging control in the absence of ozone), represent WSOC recovered from airborne *A. versicolor* spores following ozone exposure of 600ppb-hr. (**Right, top**) is from whole spores; and (**right, center**) is from spore lysate. Relative humidity was controlled at 85%.

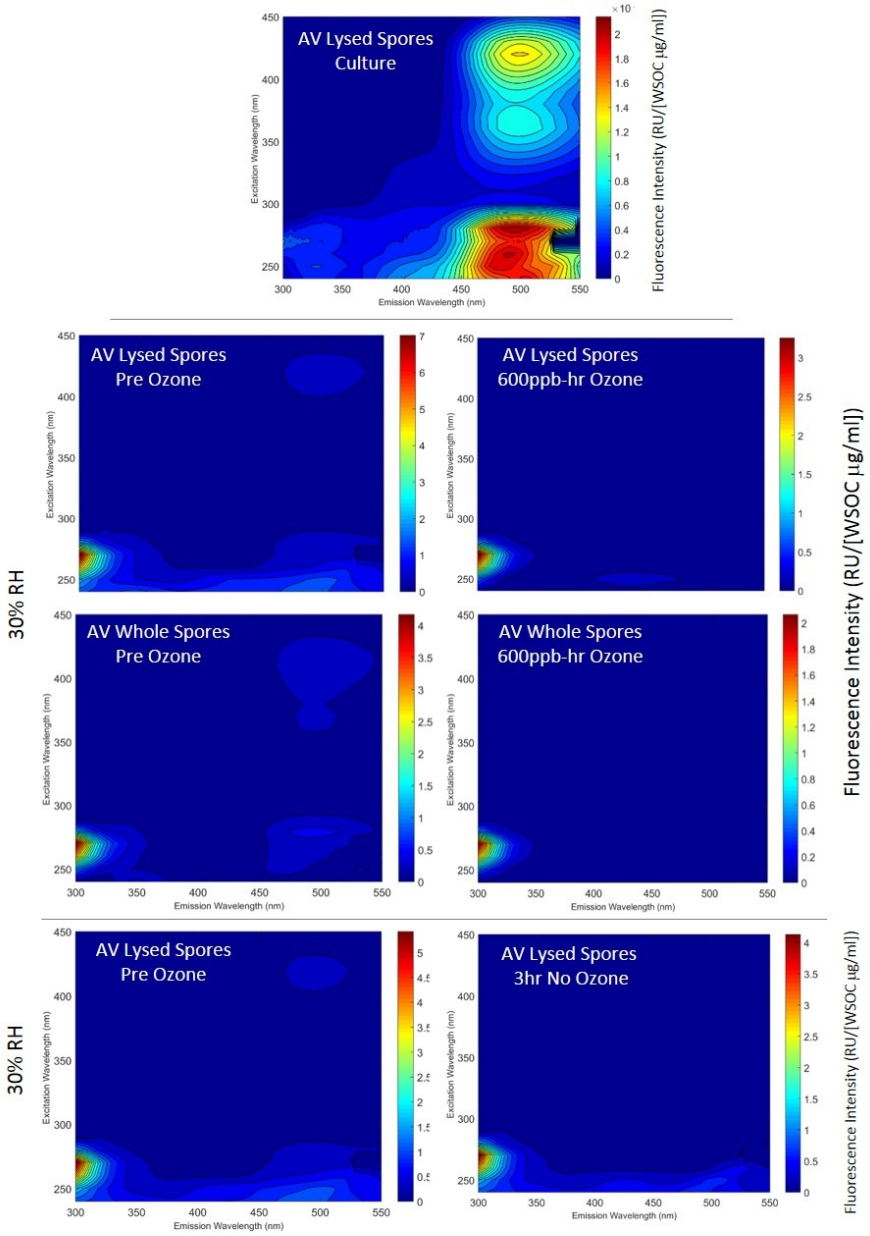

Figure 4-6. EEMs of WSOC recovered from *A. versicolor* spores immediately harvested from controlled fungal culture (**center, top**). **Left panels**, represent WSOC recovered from airborne *A. versicolor* spores following an hour of aerosol aging in the absence of ozone, where (**left, top**) is from spore lysate; (**left, center**) is from whole spores; and (**left, bottom**) is from spore lysate. **Right panels**, with exception to bottom right (an aerosol aging control in the absence of ozone), represent WSOC recovered from airborne *A. versicolor* spores following ozone exposure of 600ppb-hr. (**Right, top**) is from whole spores; and (**right, center**) is from spore lysate. Relative humidity was controlled at 30%.

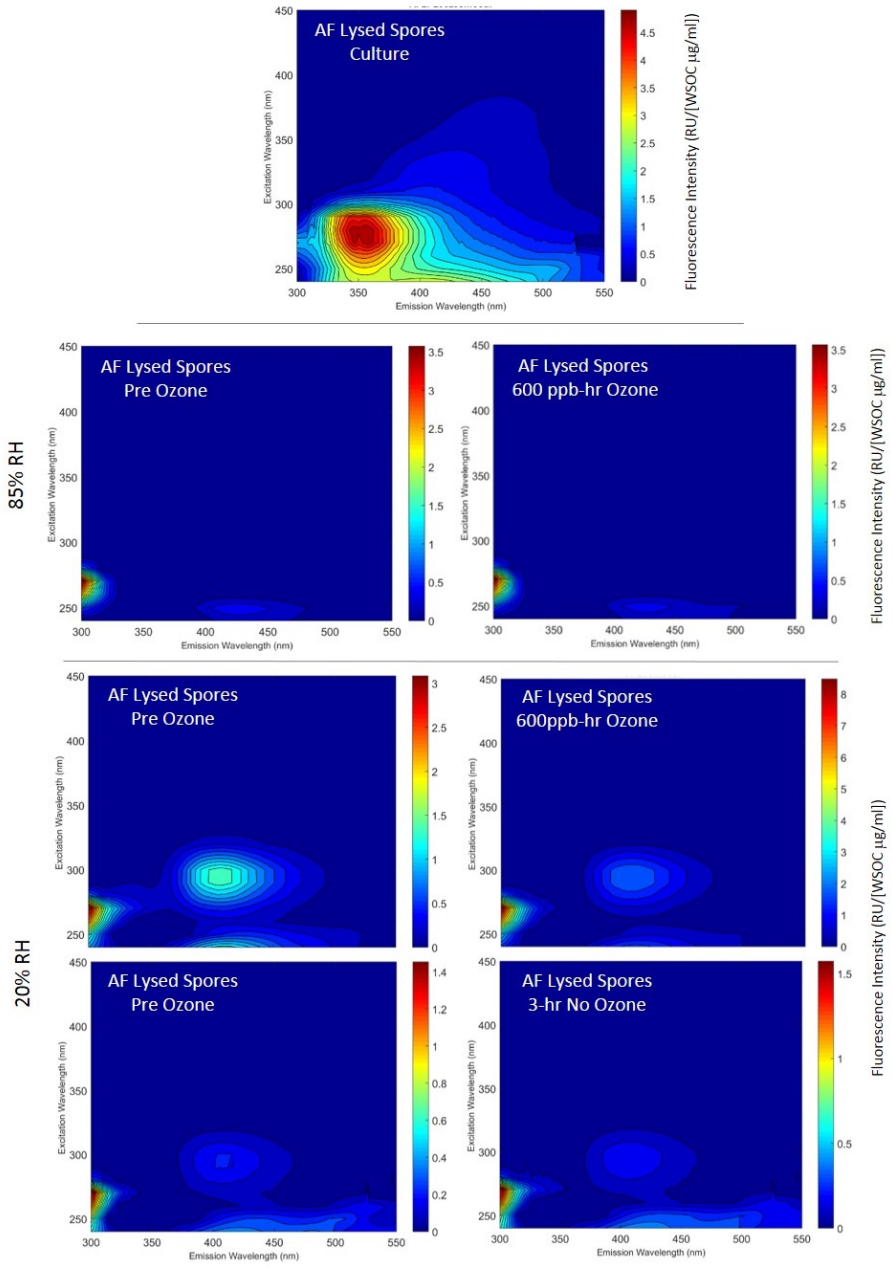

Figure 4-7. EEMs of WSOC recovered from *A. fumigatus* spores immediately harvested from controlled fungal culture (**center, top**). **Left panels**, represent WSOC recovered from airborne *A. versicolor* spores following an hour of aerosol aging in the absence of ozone, where (**left, top**) is from spore lysate at 85% RH; (**left, center**) is from whole spores at 20% RH; and (**left, bottom**) is from spore lysate at 20% RH. **Right panels**, with exception to bottom right (an aerosol aging control in the absence of ozone at 20% RH), represent WSOC recovered from airborne *A. fumigatus* spores following ozone exposure of 600ppb-hr. (**Right, top**) is from whole spores at 85% RH; and (**right, center**) is from spore lysate at 20% RH.

As demonstrated in the EEMs presented above, the fluorescence profiles between *Aspergillus versicolor* and *Aspergillus fumigatus* are distinctly different from each other, and this observation extends to their extracts following their recovery from an aerosolization. Additionally, in both *Aspergillus* species, significant changes in fluorescence profiles occur between WSOC immediately harvested from their respective cultures, and that collected after aerosolization in the presence or absence of ozone exposure. The most significant change for both cases (between culture and aerosolization) is a blue shift of the maximum intensity from the tryptophan-like region (B) toward the tyrosine-like region (A).

Dominant fluorescence peaks identified from WSOC harvested directly from *A. versicolor* cultures included fluorophore regions C-H, associated with metabolites, chitin, lignin, riboflavin, sporopollenin, and carotenoids. After immediately aerosolizing harvested spores, fluorescence intensity decreased markedly in all regions, with the exception of a blue-shifted, intensity increase in the region corresponding to bulk protein fluorescence (peak A). This blue-shift in the protein-like region occurred with both lysed and whole spore extracts. Spore lysates however, displayed additional fluorescence in regions C through E, which have been associated metabolites, terpenoids, and cell wall components released during the lysing process. Fluorescence from regions corresponding to riboflavin (H, F & E) was present in WSOC recovered from whole *A. versicolor* spores, as well as their lysed extracts, which were relatively more intense when recovered from the higher RH condition. WSOC from spores corresponding to the riboflavin regions, significantly decreased with aerosol suspension with and without ozone exposure. Note that this fluorescence region contributes to the calculated fluorescence index (FI).

Table 4-3. Descriptive fluorescence indices of WSOC liberated by lysed and whole *Aspergillus* spores aerosolized under different ozone challenge conditions.

Sample	RH(%)	Ozone (ppb)	SUVA 254	FI	HIX	FRI	Tyr/P	P/Po (%)
A. versicolor (lysed)	85	0	0.035	1.1	0.81	0.74	0.61	88.3
A. versicolor (lysed)	85	0	0.018	1.4	0.40	0.87	0.69	
A. versicolor (lysed)	85	0	0.042	1.0	1.00	0.75	0.68	127.2
A. versicolor (lysed)	85	600	0.023	1.6	0.46	0.86	0.71	
A. versicolor (whole)	85	0	0.015	0.9	0.36	0.87	0.74	185.6
A. versicolor (whole)	85	600	0.005	65535.0	0.11	0.78	0.76	
A. versicolor (lysed)	30	0	0.067	0.9	0.43	0.86	0.70	116.2
A. versicolor (lysed)	30	0	0.054	1.1	0.33	0.90	0.72	
A. versicolor (lysed)	30	0	0.051	0.9	0.54	1.01	0.68	238.2
A. versicolor (lysed)	30	600	0.018	1.8	0.32	1.14	0.74	
A. versicolor (whole)	30	0	0.014	0.9	0.32	1.30	0.70	44.9
A. versicolor (whole)	30	600	0.003	1.8	0.00	1.24	0.75	
A. versicolor (lysed)	culture	culture	0.048	0.9	4.15	0.60	0.39	-
A. fumigatus (lysed)	85	0	0.023	1.7	0.32	0.71	0.77	77.8
A. fumigatus (lysed)	85	600	0.018	1.9	0.34	0.58	0.84	
A. fumigatus (lysed)	20	0	0.015	1.5	0.90	0.63	0.80	63.6
A. fumigatus (lysed)	20	0	0.014	1.5	1.18	0.59	0.83	
A. fumigatus (lysed)	20	0	0.013	1.5	0.44	0.57	0.82	222.7
A. fumigatus (lysed)	20	600	0.017	1.8	0.45	0.57	0.70	
A. fumigatus (lysed)	culture	culture	0.024	1.4	0.84	0.96	0.21	-

Wavelength specific absorbance was determined from WSOC extracted from the spores prior to, and following, their aerosolization (and ozone exposure); this was normalized to the classic specific UV absorbance at 254nm ($SUVA_{254}$, reported in Table 4-3). This metric is traditionally associated with the degree of aromaticity and ozone reactivity of dissolved organic matter [64]. Generally, initial $SUVA_{254}$ values were smaller for WSOC liberated from *A. versicolor* spore walls, than for the lysate of those same spore samples, suggesting the presence of more aromatic organic compounds either inside and/or attached to the spore coat than those simply liberated from the spore surface. The largest decreases in $SUVA_{254}$ occurred with lysates

recovered from *A. versicolor* exposed to ozone at low RH (30%), than otherwise identical conditions at high RH. The $SUVA_{254}$ values for *A. fumigatus* were generally lower than *A. versicolor*, and did not exhibit significant change during aerosol aging in the presence or absence of ozone.

The fluorescence index (FI) is another accepted measure of WSOC aromaticity, as judged by optical properties [64]. Lower FI values indicate a higher degree of aromaticity (inverse trend of $SUVA_{254}$), and have been associated with lower weight microbially-sourced organic material (FI <1.5). FI values reflected the same trend as the $SUVA_{254}$ in regard to the lysate of *A. versicolor* exposed to ozone. The FI also has been used to determine sources (microbial or terrestrial) of organic matter in aqueous systems [19]; however, in this work, compounds associated with this type of fluorescence have spectral overlap with fulvic-acids (as judged by FI values reported in water research), yet are more likely to include species-dependent constituents (including riboflavin, chitin, lignin, sporopollenin). These results suggest that fungal spores might contribute to both microbial and terrestrial fractions of organic matter in aquatic environments.

Several component peaks have been identified in EEMs in an apportionment context; these represent compounds derived from different sources, and ultimately used to identify fluorescence indices that aid in environmental sample characterization[74]. The humification index (HIX) has been developed to assess the degree of humification that organic matter experienced, and is based on a ratio of two fluorescence emission areas corresponding to young (fresh) organic matter, and generically weathered (humified) organic material[65]. Higher HIX values indicate polycondensation processes through a shift to longer wavelengths. The HIX

value can increase with organic aerosol aging and transformation [62], and can vary by season [60] and location[18]. In this work, the HIX values generally decreased in response to simple aerosol aging (no ozone), as well as in the presence of ozone; however, specific HIX reduction trends are difficult to quantify as the initial HIX values (pre ozone or aging) were variable between experiments.

4.4. **Discussion**

A more detailed discussion of WSOC liberation, will be given in Chapter 6, in relation to other water soluble proteins cited to have negative environmental health effects (e.g. allergens). Here it is important to note the WSOC liberation from both *Aspergillus* species increased in response to spore aging and ozone exposure. Changes in the specific fluorescence contribution per microgram of WSOC liberated can give an indication of the components contributing to these fluorescence regions associated with proteins, biopolymers and oxidation products. The composition of *Aspergillus* spore walls incorporate hydrophobic biopolymers and structural components[75], Figure 4-8. With time these components may age or oxidize such that their properties become more hydrophilic, subsequently lending the spore lysate process to facilitate their contribution to the total WSOC content.

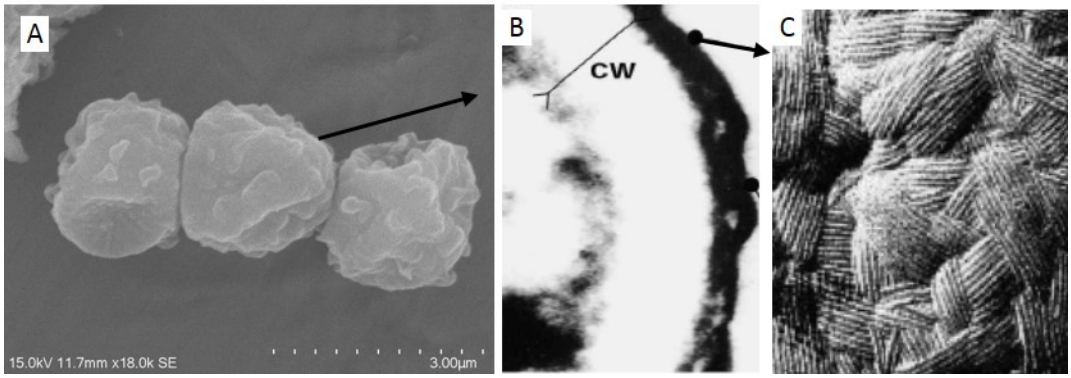

Figure 4-8. Morphological features of *A. fumigatus* cell walls. Scanning electron micrograph (SEM image of spores post aerosolization at magnification of 18,000x [current study] (A). Transmission electron microgram (TEM) showing a cross section of *A. fumigatus* spores, with biopolymer layers including chitin and a dense melanin (B); and hydrophobic rodlet protein structures at high magnification (C) [Bernard et al. 2001].

Under identical exposure conditions, analyzing WSOC liberated from whole spores, as compared to that WSOC liberated from pulverized cell extracts, can isolate the effect of oxidation of the spore surface. As a conglomerate, these data suggest that it is unlikely ozone is penetrating deep into the spore coat during the time frames of these experiments. This observation is consistent with modeling of ozone uptake, which in amorphous proteins, has been recently been show oxidation is diffusion-limited, but reportedly increases with increasing RH [55].

Ergosterols occupy a unique region of EEMs, illustrated as region (I) in the near the center of the example EEM plot in Figure 4-4. Ergosterols are a primary component of fungal wall structure, making it a prime target for antifungal agents, and *A. fumigatus* has been cited as one of the most resistant species to antifungal agents that target ergosterol [76]. Ergosterol has been reported to be a fairly stable steroid, slow to degrade in the environment [77]; and may

explain why ozone did not demonstrate a significant impact on the fluorescence properties associated with this region. The ergosterol content in *A. versicolor* relative to *A. fumigatus* been not reported in the literature, but in a study comparing ergosterol content with other fungal types, *A. versicolor* ranked in the lower percentiles [78]; a potential reason why this component is not as apparent in the *A. versicolor* EEMs.

Aspergillus spp. with darker pigments contain aspergillin, which can contribute to humic-like substances found in soil [79]. Additionally, oxidative degradation of melanin, a cited component in *Aspergillus* spore walls [75, 80], can also produce similar products as those found in humic acids [81]. These components may explain the manifestation of fluorescence associated with marine and terrestrial humic-like compounds on the EEMs (ex: 254nm, Em: 435-480nm), and ultimately the HIX. These HIX values are on the lower end of the HIX ranges typically encountered in natural waters and collected aerosol samples (note that wildfire aerosol samples indicated HIX values between 0.5 and 3.5, Chapter 7).

The EEM profiles reported here for culture-harvested spores are very similar to those reported for *Apsergillus flavus* by Wlodarski et al. 2006[82], where the dominant fluorescent region aligns with tryptophan-like fluorescence, and a smaller fluorescence contribution to the NADPH and flavin region. Note that the fluorescence enhancement and shift to the tyrosine-like regions here occurs after spore aerosolization. It is still not clear whether fungal spores contain any appreciable amounts of NADPH at all, as spores are classified as dormant, thus should not participate in major energy-yielding reactions until germination. However, it has been suggested that *Aspergillus* spores can exhibit a basal level of metabolism in preparation for germination, as judged by changes in composition of internal lipid and sugars over time [83]. NADPH is

involved in mannitol production, a carbohydrate favored for germination and growth of *Aspergillus*, but it still remains unclear on the extent of the presence of NADPH in spores [84]. Other more likely fungal compounds that can fluoresce in the same region as NADPH include riboflavin, which inhabits an EEM region clearly present in the WSOC liberated from *A. versicolor.* Riboflavin is a metabolite present at different levels in fungal spores (depending on species) that absorbs UV and aids in UV resistance of the spore wall [85]. The EEM produced for isolated riboflavin[48] is strikingly similar to regions shown for *A. versicolor*, but not seen in *A. fumigatus*. Fouillaud et al.[86] note clear visible absorption between 420nm and 500nm due to carotenoids from *Aspergillus versicolor* isolated from coastal waters around Reunion Island.

Both $SUVA_{254}$ and FI have been reported as indicators of aromaticity in dissolved organic carbon samples [19, 64]. The FI also has been used to determine sources (microbial or terrestrial) of organic matter in aqueous systems. However in this work, suggested components that fluoresce in these traditionally fulvic-acid associate regions are more likely to include constituents dependent on fungal species (including riboflavin, chitin, lignin, sporopollenin) than conventionally described terrestrial sources. This also suggests that fungal material present in water (either deposited from air, picked up from runoff, or growing in water) might contribute measurements in both microbial and terrestrial fractions of organic matter in aquatic environments. In the context of this work, FI and $SUVA_{254}$ indicated some level of modification to WSOC components, before and after ozone exposure, in both *A. versicolor* and *A. fumigatus*. The FI of *A. versicolor* WSOC extracts resembled values conventionally reported for terrestrially derived, more aromatic compounds (FI: 0.9 – 1.1) for both low and high RH exposures; however, after ozone exposures FI values increased to those conventionally reported from

microbial sources and with lower aromaticity (FI: 1.6 – 1.8). Decreases in FI values were slightly less in spores suspended for 3 hours without the presence of ozone, than those exposed to ozone, indicating the role ozone has on decreasing aromaticity of some WSOC components. Double carbon-carbon bonds and delocalized electrons present in many aromatic compounds also reflects the declining $SUVA_{254}$ trends observed here with decreasing absorption for both aerosol aging and ozone exposure. However, the specific influence of ozone on reducing this measure is unclear.

Species dependent differences in liberated WSOC constituents, and the extent of ozone oxidation, become is apparent when comparing 'pre' (initial, no ozone) and 'post' (with or without ozone) FI values for *A. versicolor* and *A. fumigatus*. For *A. versicolor*, the FI values are lower indicating the presence of components in the G region (stable spore wall components) and the F region (riboflavin and sporopollenin). With either exposure or aging, the F region decreases to a greater extent than the G region, indicating a potential greater loss of riboflavin with respect to spore wall components, like chitin and lignin, during oxidation. For *A. fumigatus*, the pre-exposure FI values were larger than for *A. versicolor*, and the final FI values are similar, indicating a lesser fluorescence contribution of riboflavin relative to that of spore wall components for *A. fumigatus* than for *A. versicolor*.

CHAPTER 5. BIOPOLYMER AND BIOCHEMICAL ANALYSIS

5.1. Introduction

This chapter will discuss the changes in water soluble organic components, and specific allergenic and enzymatic activities that whole cell bioaerosols can experience during exposure to ozone at high and low relative humidity (RH). The following hypotheses will be addressed in this chapter:

Hypothesis II*: Exposure to environmentally relevant concentrations of gaseous ozone, a common oxidizing air pollutant, will modify biopolymers on the surface of common airborne microorganisms (bioaerosols).*

Hypothesis IIa: *Environmentally-relevant levels of ozone will modify cell-bound biopolymers to such a degree that recognition by sensitive, highly-specific, biological analyses will be significantly reduced, with a focus on: water soluble organic carbon, total water soluble protein, antibody recognition of allergic epitopes and fungal spore wall enzymatic activity.*

Hypothesis IIb: *Relative humidity will play a significant role in the extent of oxidative biopolymer modification during bioaerosol exposure to ozone.*

5.2. Background and Context of Bioaerosol Biopolymer and Biochemical Analyses

The characterization of potential modifications to bioaerosols by oxidative air pollutants has been gaining increased interest because of environmental health concerns and ecological implications [13, 87]. Bioaerosols have recently been reported to constitute a significant portion of airborne organic carbon, and can experience atmospheric residence time which span minutes to many days; where, bioaerosols have been documented to travel vast (intercontinental) distances [27]. Depending on their sources and the meteorological conditions encountered, bioaerosols can become entrained in air masses and have extended interactions with anthropogenic pollutants on local and regional scales [2, 88]. In the context of oxidation processes, much of the work associated with atmospheric processing of bioaerosols has been on the potential impacts of air pollution on pollen germination and associated allergenic properties [6, 89-92]. These investigations have been motivated by the increasing occurrence of allergic and hypersensitivity diseases associated with rising air pollution levels, particularly in urban environments [93], and concern for ecological implications [91, 92].

More recently, the fluorescence properties of the water soluble organic carbon (WSOC) eluted from ambient aerosols has been investigated for its utility as a robust tracer for PM source apportionment (i.e. combustion, urban and rural aerosol sources) [94, 95]. For example, relatively toxic polyaromatic hydrocarbons (PAHs) can be found in the WSOC fraction of anthropogenically-sourced organic aerosols[96]. Additionally, the WSOC fraction can contain a cohort of allergenic constituents including microbial spores, vegetative cells, pollen grains and fractions thereof [70]. There is emerging evidence that when WSOC components associated with airborne microbes (β-glucan or lipopolysaccharies) and anthropogenically-sourced air

pollutants (PAHs) are encountered together, synergistic toxicological effects can result, and manifest in cytotoxic pathways associated with serious respiratory disease [97, 98]. However, as judged by fluorescence properties (EEMs), the contribution of bioaerosols to the overall pool of airborne WSOC remains largely unknown. Specific bioaerosol WSOC fractions have yet to be associated with airborne microbial ecology in the atmospheric environment; nor has bioaerosol-derived WSOC been isolated and characterized for its reactivity with oxidative atmospheric pollutants in any systematic manner.

Airborne microbes contain an abundance of water soluble biopolymers. These biopolymers comprise a formidable portion of microbial cell mass, and include a large diversity of proteins and polysaccharides. Proteinaceous components have been noted to contribute to WSOC in ambient aerosols, and have been used as an estimate for the contribution of bioaerosols to the total measured aerosol load in a given environment[99-102]. However, the lack of sample processing standards and the relative variability in protein quantitation techniques have yielded conflicting results, thereby producing observations and associated uncertainties that can range orders of magnitude (1 ng protein/m^3 – 10 ug protein/m^3). This poses an analytical and interpretive challenge to the aerobiology community in forming a consensus on the magnitude of aerobiological loads in the literature. It is clear however, that certain fractions of the airborne water soluble proteins are potent environmental health threats. This fraction of airborne protein include the antigenic determinates of common allergens, which induce atopic asthma or can otherwise trigger other negative respiratory health responses. Many observations of indoor allergen loads are determined from immunoassays of aqueous extracts from dust or aerosol

samples, as quantified with sensitive colorimetric, fluorescent or radioactive reporters [70, 103, 104].

The literature also contains perspectives that associate increased occurrence of allergenic diseases with climate change and air pollution [93, 105]. Climate change factors and anthropogenic pollution sources have been suggested to directly impact allergic responses in a number of ways, including the following mechanisms: 1) enhanced sensitization to airborne allergens by previous exposure to elevated levels of anthropogenic air pollutants [106]; 2) increasing levels of fine particulate matter that can serve as additional carriers, or adjuvants, for allergens [107]; 3) increased probability of exposure to combinations of anthropogenic pollutants and allergens, which have the potential to synergistically exacerbate inflammation beyond that of exposure to either alone [97, 98, 108]; 4) influence of changing ambient temperature (extended warm periods) and elevated concentrations of CO_2 and O_3 encountered during the growth phase of bioaerosol precursors can increase the allergenic activity and soluble protein content of fungal spores [70, 109] and pollens [90, 110]; and finally, 5) elevated levels of gaseous air pollutants (e.g. O_3, NO_2, and SO_2) can either directly or indirectly influence the magnitude of allergenic response in mammalian receptors (IgE recognition) [89, 90, 92] by modifying allergens and compounds in pollens believed to initiate or enhance inflammatory responses [6, 7, 111].

The literature emerging in this arena is tenuous and limited, much of which demonstrates the potential for specific allergen modification using experiments that immobilize allergen-carrying microbes, or their extracts, on fixed surfaces in the presence of gaseous oxidant, as opposed to studying these effects on aerosolized microbes for extended periods[6, 89, 90, 92]. In response to the limitations of existing experimental designs in this area of work, observations of

total water soluble protein, enzymatic activity and allergen modification of well characterized bioaerosols are reported here under well defined and controlled environmental conditions (RH and O_3), as well as sustained airborne residence times (hours).

Inahling airborne fungal cells, and their fragments, remains a major health concern [112, 113], particularly for immunocompromised and otherwise sensitive or aged populations. Elevated levels of airborne fungal material have been widely observed in water damaged buildings and associated with chronic and acute health effects ranging from respiratory and eye irritation to asthmatic inflammation and even major infections [112, 114]. The identification, distribution and abundance of airborne fungi in the built environment has been widely studied for decades, with numerous reviews reporting different perspectives on the association of microbes with building material characteristics and effects on occupants [115].

Most inventories of bacterial and fungal occurrence in the built environment rely on culture-based techniques, which can at best recover between 1-10% of the microbes present in aerosols or on surfaces, and unfortunately introduce tremendous biases into both ecological and biomass estimates [116]. High throughput genetic amplification techniques have more recently been used to describe the ecology and abundance of microbes in the built environment. However, because of the relative abundance of genetic targets (ribosomal DNA), the variance in DNA extraction and amplification efficiency, and the statistical cluster analyses techniques employed, there are significant concerns in the variance and uncertainties of these techniques as they apply to environmental applications [117].

With respect to estimating airborne fungal biomass in the built environment, an assay that leverages correlations between measured activity of a unique fungal enzyme, β-N-

acetylhexosaminidase (NAHA) , utilized in the germination process and total fungal biomass has been developed for estimations of total airborne fungal spore loads [118, 119]. The NAHA enzyme is widely present across the fungal world, and its specific activity has been well correlated to total fungal biomass and adopted into a method validated for use air and surface samples [120]. Since its validation by the USEPA (2011), this approach has been commercialized and used to estimate fungal biomass in a number of water damaged indoor environments as a means to assess fungal exposure from indoor air [113, 120, 121].

Though the NAHA activity in aerosol samples collected from water damaged homes is typically higher than those with no apparent water damage [113, 120-122], the specific relationship between measured NAHA activity from environmental aerosol samples and biomass remains unclear. It has been reported that specific NAHA activity is species and maturity dependent across some laboratory fungal cultures [119]. Further, there is a scarcity of controlled studies relating to specific aminidase activity under different airborne environmental conditions. These factors (species and culture maturity), as well as environmental exposure effects (varying RH and pollutant levels), are addressed by hypotheses tested here.

In addition to leveraging enzyme activity assays to better understand the abundance of fungal spores in the built environment, systematically defining aminidase activity under a broad range of environmental conditions is also important for ecological studies. Assessing NAHA activity during bioaerosol oxidation studies can shed light on the potential implications of modifying an important part in the enzyme cascade involved in spore germination. Investigating the impact of environmental exposure of airborne fungal material, and their enzymatic activity (particularly those that facilitate germination), can provide some important insight on how

pollutants may impact downstream microbial viability. Given that atmospheric transport of bioaerosols, specifically with respect to fungal spores, can occur on time scales of minutes to days [2, 27, 88] and can include significant influences from local and regional pollution [88], understanding the behavior of enzymes that facilitate fungal germination under different environmental conditions has important ecological implications.

The investigations presented here are designed to challenge the hypotheses outlined in Section 5.1. These were compiled in response to gaps in the literature as they relate to the interactions of oxidizing air pollution and bioaerosols, specifically focusing on modification of: water soluble organic carbon (WSOC); total water soluble proteins; specific allergen content (Asp f 1), and specific fungal enzymatic activity (NAHA). *Aspergillus fumigatus* and *Aspergillus versicolor* were chosen as microbial models for this study because they are recognized pathogens; their physiology is well-know; they are considered as indicator species of water damage in built environments; and, they are generally ubiquitous in temperate climate aerosols (as judged by conventional culture and microscopy).

5.3. Chapter Specific Methods and Materials

The following methods are specific to biopolymer and biochemical analysis, including details for determining total water soluble protein content, Asp f 1 allergen analysis, and β-N-acetylhexosaminidase (NAHA) activity. Characterization methods used in this chapter were selected based on their current implementation in bioaerosol research and their high sensitivity. Details on experimental chamber design and operation as well as *Aspergillus spp.* culturing

methods can be found in Chapter 2, and information on sample preparation and quantification of water soluble organic carbon (WSOC) can be found in Chapter 6.

5.3.1. NanoOrange® Total Water-Soluble Protein Quantitation

The total water-soluble protein eluted from spores was quantified using modifications to the commercially available NanoOrange protein quantitation assay (Invitrogen). This highly-sensitive protein assay relies on standardized fluorescence analysis where the NanoOrange reagent interacts with detergent-coated proteins creating a fluorescent complex measured at 590nm when excited at 470nm [123]. The limit of detection, as modified for this assay was, 0.05 µg/ml aqueous sample. After bioaerosol (fungal spore) capture with the Sequential Spot Sampler (Series 100, Aerosol Devices Inc.), collected spores were eluted directly from the wells of the Spot Sampler collection plate (refer to Chapter 2), using the proprietary NanoOrange surfactant provided - without the fluorophore (Component A) added - and transferred into 1.5 ml baked glass vials. The NanoOrange Working Solution was directly used for sample elution instead of water (as per the product protocol), to minimize losses of hydrophobic *Aspergillus* spores to the collection plate. Each well was washed 5 times with 50 µl of the NanoOrange® Working Solution (without Component A) for a final suspended sample volume of 250 µl. Samples were then vortexed vigorously for 30 seconds and left to incubate shaking at 120 rpm at room temperature for 1 hour. After a second vortex for 30 seconds (to resuspend spores), 150 µl of each sample was placed in clear sterile 2ml screw cap tubes for protein quantitation, while the remainder of the samples were stored at 4°C until enumerated by microscopy counts with a hemocytometer.

All protein samples were centrifuged at 4°C for 2 minutes at 10,000g to pelletize the spores, then 125 µl of each sample supernatant was carefully transferred into sterile 2ml amber tubes (screw cap) and combined with 125 µl Working Solution prepared with 2X Component A - the fluorophore was added at a 2X concentration to make the final concentration commensurate with the assay's recommended concentration (the fluorophore was added in this step to avoid photo bleaching during the initial spore elution process). The bovine serum albumin (BSA) standards were prepared per manufacturer's protocol, using BSA concentrations of 0 µg/m, 0.05 µg/ml, 0.1 µg/ml, 0.5 µg/ml, 1 µg/ml, and 10 µg/ml to construct the standard curve as a reference to determine the spore protein concentrations. All samples and standards were incubated at 95°C for 10 minutes and cooled to room temperature (20 minutes), vortexed and transferred in 200 µl aliquots to clear 0.5ml PCR tubes before measuring the sample fluorescence emission at 590 nm (excitation of 470 nm) with the Quantus™ Fluorometer (Promega Corporation).

5.3.2. Multiplex Array for Indoor Allergens (MARIA®) for Detection of Asp f 1

The quantitation of *Aspergillus fumigatus* allergen protein (Asp f 1) was conducted by Indoor Biotechnologies using the multiplex array for indoor allergens (MARIA), which has a greater range of sensitivity and degree of reproducibility for allergen detection than the conventional enzyme-linked immunosorbent assay (ELISA) for many common indoor allergens [124, 125]. The quantitation of Asp f 1 allergen from *Aspergillus fumigatus* bioaerosol samples was determined using a monoclonal antibody 4A6, an Asp f 1 analog derived from the *Aspergillus restrictus* mitogillin cytotoxin Asp r 1. Proteomic analyses of Asp r 1 and Asp f 1

show these proteins are 95% sequentially homologous, and antigenically and functionally indistinguishable from each other [126].

Aerosolized *Aspergillus fumigatus* spores were collected in 30 minute increments with the Sequential Spot Sampler (Series 100, Aerosol Devices, Inc.). The Spot Sampler, a high-efficiency condensation particle capture sampler, uses aerodynamic lenses to focus airborne particulate matter into a water condensation regime which deposits and concentrates aerosols in at the bottom of 75ul wells in a collection plate [127]. An instrument schematic, specific sampling details and experiment-specific limitations of the Sequential Spot Sampler are covered in Chapter 2. The aerosol sampling time required for Asp f 1 allergen analysis was dependent on the spore concentration in the chamber (established with the pWIBS), and based on the lower limit of detection established by a cohort of preliminary range-finding studies. Prior to this study, this immunoassay has been mainly used to determine the allergen content of settled dust samples (much higher concentrations) and required experimental range finding for these collected aerosol samples. See the Appendix for calculations of the following experiment-specific detection limits: MARIA analyses based on ATCC biomass standards; estimated chamber sampling time calculations; and "look up" tables constructed for side-by-side use of the pWIBS and the Sequential Spot Sampler. At spore concentrations above 5.4×10^4 spores/L (>750 particle counts per second by pWIBS), the Spot Sampler sampling durations were typically 30 minute at 1.5 lpm to ensure enough spore biomass was collected to be above the detection limit for Asp f 1 allergen quantitation. Because the detection limits required for MARIA (Asp f1) analyses were almost 10 folder higher than other biochemical experiments conducted on airborne *Aspergillus* spores, they only exposed to the following for 1hr at 85% RH

to maintain required bioaerosol concentrations; tested ozone concentrations (and exposures) included: baseline (no ozone) (0ppb-hr), 600 ppb (600 ppb-hr), 1200 ppb (1200 ppb-hr), and 7500 ppb (7500 ppb-hr). The Ct exposure time frame equivalents here, as they relate to 2015 EPA NAAQ O_3 standards of 70ppb for 8 hours, are: 8.5, 17, 34 and 107 environmental exposure hours at 70 ppb ozone, respectively.

All MARIA analyses for these experimental samples focused on the Asp f 1 allergen liberated from the *Aspergillus fumigatus* spore wall into 0.05%Tween 20:DI water (typical procedure for allergen analysis) after centrifugation at 10,000g for 2 minutes. All samples collected for Asp f 1 analysis had an additional sequential sample collected for total water-soluble protein content and assays were normalized by their respective spore microscopy counts. Each Spot Sampler collection well was eluted with 300µl of 0.05% Tween 20: DI water in 6 well wash volumes of 50µl to elute the spores for both Asp f 1 analysis (200µl volume) and microscope enumeration (100µl). All samples were stored in glass ½ drams (baked at 550C) to reduce hydrophobic spore losses to plastic tube walls.

The MARIA assay incorporates polystyrene microspheres covalently conjugated to monoclonal antibodies, here mAB 4A6, that are then exposed to the sample eluent, washed and exposed to biotinylated detection antibodies that selectively bind to Asp f 1 and contain a reporting fluorophore quantified with a Bio-Plex fluorescent suspension array reader (Bio-Rad Laboratories). The reported fluorescent quantities are then compared to a standard curve constructed with a varying concentrations of purified allergen Asp r 1 (reported as 95% homologous with Asp f 1). The typical lower limit of Asp f 1 detection, depending on the specific experimental standard curve, ranges from 0.02 ng/ml to 0.04 ng/ml.

5.3.3. Fungal Spore Enzyme β-N-acetylhexosaminidase (NAHA) Activity Assay

The Mycometer-Air® assay was selected for specific fungal enzyme activity (β-N-acetylhexosaminidase (NAHA)) studies because of its sensitivity and reproducibility; it has been previously evaluated and approved by the EPA for use in these settings [128]. Aerosolized spore samples were collected onto filters in sequential triplicates at the beginning (before exposure) of each chamber experiment and after a suspension time of 3 hours, either in the presence of 200ppb ozone or baseline (no ozone) conditions. All filter sampling was conducted for 15 minutes at flow rate of 20 L/min, for a total collected air volume of 300 L. All filter samples were stored at 4C, and analyzed for NAHA enzyme activity within 96 hrs of sample capture.

The NAHA enzyme activity for each sample was determined by the hydrolysis of an enzyme substrate coupled with a fluorophore by an active NAHA enzyme, producing free fluorophore in solution that is fluorimetrically quantified at an excitation of 365nm, as illustrated in the figure below:

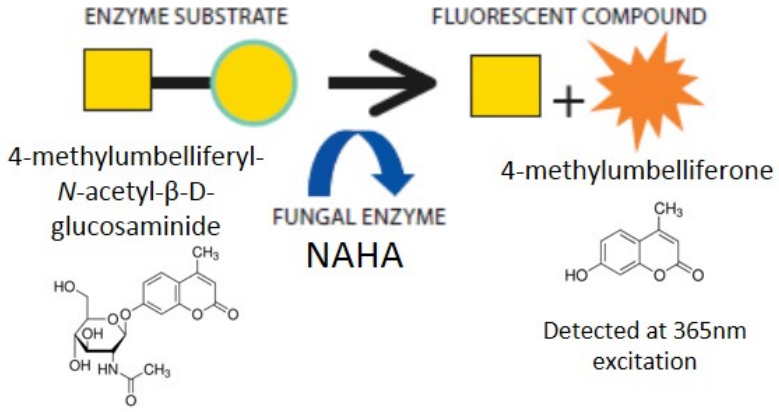

Figure 0-1. Principle of quantifying NAHA activity by detection of resulting cleaved fluorophore product using the Mycometer-Air assay.

All samples were analyzed following the Mycometer-Air protocol, where 1 ml fluorogenic substrate, 4-methylumbelliferyl N-acetyl-β-D-glucosaminide, is added directly to the sample filter cassette. After reacting for approximately 30 minutes (determined based on the room temperature), 2 ml of developer was added to stop the reaction. The resulting product solution was placed in a sterile polyacrylic cuvette and the fluorescence intensity at an excitation wavelength of 365nm was reported as referenced fluorescence units. A filter blank was analyzed with each sample set and subtracted from each measured sample. The resulting enzymatic activity is reported as NAHA enzyme activity (EU/m^3).

Statistical methods for assessing significant differences between means of serial triplicate measurements for each condition (before and after 3 hour suspension with or without ozone exposure within a given chamber experiment) included the F-Test for determining equal variances followed by the two-tailed, two-sample t-Test (alpha=0.05) for data sets with equal variance or unequal variance. All p-values (alpha=0.05) are reported.

5.4. Results

The following results, that challenge Hypotheses 2a and 2b, are presented in the following order: how ozone exposures affect water soluble organic carbon (WSOC) liberation from airborne *Aspergillus versicolor* and *Aspergillus fumigatus*; the total water soluble protein content and specific water soluble allergen, Asp f 1, specifically for *Aspergillus fumigatus*, and finally, total NAHA enzyme activity for both *Aspergillus versicolor* and *Aspergillus fumigatus*.

5.4.1. Estimation of WSOC Content of Aerosolized Fungal Spores

The WSOC content of airborne *Aspergillus versicolor* and *Aspergillus fumigatus* spores (presented in Figure 0-2 and Figure 0-3) was determined from samples taken before and after 3 hour suspension in the presence or absence of ozone, where RH was maintained at a high level (85% (± 5%)), or a low level (20% or 30% (± 5%)). The lower RH condition was determined by the ambient RH levels on the days of these experiments. As a function of aerosol suspension time, the mass of WSOC liberated per 10,000 spores is presented in Figure 0-2. Here, the first three data points for each experiment were collected in sequential triplicates every 15 minutes, up to 70 minutes (shown to the left of the blue line). After 3 hours of suspension with or without ozone present, subsequent sets of sequential triplicate aerosol samples were collected in 15 minute intervals, under the following experimental conditions: (i) with 200 ppb ozone; or (ii) no ozone (< 10 ppb (detection limit)).

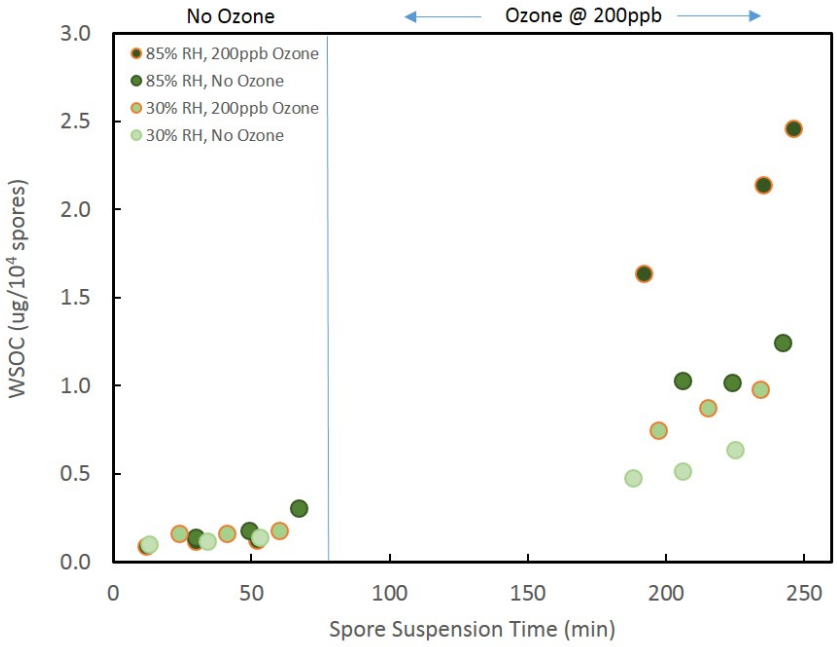

Figure 0-2. Sequential measurements of WSOC liberated from aerosolized Aspergillus versicolor spores near the beginning and end of 4 continuous hours of suspension in an environmentally controlled chamber—in the presence and absence of ozone. Where exposed, ozone was introduced around 60 minutes of aerosol suspension time. Low RH conditions are represented by light green circles (●); high RH conditions are represented by dark green (●) circles. Exposure to 200 ppb ozone is denoted by an orange ring around the symbol (**O**).

When normalized on a spore number basis (by direct microscopic count), the amount of WSOC liberated from these aerosolized spore cultures remains consistent during the first hour, and steadily increases with aerosol suspension time, regardless of RH condition. Whether they are aged as an aerosol in the presence or absence of ozone, the amount of WSOC liberated by airborne *Aspergillus* spores markedly increases after 3 hours; however, the combination of a high RH condition in the presence of ozone had the most influence on WSOC liberation potential with increasing residence time. This was phenomenon of increased WSOC liberation with elevated RH was demonstrated with *A. versicolor* spores, where the amount of WSOC liberated per spore

was substantially higher in the absence of ozone at high RH levels (85%) than even low RH (30%) ozone exposure conditions for the same time period and spore type.

The WSOC liberated from airborne *A. versicolor* and *A. fumigatus* spores are reported in Figure 0-3; these data are presented as averages with standard deviations estimated from triplicate observations taken the beginning and end of independent ozone exposure experiments. The data is reduced into cohorts of airborne *Aspergillus spp.* prior to (pre-), and during (post-), ozone exposure. As judged by WSOC liberated on a spore-normalized basis, both species of airborne *Aspergillus* spores observed here, had a significant response to ozone when airborne, particularly at higher RH levels as is indicated by t-test results (p-value less than 0.05). At 85% RH, airborne *A. versicolor* spores liberated more WSOC than did *A. fumigatus*. Unlike *A. versicolor*, WSOC liberation from *A. fumigatus* was not substantially different between the high and low RH levels tested; however, ozone exposure enhanced WSOC liberation in all cases. For all experiments, WSOC was measured from airborne spore samples collected in sterile water with liquid impingers.

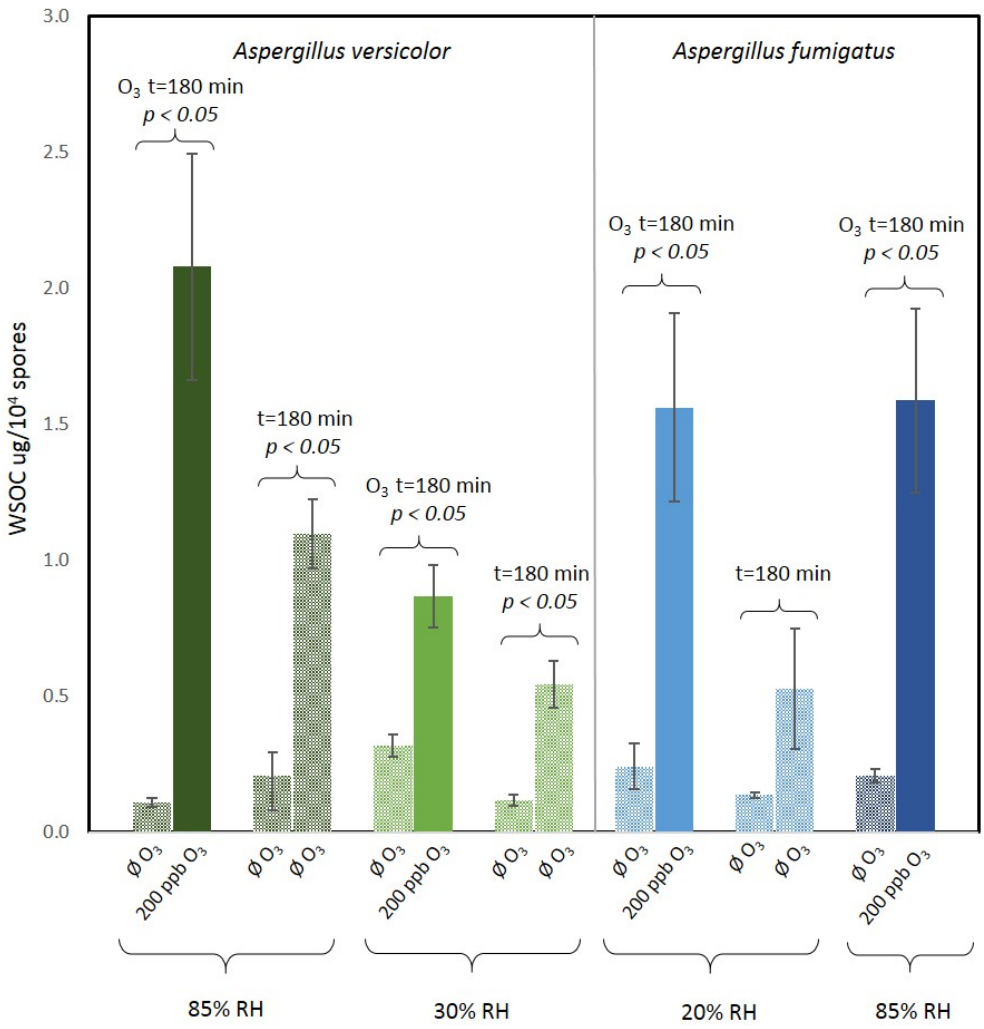

Figure 0-3. Average WSOC liberated from airborne *Aspergillus spp.* spores (n=3, error bars are SD). Patterned bars indicate averaged responses in the absence of ozone (▒) and solid-filled bars correspond to ozone exposed samples (■). Aspergillus versicolor are dark green (■) for 85% RH, and light green (■) for 30% RH. Aspergillus fumigatus are displayed in dark blue (■) for 85% RH, and light blue (■) for 20% RH. P-values are reported for significant differences between initial WSOC measurements (no ozone) and after an additional 3 hour suspension (with or without 200 ppb ozone exposure).

WSOC liberation was determined for both whole spores (simply liberated from the spore surface into water by gentle agitation), and for lysed spore. It should be noted that collected

spores encountered physical shear stress, but not rupture, during the collection process (high impinger flow rates); and if lysed by bead-beating, an additional shear stress from small borosilicate beads during the lysate process. This bead-beating method was adopted from a widely-accepted protocol used to lyse cells in laboratory and environmental samples and kept consistent over all sample processing. The effect of WSOC liberated from the just the fungal spore wall, as opposed to the spore lysate, was investigated with *A. versicolor* spores in this work. This is an important comparison to demonstrate the potential contribution intact whole spores may have on WSOC measured from environmental samples. The results from this work indicate that a baseline (no ozone) spore residence time of 1 hour at low RH (< 30%), reporting spore WSOC mass per 10^4 spores, from whole and lysed *A. versicolor* spores was 0.11 μg and 0.16 μg WSOC, respectively. After a subsequent 3 hour 200ppb ozone exposure (600 ppb-hr), whole and lysed *A. versicolor* spores respectively liberated 0.44 μg and 0.88 μg of WSOC.

When this same exposure scenario was repeated at 85% RH, the WSOC liberated from whole and lysed airborne *A. versicolor* spores was respectively 0.06 μg and 0.12 μg per 10^4 spores, after an hour of aerosol residence time in the absence of ozone. However, an additional three hours of ozone (200ppb) exposure substantially increased the WSOC liberation per 10^4 *A. versicolor* spores to 1.71 μg and 2.14 μg, for whole and lysed spores respectively. These results suggest that in both the presence and absence of ozone, the fraction of WSOC readily liberated from the surface of an airborne spore can be a significant contributor to the overall WSOC mass, and sensitive to humidity levels on relatively short time scales (1 hour). Without the presence of ozone at low RH (30%), the WSOC liberated from the spore surface makes up approximately 2/3 of the total WSOC mass that could be recovered from lysed spores; and at high RH (85%)

conditions with no ozone, the liberated WSOC fraction contributes approximately half of the total WSOC mass recovered from lysed spores. However, when ozone is present, the overall WSOC measured from both whole and lysed spores is substantially higher, but the contribution of WSOC liberated from the spore surface to the total WSOC from the entire lysed spore is substantially less, suggesting that ozone modifies biopolymer properties below the spore surface.

Table 0-1 lists the magnitude of change between means of the total WSOC mass liberated from aerosolized spores during suspension, either in the presence or absence of ozone. The smallest fold change reported below is defined here as the difference encountered with one standard deviation removed from the mean WSOC measured prior to exposure/aging and one standard deviation added to the mean WSOC measured after a 3 hour suspension in either the presence or absence of ozone (i.e. fold change encountered between the error bars, to account for variances).

Table 0-1. Fold change in WSOC liberated by fungal spores after 4 hours of aerosol suspension, with or without the presence of ozone (in the final three hours)

Type of aerosolized fungal spore	**RH [%]**	**Ozone [ppb]**	**Mean fold change**	**Smallest fold change [($Post_{Avg}$-SD) – (Pre_{avg}+SD)]**
A. versicolor	85	200	19	13
A. versicolor	85	0	5	3
A. versicolor	30	200	5	4
A. versicolor	30	0	5	3
A. fumigatus	20	200	6	4
A. fumigatus	20	0	4	2
A. fumigatus	85	200	8	5

The largest differences seen between measurements taken at the beginning and end of an ozone exposure experiment was a 19-fold increase in WSOC liberated with *A. versicolor* at 85%RH, after a 3 hour exposure to 200ppb. At low RH, the differences were significantly less. Culture maturity (spores between two weeks and three months old) had little effect on the magnitude of WSOC liberation in response to humidity conditions when ozone was absent. As judged by WSOC liberation, *A. fumigatus* was less sensitive to ozone than *A. versicolor*, but the difference in sensitivity diminished at low RH.

5.4.2. Asp f 1 and Total Water Soluble Protein for *Aspergillus fumigatus*

Quantitative MARIA analysis of the widely recognized *Aspergillus spp.* allergen, Asp f 1, was conducted to isolate the potential effects of ozone associated weathering at higher relatively humidity levels. As judged by this standardized immunoassay, the Asp f 1 allergen protein content was normalized by *Aspergillus fumigatus* spore count, and the corresponding total water soluble protein content of these spores (referred from here on as simply "protein"). All allergen and protein values reported here are for those liberated directly from the whole spore surface into solution (not lysed). To maintain high enough spore concentrations to exceed the lower limit of detection for Asp f 1 and protein measurements, all experiments were conducted at 85% RH with a 1 hour suspension time, where initial sampling was conducted before exposure or aging and final sampling occurred after an hour of suspension. Tested ozone concentrations during 1 hour exposures included: 0 ppb, 600 ppb (equivalent to 3 hours at 200 ppb), 1,000 ppb, 1200 ppb, and 7,500 ppb. Additional culture control samples for allergen and protein content

were reported (from the mother culture, not aerosolized). Figure 0-4 presents the Asp f 1 content (nanograms) per *A. fumigatus* spore on left axis reported on a log scale, while the liberated protein content for the same exposure condition, in nanograms per spore, is reported on the right axis, reported on normal scale. Experimental triplicate measurements are reported as means, with error bars as standard deviations; duplicate measurements for a given exposure condition are shown as separate points.

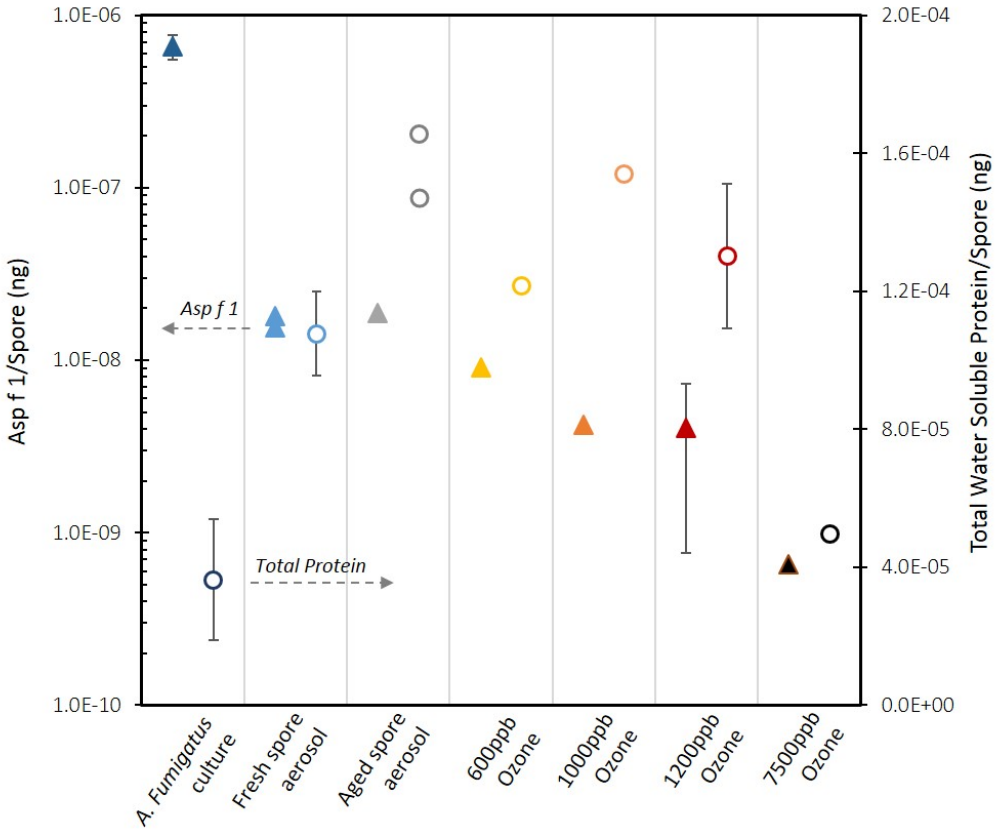

Figure 0-4. The Asp f 1 (triangles, left axis) and total water soluble protein (circles, right axis) reported for *Aspergillus fumigatus* spores. Triplicate measurements are reported as means, with error bars as SD.

The spore normalized allergen content (Asp f1) significantly decreases by more than two orders of magnitude when comparing spores harvested directly from the *A. fumigatus* culture and that immediately following spore aerosolization. The opposite trend was true for protein content, where freshly aerosolized spores released more than double the amount of protein (per spore) than those immediately following culture harvest. There was no significant difference in the Asp f 1 content of spores immediately following aerosolization and those suspended for 1 hour (aged); however, there is a decreasing trend in the measureable Asp f 1 levels after exposure to increasing levels of ozone. There was no significant difference in protein levels liberated from spores until the most extreme ozone exposure at 7,500 ppb (demonstrating extreme oxidation potential). Figure 0-5 highlights how Asp f 1 varies with respect to protein with different exposure conditions, and note that Asp f 1 is included in the protein measurement.

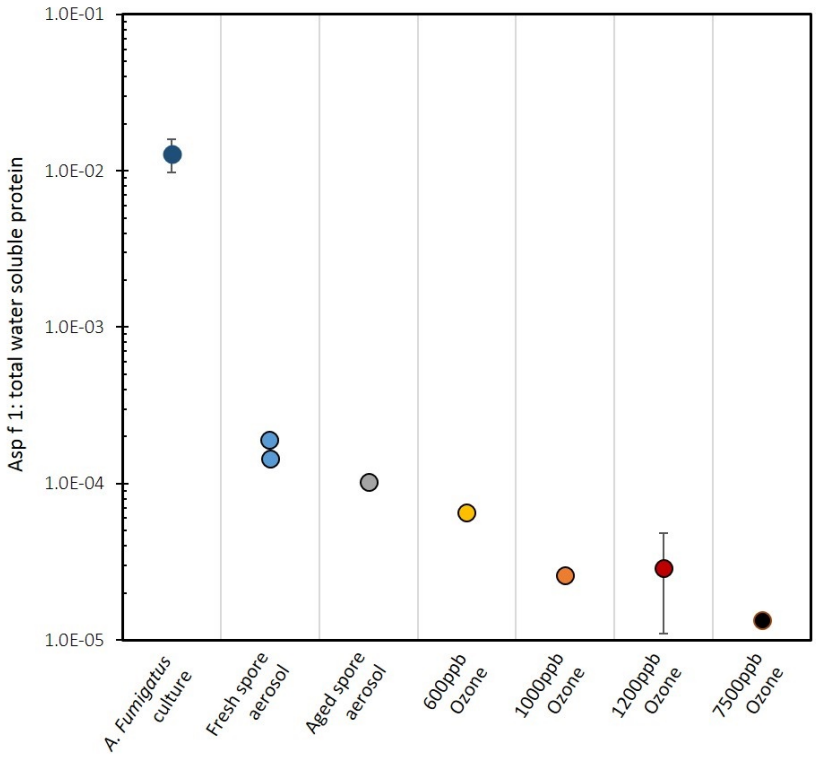

Figure 0-5. Ratios of Asp f 1 to total water soluble protein content per *Aspergillus fumigatus* spore, reported for harvested and aerosolized spores. Aerosolized spores were suspended in 85% RH conditions for 1 hour at the specified conditions. Triplicate data points are reported as means with error bars as SD.

A clear decrease in the Asp f 1 fraction of total protein occurs when freshly harvested *A. fumigatus* spores were aerosolized. The contribution of Asp f 1 to the total spore protein content continued to decrease in response to increasing levels of ozone. Although the amount of Asp f 1 content per spore did not change significantly after an hour without ozone present (baseline), a

noted decrease in Asp f1 contribution to the total protein content per spore occurred due to the increase in protein liberated with suspension time.

Figure 0-6 displays the Asp f 1 mean values on a log scale (n=3, SD error bars) for cases where spores were freshly harvested, freshly aerosolized in the absence of ozone, and then exposed to 1,200 ppb ozone for 1 hour at 85% RH.

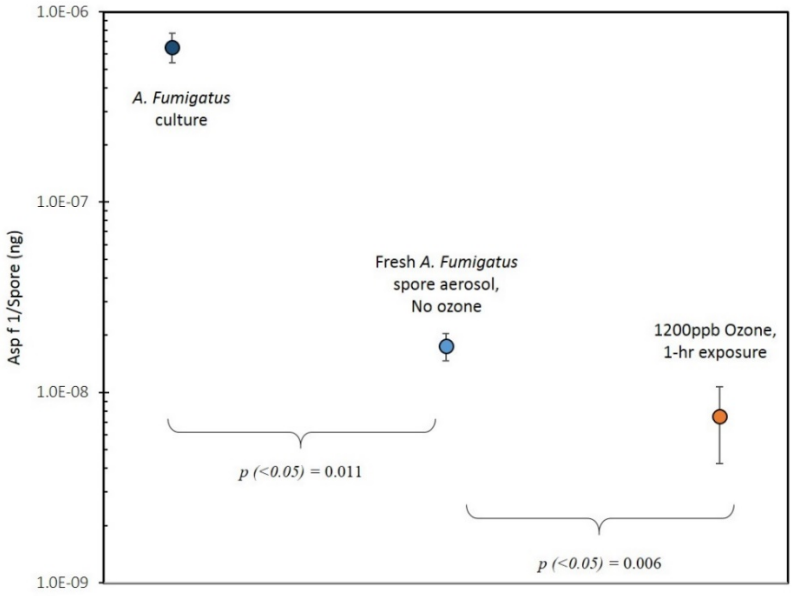

Figure 0-6. Replicates (n=3) of Asp f 1 measurements for fresh cultured *Aspergillus fumigatus* spores (dark blue), aerosolized spores with no ozone exposure (light blue), and aerosolized spores with ozone exposure (orange). Significance (P-values) between sample sets was determined from two-sample Student's t-tests (α=0.05).

There is a significant decrease in Asp f 1 per spore, as judged by the Student's t-test, between those directly harvested from cultures (M = 6.55×10^{-7} ng/spore, SD= 1.16×10^{-7} ng/spore) and those immeditaley aerosolized without ozone present (M= 1.75×10^{-8} ng/spore,

SD= 2.87×10^{-9} ng/spore), p-value = 0.011. Additionally, there was also a significant decrease in Asp f 1 content between aerosolized spores not exposed to ozone and those exposed to 1,200 ppb ozone for 1 hour (M= 4.02×10^{-9} ng/spore, SD= 3.25×10^{-9} ng/spore), p-value = 0.006.

5.4.3. Fungal Spore Enzyme β-N-acetylhexosaminidase (NAHA) Activity

Aerosolized spores from two fungal culture types, *A. fumigatus* and *A. versicolor*, were tested for specific aminidase enzymatic activity under different humidity and ozone exposure conditions. Fungal culture maturity was also considered with respect to NAHA activity, Figure 0-7. Sequential triplicate aerosol samples were collected at the beginning and the end of each chamber experiment; including after 3 hours of aerosol aging in the absence of ozone, or 3 hours in the presence of ozone at 200 ppb (600 ppb-hr ozone exposure).

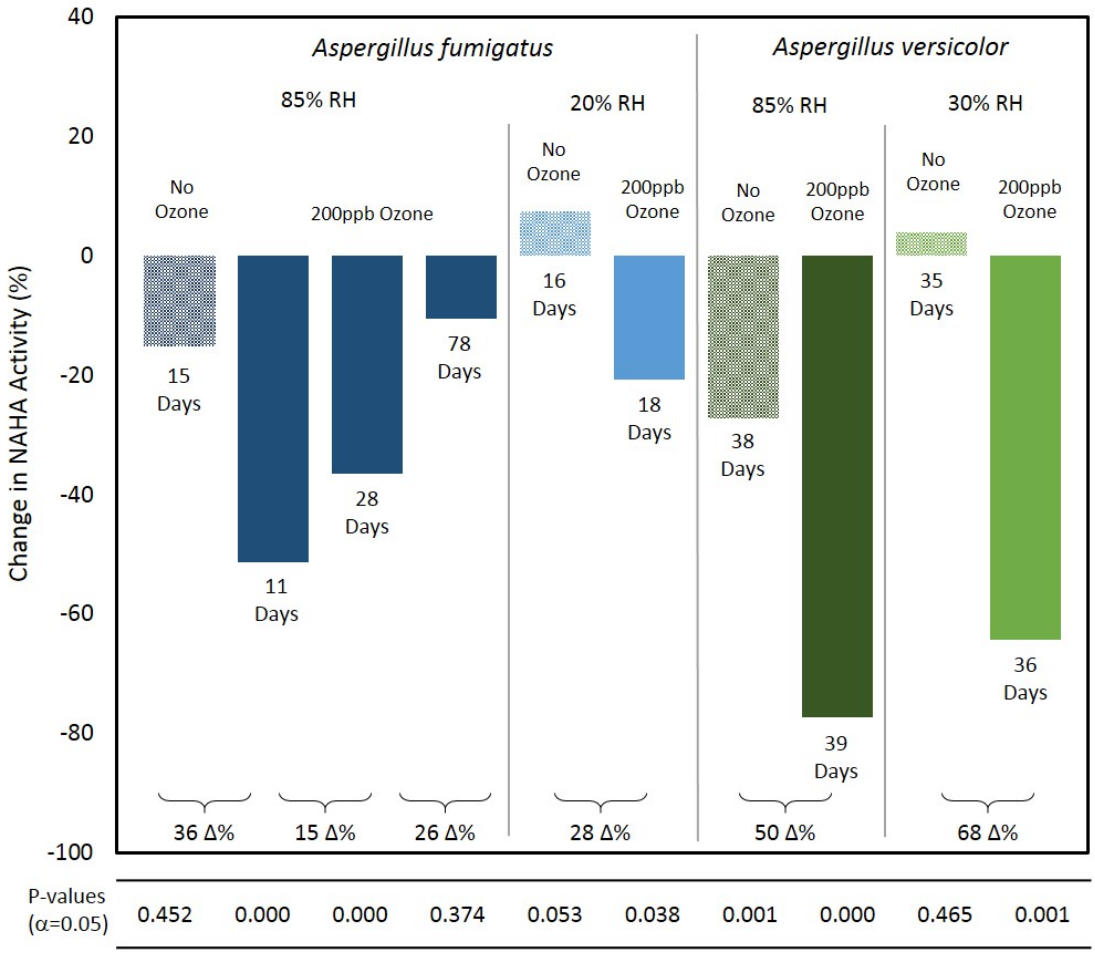

Figure 0-7. Change in NAHA activity for aerosolized *Aspergillus fumigatus* and *Aspergillus versicolor* spores in the presence and absence of ozone. Spore type, RH levels, and ozone concentrations are indicated on the top section of the graph, while culture maturity (days old) and the percent difference in NAHA activity between exposure conditions are shown in the lower portion of the graph. Patterned bars indicate averaged responses in the absence of ozone (▒) and solid-filled bars correspond to ozone exposed samples (■). *Aspergillus versicolor* are dark green (■) for 85% RH, and light green (■) for 30% RH. *Aspergillus fumigatus* are displayed in dark blue (■) for 85% RH, and light blue (■) for 20% RH P-values, for significance between freshly aerosolized spores and aged/exposed spores are reported below the graph for each case.

All experimental conditions influenced changes in NAHA activity; however, not all were statistically significant (p-values comparing significance between initial and final measurements for each experimental scenario are reported at the bottom of each condition). The following factors affecting NAHA activity were investigated: between species (*A. fumigatus* and *A. versicolor*), with fungal culture maturity (reported as 'Days' old), between high and low RH conditions, and after a 3 hour suspension in absence or presence of ozone at 200ppb (600 ppb-hr ozone exposure). Changes in NAHA activity occurred to a greater extent in *A. versicolor* than *A. fumigatus* with variable ozone and humidity levels. At low RH, there was no significant change in NAHA activity for either species in the absence of ozone over the 3 hour suspension times. However at high RH, *A. versicolor* responded with significant decreases in NAHA activity (27%) after 3 hours of suspension time without ozone present. Additionally, *A. versicolor* spores exposed to 200ppb ozone for 3 hours demonstrated a significant NAHA activity decrease of 64% at low RH and a decrease in activity by 77% a high RH.

As with WSOC, RH did not have as big of an impact on NAHA activity in *A. fumigatus* as with *A. versicolor*. However, *A. fumigatus* experienced significant decreases in NAHA activity with the presence of ozone for fungal cultures 11 days old and 28 days old, but 78 day old *A. fumigatus* did not present a significant NAHA activity reduction. These results suggest that along with relevant environmental exposure conditions (RH and ozone levels), an intrinsic loss of NAHA activity can occur with increasing fungal culture maturity.

5.5. Discussion

Using airborne spores from ubiquitous of fungi species as bioaerosol models, this chapter presented a cohort of evidence demonstrating relevant environmental exposure conditions can significantly modify biopolymers in and on the surface of airborne microbes. This conclusion was drawn from independent observations of the response important catalytic and allergenic proteins, present in two common species of *Aspergillus* spores, after exposure to environmentally-relevant oxidative conditions. These results demonstrate potential influences anthropogenic ozone have on specific fungal spore biopolymer integrity, as well as bulk WSOC properties present in bioaerosols. Specific ozone influence on the aminidase enzyme system (NAHA) that is integral to the germination process, was demonstrated on both young and aged *Aspergillus spp.* spores. This work further demonstrated the potential impact ozone on widely cited specific *Aspergillus* allergens of particular concern to the public health arena. While the literature contains sound immunological methods to identify and quantify *Aspergillus* antigens from the indoor environment, there is a paucity of studies that are able to reliably recover and measure these allergens from aerosol samples; thus, this work was designed to fill this knowledge gap by adapting the most modern immunological tools for actual bioaerosol characterization. These observations presented here form the biochemical basis that challenge the main hypotheses presented in this dissertation. Previous chapters presented complementary, but independent optical approaches to challenge these same hypotheses.

Characterization of aerosol WSOC has recently been leveraged for source apportionment driven by environmental health concerns. Determining the contribution bioaerosols can have to the overall ambient aerosol pool is an important link in understanding their role in the overall

aerosol mass balance and reactive potential of biogenic organic carbon in indoor and outdoor environments. Here, WSOC measurement and characterization was utilized as a tool for observing changes in airborne *Aspergillus* spores during ozone exposure. In this context, this work demonstrated the potential impacts a range of atmospheric conditions can have on the WSOC liberation of common bioaerosols. The WSOC liberated from airborne spores was shown to significantly increase with suspension time in almost every scenario tested. Ozone clearly induced enhanced WSOC liberation by airborne fungal spores; the magnitude of which was influenced by varying RH levels.

The total carbon content of a number of different fungal strains was has been previously estimated by Bauer and coworkers [129]. When normalized by spore count, the total carbon content of *Aspergillus niger* and *Aspergillus versicolor* previously reported (0.14 ug spores and 0.07ug, respectively) agrees with the magnitude of the WSOC recovered from the *Aspergillus* spores cultured in this work (prior to aerosol aging or ozone exposure). As judged by WSOC liberation, the effects of RH were greater on *A. versicolor* with and without ozone exposure than with *A. fumigatus,* most likely due to differences in fungal spore wall composition. The phenomenon of increasing liberation of WSOC from microorganisms exposed to ozone has been previously reported in drinking water treatment research for a number of microorganisms [130, 131]. However, its analogy in the atmospheric environment had yet to be investigated, providing the motivation for this work. In the potable water treatment engineering sector, the ozone-induced liberation of organic carbon from microbes is common, and simply quantified as dissolved organic carbon (DOC).

In aqueous environments, for example, common algae species (e.g. *Scenedesmus spp.)* exposed to ozone had a 4 fold increase in DOC released (WSOC) with a dose of 1 mg/L ozone after 30 minutes of exposure (30 mg-min/L), and a 5 fold increase with a 30 minute exposure of 3 mg/L ozone (90 mg-min/L) *[130]*. For context, 200 ppb gaseous ozone in the air for 180 minutes would be the equivalent of an aqueous exposure 0.085 mg-min/L in the absence of any other ozone demand. This is an ozone exposure robust enough for a 2-log inactivation of *E. coli* and Rotavirus under common potable water conditions [132].

How the atmosphere hosts physical and chemical disinfectants is dictated in part by its ability to hold variable amounts of water vapor through a relatively large range (RH). Relative humidity has a tremendous effect on bioaerosol inactivation concerning UV exposure [133]. The degree to which microbial biopolymers are hydrated changes their steric and electrochemical configurations (i.e. DNA and protein structure), and can in turn influence their specific UV absorbance and photoreactivity. The data from these studies suggest a responsive analogy exists concerning airborne ozone-microbe interactions under the range of RH and culture conditions tested here.

Equilibrium occurs between atmospheric water vapor and whole cell microbial bioaerosol on the order of 10 minutes under high humidity conditions—significantly less time is required for equilibrium at low RH levels [133]. Because of their residence time, the spores aerosolized in these chamber studies were in equilibrium with chamber humidity throughout these ozone exposures. With the *Aspergillus spp*. tested here, RH levels had a significant influence on the amount of WSOC these spores liberated with suspension time depending on the presence or absence of ozone. When challenged with ozone, the contribution of the spore wall protein to the

liberated pool of WSOC increased markedly in response to RH for the same ozone exposure, from 50% (low RH) to 80% (high RH) of the total WSOC pool. These results imply biopolymer hydration can enhance the impact of ozone on airborne microbes under these conditions.

In the context of allergen and protein response to ozone exposure, humidity levels have also been noted to influence protein modification. Humidity can serve to hydrate proteins, or facilitating the production of additional reaction intermediates, and can increasing protein nitration in the presence of O_3 and NO_2 [6, 111]. Ozone has been reported to have significant effects on the water soluble protein content of aerosolized pollen grains, depending on the species and ozone concentration [90]. In this work, the soluble protein content of fungal spores increased over an order of magnitude upon aerosolization, but did not decrease until ozone exposure were sustained at 7500 ppb for at least an hour. However, the spore normalized allergen (Asp f1) content did significantly decrease during aerosolization, a critical observation which is in agreement with Arruda et al. 1992 (noting disrupted fungal cultures presented a 10^3 fold lower Asp f 1)[134]. Further, this work found that after aerosolization, decreases in specific Asp f 1 allergen content were observed in response increasing ozone exposure, both per spore and in relation to the total soluble protein content.

Related research in this arena has reported the recovery Asp f 1 allergen mainly from settled dust samples, and the quantitative work in the aeroallergen arena has been limited in part due to the particulate biomass required to reach allergen detection limits. Those that have quantitative reports of Asp f 1 allergen levels recovered from indoor samples usually do so from relatively large masses of settled dust; but, in general there is low level of success in detecting Asp f 1 in collected aerosol [103]. This is the first work to document changes in the specific

allergen Asp f 1 in response to environmentally relevant oxidizing conditions, and incorporated the modified immunoassay, MARIA [125], for the analytical sensitivity to demonstrate significance. Further, an emerging condensation particle capture technique (the Spot Sampler) was used to collect, concentrate and preserve allergen-containing spores from the air during experiments. This was the first adaptation of this technology for quantitative biopolymer characterization.

At high RH levels, increasing ozone exposures was associated with corresponding decreases in the Asp f 1 content of *A. fumigatus* spores. In other allergen related exposure studies, specific protein modifications including acidification, nitration, or basic inflammatory responses have been observed where immobilized pollen grains, or their extracts, were exposed to high RH levels and oxidizing pollutant conditions; however, none of these have convincingly demonstrated allergen modification in the aerosol phase [6, 90, 111]. Using allergen reporting protocols other than MARIA, related studies suggesting oxidative modifications to pollen-associated allergens are summarized in the table below [6, 89, 90, 107].

Table 0-2. Overview of pollen oxidations studies from the literature

Allergen	Oxidizing Conditions	Major Outcomes	References
Timothy grass pollen	O_3 (100ppb, 4hrs), NO_2 (2000ppb, 4hrs), SO_2 (2000ppb, 4hrs), Dry air (low RH)	No change in soluble protein (judged by Bradford assay); Decrease in allergen recognition by IgE; Acidification of allergens	Rogerieux et al. 2007
Acer negundo pollen	NO_2 (~100-300ppb, 6hrs), SO_2 (~100-300ppb, 6hrs), RH not specified	A higher IgE recognition of exposed pollens; Pollen protein content lower in SO_2 exposed and higher in NO_2 exposed (Bradford assay); Decrease in germination	Sousa et al. 2011
Zinnia pollen	Urban air exposure, 10-20 days	Protein content decreased (Lowry method); IgE response increased with exposed pollen; Allergic sensitivity doubled with exposed pollen (skin prick test)	Chehregani et al. 2004
Ragweed pollen	O_3 (100nl/L, 5 hrs x 7days) 60-75% RH	Increase in ROS-generating enzyme NAD(P)H oxidase; detection of allergen Amb a 1 not affected (no decrease, judged by mRNA); No change in protein content (Bradford assay)	Pasqualini et al. 2011
A. negundo; P. x acerifolia; Q. robur pollens	O_3 (30ppb, 60ppb & 230ppb, 6 hrs) RH not specified	IgE binding increase for A. negundo and Q. robur, IgE decrease for P. x acerifolia (signaling species dependent modification); Protein content decreased or no change depending on species (Bradford assay)	Ribeiro et al. 2013
Birch pollen extract	O_3 (50, 100, 200 ppb, 4hr), NO_2 (50, 100, 200 ppb, 4hr), Dry air & 40%RH	Largest increase in protein nitration, as judged by enzyme immunoassays, occurred with 40%RH and combined O_3 and NO_2	Franze et al. 2005

Decreases in Asp f 1 allergen detection may occur after ozone exposure because of the oxidation of specific aromatic amino acids defining the allergen protein sequence. Because of their structure, different amino acids are more susceptible to react with ozone than others. Sharma and coworkers [135] have cited that tryptophan residues, depending on their location, are more likely to react with ozone than most other amino acids. Peccia et al. (2001) demonstrated that bioaerosol cellular uptake of atmospheric water (humidity) may change the nature of the cell

wall, or cell-bound biopolymers, such that the impact of UV and reactive gases on bioaerosols, may vary significantly under different RH conditions [133]. In this work, the relationship between RH and NAHA activity, as well as WSOC content, clearly demonstrate the influence humidity can have on the character of the bioaerosol in the presence and absence of ozone. Because the composition biopolymers present in the fungal spore wall varies between species [136], it follows that the extent of RH influence on biopolymer modification by ozone will also vary by species. In the case of both NAHA activity and WSOC content, higher RH seemed to play a larger role in the extent of biopolymer modification for *A. versicolor* than for *A. fumigatus* – and though these species are closely related as judged by genetic sequences, their protein composition varies.

The NAHA enzyme present in fungal spore walls, has been quantified in air samples in a number of water damaged indoor environments as a means to assess fungal exposure from indoor air [113, 120-122]. The NAHA enzyme is responsible for the second step of a two-component chitinolytic enzyme system that degrades chitin, a structural biopolymer, to aid in the reorganization of the cell wall for germination [137]. Specifically, NAHA converts chitooligosaccharides, formed from the degredation of chitin polymers by a chitinases, into monomers. Both NAHA enzymes and chitin polymers can be found widely in animal tissues, insects, plants, bacteria, and fungi [137]. The specific NAHA enzyme associated with fungi is unique in that it is present as a dimer (intracellular bacterial NAHA is monomeric) and contains an extra loop structure for stability and protection of the active binding site on the enzyme [138]. At high humidity, atmospheric water can sorb to biopolymers, including enzymatic proteins, potentially changing their steric and electrochemical configuration.

In the context of pharmaceutical applications, the stability of many aerosolized (nebulized) proteins and enzymes have been noted to quickly degrade due to shear stress and forces between microdroplets at the water-air interface [139, 140]. Sorbed water can enhance structural changes to the protein (unfolding) and possibly decrease the stability of the structural protein environment [140] around the NAHA enzyme active site, potentially affecting the ability for the NAHA enzyme to bind to a substrate [138]. If ozone is introduced at high RH, the active site of this enzyme may be more vulnerable to oxidative attack due to hydration induced changes in the protein structural conformation. Consistent with this report is the loss of lysozyme activity, another ubiquitous lytic enzyme, which can be significantly decreased with ozone exposure [141, 142]. Activity loss in lysozyme during ozone challenges has been attributed to the oxidation of tryptophan residues present in this enzymes active site, which then resulted in a decrease in the ability to form an enzyme-substrate complex [141]. The active site present in NAHA has at least two tryptophan residues important for substrate binding [138], and may have a similar mechanism of liability to ozone.

Ozone exposure in the range between 5 and 60 ppm has been reported to have an impact on the ability of spores to germinate [91]; however, the duration of exposure and mechanism behind this inhibition has not been described. Reductions in NAHA activity (a necessary component in cell wall reorganization during germination) may contribute to this phenomenon. Indeed, aminidases are an important family of proteins, many of which are conserved across the fungal world, and thus these results have greater ecological implications for fungal propagation in air sheds that carry spores through polluted air on time scales of hours to days. Converging independent lines of evidence reported in this work have successfully demonstrated the potential

of environmentally-relevant levels of ozone and RH to modify biopolymers present in and on whole cell bioaerosols; and may inform potential ecological, environmental and human health implications from anthropogenic air pollutants.

CHAPTER 6. WILDFIRE AEROSOL CHEMICAL AND FLUORESCENCE SIGNATURES: INDICATION OF ENVIRONMENTAL AEROSOL PROCESSING AND BUILDING INFILTRATION POTENTIAL

6.1. Introduction

The work in this chapter touches on both Hypothesis I and Hypothesis II by exploring potential biochemical and fluorescence modification of environmental aerosols during extreme oxidation processes encountered during wildfire combustion and subsequent atmospheric transport of wildfire emissions. Types of size segregated particulate matter (PM) collected during a local wildfire including size segregated mixtures of organic particulate material, secondary organic aerosols condensed from biomass combustion VOCs (biogenic aerosols) and microbial and plant debris (bioaerosols) either combusted, partially combusted, or simply lifted into the air via convective action.

The increasing frequency and magnitude of wildfires has raised concern over their potential impacts on nearby indoor environments. Here, a high-occupancy university structure served as a model to demonstrate the performance of a modern building envelope against pollution challenges presented by sub-alpine wildfire. Size segregated particulate matter (PM10 and PM2.5) was simultaneously collected indoors and outdoors before, during and after a proximal wildfire. As judged by time-resolved profiles of elemental carbon, organic carbon, and the fluorescent fraction of water soluble organic carbon, wildfire emissions penetrated the building envelope regardless of high-efficiency filter operations. Organic carbon levels in PM2.5 were comparable to those recovered from PM10 fractions suggesting that the majority of the organic content was in the finer aerosol fractions. Analysis of fluorescence profiles of

excitation-emission matrices (EEMs) of the size-segregated water soluble organic carbon (WSOC) fraction, and levels of liberated PM WSOC were conducted in a similar fashion as for the controlled bioaerosol studies in Chapter 3 and Chapter 4. As the wildfire progressed, the formation of distinct humic-like signatures in fluorescence spectra dominated the profile and became more apparent in all aerosol size modes from both outdoor and indoor samples.

6.1.1. Biomass Burning Impact on Outdoor and Indoor Environments

Over the past few decades, wildfire occurrence and burn area has been significantly increasing in the western United States [143]-[144]. The frequency of large wildfire events have been predicted to increase due to increases in spring and summer temperatures, and has been noted that 72% of burn area has occurred in early snow melt years [Westerling 2006]. In fact, the annual mean burn area has been predicted in increase by 175% by 2050 [Spracklen 2009]. During wildfire events, concentrations of coarse and fine fractions of particulate matter (PM), as well as gaseous pollutants, can be significantly increased. Increases in burn area are also estimated to double wildfire carbonaceous aerosol emissions by 2050, and dominate the summertime estimated increases in aerosol organic carbon (20% overall increase from climate change, 75% of that from wildfire contribution) and aerosol elemental carbon (overall summertime increases by 40%, where 95% contributed by wildfire) [Sprecklen 2009].

Wildfire emissions, including aerosols and other hazardous constituents [145, 146], can penetrate indoor environments and present an increased environmental health risk [147-149]. Wildfire emissions can include CO_2, CO, ozone, VOCs, SO_2, NO_X, PAHs, secondary organic

aerosols (SOA), particulate matter (PM), metals, and water-soluble components, the extent of formation and contribution to overall emissions are based on combustion characteristics (flaming vs. smoldering), the nature of the fuel, proximity and meteorological conditions [56, 150-153]. During wildfire events, reported elevated indoor levels of $PM_{2.5}$ were between 58% and 100% of outdoor levels [148], and indoor penetration of PM between 100 nm and 300 nm has been measured [147], a size fraction of particular concern for respiratory health [146, 154]. Respiratory health studies indicate exposure to wildfire PM can lead to cellular membrane and DNA damage [Leonard 2007], induce strong pro-inflammatory response and increased oxidative stress [wegesser 2009;Wong 2011], and increased frequency of emergency room visits for cardiovascular and respiratory syptoms, including asthma, COPD, acute bronchitis, and pneumonia [Kochi 2010; Delfine 2008]. However, in light of public health recommendations to remain indoors during fire events, limited work has been conducted on the effectiveness of the built environment to protect occupants from wildfire emissions.

Depending on intensity and duration, wildfires impact the elemental carbon (EC) and total organic carbon (OC) loads of proximal aerosol in all size modes, as well as the water soluble (WSOC) fraction [58, 150, 155]. The WSOC fraction of PM, has been receiving increased attention in broad atmospheric contexts, due to the potential impact on climate (cloud nucleation and radiative balance) [56], visibility [57], and public health [58]. Carbon emissions from biomass burning have been reported to contain as much as 72% WSOC [155, 156], and increase by a factor of 2 on fire days over baseline days [58]. The increased ratio of aerosol WSOC to OC has been used as an indicator of the presence of biomass burning emissions. There has been a noted spectroscopic resemblance of lignin breakdown products present in biomass

burning emissions WSOC, to humic-like substances reported in aquatic research [61]. The HUmic-LIke Substances (HULIS) present in atmospheric aerosols have unique optical properties, and have been gaining interest due to their strong associations with biomass combustion and potential role in atmospheric processes [57, 157]. Up to 70% of the compounds present in WSOC derived from biomass burning aerosols have been noted to be associated HULIS [Mayol-Bracero 2002]. Many identified compounds associated with HULIS have included monocarboxylic acids, and polycarboxylic acids most likely sourced from combustion processes (thermal breakdown) involving polymeric carbohydrates and lignin, as well as convective lofting of humic matter from soil and decaying leaf debri into the air [Mayol-Bracero 2002]. Recent work has utilized fluorescence excitation-emission matrices (EEMs) in characterizing airborne WSOC, including HULIS, from different environments [15, 17, 18, 60, 62]; none however, have used EEMs to understand the fate and transport of wildfire aerosol.

In this work, EEMs were constructed from longitudinal wildfire aerosol samples to compliment conventional carbon signatures in tracking the influence of wildfire aerosol in the built environment. Size segregated aerosols (PM_{10} and $PM_{2.5}$), collected during a local wildfire in the Rocky Mountain Front Range, were analyzed for their content of elemental carbon (EC), total organic carbon content (OC), and water soluble organic carbon (WSOC), along with fluorescence properties (EEMs). A high-occupancy university building, vacant during the course of the wildfire, served as a model to determine the performance of a modern building envelope, fitted with a high efficiency filtration system, against the aerosol challenges presented by wildfire.

6.2. Chapter Specific Methods and Materials

6.2.1. Overview of Aerosol Sample Collection

Samples of indoor and outdoor particulate matter, ≤ 10 μm (PM_{10}) and ≤ 2.5 μm ($PM_{2.5}$), were continuously collected over 24 hour periods in June of 2012 (n=7), before and during a local wildfire. The wildfire started by lightning on 6/26/2012, lasting 8 days and burning over 300 acres. The burn area was approximately 4 km southwest from the building site in Boulder, Colorado (left panel of Figure 0-1), and predominantly migrated East (ESE) in response to the prevailing winds (right panel of Figure 0-1), with calm conditions approximately 33% of the time. Wind roses were generated with Lakes Environmental WRPLOT View (V.7.0.0) using meteorological data obtained from the University of Colorado ATOC Weather Network [158].

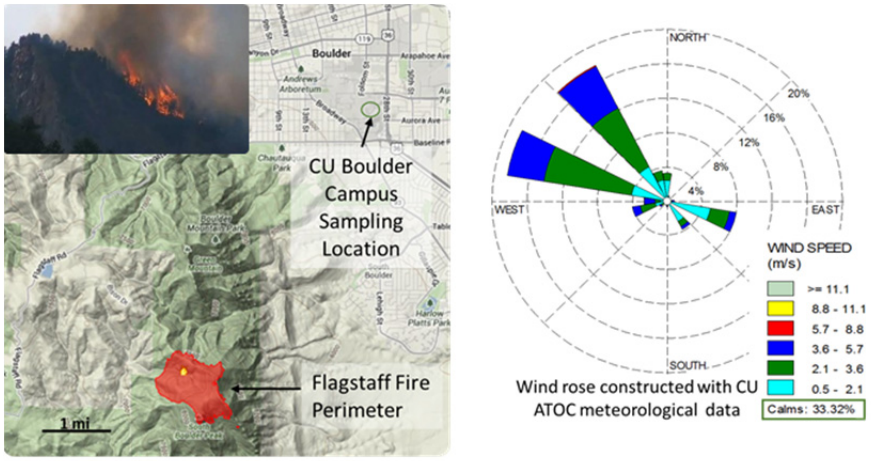

Figure 0-1. Location of the 2012 Flagstaff Wildfire with respect to the sampling location (left). A compilation of the wind direction and speed encountered over the course of sampling (right).

Concurrent sampling occurred in a vacant, centrally located university classroom (246 m^3), and on the roof of the same building using two Medium Volume Particulate Samplers (URG 3000) fitted with prebaked (at 550C for 3 hours) quartz fiber filters (Pallflex Tissuquartz, Pall Life Sciences) for a total flow rate of 66 lpm split through 8 channels, 4 channels for PM_{10} collection and 4 channels for $PM_{2.5}$ collection. The room air change rate was 6 hr^{-1} with filtered (MERV 8 and 14 bag filters in series) supply air sourced from outside. Figure 0-2a indicates the indoor and outdoor sampling sites, as well as the size and types of aerosols MERV filters of a similar rating as installed here can handle rated for the air handling system here. Figure 0-2b displays the outdoor sampling location, as well as how the filter holders are arranged in the URG sampler.

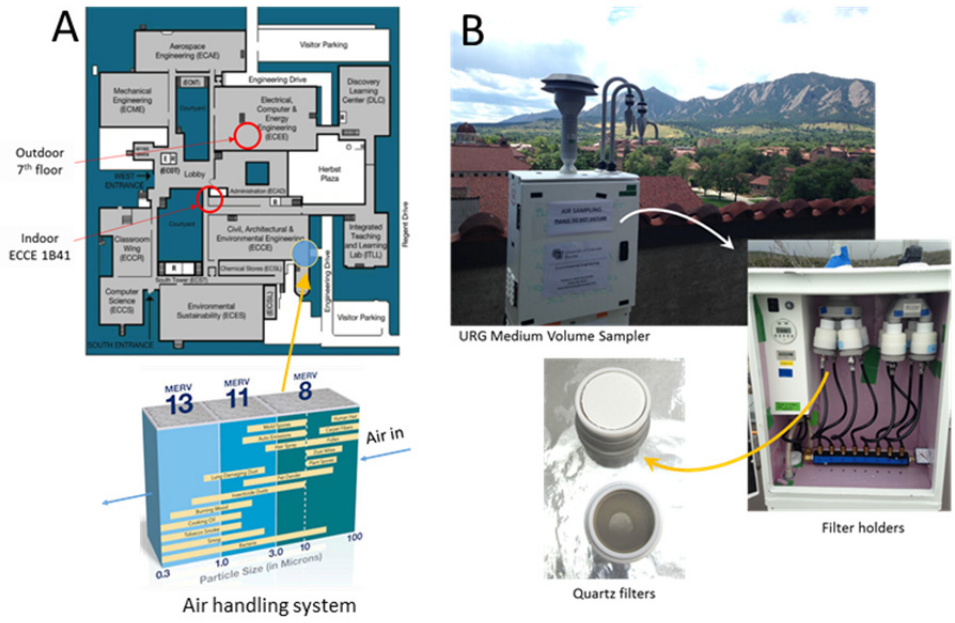

Figure 0-2. The location of both indoor and outdoor sampling sites, the supply outdoor supply air location, and ranges of particle the associated MERV filters can handle (A). The outdoor filter sampling setup with filter holders and quartz filters on display (B).

Additional baseline air sampling occurred in the same locations over three separate 48-hour periods during October of 2014 to verify baseline ambient and vacant indoor carbon concentrations on non-fire days when contamination from additional anthropogenic activity was reduced.

6.2.2. Collected Aerosol Sample Processing and Analysis

A 1.5 cm^2 portion of selected quartz sample filters were analyzed for carbon content (OC and EC) using a thermal-optical method [159] with a Lab OC-EC Aerosol Analyzer (Sunset Laboratory, Inc.). Aqueous extracts of the remainder of the filters were prepared in sterile water using a modified bead-beating extraction method [69]. Water soluble organic carbon (WSOC) content was determined from the aqueous extracts using a Model 700 TOC Analyzer (O.I. Analytical). See Chapter 5 for expanded methods for WSOC extraction and quantitation.

Fluorescence spectra of the aqueous extracts were measured using a Fluoromax-4 spectrofluorometer (Horiba), where the emission intensity was measured in 2 nm wavelength increments between 300nm and 550nm in response to excitation in 10nm increments in the range between 240nm to 500nm. The EEMs were constructed and corrected with MATLAB software (MathWorks). Instrument and inner-filter corrections, as well as Raman normalization and blank subtractions, were applied to all EEMs [18]. All EEM spectrum were smoothed with standard splines, and had their primary and secondary scattering removed, where the spectra in those regions were interpolated for presentation. Corrected and normalized EEMs are presented in Raman Units per microgram WSOC per cubic meter air (RU/[$\mu g/m^3$]). Degree of aerosol humification, adapted from a humification index (HIX) of aquatic natural organic matter[65], is

defined here as the ratio of emission intensities in the range between 435-480 nm, to that between 330-345 nm, where excited at 254 nm. The Freshness Index (known as BIX, referred to here as 'FRI') traditionally indicates a measure of freshly produced dissolved organism matter in aqueous environments by comparing an EEM region associated with recently created organic matter (ex:310 nm /em:380 nm) with older, decomposed organic matter (ex: 310 nm /em: 420-435 nm) [66]; however, in the context of this work a decreasing FRI value may be an interesting indicator of a more aged material present in the aerosol, or a certain stage of combustion during the wildfire (flaming vs. smoldering). Figure 0-3 illustrates an example EEM with the HIX and FRI regions highlighted with respect to other noted fluorescence regions.

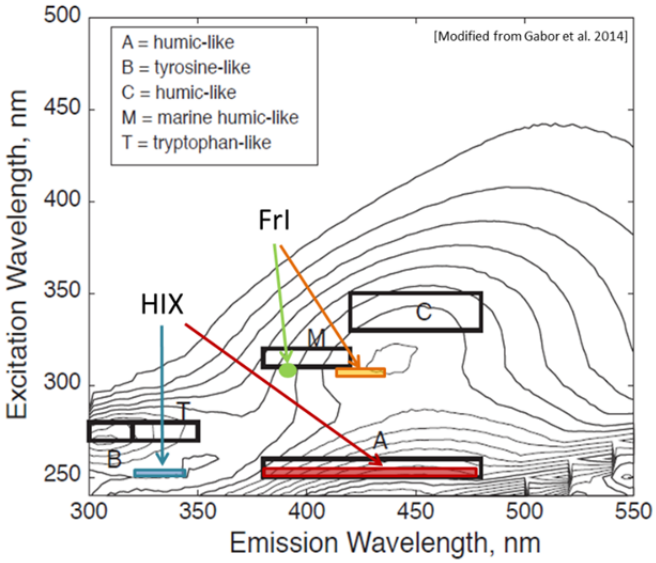

Figure 0-3. Fluorescence regions indicating the HIX and FRI indices on an example excitation-emission matrix, adapted from Gabor et al. 2014.

6.3. Results

6.3.1. Aerosol Carbon Concentration

The total aerosol carbon content, including its organic and elemental fractions, has been reported to substantially increase in aerosols generated by biomass burning[155]. Generally, WSOC inventories of airborne PM in all size fractions have been reported to increase with aerosol aging and oxidation; this may be accelerated by conditions sustained in biomass burning and wildfire events. The total outdoor and indoor carbon concentrations encountered in this study on wildfire days were more than double those experienced on baseline (no fire) days, including substantial increases in the OC and WSOC portion of the collected aerosols (Figure 0-4). Levels of EC only increased outdoors on the fire days, where OC and WSOC substantial increased in both locations for each size fraction on wildfire days. The slight elevated indoor PM concentrations over outdoor PM levels on baseline days was likely due to construction activity in other parts of the building - these were insignificant in light of the indoor PM2.5 increases that occurred as the fire progressed.

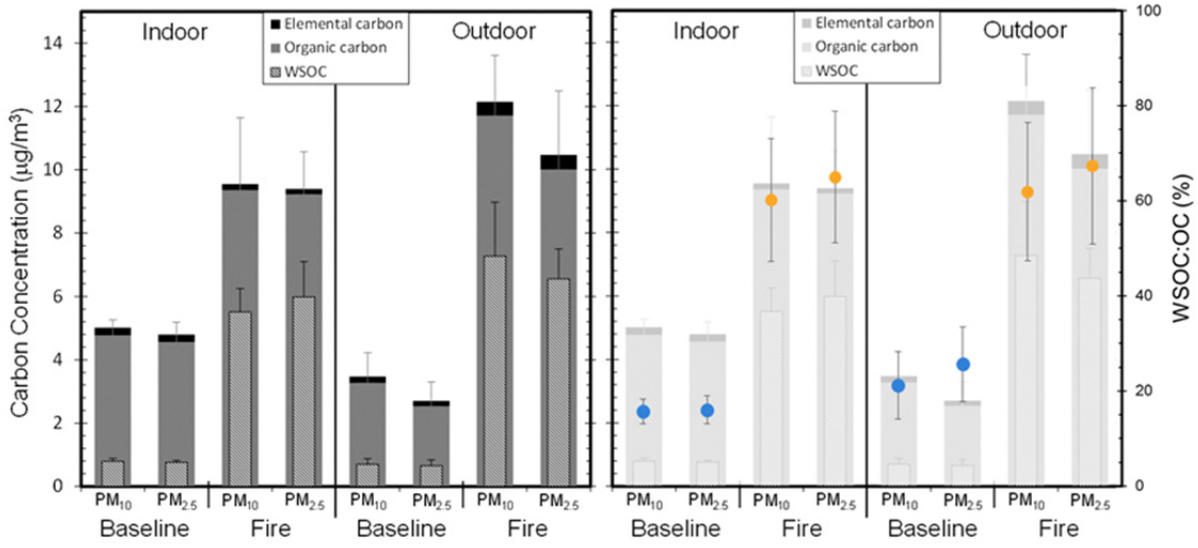

Figure 0-4. Bars represent average total carbon present in collected wildfire aerosol emissions, separated into average concentrations (error bar = +/- SD) of elemental carbon (black), organic carbon (grey), and water soluble organic carbon (patterned). Baseline (n=3, 48 hr samples) results are on the left half of each Indoor and Outdoor panel, while fire days results (n=7, 24 hr samples) are on the right half of the left plot. The right plot overlays the average percentage (error bar = +/- SD) of WSOC in OC contribution for each sample set on the data from the left plot.

The maximum contribution of indoor WSOC to OC during the wildfire was 81% and 82% for PM_{10} and $PM_{2.5}$ respectively, while the corresponding outdoor WSOC to OC maximum contributions were 81% and 87%. The WSOC contribution to OC was higher for $PM_{2.5}$ than for PM_{10}, indicating that WSOC dominated the fine fraction, with little additional contribution to the coarse aerosol fraction. On baseline days, the maximum contribution of indoor WSOC to OC was 19% and 20% for PM_{10} and $PM_{2.5}$ respectively; corresponding outdoor WSOC to OC maximum contributions were 30% and 35%. The contribution of the fire-associated WSOC to OC observed here is consistent with other studies investigating biomass burning and atmospheric aerosols[61, 155, 160, 161]. During this wildfire event, there was a slight decrease in indoor EC

over its outdoor counterparts; however they were not significantly elevated over baseline observation days (Figure 0-4). This is consistent with the fact that EC has not been reported as a major carbon constituent of biomass burning emissions[162].

6.3.2. Wildfire Aerosol Fluorescence Properties

Fluorescence excitation-emission matrix (EEMs) spectra have been widely used to map natural organic matter in aqueous environments [163] and have recently been utilized as a tool for characterization of WSOC in aerosols [17, 18, 60, 62]. In order to compare fluorescence properties of collected PM as they occur in aerosol phase, results in this work are reported as a specific fluorescence intensity, where Raman Units (RU) are normalized by aerosol WSOC concentration in the air (RU/[μg WSOC]/m^3). The EEMs constructed from the PM collected on baseline (non-fire) days exhibit normalized fluorescence, at least an order of magnitude lower than wildfire aerosol samples (Figure 0-5). As the wildfire progressed, the indoor aerosol fluorescence signatures clearly reflect the character of WSOC found in outdoor aerosols. Additionally, the similarity of the $PM_{2.5}$ EEMs fluorescence signatures to those including both $PM_{2.5}$ and coarse PM_{10} indicate that the majority of the fluorescence unique to the wildfire WSOC contribution are found in the $PM_{2.5}$ fraction. In some cases the maximum fluorescence intensity is lower in the PM_{10} samples than in the $PM_{2.5}$ samples (see Figure 0-5, Fire Day 1), indicating the presence of more non-fluorescent compounds in the coarse fraction of collected PM_{10} than in the $PM_{2.5}$ fraction.

Further, a change in wind direction occurred during the first two sampling days, starting from the South-East and shifting to the North-West (the fire was located South-West of the sampling site). This shift in wind direction and speed, along with the progression of the fire, is consistent with the shift in fluorescence patterns observed in the EEMs reported here, where the organic content of smoke aerosols increases with the transition from flaming to smoldering[162]. The predominant wind directions during sampling were from W and NW with calm conditions 33% of the time, with the exception of the first two days of sampling where the wind was blowing from the E and SE directions (opposite the wildfire location relative to the sampling site). This organic fraction includes a complex mixture of condensed high molecular weight polyacidic compounds resembling humic-like substances (HULIS) from terrestrial and aquatic sources [157, 162]. As the fire aged, fluorescent HULIS fractions increased, both outdoors and indoors.

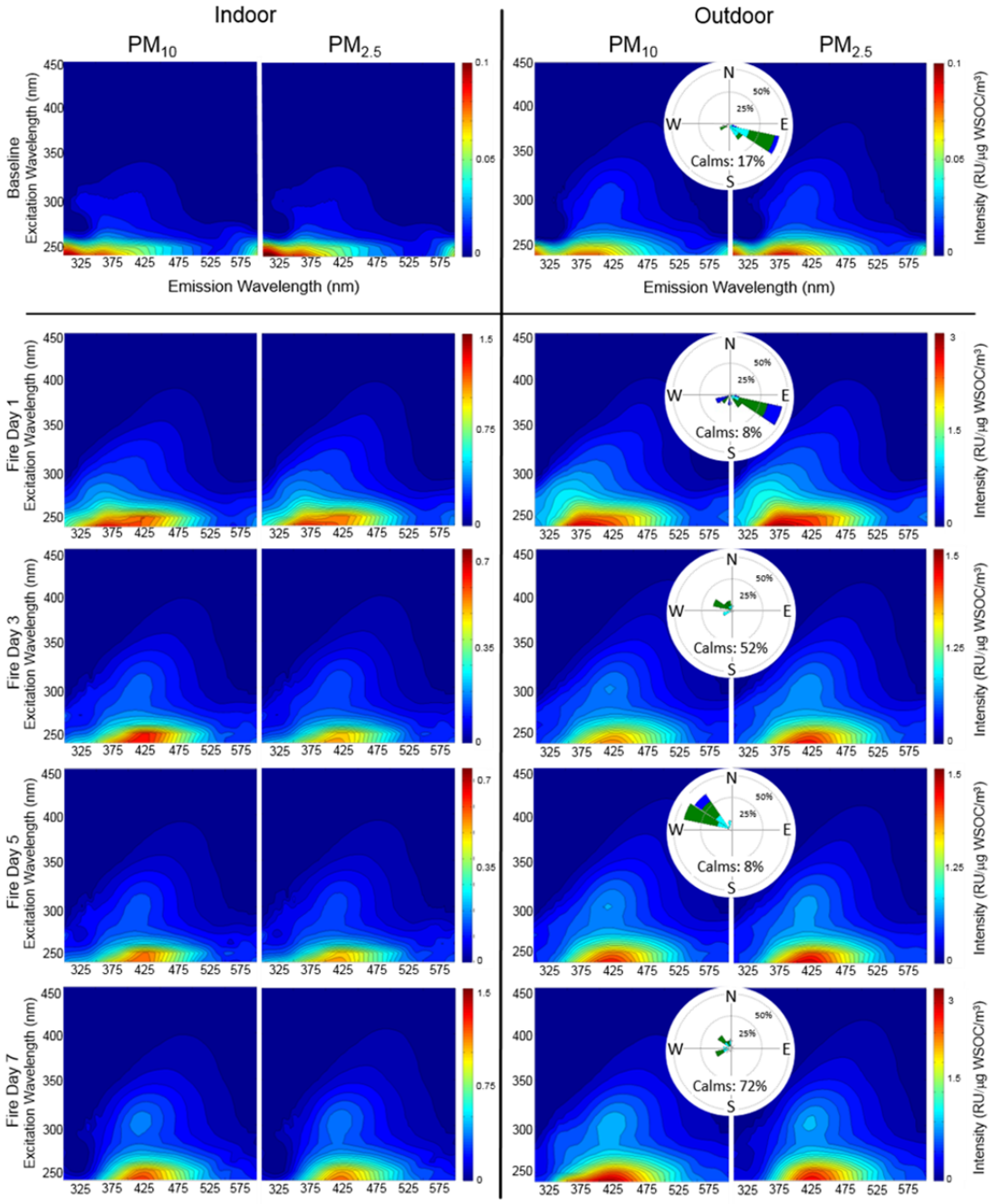

Figure 0-5. Excitation-emission matrices (EEMs) were constructed for Indoor (left half) and outdoor (right half) samples for Fire Days 1, 3, 5, and 7. The color scale on right of each set of size segregated EEMs represents fluorescence intensity in Raman Units per microgram WSOC per cubic meter of air. Inset wind roses on the outdoor EEMs indicate direction the wind was blowing from, where the percentage of the time conditions were calm, and the percentage of time wind was blowing at a given speed presented in the following triangle colors: 'teal' = 0.5-2.1 m/s, 'green' = 2.1-3.6 m/s and 'blue' = 3.6-5.7 m/s.

Several component peaks have been identified in EEMs in an apportionment context; these represent compounds derived from different sources, and ultimately used to identify fluorescence indices that aid in environmental sample characterization[74]. An index (HIX) has been developed to assess the degree of humification that organic matter experienced, and is based on a ratio of two fluorescence emission areas corresponding to young (fresh) organic matter, and generically weathered (humified) organic material[65]. Higher HIX values indicate condensation processes, through a shift to longer wavelengths. The HIX increase can with organic aerosol aging and transformation[62], and can vary by season[60] and location[18]. Here, HIX values increased almost an order of magnitude in some cases for $PM_{2.5}$ and PM_{10} in both indoors and outdoors over the course of wildfire event (Figure 0-6, left). This suggests an increase in humification of the organic matter in the aerosol as the wildfire progress from flaming to smoldering stages. It is important to note that the HIX is a ratio of fluorescence intensities - even though outdoor maximum intensities are higher than those observed indoors, HIX values can be similar. Further, in some cases the HIX was higher in $PM_{2.5}$ samples than in PM_{10}, suggesting the largest contribution to aerosol humification was associated with wildfire progression in the fine PM fraction.

The FRI for all collected samples show similar inverse trends as the HIX, however the impact is not as apparent (Figure 0-6, right). The FRI values do not seem to have the same dependence on PM size as with HIX, where for both PM size fractions trend together and slightly decrease over the course of the wildfire. The most apparent decrease is from Fire Day 1 through Day 4 (FRI values above 1 to below 0.6), with fairly consistent FRI values around 0.6 each day, location, and size fraction thereafter.

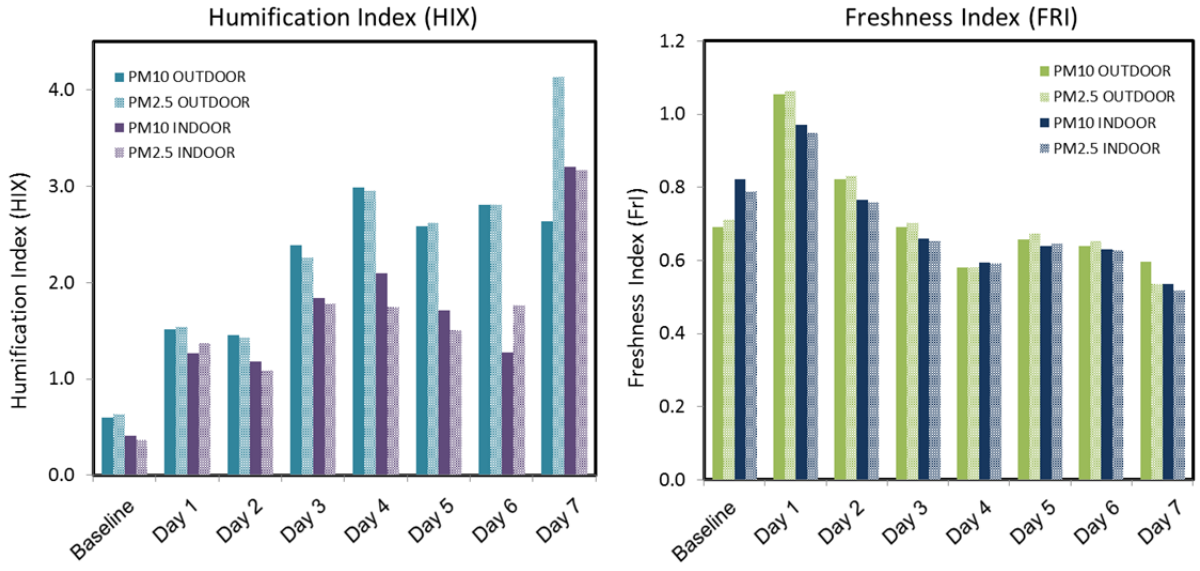

Figure 0-6. Calculated HIX (left plot) and FRI (right plot) for all collected samples from wildfire days and baseline days for both indoor and outdoor locations and PM_{10} and $PM_{2.5}$ size fractions.

6.4. Discussion

On wildfire days, the building was effective in removing the majority of coarse PM contribution to the indoor carbonaceous aerosol load; however, following the onset of the fire, indoor OC $PM_{2.5}$ levels rose to those observed immediately outdoors, indicating significant wildfire impact on the indoor aerosol in respirable size ranges. In this context, reported biomass burning emissions can range 0.26 – 0.35 μm[147, 162], suggesting that a substantial fraction can be found in the fine PM fraction, consistent with the observations here. In many environments, the organic carbon (OC) association with atmospheric aerosols can account for more than 90% of its total carbon (TC) content, where levels of water soluble organic carbon (WSOC) can greatly vary but contribute up to 85 % of OC [155, 161, 164]. Aerosol aging, accelerated here by wildfire conditions, has been reported to increase WSOC/OC ratios in atmospheric aerosols[164]. The character of particulate carbon, including WSOC, has received appreciable attention for its utility in source apportionment of atmospheric aerosols[61, 155, 157, 164] – this same approach was extended here by leveraging EEMs to describe wildfire aerosol signatures. With this forensic perspective, we demonstrated that fine WSOC generated by wildfire can penetrate indoors, even in the most modern of buildings. Though the complex nature of WSOC can make it difficult to assess the relative contribution of each source, it is important to note that the OC and WSOC levels are substantially higher on wildfire days and conventional carbon analysis may not capture the penetration potential of wildfire aerosol.

In the context of air quality, there has been an increasing focus on evaluating airborne WSOC and its properties. While some attempts have been made to evaluate individual compounds responsible for aerosol fluorescence, few studies have looked at fluorescence

excitation emission matrices (EEMs) of water soluble components associating with particulate matter. In response, EEMs were utilized to characterize aerosols generated by wildfires and to compliment other chemical signatures used to track the influence of wildfire aerosols on the indoor environment.

Several component peaks have been identified in EEMs in an apportionment context; these represent compounds derived from different sources, and ultimately used to identify fluorescence indices that aid in environmental sample characterization[74]. An index (HIX) has been developed to assess the degree of humification that organic matter experienced, and is based on a ratio of two fluorescence emission areas corresponding to young (fresh) organic matter, and generically weathered (humified) organic material[65]. Higher HIX values indicate condensation processes, through a shift to longer wavelengths. The HIX increase can with organic aerosol aging and transformation[62], and can vary by season[60] and location[18]. Here, HIX values increased almost an order of magnitude in some cases for $PM_{2.5}$ and PM_{10} in both indoors and outdoors over the course of wildfire event (Figure 0-3). This suggests an increase in humification of the organic matter in the aerosol as the wildfire progress from flaming to smoldering stages. It is important to note that the HIX is a ratio of fluorescence intensities - even though outdoor maximum intensities are higher than those observed indoors, HIX values can be similar. Further, in some cases the HIX was higher in $PM_{2.5}$ samples than in PM_{10}, suggesting the largest contribution to aerosol humification was associated with wildfire progression in the fine PM fraction.

The Freshness Index (FRI) has been investigated in a limited context in aerosol research. In this work, the FRI decreased over the course of the wildfire event, inversely proportional to

HIX and also consistent with shifts in wind direction and the changes in the wildfire progress (flaming to smoldering). Wildfire smoldering conditions have been noted to produce large amounts of VOCs [165] that can condense into secondary organic aerosols (SOA) and continue to age with transport. Large increases in SOA formation and ozone concentrations have been cited to from wildfire emissions, due to atmospheric processing of elevated concentrations of VOC from wildfires [166]. Lee et al. 2013 reported decreases in the measured FRI of relevant biogenic SOA after aging with ozone, a noted constituent in wildfire emissions [167].

Size segregated particulate matter (PM_{10} and $PM_{2.5}$) was simultaneously collected indoors and outdoors before, during and after a wildfire in the Rocky Mountain Front Range. The collected aerosols were analyzed for elemental carbon content (EC), total organic carbon content (OC), water soluble organic carbon (WSOC), and their fluorescent properties. As judged by time-resolved profiles of EC, OC, and the fluorescent fraction of WSOC, wildfire emissions penetrated this building envelope regardless of high-efficiency air filter operations. Organic carbon levels in $PM_{2.5}$ were comparable to those recovered from PM_{10} fractions suggesting that the majority of the organic content was in the finer aerosol fractions, consistent with other combustion processes. As the wildfire progressed, the formation of distinct humic-like signatures in fluorescence spectra became more apparent in all size modes from both indoors and out. It was demonstrated that wildfires have unique aerosol EEM signatures, that these signatures can be used to assess the penetration performance of buildings, and that modern HVAC systems may not be able isolate high-occupancy indoor environments from some of the unique air pollution challenges presented by wildfires.

This study demonstrated that fluorescence properties can provide a more detailed chemical characterization of wildfire impacted aerosol than conventional carbon analysis alone. Further, this work highlighted the impact environmental combustion processes and subsequent atmospheric aging can play on particle carbon content and fluorescence properties, relating to the proposed hypotheses tested in the previous chapters of this thesis. These results, taken individually and collectively, also indicate a significant influence on the indoor environment monitored during this wildfire and clearly demonstrated the influence of outdoor air on the indoor environment of a modern building fitted with relatively high efficiency filters. In combination with the limited body of literature describing the potential impacts of wildfires on the indoor air quality of residential buildings, this study clearly elucidated the longitudinal progression of wildfire aerosol signatures penetrating indoors during an actual fire event; contributing to the evidence that buildings, both residential and commercial, may not be effective in protecting its occupants from exposure to wildfire emissions. With concerns of increasing wildfire activity in the United States, preparing the indoor environment for these pollution challenges should to be a critical component defining future public health agenda.

CHAPTER 7. CONCLUDING REMARKS

7.1. Conclusions

Due in part to increasing concerns of urbanization and climate change, research in the bioaerosol field is relatively young and experiencing rapid expansion. Further, research on atmospheric interactions with aerosols, both biological and otherwise, has now become an interdisciplinary arena and driven by concerns of negative impacts on the atmosphere, environment, public health, national security, and ecology. The airborne biosphere is an important research frontier, and how we understand and steward this component of our atmosphere has tremendous implications for our immediate future. The investigations reported here were designed to isolate selected physiological responses of sporulated airborne microbes to common oxidative atmospheric conditions. The work was motivated by the negative impacts bioaerosols, particularly fungal spores, can present to human and environmental health at large; including, but not limited to, atmospheric processes, non-infectious human respiratory diseases, sustainable botanical progression and regional ecological concerns.

Any new research direction in environmental engineering has scaling challenges, and as such, models must be chosen to control and extrapolate findings from the bench scale to the environment, in the context of both indoor and outdoor settings. In this work, models to demonstrate environmental processes were based on their relevance, ubiquitous nature, and general concern in the research arena. In order to challenge the hypotheses developed here to investigate modifications to biopolymers present in and on whole airborne microorganisms by ozone in environmentally relevant concentrations and time frames, a tightly controlled

environmental chamber was designed and operated to mimic relevant environmental conditions encountered by common bioaerosols. The work presented here was executed at a scale of 11 m^3, which is large enough to achieve substantial bioaerosol residence times, but small enough to carefully control exposure conditions – thus presenting a platform to translate bench scale results to environmental relevancy. Here, ozone was selected as the oxidizing air pollutant of interest because of its potency and ubiquitous occurrence. The bioaerosol models in this work were spores from pure cultures of *Aspergillus* and *Bacillus spp*. because they are well characterized microbes with pathogenic potential and widely present in the terrestrial and atmospheric environment.

Three analytical approaches were leveraged to help understand how these types of microbes may respond to atmospheric ozone: 1) classical real-time bioaerosol optical properties and intrinsic fluorescence; 2) bioaerosol water soluble organic carbon optical properties; and 3) bioaerosol protein biochemistry and immunology. These independent lines of investigation converged to provide evidence that ozone, isolated as a sole oxidant, at levels and with RH ranges relevant to what bioaerosols can experience in the atmosphere and in urban environments, can modify the surface of airborne microbes. An overview of these major conclusions is outlined below as they pertain to their proposed hypotheses.

7.1.1. General Conclusions Challenging Hypothesis Ia

The detailed results reported from testing Hypothesis Ia: "Real-time fluorescent measurements will detect a decrease in intrinsic fluorescence intensities of model bioaerosols during ozone exposure" are presented in Chapter 3. In general, conclusions drawn from these results are as follow:

- Bioaerosol size and bulk cellular structures were not significantly influenced by ozone exposure at either high or low RH, as judged by normalized particle size distributions, Kolmogorov-Smirnov test statistics on cumulative frequency distributions of particle size, and SEM images of collected bioaerosols.
- Ozone exposure had relatively little effect on the fluorescent distributions of bioaerosols, as measured by three fluorescent channels in pWIBS, with the exception of mature fungal spores (78 days old).
- Mature fungal spores (78 days old) were the most susceptible to changes in fluorescence intensity with 600 ppb-hr ozone exposure.
- Ozone exposures exceeding 1000 ppb-hr were required to observe appreciable fluorescence changes in younger fungal spores (less than 78 days old), as judged by the relative DiF Measure.

7.1.2. General Conclusions Challenging Hypothesis Ib

The detailed results reported from testing Hypothesis Ib: "Changes in intrinsic fluorescence intensities of exposed bioaerosol aqueous extracts, over those of fresh bioaerosols, can be determined from excitation-emission matrices" are presented in Chapter 4. In general, conclusions drawn from these results are as follow:

- As judged by the amount of water soluble organic carbon (WSOC) airborne spores liberate, aerosol aging, on the order of hours to a day, can increase the potential for bioaerosol WSOC liberation. The WSOC liberation increased in response to elevated RH, residence time, and ozone exposure.
- The specific ultraviolet absorbance of water soluble organic carbon that can be liberated by airborne microbes is different, depending on environmental conditions and ozone exposure. In general, the classic $SUVA_{254}$ decreased with increasing ozone exposure and was sensitive to lower RH conditions. $SUVA_{254}$ results suggest that ozone preferentially reduces the aromaticity of soluble proteins.
- The water soluble organic carbon liberated by airborne spores could be characterized with excitation emission matrices (EEMs). EEMs revealed that the optically active fraction of WSOC was different among closely related fungal species, and also between spores harvested directly from fungal cultures and those immediately aerosolized. Identified regions on EEMs associated fluorescently active biochemicals and metabolites responded to ozone exposure.

- Changes in established EEM fluorescent indices revealed microbial sensitivity to ozone and RH levels in the atmospheric environment, as well as suspension in the absence of ozone.
- EEM results were consistent with $SUVA_{254}$ suggesting airborne ozone attacks the aromatic biochemical constituents present in and on airborne fungal spores.

7.1.3. General Conclusions Challenging Hypothesis II

The detailed results reported from testing Hypothesis II: "Bioaerosol exposure to gas-phase ozone, under environmentally relevant conditions, will modify biopolymers on the surface of common airborne pollens, fungi, and bacterial spores." are presented in Chapter 5. In general, conclusions drawn from these results are as follow:

- The total water soluble protein pool, as well as selected structural proteins, catalytic proteins and allergenic proteins were sensitive to aerosolization, RH levels and ozone exposure. The total water soluble protein liberated by fungal spores increased in response to aerosolization, but decreased in response to suspension with increasing levels of ozone.
- Detection of the widely cited allergenic protein associated with *Aspergillus fumigatus* spores, Asp f1, dramatically decreases with aerosolization, atmospheric aging and ozone exposure.
- The activity of an important aminidase enzyme, NAHA, integral to the germination process of all fungal spores, rapidly degrades in response to spore maturity and ozone

exposure. This degradation is also sensitive to the atmospheric elevated RH conditions. Loss of NAHA activity in fungal spores from atmospheric processing may have serious ecological implications.

These independent lines of investigation (both optical and biochemical) converge to provide evidence that ozone can modify airborne spores in environmentally-relevant scenarios. The magnitude of differences in sensitivity to aerosol aging, humidity and ozone exposure between closely related species was significant and also sensitive to culture maturity. Given the variance across the pure culture bioaerosols tested, the trends of environmental behaviors observed here cannot necessarily be generalized or extrapolated across the diversity of airborne spores, but do demonstrate the potential for ozone-mediated bioaerosol modification.

7.1.4. General Conclusions: Air Quality Engineering Application to Practice

The characterization of concurrently collected environmental wildfire aerosol samples from both indoor and outdoor locations was conducted by applying many of the bioaerosol characterization methods and principles used to challenge the bioaerosol oxidation hypotheses present in this thesis. Size segregated particulate matter (PM_{10} and $PM_{2.5}$) was simultaneously collected indoors and outdoors before, during and after a local wildfire event in Boulder, Colorado. As judged by the time-resolved profiles of elemental carbon, organic carbon, and the fluorescent fraction of water soluble organic carbon, wildfire emissions rapidly infiltrated the

building regardless of high-efficiency filter operations. Organic carbon levels in $PM_{2.5}$ were comparable to those recovered from $PM_{10,}$ fractions suggesting that the majority of the organic content was in the finer aerosol fractions. Analysis of fluorescence profiles from excitation-emission matrices (EEMs) of the size-segregated water soluble organic carbon (WSOC) liberated from wildfire-associated PM were conducted in a similar fashion as for the controlled bioaerosol studies in Chapter 3 and Chapter 4. As the wildfire progressed, the formation of distinct humic-like signatures in fluorescence spectra dominated the profile and became more apparent in all aerosol size modes from both outdoor and indoor samples. In combination with the limited body of literature describing the potential impacts of wildfires on indoor air quality, this study clearly demonstrated the longitudinal progression of wildfire aerosol signatures present indoors during an actual fire event; contributing to the evidence that buildings, both residential and commercial, may not be effective in protecting its occupants from exposure to wildfire emissions.

This thesis successfully utilized a number of accepted aerosol characterization tools, as well as developed new methods for characterizing the impacts of oxidizing atmospheric environments on both bioaerosols in a controlled laboratory setting, and aerosols recovered from actual wildfire emission samples. The results obtained from this thesis work contribute to the small, but growing body of work on the impact of atmospheric processes on aerosols (including biological) important to public health, environmental welfare, and ecology. Though this work focused on isolating only a few of the many environmental variables responsible for atmospheric oxidative processes encountered by bioaerosols, these results inform important directions for research on investigating the potential impacts of changing climate and urbanization on our health and environment.

REFERENCES

1. Després VR, Huffman AJ, Burrows SM, Hoose C, Safatov AS, Buryak G, Fröhlich-Nowoisky J, Elbert W, Andreae MO, Pöschl U *et al*: **Primary biological aerosol particles in the atmosphere: a review**. *Tellus B* 2012, **64**(0).
2. Yeo H-G, Kim J-H: **SPM and fungal spores in the ambient air of west Korea during the Asian dust (Yellow sand) period**. *Atmospheric Environment* 2002, **36**(35):5437-5442.
3. Mandal J, Brandl H: **Bioaerosols in Indoor Environment - A Review with Special Reference to Residential and Occupational Locations**. *The Open Environmental & Biological Monitoring Journal* 2011, **4**:83-96.
4. Schumacher CJ, Pöhlker C, Aalto P, Hiltunen V, Petäjä T, Kulmala M, Pöschl U, Huffman JA: **Seasonal cycles of fluorescent biological aerosol particles in boreal and semi-arid forests of Finland and Colorado**. *Atmospheric Chemistry and Physics* 2013, **13**(23):11987-12001.
5. Chehregani A, Majde A, Moin M, Gholami M, Ali Shariatzadeh M, Nassiri H: **Increasing allergy potency of Zinnia pollen grains in polluted areas**. *Ecotoxicology and environmental safety* 2004, **58**(2):267-272.
6. Franze T, Weller MG, Niessner R, Pöschl U: **Protein nitration by polluted air**. *Environmental science & technology* 2005, **39**(6):1673-1678.
7. Pasqualini S, Tedeschini E, Frenguelli G, Wopfner N, Ferreira F, D'Amato G, Ederli L: **Ozone affects pollen viability and NAD (P) H oxidase release from Ambrosia artemisiifolia pollen**. *Environmental pollution* 2011, **159**(10):2823-2830.
8. Sarkar A, Agrawal S: **Elevated ozone and two modern wheat cultivars: an assessment of dose dependent sensitivity with respect to growth, reproductive and yield parameters**. *Environmental and Experimental Botany* 2010, **69**(3):328-337.
9. Seinfeld JH, Pandis SN: **Atmospheric Chemistry and Physics - From Air Pollution to Climate Change (2nd Edition)**: John Wiley & Sons; 2006.
10. Möhler O, DeMott PJ, Vali G, Levin Z: **Microbiology and atmospheric processes:the role of biological particles in cloud physics**. *Biosciences Discussions* 2007, **4**:2559-2591.
11. Sun J, Ariya PA: **Atmospheric organic and bio-aerosols as cloud condensation nuclei (CCN): A review**. *Atmospheric Environment* 2006, **40**(5):795-820.
12. Franze T, Weller MG, Niessner R, P□schl U: **Enzyme immunoassays for the investigation of protein nitration by air pollutants**. *The Analyst* 2003, **128**(7):824-824.
13. Franze T, Weller MG, Niessner R, Pöschl U: **Protein nitration by polluted air**. *Environmental science & technology* 2005, **39**(6):1673-1678.
14. Pan Y-L, Santarpia JL, Ratnesar-Shumate S, Corson E, Eshbaugh J, Hill SC, Williamson CC, Coleman M, Bare C, Kinahan S: **Effects of ozone and relative humidity on fluorescence spectra of octapeptide bioaerosol particles**. *Journal of Quantitative Spectroscopy and Radiative Transfer* 2014, **133**:538-550.
15. Pöhlker C, Huffman Ja, Pöschl U: **Autofluorescence of atmospheric bioaerosols – fluorescent biomolecules and potential interferences**. *Atmospheric Measurement Techniques* 2012, **5**(1):37-71.

16. Santarpia JL, Pan Y-L, Hill SC, Baker N, Cottrell B, McKee L, Ratnesar-Shumate S, Pinnick RG: **Changes in fluorescence spectra of bioaerosols exposed to ozone in a laboratory reaction chamber to simulate atmospheric aging**. *Optics express* 2012, **20**(28):29867-29881.
17. Duarte RBO, Pio C, Duarte A: **Synchronous Scan and Excitation-Emission Matrix Fluorescence Spectroscopy of Water-Soluble Organic Compounds in Atmospheric Aerosols**. *Journal of Atmospheric Chemistry* 2004, **48**(2):157-171.
18. Mladenov N, Alados-Arboledas L, Olmo FJ, Lyamani H, Delgado A, Molina A, Reche I: **Applications of optical spectroscopy and stable isotope analyses to organic aerosol source discrimination in an urban area**. *Atmospheric Environment* 2011, **45**(11):1960-1969.
19. McKnight DM, Boyer EW, Westerhoff PK, Doran PT, Kulbe T, Andersen DT: **Spectrofluorometric characterization of dissolved organic matter for indication of precursor organic material and aromaticity**. *Limnology and Oceanography* 2001, **46**(1):38-48.
20. Fellman JB, Hood E, Spencer RGM: **Fluorescence spectroscopy opens new windows into dissolved organic matter dynamics in freshwater ecosystems: A review**. *Limnology and Oceanography* 2010, **55**(6):2452-2462.
21. Zhang T, Lu J, Ma J, Qiang Z: **Fluorescence spectroscopic characterization of DOM fractions isolated from a filtered river water after ozonation and catalytic ozonation**. *Chemosphere* 2008, **71**(5):911-921.
22. Sharma VK, Graham NJD: **Oxidation of Amino Acids, Peptides and Proteins by Ozone: A Review**. *Ozone: Science & Engineering* 2010, **32**(2):81-90.
23. Peccia J, Werth HM, Miller S, Hernandez M: **Effects of Relative Humidity on the Ultraviolet Induced Inactivation of Airborne Bacteria**. *Aerosol Science and Technology* 2001, **35**(3):728-740.
24. Bhetanabhotla M, Crowell B, Coucouvinos A, Hill R, Rinker R: **Simulation of trace species production by lightning and corona discharge in moist air**. *Atmospheric Environment (1967)* 1985, **19**(9):1391-1397.
25. Tamir H, Gilvarg C: **Density gradient centrifugation for the separation of sporulating forms of bacteria**. *Journal of Biological Chemistry* 1966, **241**(5):1085-1090.
26. Dow SM, Barbeau B, von Gunten U, Chandrakanth M, Amy G, Hernandez M: **The impact of selected water quality parameters on the inactivation of Bacillus subtilis spores by monochloramine and ozone**. *Water research* 2006, **40**(2):373-382.
27. Gabey A, Gallagher M, Whitehead J, Dorsey J, Kaye PH, Stanley W: **Measurements and comparison of primary biological aerosol above and below a tropical forest canopy using a dual channel fluorescence spectrometer**. *Atmospheric Chemistry and Physics* 2010, **10**(10):4453-4466.
28. Huffman J, Sinha B, Garland R, Snee-Pollmann A, Gunthe S, Artaxo P, Martin S, Andreae M, Pöschl U: **Size distributions and temporal variations of biological aerosol particles in the Amazon rainforest characterized by microscopy and real-time UV-APS fluorescence techniques during AMAZE-08**. *Atmospheric Chemistry and Physics* 2012, **12**(24):11997-12019.

29. Huffman J, Treutlein B, Pöschl U: **Fluorescent biological aerosol particle concentrations and size distributions measured with an Ultraviolet Aerodynamic Particle Sizer (UV-APS) in Central Europe**. *Atmospheric Chemistry and Physics* 2010, **10**(7):3215-3233.
30. Pinnick RG, Hill SC, Pan Y-L, Chang RK: **Fluorescence spectra of atmospheric aerosol at Adelphi, Maryland, USA: measurement and classification of single particles containing organic carbon**. *Atmospheric Environment* 2004, **38**(11):1657-1672.
31. Handorean A, Robertson CE, Harris JK, Frank D, Hull N, Kotter C, Stevens MJ, Baumgardner D, Pace NR, Hernandez M: **Microbial aerosol liberation from soiled textiles isolated during routine residuals handling in a modern health care setting**. *Microbiome* 2015, **3**(1):1.
32. Bhangar S, Huffman J, Nazaroff W: **Size-resolved fluorescent biological aerosol particle concentrations and occupant emissions in a university classroom**. *Indoor air* 2014, **24**(6):604-617.
33. Pan Y-L: **Detection and characterization of biological and other organic-carbon aerosol particles in atmosphere using fluorescence**. *Journal of Quantitative Spectroscopy and Radiative Transfer* 2015, **150**:12-35.
34. Kopczynski K, Kwasny M, Mierczyk Z, Zawadzki Z: **Laser induced fluorescence system for detection of biological agents: European project FABIOLA**. *Proceedings of SPIE* 2005, **5954**:595405-595405-595412.
35. Schumacher C, Pöhlker C, Aalto P, Hiltunen V, Petäjä T, Kulmala M, Pöschl U, Huffman J: **Seasonal cycles of fluorescent biological aerosol particles in boreal and semi-arid forests of Finland and Colorado**. *Atmospheric chemistry and physics* 2013, **13**(23):11987-12001.
36. Gabey A, Vaitilingom M, Freney E, Boulon J, Sellegri K, Gallagher M, Crawford I, Robinson N, Stanley W, Kaye PH: **Observations of fluorescent and biological aerosol at a high-altitude site in central France**. *Atmospheric Chemistry and Physics* 2013, **13**(15):7415-7428.
37. Sivaprakasam V, Lin H-B, Huston AL, Eversole JD: **Spectral characterization of biological aerosol particles using two-wavelength excited laser-induced fluorescence and elastic scattering measurements**. *Optics express* 2011, **19**(7):6191-6208.
38. Kaye P, Stanley W, Hirst E, Foot E, Baxter K, Barrington S: **Single particle multichannel bio-aerosol fluorescence sensor**. *Optics express* 2005, **13**(10):3583-3593.
39. Toprak E, Schnaiter M: **Fluorescent biological aerosol particles measured with the Waveband Integrated Bioaerosol Sensor WIBS-4: laboratory tests combined with a one year field study**. *Atmospheric Chemistry and Physics* 2013, **13**(1):225-243.
40. Perring A, Schwarz J, Baumgardner D, Hernandez M, Spracklen D, Heald C, Gao R, Kok G, McMeeking G, McQuaid J: **Airborne observations of regional variation in fluorescent aerosol across the United States**. *Journal of Geophysical Research: Atmospheres* 2015, **120**(3):1153-1170.
41. Hernandez M, Perring A, McCabe K, Kok G, Granger G, Baumgardner D: **Composite Catalogues of Optical and Fluorescent Signatures Distinguish Bioaerosol Classes**. *Atmos Meas Tech Discuss* 2016, **in review**.

42. O'Connor DJ, Iacopino D, Healy DA, O'Sullivan D, Sodeau JR: **The intrinsic fluorescence spectra of selected pollen and fungal spores**. *Atmospheric Environment* 2011, **45**(35):6451-6458.
43. Robinson NH, Allan J, Huffman J, Kaye PH, Foot V, Gallagher M: **Cluster analysis of WIBS single-particle bioaerosol data**. *Atmospheric Measurement Techniques* 2013.
44. Baumgartner D, McCabe K, Kok G, Granger G, Hernandez M: **Using Real-time Multiband Fluorescence Signatures to Discriminate between Bioaerosol Classes**. In: *The American Association for Aerosol Research: 2013; Portland, OR*; 2013.
45. Kanaani H, Hargreaves M, Ristovski Z, Morawska L: **Performance assessment of UVAPS: Influence of fungal spore age and air exposure**. *Journal of Aerosol Science* 2007, **38**(1):83-96.
46. Jung JH, Lee JE: **Variation in the fluorescence intensity of thermally-exposed bacterial bioaerosols**. *Journal of Aerosol Science* 2013, **65**:101-110.
47. Healy DA, O'Connor DJ, Sodeau JR: **Measurement of the particle counting efficiency of the "Waveband Integrated Bioaerosol Sensor" model number 4 (WIBS-4)**. *Journal of Aerosol Science* 2012, **47**:94-99.
48. Pöhlker C, Huffman J, Pöschl U: **Autofluorescence of atmospheric bioaerosols–fluorescent biomolecules and potential interferences**. *Atmospheric Measurement Techniques* 2012, **5**(1):37-71.
49. Bohren CF, Huffman DR: **Absorption and scattering by a sphere**. *Absorption and Scattering of Light by Small Particles* 1983:82-129.
50. Heintzenberg J: **Properties of the log-normal particle size distribution**. *Aerosol Science and Technology* 1994, **21**(1):46-48.
51. Ratnesar-Shumate S, Pan Y-L, Hill SC, Kinahan S, Corson E, Eshbaugh J, Santarpia JL: **Fluorescence spectra and biological activity of aerosolized bacillus spores and MS2 bacteriophage exposed to ozone at different relative humidities in a rotating drum**. *Journal of Quantitative Spectroscopy and Radiative Transfer* 2015, **153**:13-28.
52. Hill SC, Pinnick RG, Niles S, Fell NF, Pan Y-L, Bottiger J, Bronk BV, Holler S, Chang RK: **Fluorescence from airborne microparticles: dependence on size, concentration of fluorophores, and illumination intensity**. *Appl Optics* 2001, **40**(18):3005-3013.
53. Agranovski V, Ristovski ZD: **Real-time monitoring of viable bioaerosols: capability of the UVAPS to predict the amount of individual microorganisms in aerosol particles**. *Journal of Aerosol Science* 2005, **36**(5):665-676.
54. Rubel GO: **Measurement of water vapor sorption by single biological aerosols**. *Aerosol science and technology* 1997, **27**(4):481-490.
55. Shiraiwa M, Ammann M, Koop T, Poschl U: **Gas uptake and chemical aging of semisolid organic aerosol particles**. *P Natl Acad Sci USA* 2011, **108**(27):11003-11008.
56. Andreae MO, Merlet P: **Emission of trace gases and aerosols from biomass burning**. *Global Biogeochemical Cycles* 2001, **15**(4):955-966.
57. Hoffer A, Gelencser A, Guyon P, Kiss G, Schmid O, Frank GP, Artaxo P, Andreae MO: **Optical properties of humic-like substances (HULIS) in biomass-burning aerosols**. *Atmospheric Chemistry and Physics* 2006, **6**:3563-3570.
58. Verma V, Fang T, Guo H, King L, Bates JT, Peltier RE, Edgerton E, Russell AG, Weber RJ: **Reactive oxygen species associated with water-soluble PM2.5 in the southeastern**

United States: spatiotemporal trends and source apportionment. *Atmospheric Chemistry and Physics* 2014, **14**(23):12915-12930.
59. Fu P, Kawamura K, Chen J, Qin M, Ren L, Sun Y, Wang Z, Barrie LA, Tachibana E, Ding A: **Fluorescent water-soluble organic aerosols in the High Arctic atmosphere**. *Scientific reports* 2015, **5**.
60. Duhl TR, Clements N, Mladenov N, Cawley K, Rosario-Ortiz FL, Hannigan MP: **Natural and Unnatural Organic Matter in the Atmosphere: Recent Perspectives on the High Molecular Weight Fraction of Organic Aerosol**. *Acs Sym Ser* 2014, **1160**:87-111.
61. Duarte RMBO, Pio CA, Duarte AC: **Spectroscopic study of the water-soluble organic matter isolated from atmospheric aerosols collected under different atmospheric conditions**. *Analytica Chimica Acta* 2005, **530**(1):7-14.
62. Lee HJ, Laskin A, Laskin J, Nizkorodov SA: **Excitation-emission spectra and fluorescence quantum yields for fresh and aged biogenic secondary organic aerosols**. *Environ Sci Technol* 2013, **47**(11):5763-5770.
63. Gabor RS, Baker A, McKnight DM, Miller MP, Coble P, Lead J, Baker A, Reynolds D, Spencer R: **Fluorescence Indices and Their Interpretation**. *Aquatic Organic Matter Fluorescence* 2014:303.
64. Weishaar JL, Aiken GR, Bergamaschi BA, Fram MS, Fujii R, Mopper K: **Evaluation of Specific Ultraviolet Absorbance as an Indicator of the Chemical Composition and Reactivity of Dissolved Organic Carbon**. *Environmental Science & Technology* 2003, **37**(20):4702-4708.
65. Zsolnay A, Baigar E, Jimenez M, Steinweg B, Saccomandi F: **Differentiating with fluorescence spectroscopy the sources of dissolved organic matter in soils subjected to drying**. *Chemosphere* 1999, **38**(1):45-50.
66. Wilson HF, Xenopoulos MA: **Effects of agricultural land use on the composition of fluvial dissolved organic matter**. *Nature Geoscience* 2008, **2**(1):37-41.
67. Korak JA, Wert EC, Rosario-Ortiz FL: **Evaluating fluorescence spectroscopy as a tool to characterize cyanobacteria intracellular organic matter upon simulated release and oxidation in natural water**. *Water research* 2015, **68**:432-443.
68. Komanapalli IR, Lau BHS: **Ozone-induced damage of *Escherichia coli* K-12**. *Appl Microbiol Biotechnol* 1996, **46**:601-614.
69. Frank DN, Spiegelman GB, Davis W, Wagner E, Lyons E, Pace NR: **Culture-independent molecular analysis of microbial constituents of the healthy human outer ear**. *J Clin Microbiol* 2003, **41**(1):295-303.
70. Low SY, Dannemiller K, Yao M, Yamamoto N, Peccia J: **The allergenicity of Aspergillus fumigatus conidia is influenced by growth temperature**. *Fungal biology* 2011, **115**(7):625-632.
71. Lawaetz AJ, Stedmon CA: **Fluorescence intensity calibration using the Raman scatter peak of water**. *Applied spectroscopy* 2009, **63**(8):936-940.
72. Westerhoff P, Aiken G, Amy G, Debroux J: **Relationships between the structure of natural organic matter and its reactivity towards molecular ozone and hydroxyl radicals**. *Water research* 1999, **33**(10):2265-2276.

73. Cory RM, Miller MP, McKnight DM, Guerard JJ, Miller PL: **Effect of instrument-specific response on the analysis of fulvic acid fluorescence spectra**. *Limnology and Oceanography: Methods* 2010, **8**(2):67.
74. Coble PG: **Characterization of marine and terrestrial DOM in seawater using excitation emission matrix spectroscopy**. *Marine Chemistry* 1996, **51**(4):325-346.
75. Bernard M, Latgé J-P: **Aspergillus fumigatus cell wall: composition and biosynthesis**. *Medical Mycology* 2001, **39**(1):9-17.
76. Song J, Zhai P, Zhang Y, Zhang C, Sang H, Han G, Keller NP, Lu L: **The Aspergillus fumigatus damage resistance protein family coordinately regulates ergosterol biosynthesis and azole susceptibility**. *中国菌物学会 2015 年学术年会论文摘要集* 2015.
77. Mille-Lindblom C, von Wachenfeldt E, Tranvik LJ: **Ergosterol as a measure of living fungal biomass: persistence in environmental samples after fungal death**. *Journal of Microbiological Methods* 2004, **59**(2):253-262.
78. Pasanen A-L, Yli-Pietilä K, Pasanen P, Kalliokoski P, Tarhanen J: **Ergosterol content in various fungal species and biocontaminated building materials**. *Appl Environ Microb* 1999, **65**(1):138-142.
79. Brodowski S, Rodionov A, Haumaier L, Glaser B, Amelung W: **Revised black carbon assessment using benzene polycarboxylic acids**. *Organic Geochemistry* 2005, **36**(9):1299-1310.
80. Pihet M, Vandeputte P, Tronchin G, Renier G, Saulnier P, Georgeault S, Mallet R, Chabasse D, Symoens F, Bouchara J-P: **Melanin is an essential component for the integrity of the cell wall of Aspergillus fumigatus conidia**. *BMC microbiology* 2009, **9**(1):1.
81. Valmaseda M, Martinez A, Almendros G: **Contribution by pigmented fungi to P-type humic acid formation in two forest soils**. *Soil Biology and Biochemistry* 1989, **21**(1):23-28.
82. Wlodarski M, Kaliszewski M, Kwasny M, Kopczynski K, Zawadzki Z, Mierczyk Z, Mlynczak J, Trafny E, Szpakowska M: **Fluorescence excitation-emission matrices of selected biological materials**. In: *Optics/Photonics in Security and Defence: 2006*: International Society for Optics and Photonics; 2006: 639806-639806-639812.
83. Morozova E, Kozlov V, Tereshina V, Memorskaya A, Feofilova E: **Changes in lipid composition and carbohydrate composition of Aspergillus niger conidia during germination**. *Applied Biochemistry and Microbiology* 2002, **38**(2):129-133.
84. Ruijter GJ, Bax M, Patel H, Flitter SJ, van de Vondervoort PJ, de Vries RP, Visser J: **Mannitol is required for stress tolerance in Aspergillus niger conidiospores**. *Eukaryotic Cell* 2003, **2**(4):690-698.
85. Stahmann K, Arst HN, Althöfer H, Revuelta JL, Monschau N, Schlüpen C, Gätgens C, Wiesenburg A, Schlösser T: **Riboflavin, overproduced during sporulation of Ashbya gossypii, protects its hyaline spores against ultraviolet light**. *Environmental microbiology* 2001, **3**(9):545-550.
86. Fouillaud M, Boyer E, Fel A, Caro Y, Dufossé L: **PIGMENTED FILAMENTOUS FUNGI ISOLATED FROM TROPICAL MARINE ENVIRONMENTS AROUND REUNION ISLAND, INDIAN OCEAN, FRANCE**.

87. Sousa R, Duque L, Duarte AJ, Gomes CR, Ribeiro H, Cruz A, Esteves da Silva JC, Abreu I: **In vitro exposure of Acer negundo pollen to atmospheric levels of SO(2) and NO(2): effects on allergenicity and germination**. *Environ Sci Technol* 2012, **46**(4):2406-2412.
88. Mims SA, Mims FM: **Fungal spores are transported long distances in smoke from biomass fires**. *Atmospheric Environment* 2004, **38**(5):651-655.
89. Rogerieux F, Godfrin D, Senechal H, Motta A, Marliere M, Peltre G, Lacroix G: **Modifications of Phleum pratense grass pollen allergens following artificial exposure to gaseous air pollutants (O3, NO2, SO2)**. *International archives of allergy and immunology* 2007, **143**(2):127-134.
90. Ribeiro H, Duque L, Sousa R, Cruz A, Gomes C, Esteves da Silva J, Abreu I: **Changes in the IgE-reacting protein profiles of Acer negundo, Platanus x acerifolia and Quercus robur pollen in response to ozone treatment**. *International journal of environmental health research* 2014, **24**(6):515-527.
91. Savi GD, Scussel VM: **Effects of ozone gas exposure on toxigenic fungi species from Fusarium, Aspergillus, and Penicillium genera**. *Ozone: Science & Engineering* 2014, **36**(2):144-152.
92. Sousa R, Duque L, Duarte AJ, Gomes CR, Ribeiro H, Cruz A, Esteves da Silva JC, Abreu I: **In vitro exposure of Acer negundo pollen to atmospheric levels of SO2 and NO2: effects on allergenicity and germination**. *Environmental science & technology* 2012, **46**(4):2406-2412.
93. Beggs PJ: **Impacts of climate change on aeroallergens: past and future**. *Clinical and experimental allergy : journal of the British Society for Allergy and Clinical Immunology* 2004, **34**(10):1507-1513.
94. Duarte RM, Pio CA, Duarte AC: **Synchronous scan and excitation-emission matrix fluorescence spectroscopy of water-soluble organic compounds in atmospheric aerosols**. *Journal of atmospheric chemistry* 2004, **48**(2):157-171.
95. Mayol-Bracero O, Guyon P, Graham B, Roberts G, Andreae M, Decesari S, Facchini M, Fuzzi S, Artaxo P: **Water-soluble organic compounds in biomass burning aerosols over amazonia 2. Apportionment of the chemical composition and importance of the polyacidic fraction**. *Journal of Geophysical Research: Atmospheres* 2002, **107**(D20).
96. Mauderly JL, Chow JC: **Health effects of organic aerosols**. *Inhalation toxicology* 2008, **20**(3):257-288.
97. Turner J, Hernandez M, Snawder JE, Handorean A, McCabe KM: **A toxicology suite adapted for comparing parallel toxicity responses of model human lung cells to diesel exhaust particles and their extracts**. *Aerosol Science and Technology* 2015, **49**(8):599-610.
98. Long CM, Suh HH, Kobzik L, Catalano PJ, Ning YY, Koutrakis P: **A pilot investigation of the relative toxicity of indoor and outdoor fine particles: in vitro effects of endotoxin and other particulate properties**. *Environmental Health Perspectives* 2001, **109**(10):1019.
99. Boreson J, Dillner AM, Peccia J: **Correlating bioaerosol load with PM2. 5 and PM10cf concentrations: a comparison between natural desert and urban-fringe aerosols**. *Atmospheric Environment* 2004, **38**(35):6029-6041.

100. Kang H, Xie Z, Hu Q: **Ambient protein concentration in PM 10 in Hefei, central China**. *Atmospheric Environment* 2012, **54**:73-79.
101. Menetrez M, Foarde K, Esch R, Dean T, Betancourt D, Moore S, Svendsen E, Yeatts K: **The measurement of ambient bioaerosol exposure**. *Aerosol Science and Technology* 2007, **41**(9):884-893.
102. Rosas I, Yela A, Salinas E, Arreguin R, Rodriguez-Romero A: **Preliminary assessment of protein associated with airborne particles in Mexico City**. *Aerobiología* 1995, **11**(2):81-86.
103. Ryan TJ, Whitehead LW, Connor TH, Burau KD: **Survey of the Asp f 1 allergen in office environments**. *Applied occupational and environmental hygiene* 2001, **16**(6):679-684.
104. Sporik R, Arruda L, Woodfolk J, Chapman M, PLATTS-MILLS T: **Environmental exposure to Aspergillus fumigatus allergen (Asp f I)**. *Clinical & Experimental Allergy* 1993, **23**(4):326-331.
105. Beggs PJ, Bambrick HJ: **Is the global rise of asthma an early impact of anthropogenic climate change?** *Ciência & Saúde Coletiva* 2006, **11**(3):745-752.
106. Svartengren M, Strand V, Bylin G, Jarup L, Pershagen G: **Short-term exposure to air pollution in a road tunnel enhances the asthmatic response to allergen**. *European respiratory journal* 2000, **15**(4):716-724.
107. Chehregani A, Majde A, Moin M, Gholami M, Shariatzadeh MA, Nassiri H: **Increasing allergy potency of Zinnia pollen grains in polluted areas**. *Ecotoxicology and environmental safety* 2004, **58**(2):267-272.
108. Parnia S, Brown J, Frew A: **The role of pollutants in allergic sensitization and the development of asthma**. *Allergy* 2002, **57**(12):1111-1117.
109. Lang-Yona N, Dannemiller K, Yamamoto N, Burshtein N, Peccia J, Yarden O, Rudich Y: **Annual distribution of allergenic fungal spores in atmospheric particulate matter in the Eastern Mediterranean; a comparative study between ergosterol and quantitative PCR analysis**. *Atmospheric Chemistry and Physics* 2012, **12**(5):2681-2690.
110. Eckl-Dorna J, Klein B, Reichenauer TG, Niederberger V, Valenta R: **Exposure of rye (Secale cereale) cultivars to elevated ozone levels increases the allergen content in pollen**. *Journal of Allergy and Clinical Immunology* 2010, **126**(6):1315-1317.
111. Franze T, Weller MG, Niessner R, Pöschl U: **Enzyme immunoassays for the investigation of protein nitration by air pollutants**. *Analyst* 2003, **128**(7):824-831.
112. Jones AP: **Indoor air quality and health**. *Atmospheric environment* 1999, **33**(28):4535-4564.
113. Terčelj M, Salobir B, Narancsik Z, Kriznar K, Grzetic-Romcevic T, Matos T, Rylander R: **Nocturnal asthma and domestic exposure to fungi**. *Indoor and Built Environment* 2012:1420326X12460255.
114. EPA: **Moisture Control Guidance for Building Design, Constuction and Maintnenece**. In.; 2013.
115. Adan O, Samson R: **Fundamentals of mold growth in indoor environments and strategies for healthy living**: Wageningen Academic Publishers; 2011.
116. Pace NR: **A molecular view of microbial diversity and the biosphere**. *Science* 1997, **276**(5313):734-740.

117. Brooks JP, Edwards DJ, Harwich MD, Rivera MC, Fettweis JM, Serrano MG, Reris RA, Sheth NU, Huang B, Girerd P: **The truth about metagenomics: quantifying and counteracting bias in 16S rRNA studies**. *BMC microbiology* 2015, **15**(1):66.
118. Madsen A: **NAGase activity in airborne biomass dust and relationship between NAGase concentrations and fungal spores**. *Aerobiologia* 2003, **19**(2):97-105.
119. Reeslev M, Miller M, Nielsen KF: **Quantifying mold biomass on gypsum board: comparison of ergosterol and beta-N-acetylhexosaminidase as mold biomass parameters**. *Appl Environ Microb* 2003, **69**(7):3996-3998.
120. Rylander R, Reeslev M, Hulander T: **Airborne enzyme measurements to detect indoor mould exposure**. *Journal of Environmental Monitoring* 2010, **12**(11):2161-2164.
121. Terčelj M, Salobir B, Harlander M, Rylander R: **Fungal exposure in homes of patients with sarcoidosis-an environmental exposure study**. *Environmental Health* 2011, **10**(1):8.
122. Adhikari A, Reponen T, Rylander R: **Airborne fungal cell fragments in homes in relation to total fungal biomass**. *Indoor air* 2013, **23**(2):142-147.
123. Jones LJ, Haugland RP, Singer VL: **Development and characterization of the NanoOrange® Protein quantitation assay: A fluorescence-based assay of proteins in solution**. *Biotechniques* 2003, **34**(4):850-861.
124. Earle CD, King EM, Tsay A, Pittman K, Saric B, Vailes L, Godbout R, Oliver KG, Chapman MD: **High-throughput fluorescent multiplex array for indoor allergen exposure assessment**. *Journal of Allergy and Clinical Immunology* 2007, **119**(2):428-433.
125. King EM, Filep S, Smith B, Platts-Mills T, Hamilton RG, Schmechel D, Sordillo JE, Milton D, van Ree R, Krop EJ: **A multi-center ring trial of allergen analysis using fluorescent multiplex array technology**. *Journal of immunological methods* 2013, **387**(1):89-95.
126. Arruda LK, Platts-Mills T, Fox J, Chapman M: **Aspergillus fumigatus allergen I, a major IgE-binding protein, is a member of the mitogillin family of cytotoxins**. *The Journal of experimental medicine* 1990, **172**(5):1529-1532.
127. Eiguren Fernandez A, Lewis GS, Hering SV: **Design and laboratory evaluation of a sequential spot sampler for time-resolved measurement of airborne particle composition**. *Aerosol Science and Technology* 2014, **48**(6):655-663.
128. EPA: **Environmental Technology Verification Report, Mycometer-test Rapid Fungi Detection**. In.; 2011.
129. Bauer H, Kasper-Giebl A, Löflund M, Giebl H, Hitzenberger R, Zibuschka F, Puxbaum H: **The contribution of bacteria and fungal spores to the organic carbon content of cloud water, precipitation and aerosols**. *Atmos Res* 2002, **64**(1):109-119.
130. Plummer JD, Edzwald JK: **Effect of ozone on algae as precursors for trihalomethane and haloacetic acid production**. *Environmental science & technology* 2001, **35**(18):3661-3668.
131. Volk C, Renner C, Roche P, Paillard H, Joret J: **Effects of ozone on the production of biodegradable dissolved organic carbon (BDOC) during water treatment**. *Ozone: science & engineering* 1993, **15**(5):389-404.

132. Von Sonntag C, Von Gunten U: **Chemistry of ozone in water and wastewater treatment: From basic principles to applications**. *Water Intelligence Online* 2012, **11**:9781780400839.
133. Peccia J, Werth HM, Miller S, Hernandez M: **Effects of relative humidity on the ultraviolet induced inactivation of airborne bacteria**. *Aerosol Science & Technology* 2001, **35**(3):728-740.
134. Arruda LK, Mann B, Chapman M: **Selective expression of a major allergen and cytotoxin, Asp f I, in Aspergillus fumigatus. Implications for the immunopathogenesis of Aspergillus-related diseases**. *The Journal of Immunology* 1992, **149**(10):3354-3359.
135. Sharma VK, Graham NJ: **Oxidation of amino acids, peptides and proteins by ozone: a review**. *Ozone: Science & Engineering* 2010, **32**(2):81-90.
136. Sentandreu R, Mormeneo S, Ruiz-Herrera J: **Biogenesis of the fungal cell wall**. In: *Growth, Differentiation and Sexuality*. Springer; 1994: 111-124.
137. Konno N, Takahashi H, Nakajima M, Takeda T, Sakamoto Y: **Characterization of β-N-acetylhexosaminidase (LeHex20A), a member of glycoside hydrolase family 20, from Lentinula edodes (shiitake mushroom)**. *AMB express* 2012, **2**(1):29.
138. Ettrich R, Kopecký V, Hofbauerová K, Baumruk V, Novák P, Pompach P, Man P, Plíhal O, Kutý M, Kulik N: **Structure of the dimeric N-glycosylated form of fungal β-N-acetylhexosaminidase revealed by computer modeling, vibrational spectroscopy, and biochemical studies**. *BMC structural biology* 2007, **7**(1):1.
139. Albasarah YY, Somavarapu S, Taylor KM: **Stabilizing protein formulations during air-jet nebulization**. *International journal of pharmaceutics* 2010, **402**(1):140-145.
140. Tronin A, Dubrovsky T, Dubrovskaya S, Radicchi G, Nicolini C: **Role of protein unfolding in monolayer formation on air-water interface**. *Langmuir* 1996, **12**(13):3272-3275.
141. Dooley M, Mudd J: **Reaction of ozone with lysozyme under different exposure conditions**. *Archives of biochemistry and biophysics* 1982, **218**(2):459-471.
142. Kuroda M, Sakiyama F, Narita K: **Oxidation of tryptophan in lysozyme by ozone in aqueous solution**. *Journal of biochemistry* 1975, **78**(4):641-651.
143. Spracklen DV, Mickley LJ, Logan JA, Hudman RC, Yevich R, Flannigan MD, Westerling AL: **Impacts of climate change from 2000 to 2050 on wildfire activity and carbonaceous aerosol concentrations in the western United States**. *J Geophys Res-Atmos* 2009, **114**.
144. Westerling AL, Hidalgo HG, Cayan DR, Swetnam TW: **Warming and earlier spring increase western US forest wildfire activity**. *Science* 2006, **313**(5789):940-943.
145. Naeher LP, Brauer M, Lipsett M, Zelikoff JT, Simpson CD, Koenig JQ, Smith KR: **Woodsmoke health effects: A review**. *Inhalation toxicology* 2007, **19**(1):67-106.
146. Wong LSN, Aung HH, Lame MW, Wegesser TC, Wilson DW: **Fine particulate matter from urban ambient and wildfire sources from California's San Joaquin Valley initiate differential inflammatory, oxidative stress, and xenobiotic responses in human bronchial epithelial cells**. *Toxicology in Vitro* 2011, **25**(8):1895-1905.
147. Phuleria HC, Fine PM, Zhu YF, Sioutas C: **Air quality impacts of the October 2003 Southern California wildfires**. *J Geophys Res-Atmos* 2005, **110**(D7).

148. Henderson DE, Milford JB, Miller SL: **Prescribed burns and wildfires in Colorado: Impacts of mitigation measures on indoor air particulate matter**. *J Air Waste Manage* 2005, **55**(10):1516-1526.
149. Fisk WJ: **Review of some effects of climate change on indoor environmental quality and health and associated no-regrets mitigation measures**. *Building and Environment* 2015, **86**:70-80.
150. Conny JM: **Black carbon and organic carbon in aerosol particles from crown fires in the Canadian boreal forest**. *Journal of Geophysical Research* 2002, **107**(D11).
151. Zauscher MD, Wang Y, Moore MJ, Gaston CJ, Prather KA: **Air Quality Impact and Physicochemical Aging of Biomass Burning Aerosols during the 2007 San Diego Wildfires**. *Environ Sci Technol* 2013, **47**(14):7633-7643.
152. Urbanski SP: **Combustion efficiency and emission factors for wildfire-season fires in mixed conifer forests of the northern Rocky Mountains, US**. *Atmospheric Chemistry and Physics* 2013, **13**(14):7241-7262.
153. Kochi I, Champ PA, Loomis JB, Donovan GH: **Valuing mortality impacts of smoke exposure from major southern California wildfires**. *J Forest Econ* 2012, **18**(1):61-75.
154. Leonard SS, Castranova V, Chen BT, Schwegler-Berry D, Hoover M, Piacitelli C, Gaughan DM: **Particle size-dependent radical generation from wildland fire smoke**. *Toxicology* 2007, **236**(1-2):103-113.
155. Mayol-Bracero OL: **Water-soluble organic compounds in biomass burning aerosols over Amazonia 2. Apportionment of the chemical composition and importance of the polyacidic fraction**. *Journal of Geophysical Research* 2002, **107**(D20).
156. Wonaschutz A, Hersey SP, Sorooshian A, Craven JS, Metcalf AR, Flagan RC, Seinfeld JH: **Impact of a large wildfire on water-soluble organic aerosol in a major urban area: the 2009 Station Fire in Los Angeles County**. *Atmospheric Chemistry and Physics* 2011, **11**(16):8257-8270.
157. Graber ER, Rudich Y: **Atmospheric HULIS: How humic-like are they? A comprehensive and critical review**. *Atmospheric Chemistry and Physics* 2006, **6**:729-753.
158. **ATOC Weather Network, CU-Boulder Campus** [http://foehn.colorado.edu/weather/atoc1/archive_index.html]
159. NIOSH: **Manual of Analytical Methods, Fourth Editions**. In: *Method 5040, Diesel Particulate Matter.* National Institute for Occupational Safety and Health; 2003: 5.
160. Decesari S, Facchini MC, Matta E, Lettini F, Mircea M, Fuzzi S, Tagliavini E, Putaud JP: **Chemical features and seasonal variation of fine aerosol water-soluble organic compounds in the Po Valley, Italy**. *Atmospheric Environment* 2001, **35**(21):3691-3699.
161. Jaffrezo JL, Aymoz G, Delaval C, Cozic J: **Seasonal variations of the water soluble organic carbon mass fraction of aerosol in two valleys of the French Alps**. *Atmospheric Chemistry and Physics* 2005, **5**:2809-2821.
162. Reid JS, Koppmann R, Eck TF, Eleuterio DP: **A review of biomass burning emissions part II: intensive physical properties of biomass burning particles**. *Atmospheric Chemistry and Physics* 2005, **5**:799-825.

163. Chen W, Westerhoff P, Leenheer JA, Booksh K: **Fluorescence excitation - Emission matrix regional integration to quantify spectra for dissolved organic matter**. *Environmental Science & Technology* 2003, **37**(24):5701-5710.
164. Snyder DC, Rutter AP, Collins R, Worley C, Schauer JJ: **Insights into the Origin of Water Soluble Organic Carbon in Atmospheric Fine Particulate Matter**. *Aerosol Science and Technology* 2009, **43**(11):1099-1107.
165. Evtyugina M, Calvo AI, Nunes T, Alves C, Fernandes AP, Tarelho L, Vicente A, Pio C: **VOC emissions of smouldering combustion from Mediterranean wildfires in central Portugal**. *Atmospheric environment* 2013, **64**:339-348.
166. Bein KJ, Zhao Y, Johnston MV, Wexler AS: **Interactions between boreal wildfire and urban emissions**. *Journal of Geophysical Research: Atmospheres* 2008, **113**(D7).
167. Jaffe DA, Wigder NL: **Ozone production from wildfires: A critical review**. *Atmospheric Environment* 2012, **51**:1-10.

APPENDIX MATERIALS

APPENDIX: Real-Time Bioaerosol Fluorescence Data

Aspergillus versicolor

RH (%)	85
Ozone (ppb)/ suspension time (hr)	200 / 3 hours
Chamber Date	10/05/2015
Culture age (days)	39
InstaScope Gain	High
I.S. Files (t=0,1hr,3hr) {points}	0005, 0017, 0026 (Igor points: 1, 13, 22)

Pre Particle Size Distribution

Gauss fit mean	2.29
SD +/- (width/sqrt(2))	0.426
Size Range	1.5 – 3.5

Post Particle Size Distribution

Gauss fit mean	2.35
SD +/- (width/sqrt(2))	0.425
Size Range	1.5 – 3.5

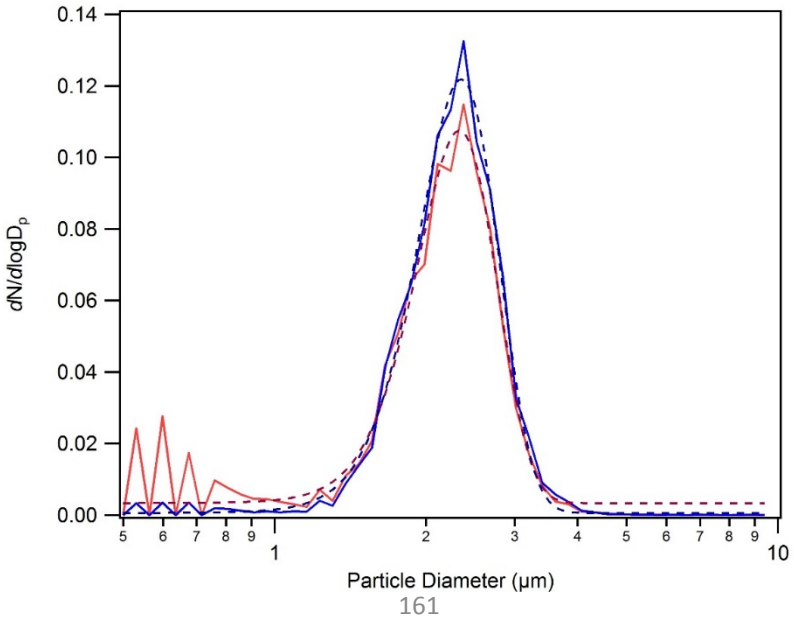

Aspergillus versicolor, 85%RH, 200ppb Ozone

Pre Particle FL1 Distribution

LogNormalFL1	344.2
SD (*,/)	0.65
Size range	1.5 – 3.5
FL1 Range	128 - 2100

Post Particle FL1 Distribution

LogNormalFL1	354.49
SD (*,/)	.64
Size range	1.5 – 3.5
FL1 Range	128 - 2100

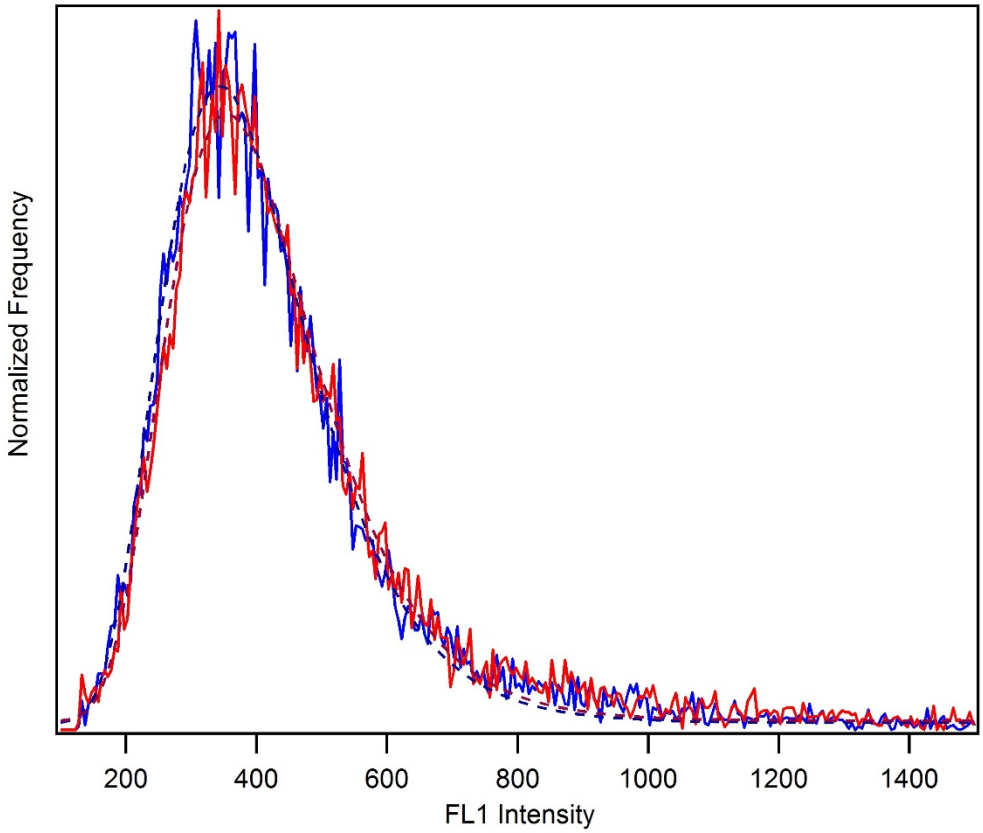

Aspergillus versicolor, 85%RH, 200ppb Ozone

	Pre O3 (%)	1hr (%)	3hr (%)
Total Particles	100.00	100.00	100.00
Nonfluorescent	0.78	2.35	2.42
Saturated FL1	0.45	0.34	0.41
Channel FL1	98.52	95.60	95.67
Channel FL2	50.01	48.95	50.86
Channel FL3	17.70	10.41	13.19

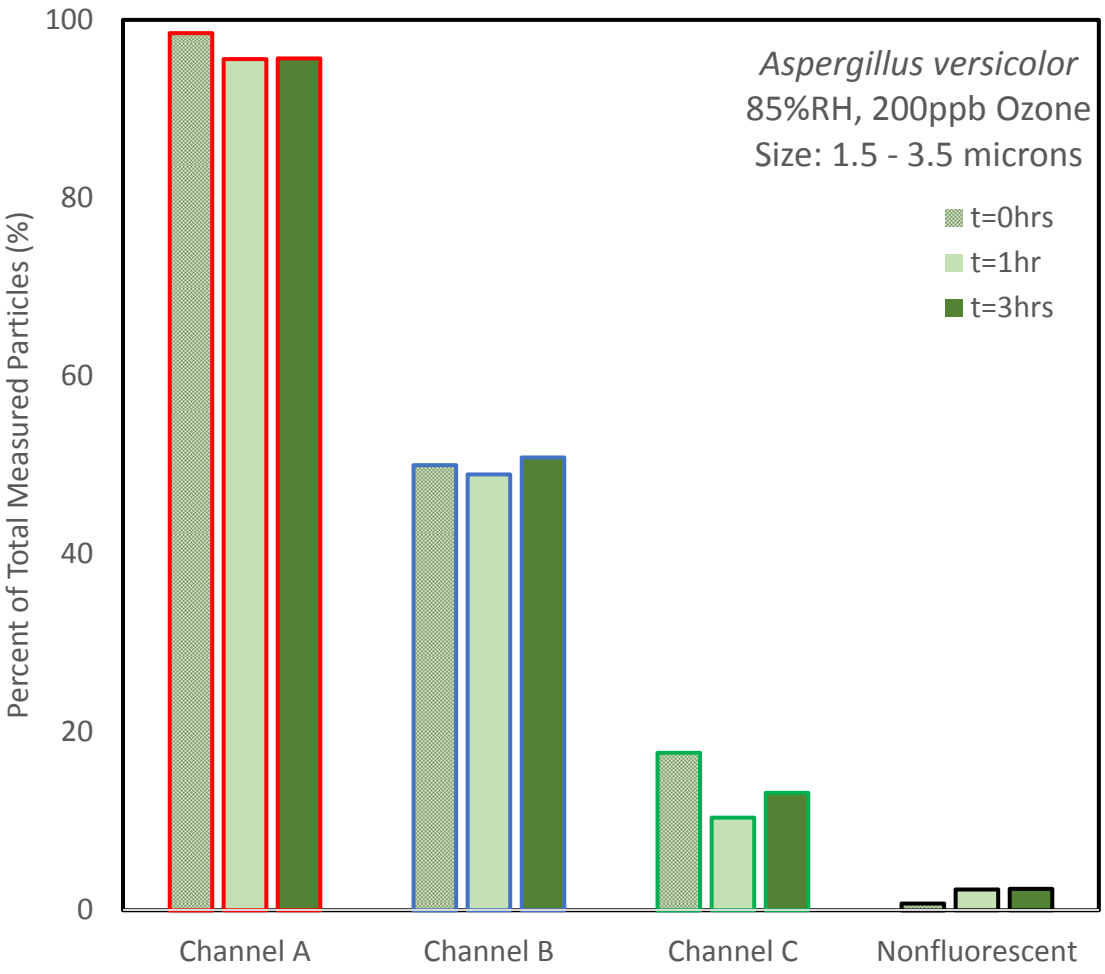

Aspergillus versicolor, 85%RH, 200ppb Ozone
KS (size, FL1, FL2, FL3)

	P value	KS Satistic	Median Pre	Median Post
Size (um)	4.77E-28	0.044716	2.35	2.29
FL1 (intensity)	1.33E-07	2.32E-02	404	410
FL2 (intensity)	4.67E-09	0.035179	69	69
FL3 (intensity)	0.0229712	0.030522	5	5

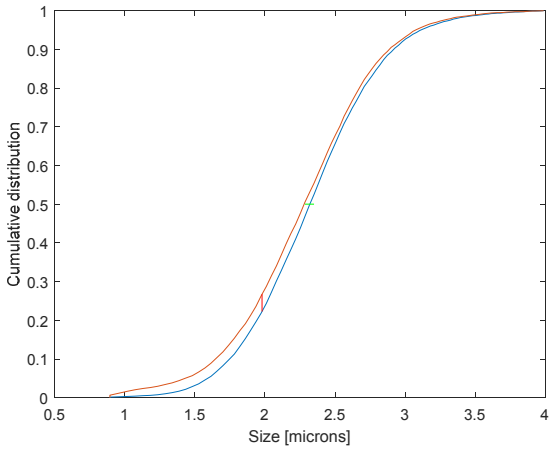

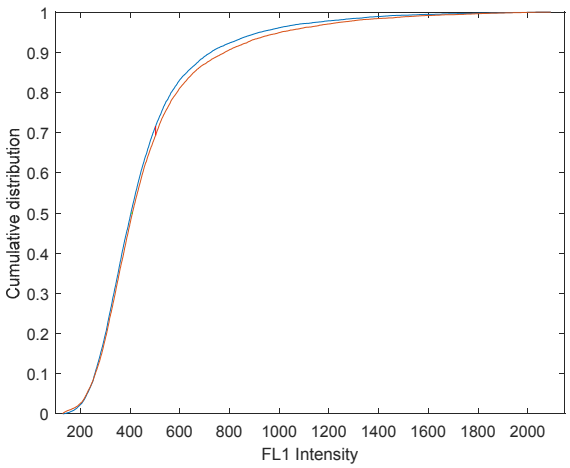

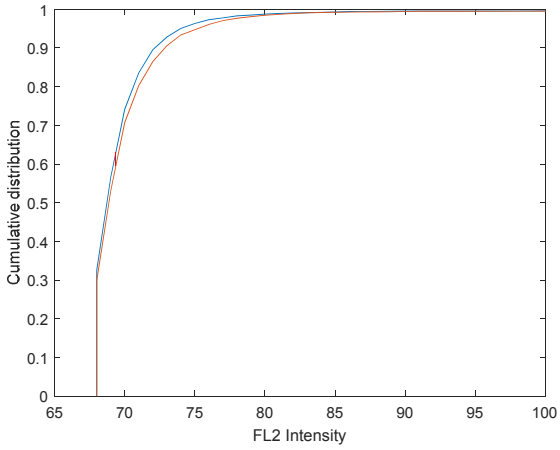

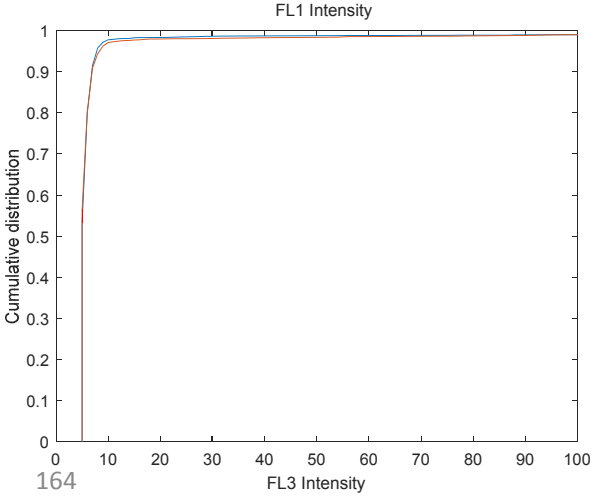

Aspergillus versicolor, 85%RH, 200ppb Ozone
Peak Stats FL1

	FL1 pre	FL1 post
Size (um)	2.380855	2.333537
Size SD	0.265444	0.270898
FL (intensity)	367.962060	370.824799
FL SD	75.131672	79.052201
Linear Fit slope	11.453	2.4371
Size_FL Corr	-0.0163	-0.0450

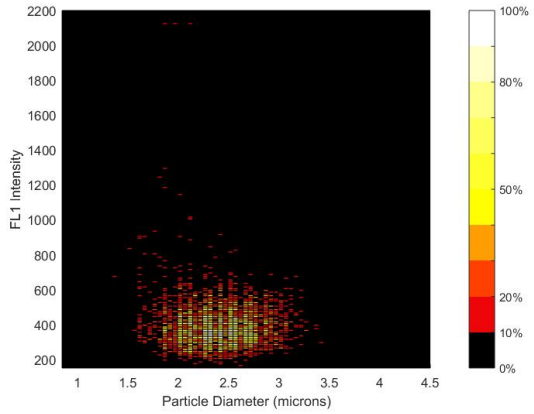

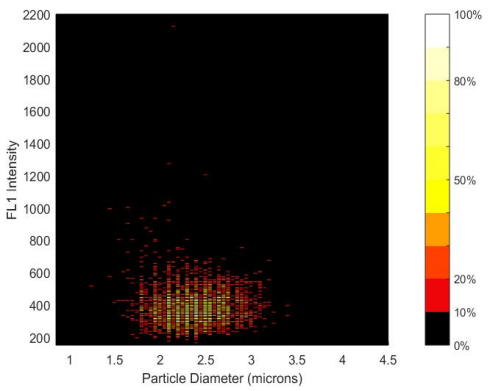

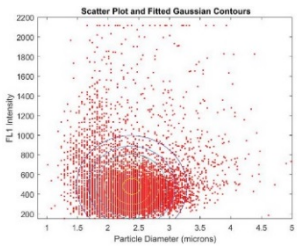

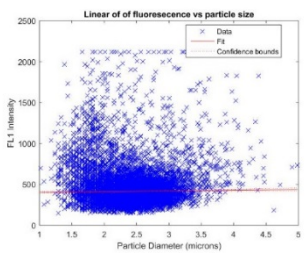

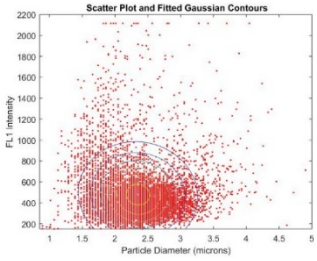

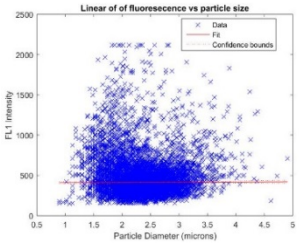

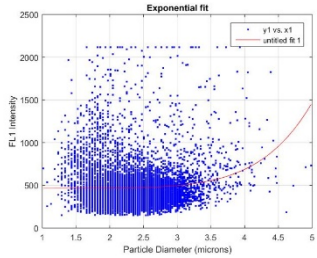

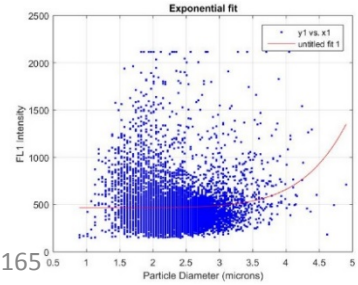

Aspergillus versicolor, 85%RH, 200ppb Ozone
Peak Stats FL1

Pre Ozone

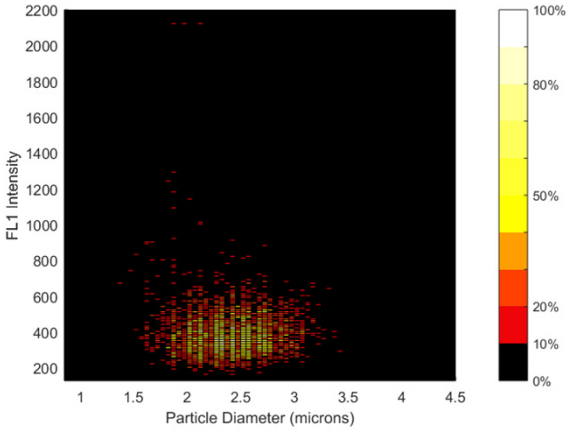

Ozone

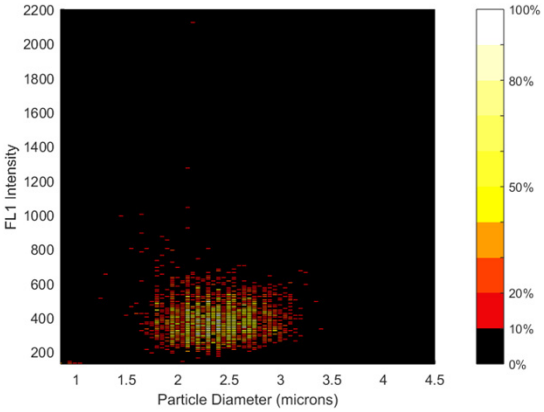

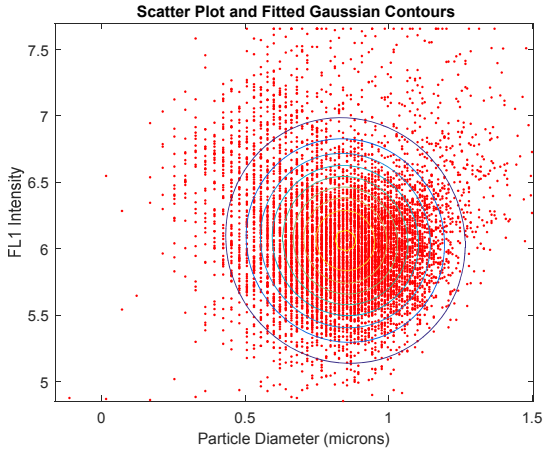

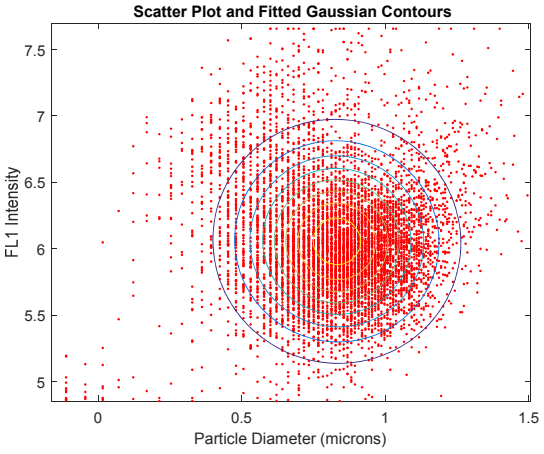

Aspergillus versicolor

RH (%)	85
Ozone (ppb)/ suspension time (hr)	0 / 3 hours
Chamber Date	10/04/2015
Culture age (days)	38
InstaScope Gain	High
I.S. Files (t=0,1hr,3hr) {points}	0006, 0015, 0029 (Igor points: 1, 10, 24)

Pre Particle Size Distribution

Gauss fit mean	2.411
SD +/- (width/sqrt(2))	0.66914
Size Range	1.5 – 3.5

Post Particle Size Distribution

Gauss fit mean	2.2545
SD +/- (width/sqrt(2))	0.61741
Size Range	1.5 – 3.5

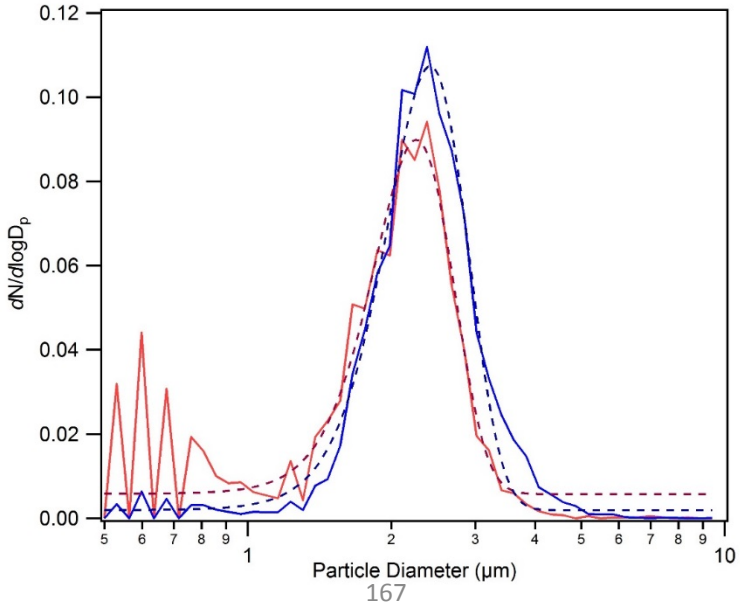

Aspergillus versicolor, 85%RH, 0ppb Ozone

Pre Particle FL1 Distribution

LogNormalFL1	356.1
SD (*,/)	0.683378
Size range	1.5 – 3.5
FL1 Range	128 - 2100

Post Particle FL1 Distribution

LogNormalFL1	349.84
SD (*,/)	0.647422
Size range	1.5 – 3.5
FL1 Range	128 - 2100

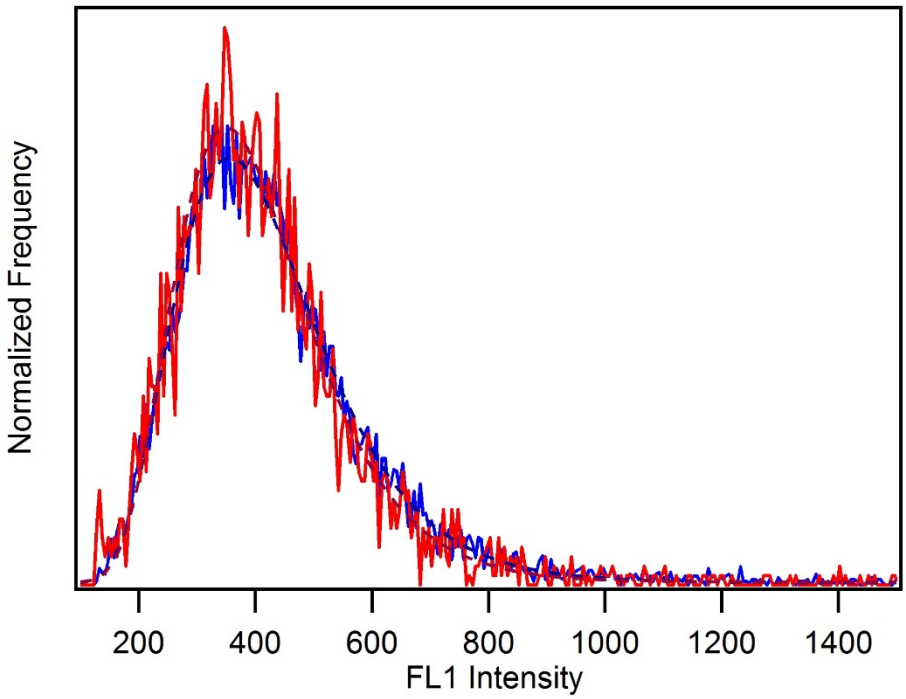

Aspergillus versicolor, 85%RH, 0ppb Ozone

	Pre O3 (%)	1hr (%)	3hr (%)
Nonfluorescent	0.54	0.76	1.56
Saturated FL1	0.47	0.53	0.32
Channel FL1	99.18	98.91	97.00
Channel FL2	48.51	49.03	50.86
Channel FL3	19.19	22.70	21.78

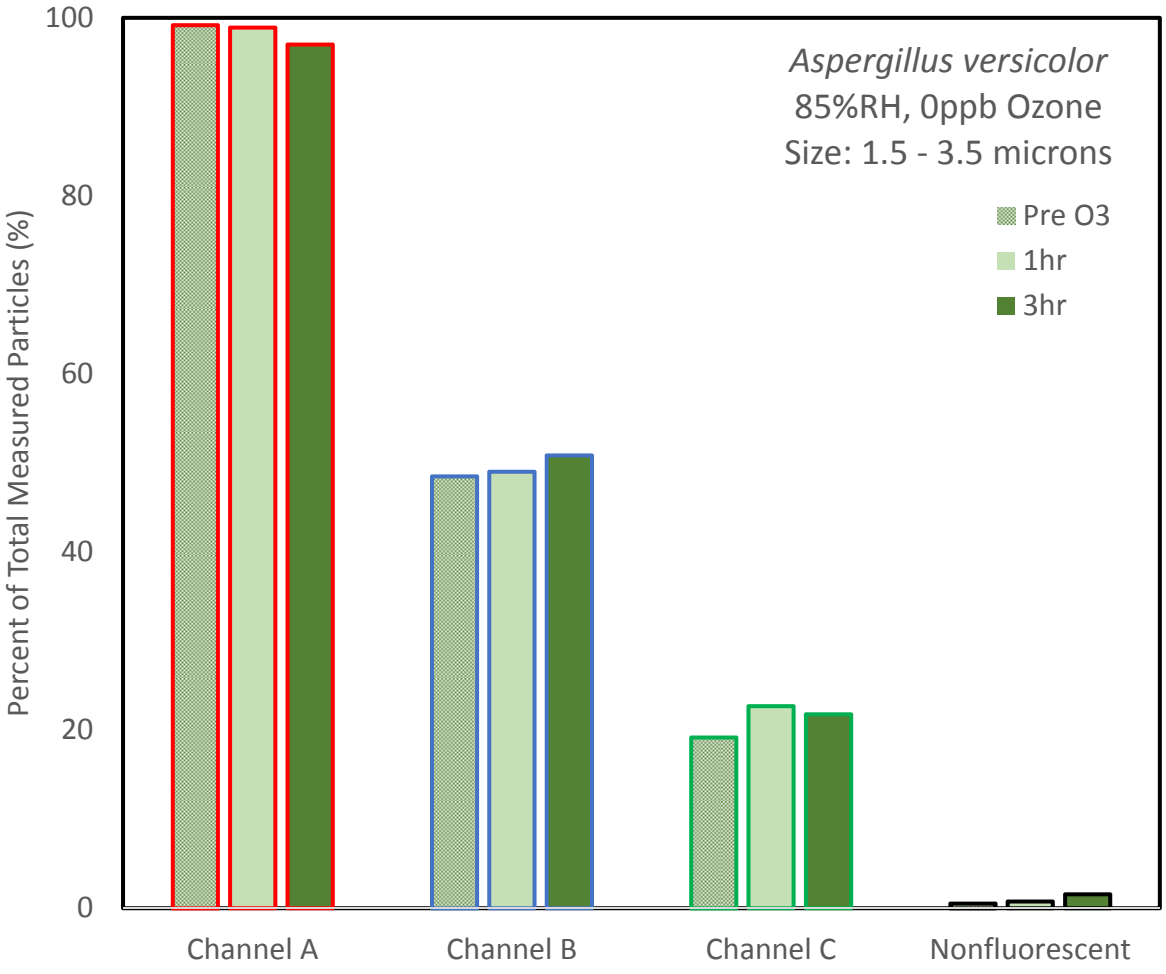

Aspergillus versicolor, 85%RH, 0ppb Ozone
KS (size, FL1, FL2, FL3)

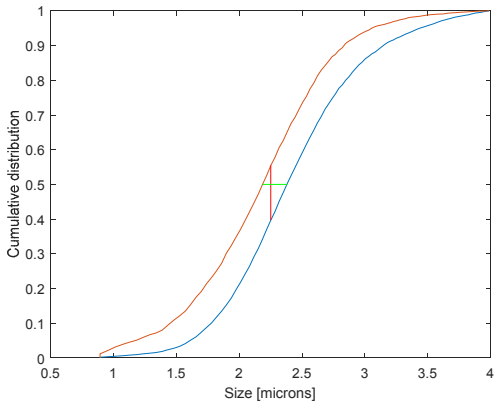

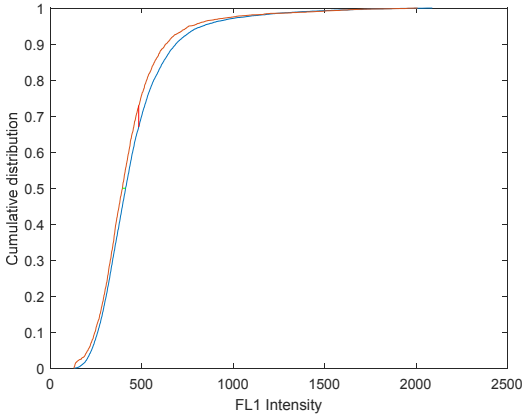

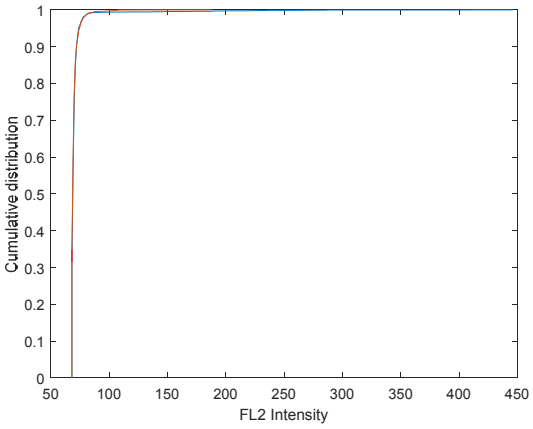

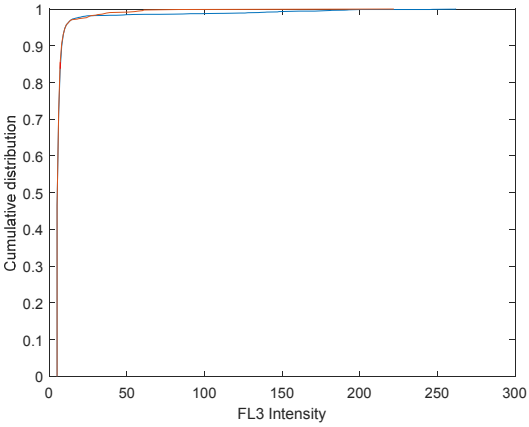

Aspergillus versicolor, 85%RH, 0ppb Ozone
Peak Stats FL1

Pre

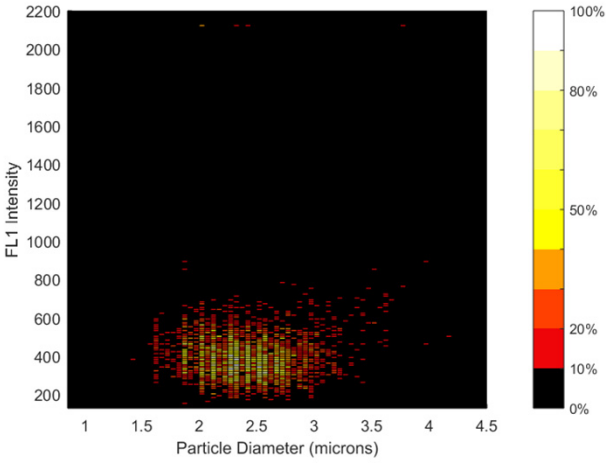

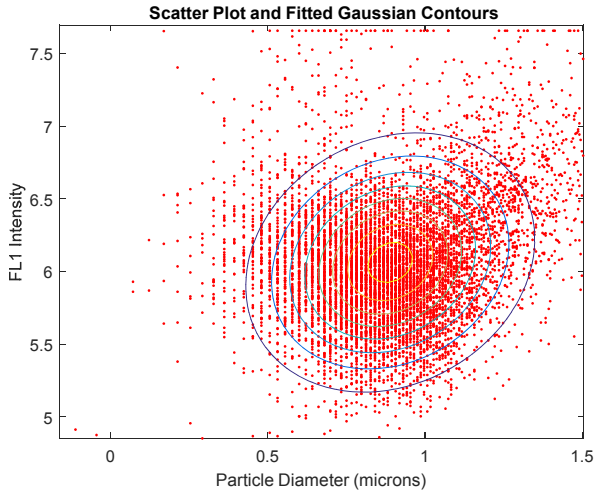

Post

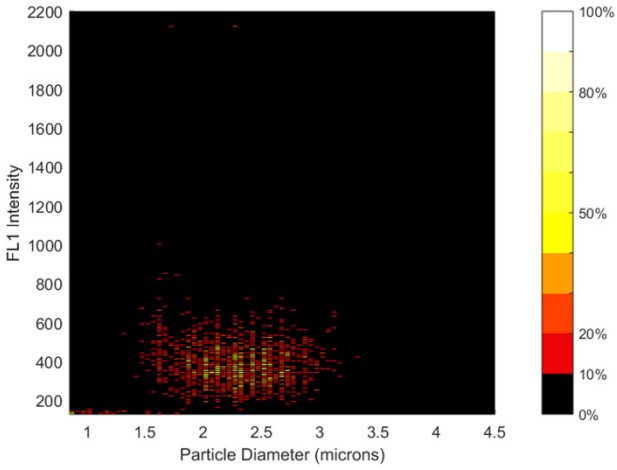

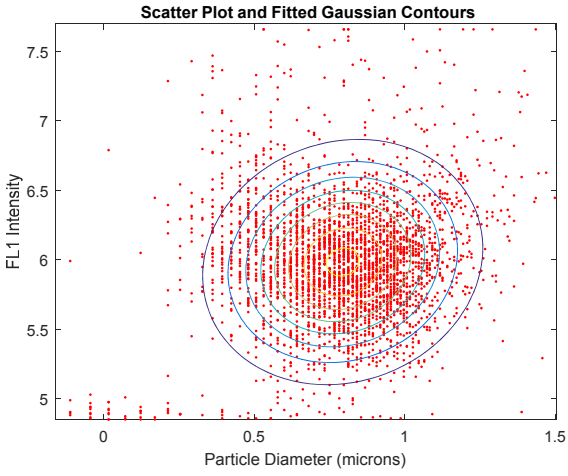

Aspergillus versicolor

RH (%)	30
Ozone (ppb)/ suspension time (hr)	200 / 3 hours
Chamber Date	10/02/2015
Culture age (days)	36
InstaScope Gain	High
I.S. Files (t=0,1hr,3hr) {points}	0002, 0019, 0028 (Igor points: 1, 18, 27)

Pre Particle Size Distribution

Gauss fit mean	2.2701
SD +/- (width/sqrt(2))	0.49899
Size Range	1.5 – 3.5

Post Particle Size Distribution

Gauss fit mean	2.1047
SD +/- (width/sqrt(2))	0.45664
Size Range	1.5 – 3.5

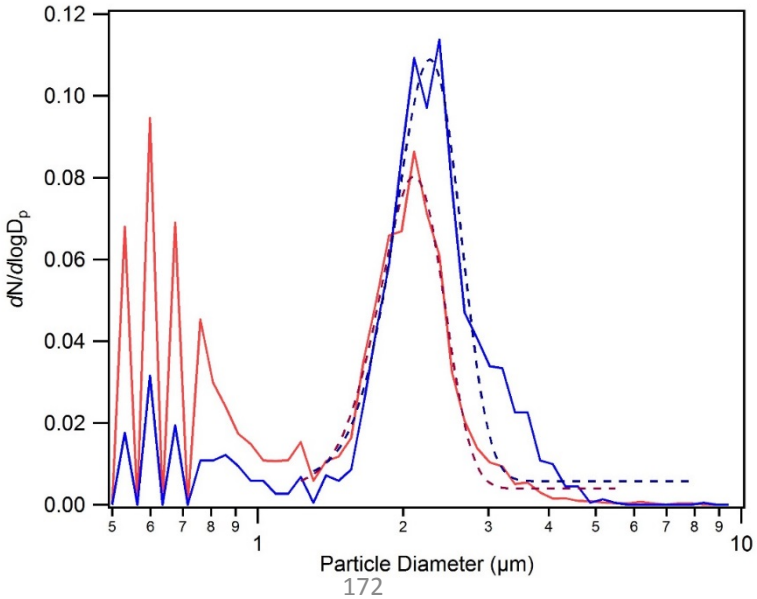

Aspergillus versicolor, 30%RH, 200ppb Ozone

Pre Particle FL1 Distribution

LogNormalFL1	393.75
SD (*,/)	0.705
Size range	1.5 – 3.5
FL1 Range	128 - 2100

Post Particle FL1 Distribution

LogNormalFL1	374.61
SD (*,/)	.699
Size range	1.5 – 3.5
FL1 Range	128 - 2100

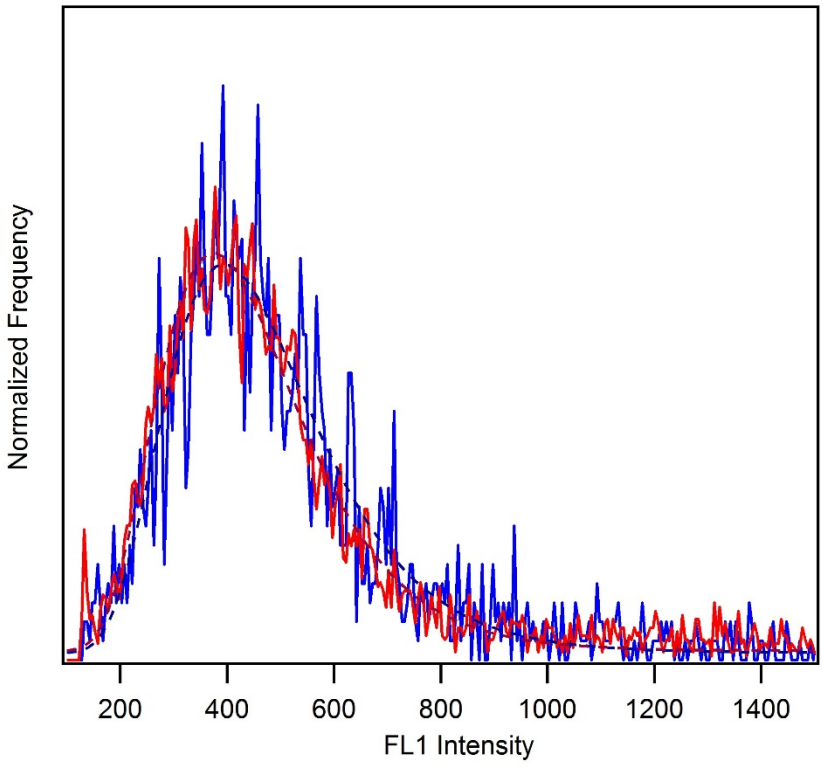

Aspergillus versicolor, 30%RH, 200ppb Ozone

	Pre O3 (%)	1hr (%)	3hr (%)
Nonfluorescent	1.37	3.70	6.29
Saturated FL1	0.69	0.74	0.52
Channel FL1	97.77	93.78	90.06
Channel FL2	63.37	57.02	53.35
Channel FL3	8.53	6.20	5.93

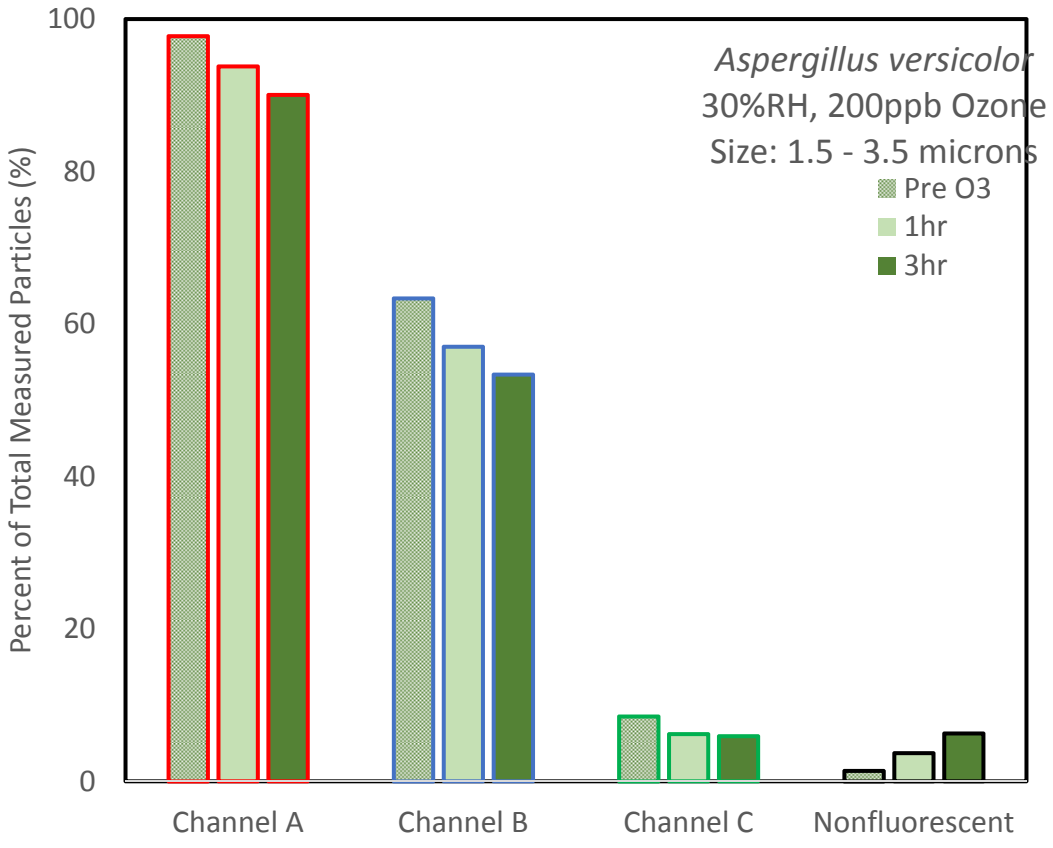

Aspergillus versicolor, 30%RH, 200ppb Ozone
KS (size, FL1, FL2, FL3)

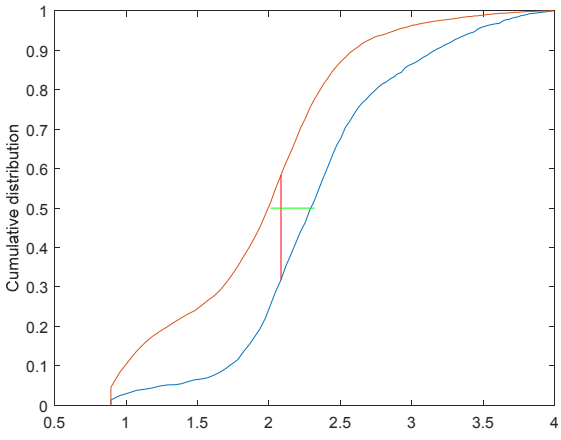

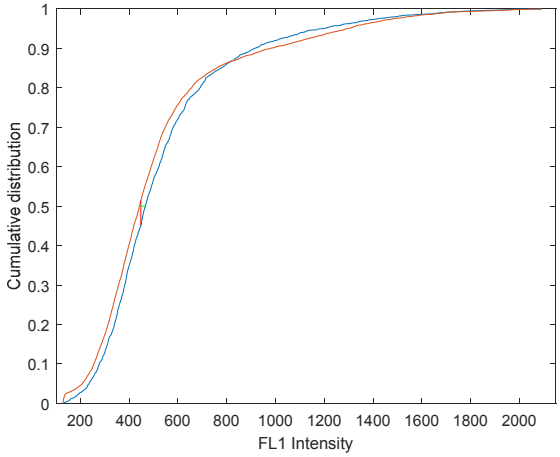

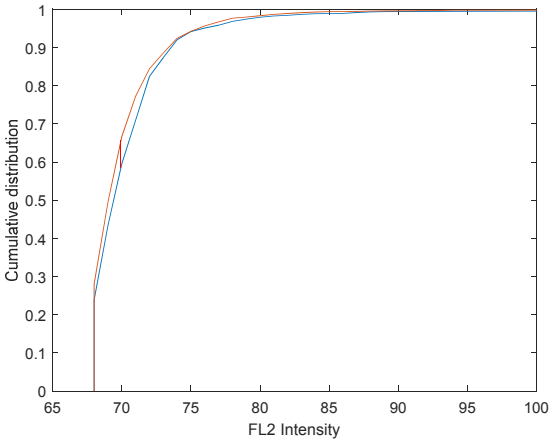

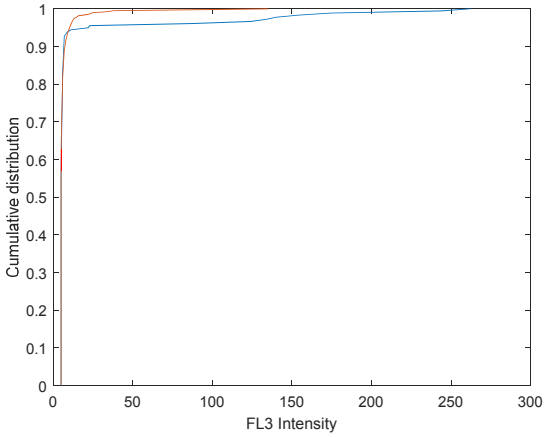

Aspergillus versicolor, 30%RH, 200ppb Ozone
Peak Stats FL1

Pre

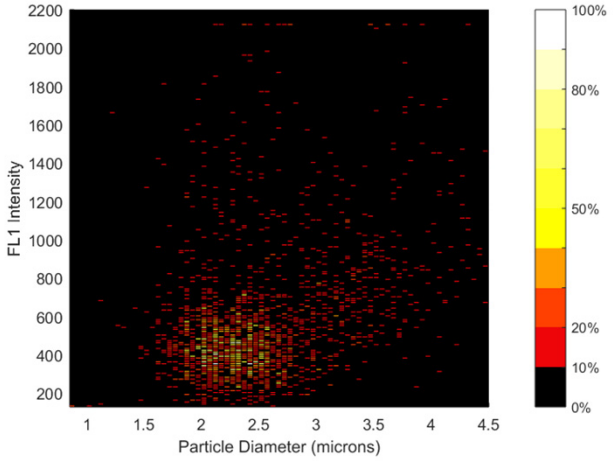

Post

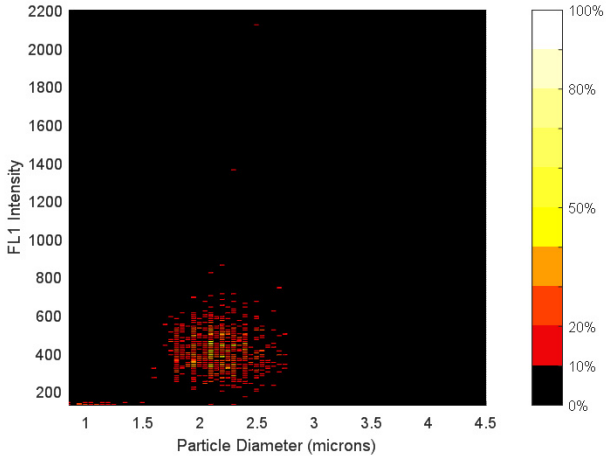

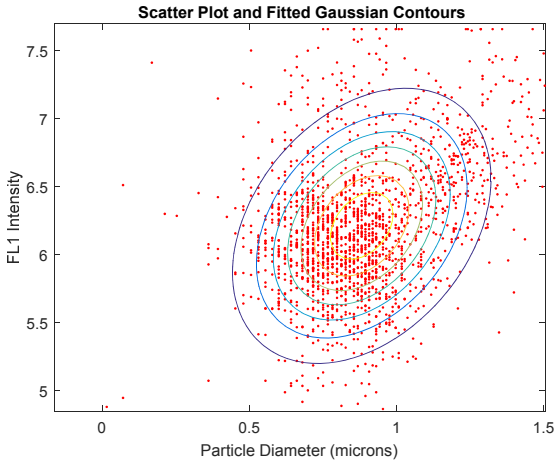

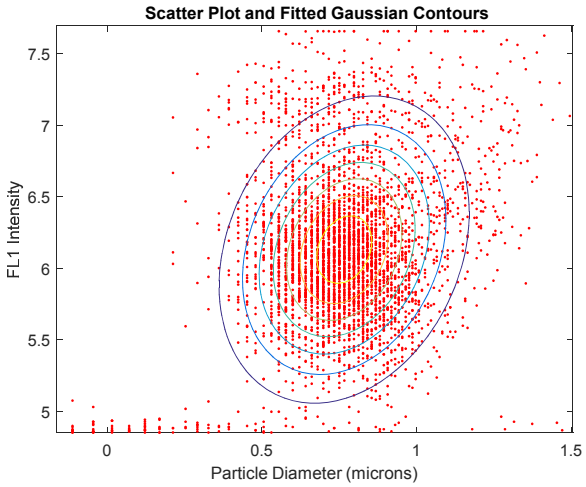

Aspergillus versicolor

RH (%)	30
Ozone (ppb)/ suspension time (hr)	0 / 3 hours
Chamber Date	10/01/2015
Culture age (days)	35
InstaScope Gain	High
I.S. Files (t=0,1hr,3hr) {points}	0002, 0019, 0028 (Igor points: 1, 18, 27)

Pre Particle Size Distribution

Gauss fit mean	2.30
SD +/- (width/sqrt(2))	0.554
Size Range	1.5 – 3.5

Post Particle Size Distribution

Gauss fit mean	2.16
SD +/- (width/sqrt(2))	0.536
Size Range	1.5 – 3.5

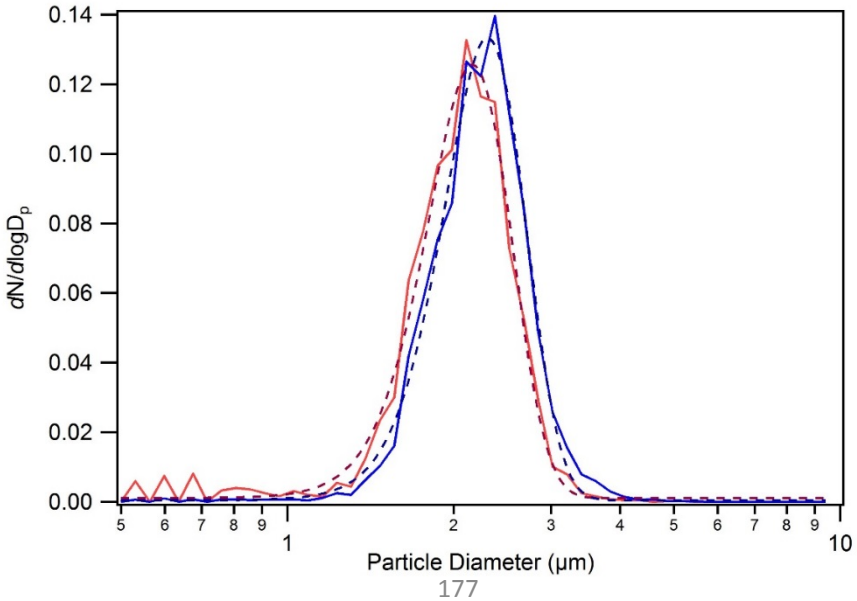

Aspergillus versicolor, 30%RH, 0ppb Ozone

Pre Particle FL1 Distribution

LogNormalFL1	333.85
SD (*,/)	0.761
Size range	1.5 – 3.5
FL1 Range	128 - 2100

Post Particle FL1 Distribution

LogNormalFL1	339.82
SD (*,/)	0.693
Size range	1.5 – 3.5
FL1 Range	128 - 2100

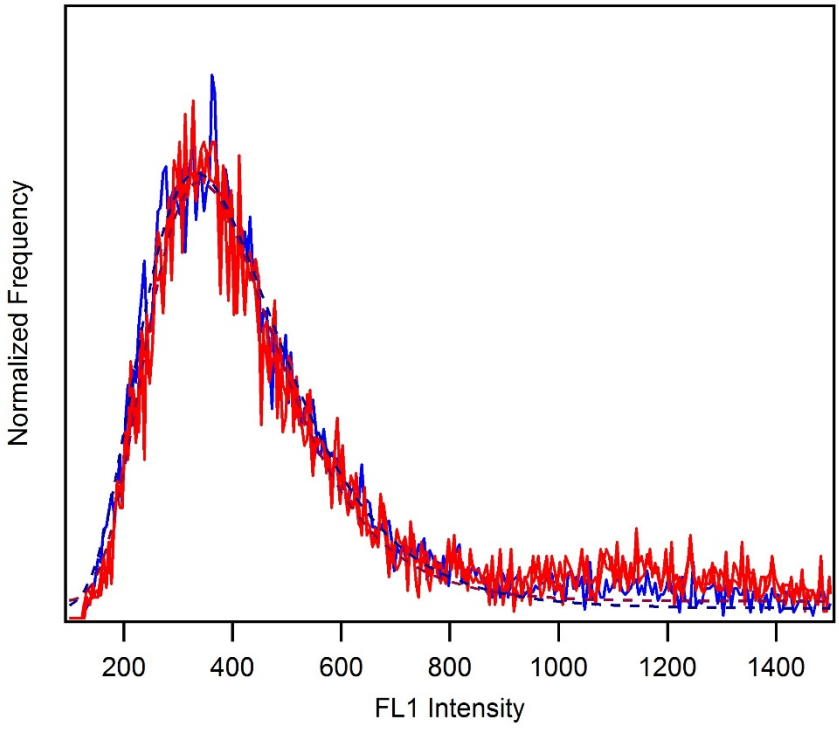

Aspergillus versicolor, 30%RH, 0ppb Ozone

	Pre O3 (%)	1hr (%)	3hr (%)
Nonfluorescent	0.26	0.44	0.72
Saturated FL1	0.43	0.49	0.37
Channel FL1	99.64	99.33	98.71
Channel FL2	60.63	58.42	59.25
Channel FL3	6.99	6.02	6.64

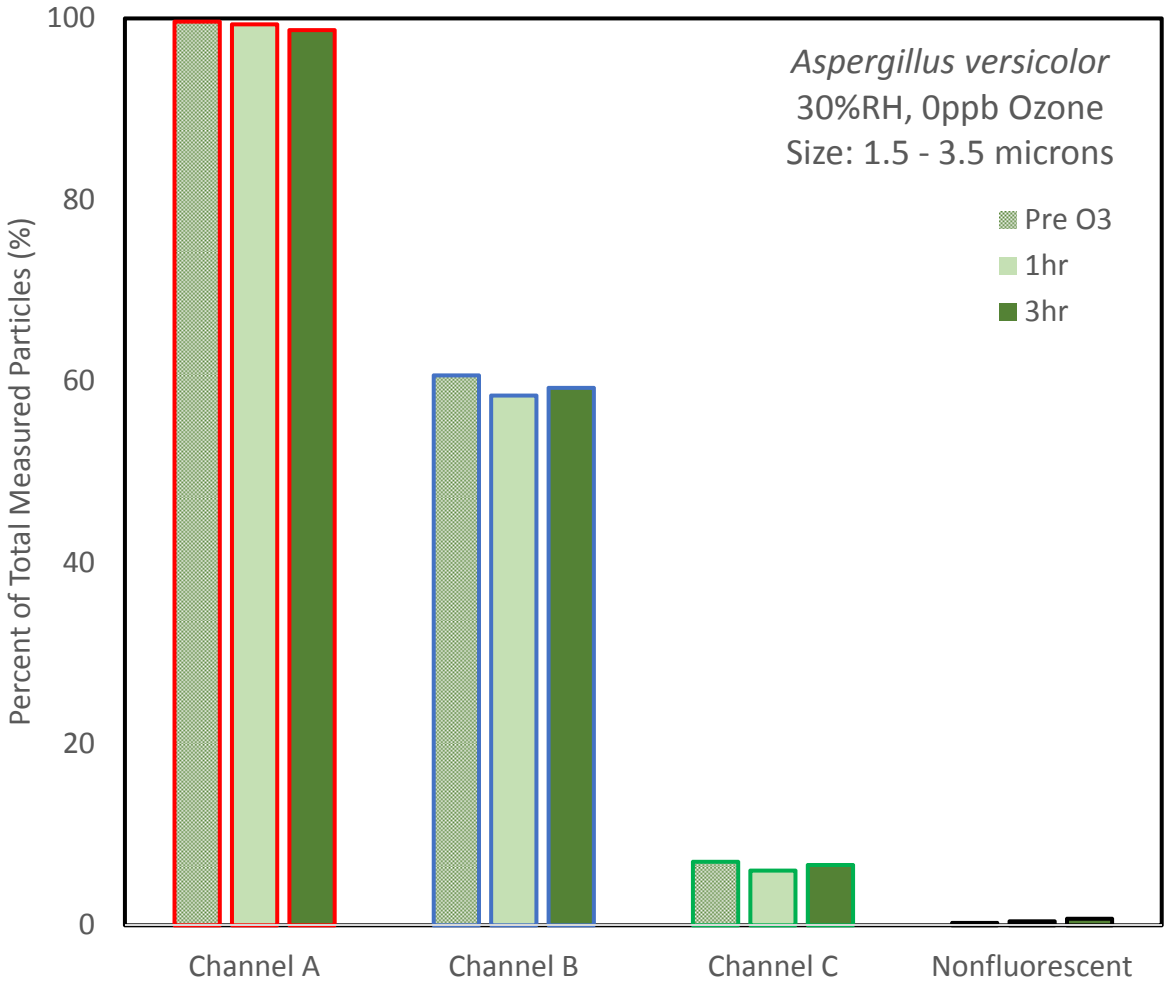

Aspergillus versicolor, 30%RH, 0ppb Ozone
KS (size, FL1, FL2, FL3)

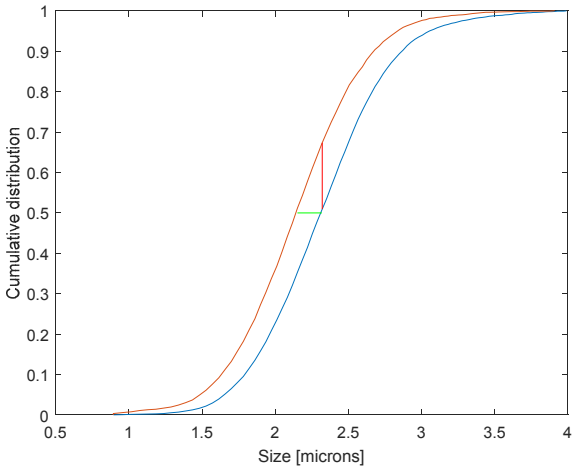

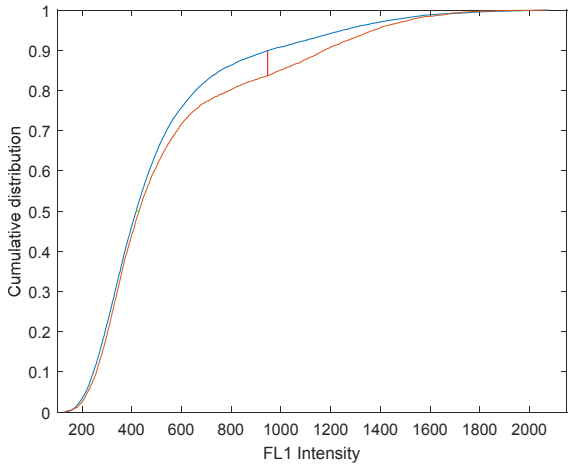

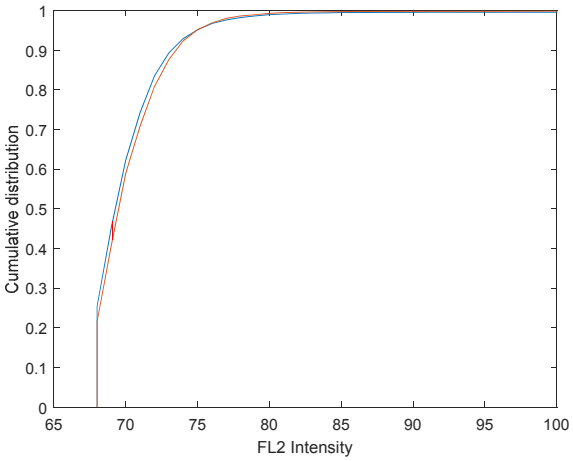

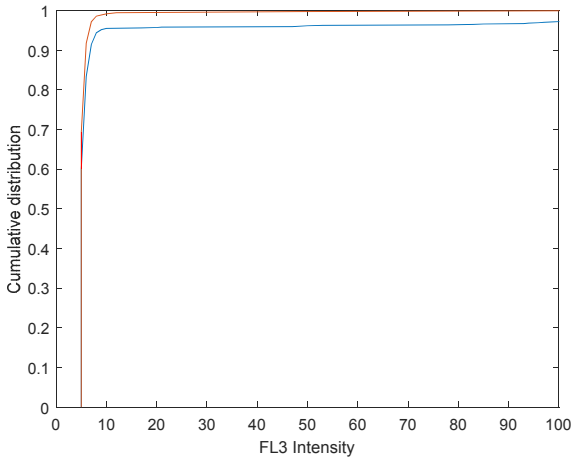

Aspergillus versicolor, 30%RH, 0ppb
Peak Stats FL1

Pre

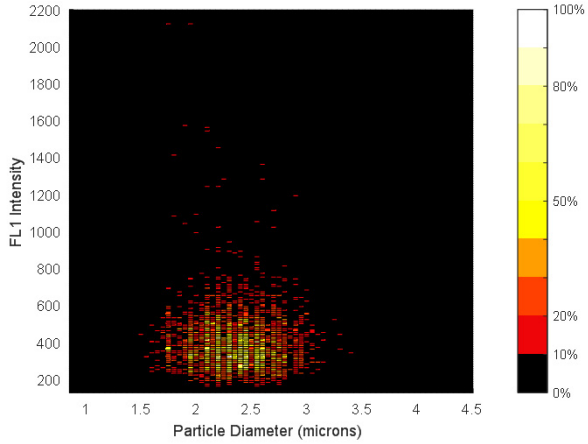

Post

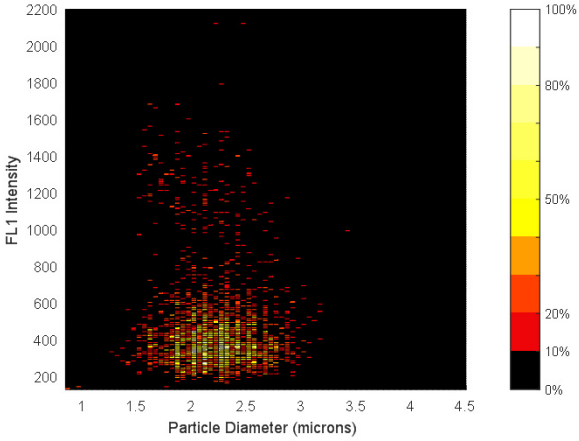

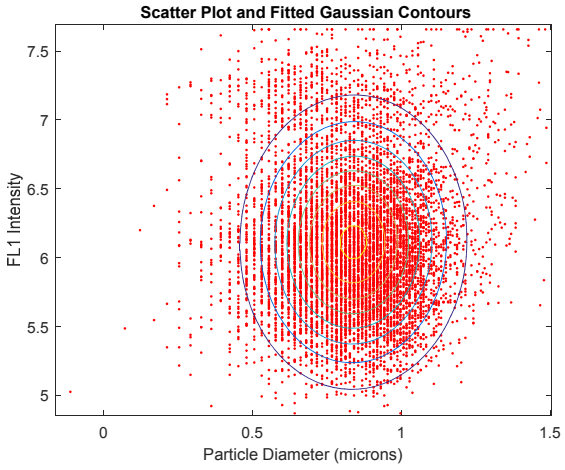

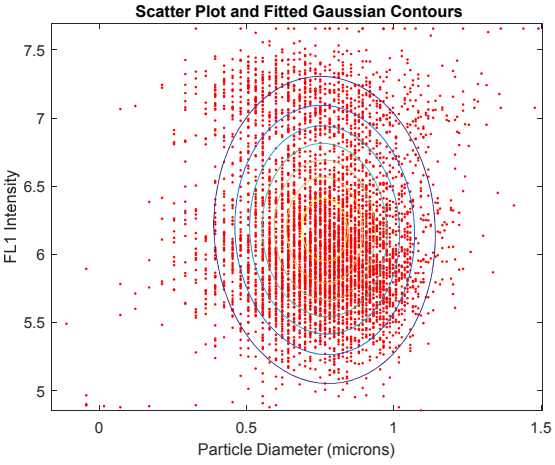

Aspergillus fumigatus

RH (%)	85
Ozone (ppb)/ suspension time (hr)	200 / 3 hours
Chamber Date	04/21/2015
Culture age (days)	78
InstaScope Gain	High
I.S. Files (t=0,1hr,3hr) {points}	0003, 0016, 0021 (Igor points: 0, 13, 18)

Pre Particle Size Distribution

Gauss fit mean	2.284
SD +/- (width/sqrt(2))	0.69452
Size Range	1.5 – 3.5

Post Particle Size Distribution

Gauss fit mean	2.1207
SD +/- (width/sqrt(2))	0.32538
Size Range	1.5 – 3.5

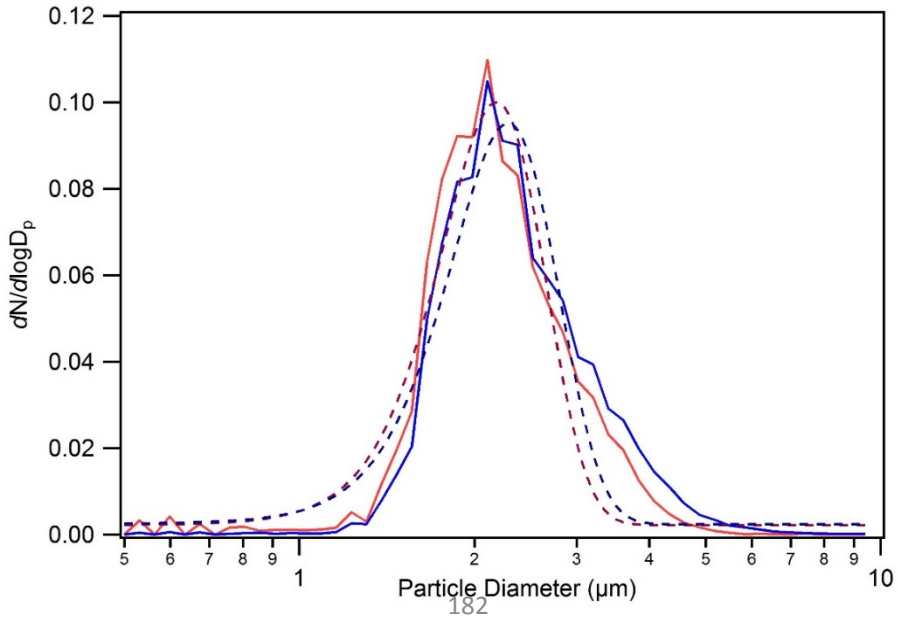

Aspergillus fumigatus (78days), 85%RH, 200ppb Ozone

Pre Particle FL1 Distribution

LogNormalFL1	1217.2
SD (*,/)	0.402247
Size range	1.5 – 3.5
FL1 Range	128 - 2100

Post Particle FL1 Distribution

LogNormal FL1	959.51
SD (*,/)	0.45613
Size range	1.5 – 3.5
FL1 Range	128 - 2100

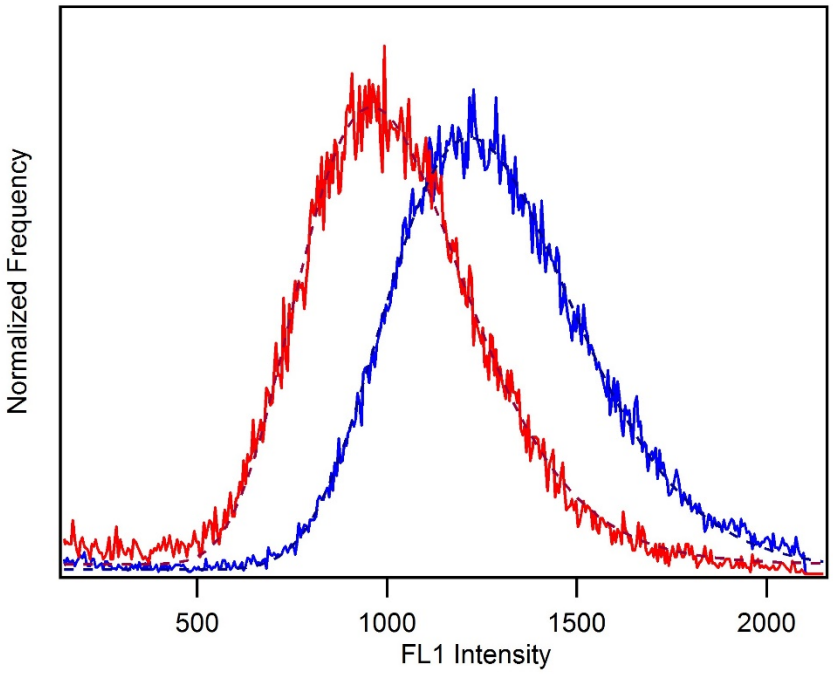

Aspergillus fumigatus (78 days)
85%RH, 600 ppb-hr Ozone
Example of peak statistic analysis limits

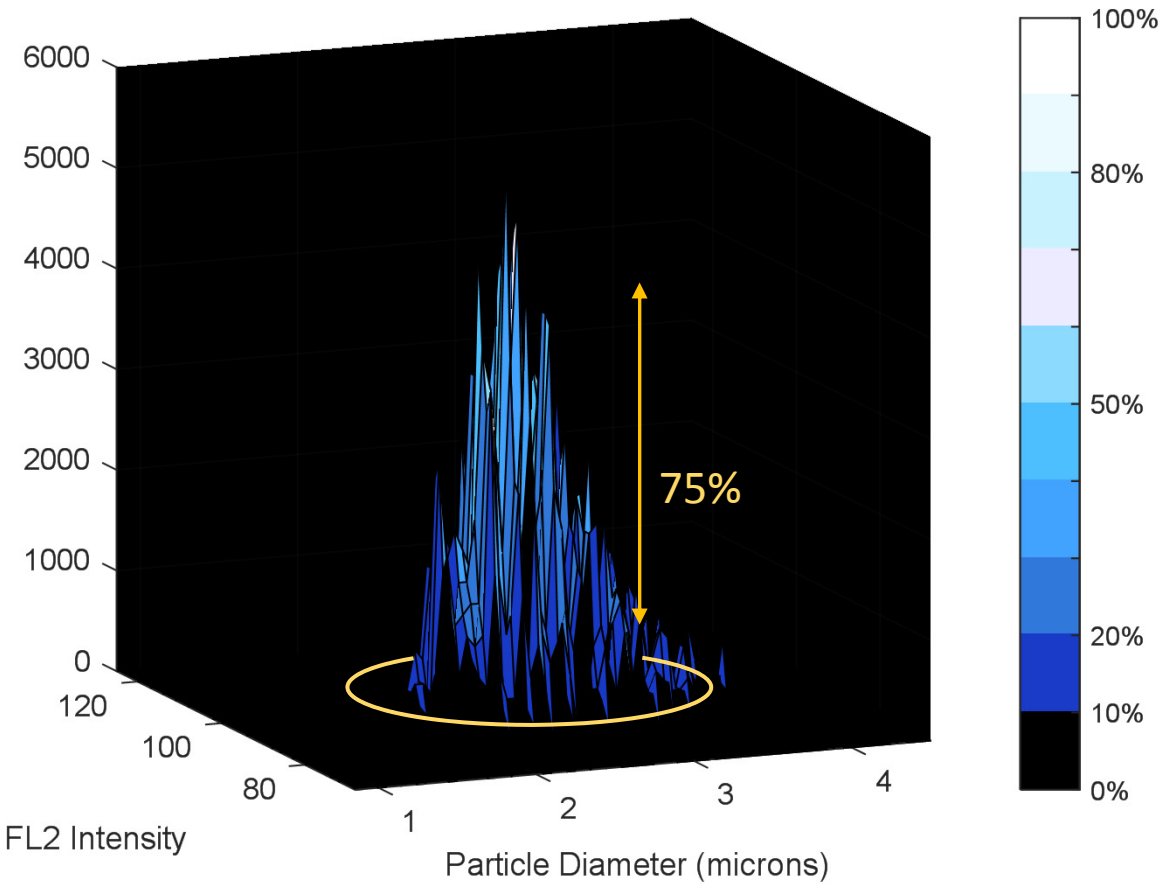

Aspergillus fumigatus (78 days)
85%RH, 600 ppb-hr Ozone

Pre Ozone

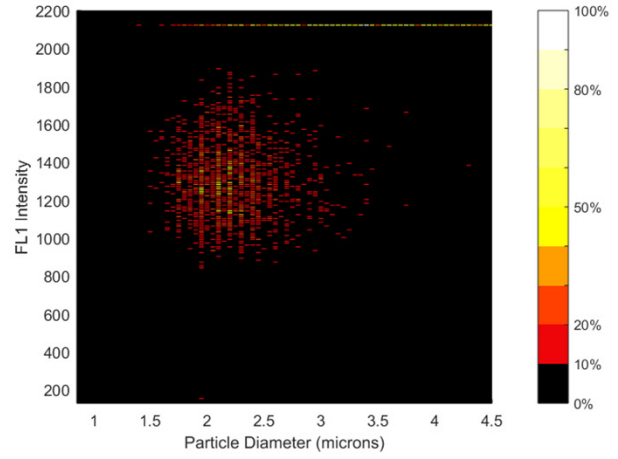

Post Ozone

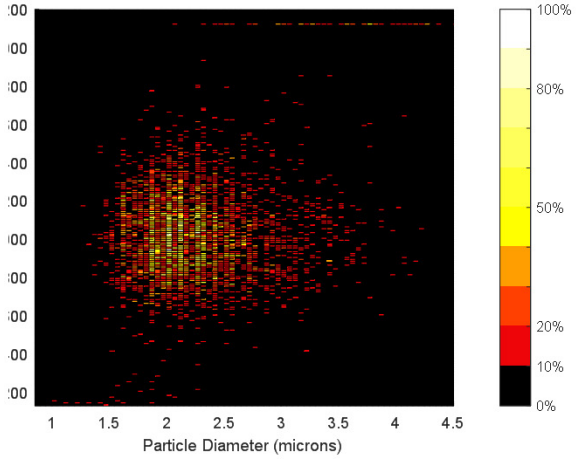

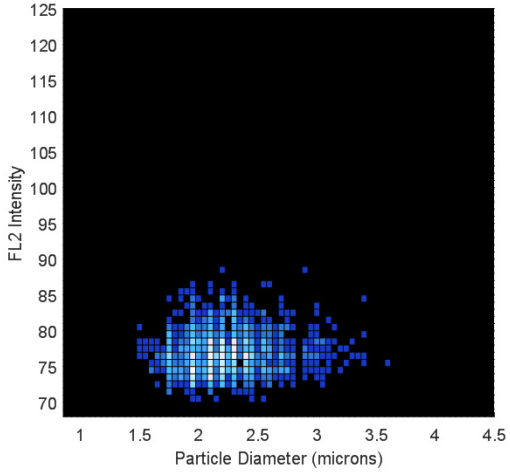

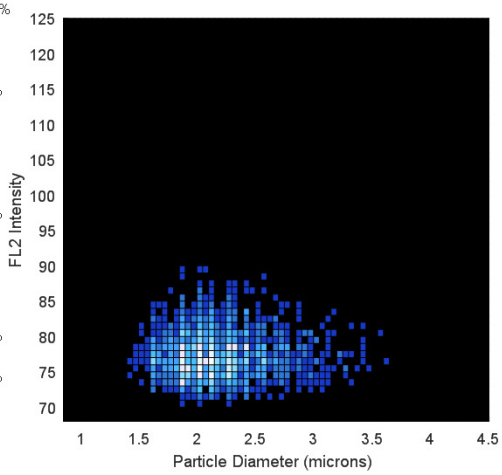

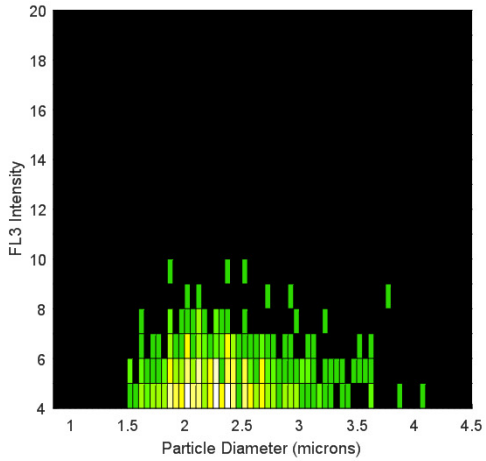

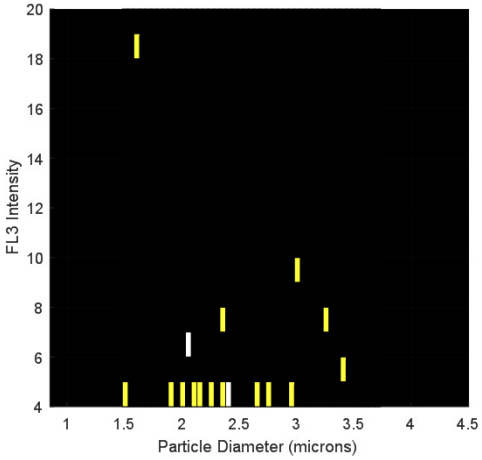

Aspergillus fumigatus (78days), 85%RH, 200ppb Ozone

	Pre O3 (%)	1hr (%)	3hr (%)
Nonfluorescent	0.14	0.13	0.19
Saturated FL1	5.212	1.277	0.911
Channel FL1	99.79	99.72	99.61
Channel FL2	99.65	99.72	99.63
Channel FL3	27.16	0.23	0.23

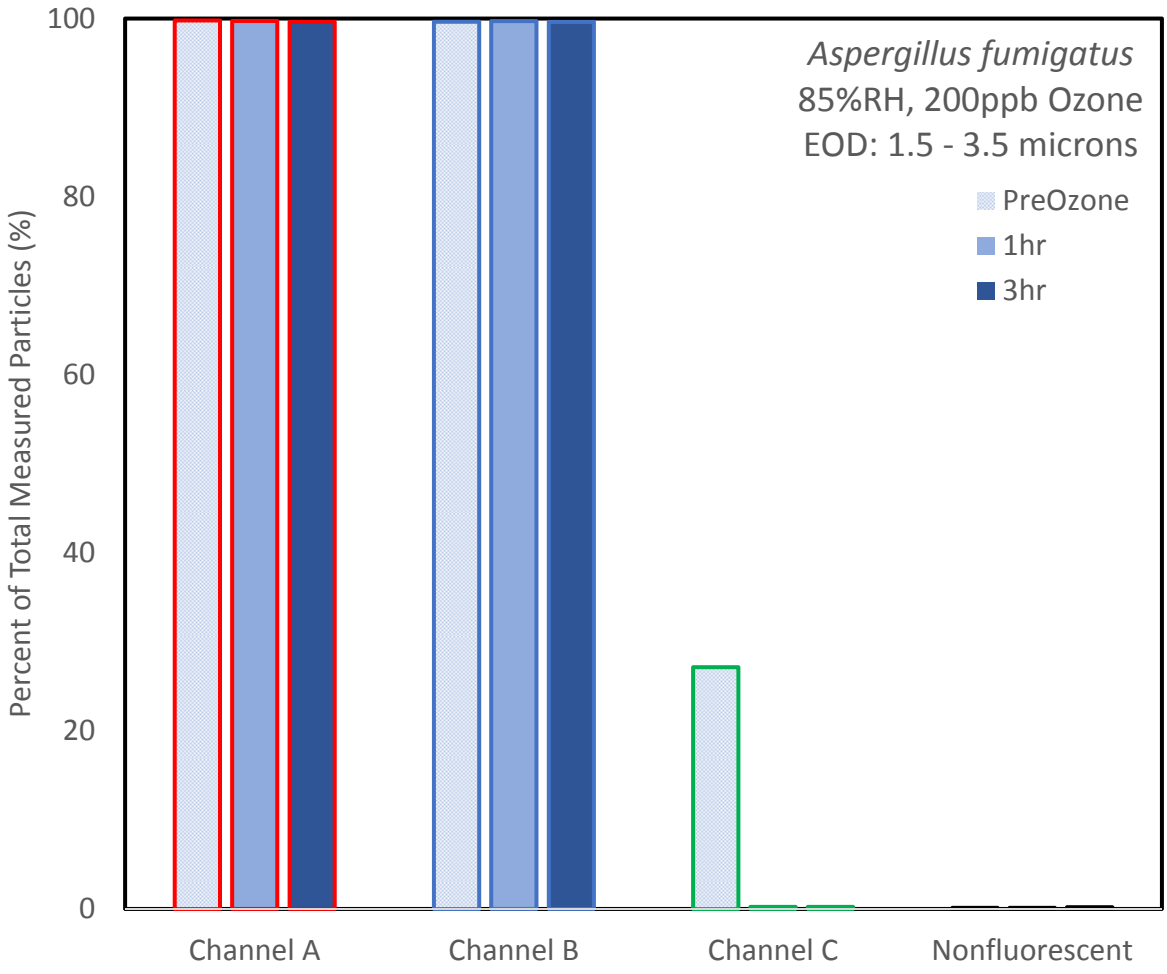

Aspergillus fumigatus (78days), 85%RH, 200ppb Ozone
KS (size, FL1, FL2, FL3)

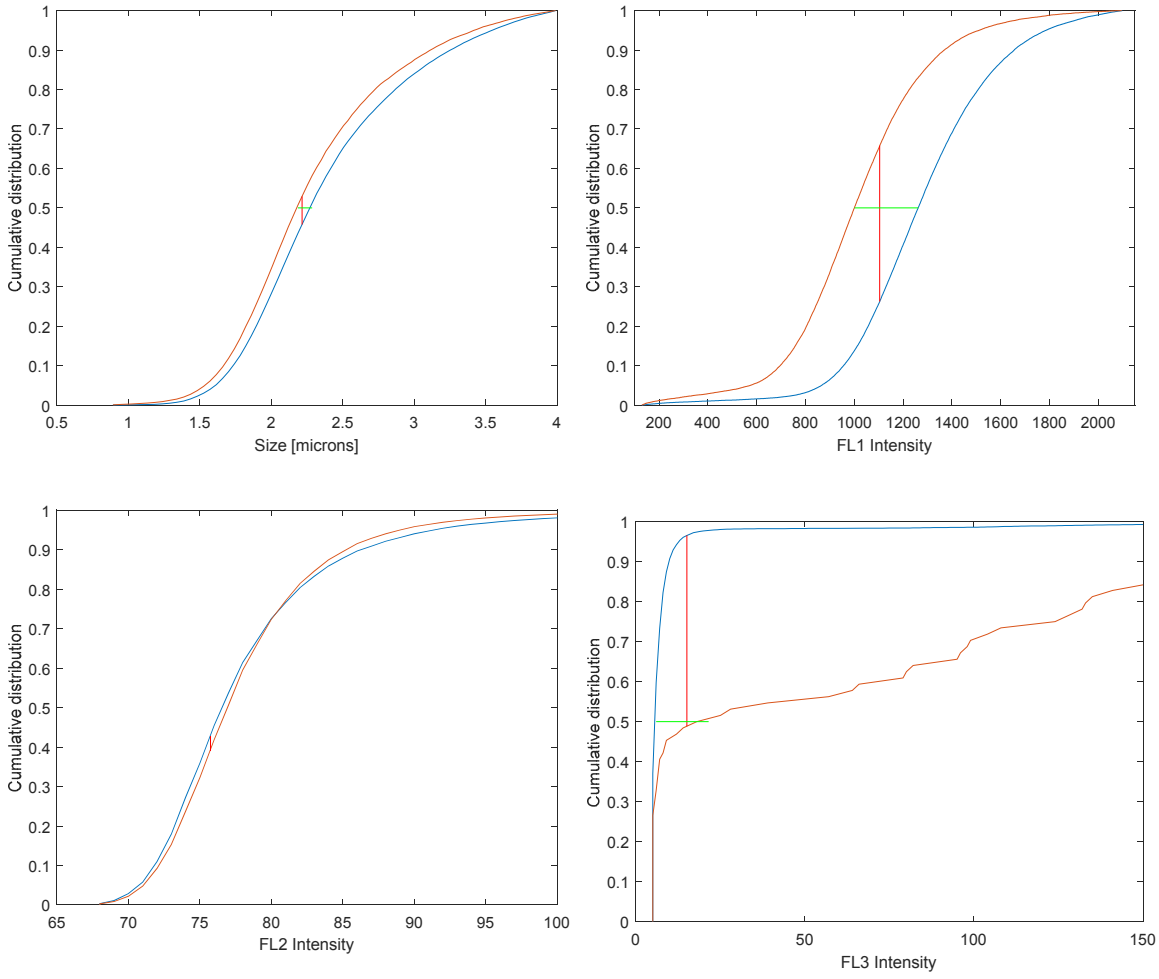

Aspergillus fumigatus

RH (%)	85
Ozone (ppb)/ suspension time (hr)	0 / 3 hours
Chamber Date	01/25/2016
Culture age (days)	15
InstaScope Gain	Low
I.S. Files (t=0,1hr,3hr) {points}	0002, 0007, 0012 (Igor points: 0, 5, 10)

Pre Particle Size Distribution

Gauss fit mean	2.0195
SD +/- (width/sqrt(2))	0.54268
Size Range	1.5 – 3.5

Post Particle Size Distribution

Gauss fit mean	1.9656
SD +/- (width/sqrt(2))	0.51748
Size Range	1.5 – 3.5

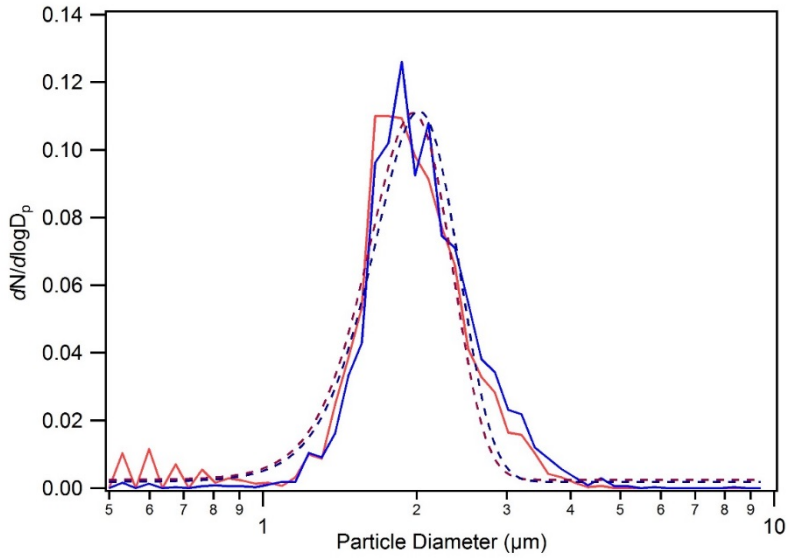

Aspergillus fumigatus (15days), 85%RH, 0ppb Ozone

Pre Particle FL1 Distribution

LogNormalFL1	352.11
SD (*,/)	0.305221
Size range	1.5 – 3.5
FL1 Range	128 - 2100

Post Particle FL1 Distribution

LogNormalFL1	351.57
SD (*,/)	0.286208
Size range	1.5 – 3.5
FL1 Range	128 - 2100

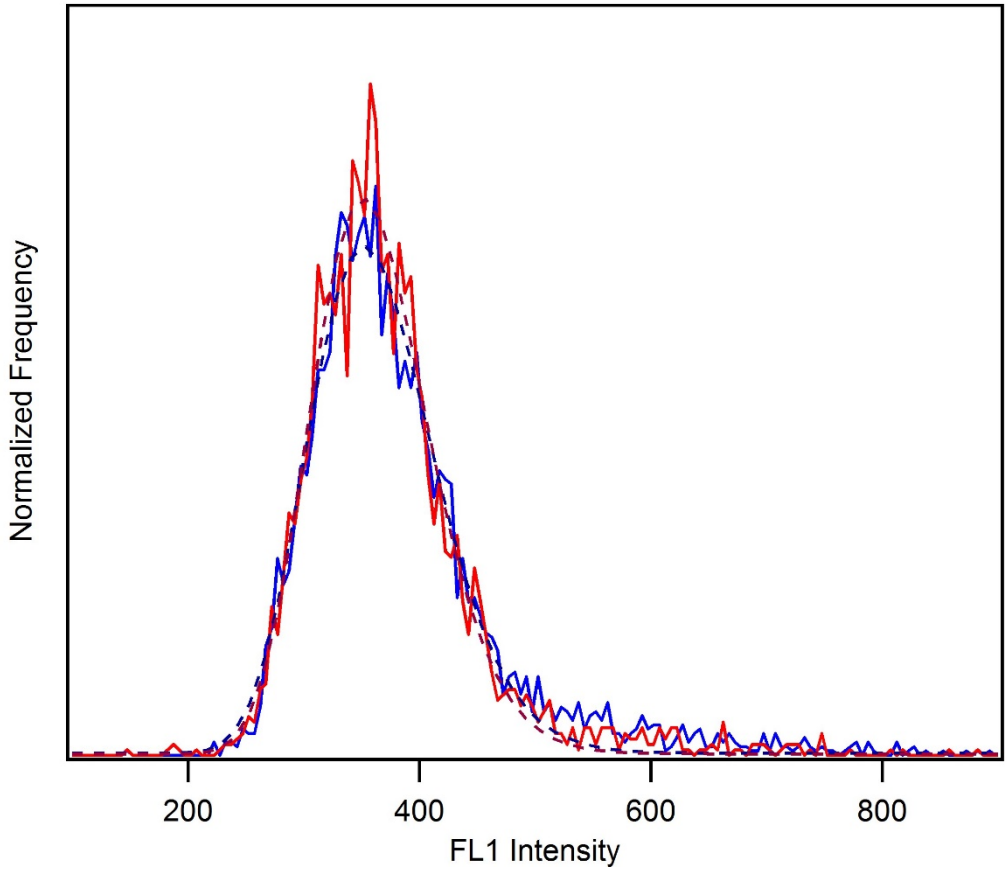

Aspergillus fumigatus (15days), 85%RH, 0ppb Ozone

	Pre O3 (%)	1hr (%)	3hr (%)
Nonfluorescent	0.12	0.13	0.18
Saturated FL1	0	0	0
Channel FL1	99.79	99.80	99.56
Channel FL2	99.68	99.67	99.67
Channel FL3	11.25	11.75	12.57

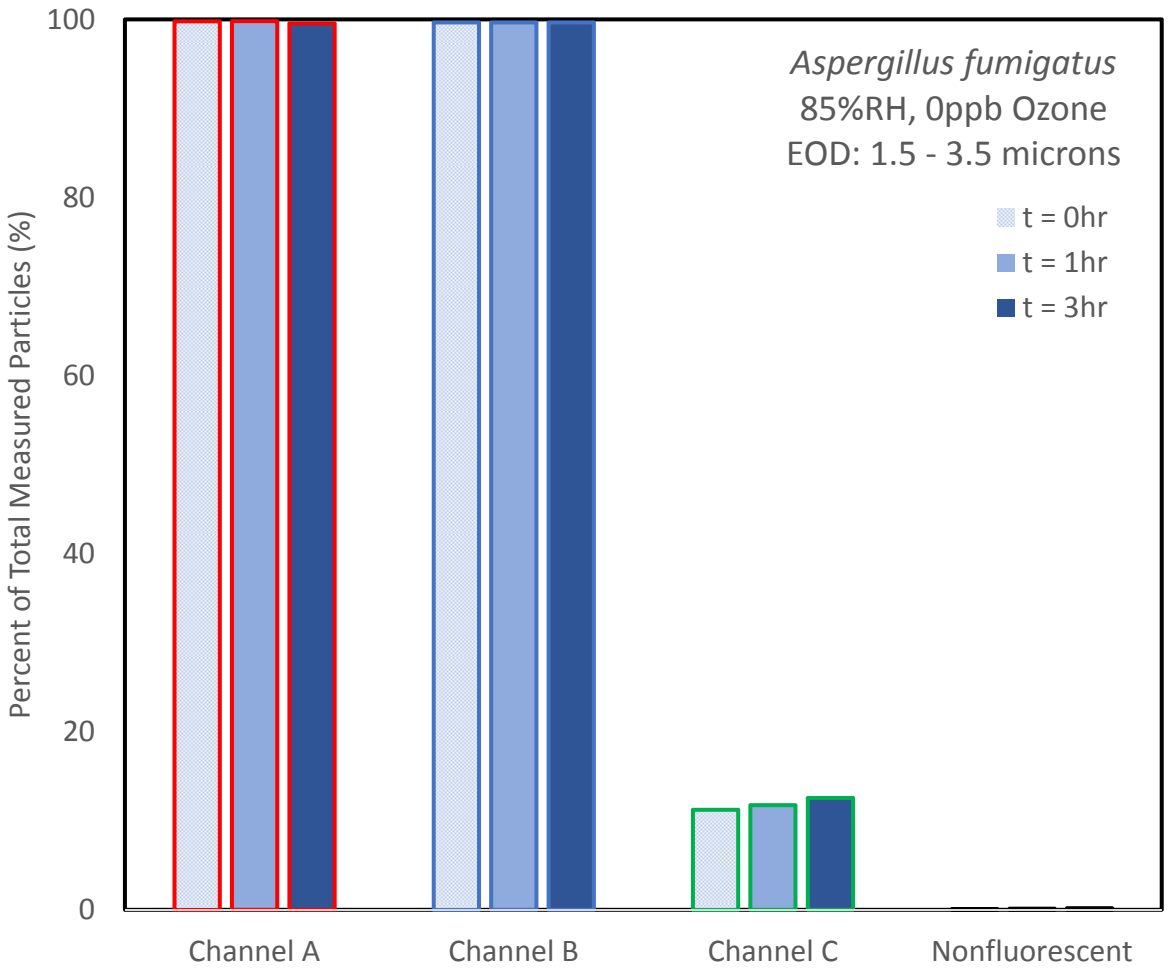

Aspergillus fumigatus, 85%RH, 0ppb Ozone(Low Gain)
KS (size, FL1, FL2, FL3)

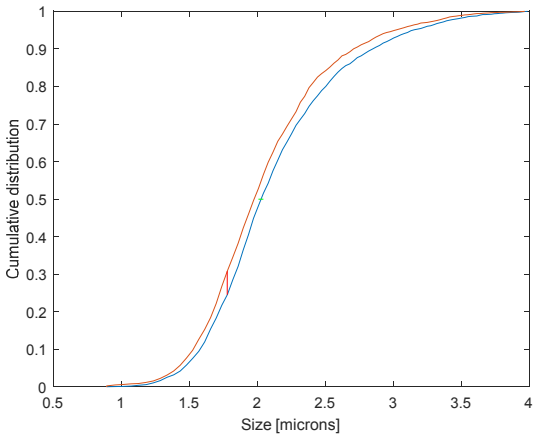

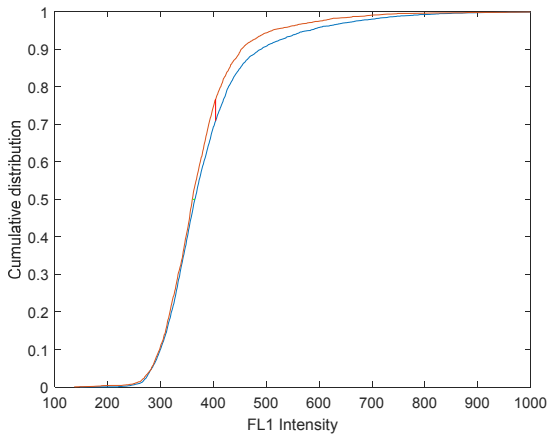

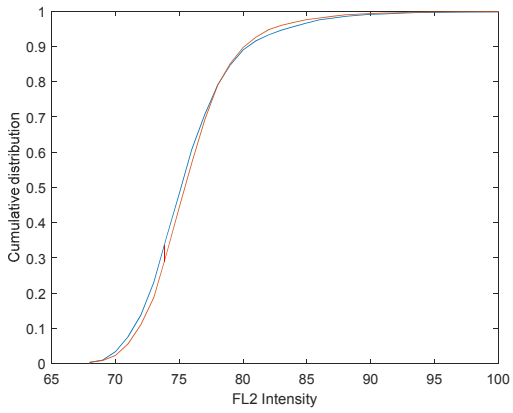

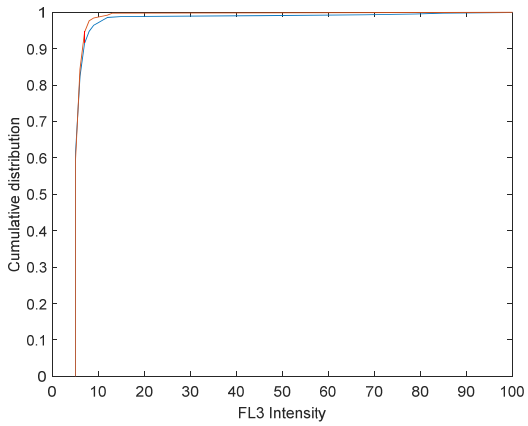

Aspergillus fumigatus

RH (%)	85
Ozone (ppb)/ suspension time (hr)	200 / 3 hours
Chamber Date	06/29/2015
Culture age (days)	11
InstaScope Gain	High
I.S. Files (t=0,1hr,3hr) {points}	0002, 0024, 0038 (Igor points: 0, 22, 36)

Pre Particle Size Distribution

Gauss fit mean	1.9111
SD +/- (width/sqrt(2))	0.54211
Size Range	1.5 – 3.5

Post Particle Size Distribution

Gauss fit mean	1.957
SD +/- (width/sqrt(2))	0.54469
Size Range	1.5 – 3.5

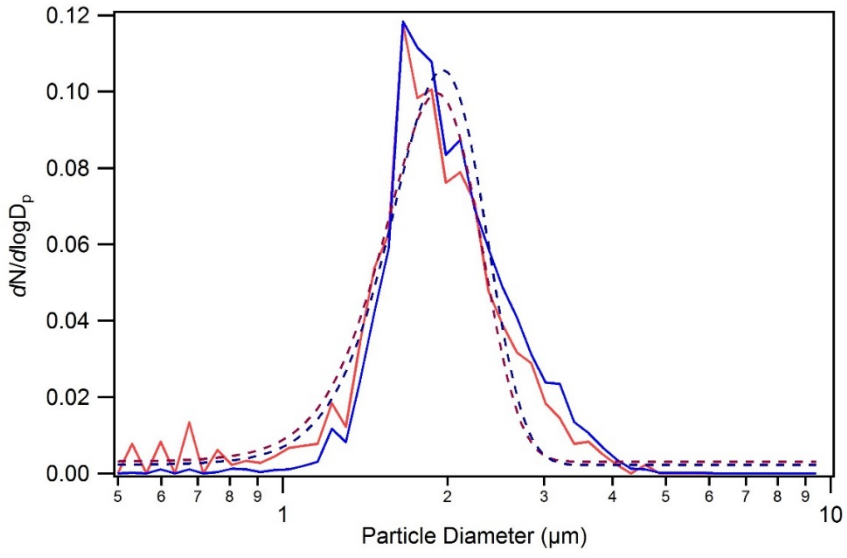

Aspergillus fumigatus (11days), 85%RH, 200ppb Ozone

Pre Particle FL1 Distribution

LogNormalFL1	1292.9
SD (*,/)	0.375877
Size range	1.5 – 3.5
FL1 Range	128 - 2100

Post Particle FL1 Distribution

LogNormalFL1	1184
SD (*,/)	0.349113
Size range	1.5 – 3.5
FL1 Range	128 - 2100

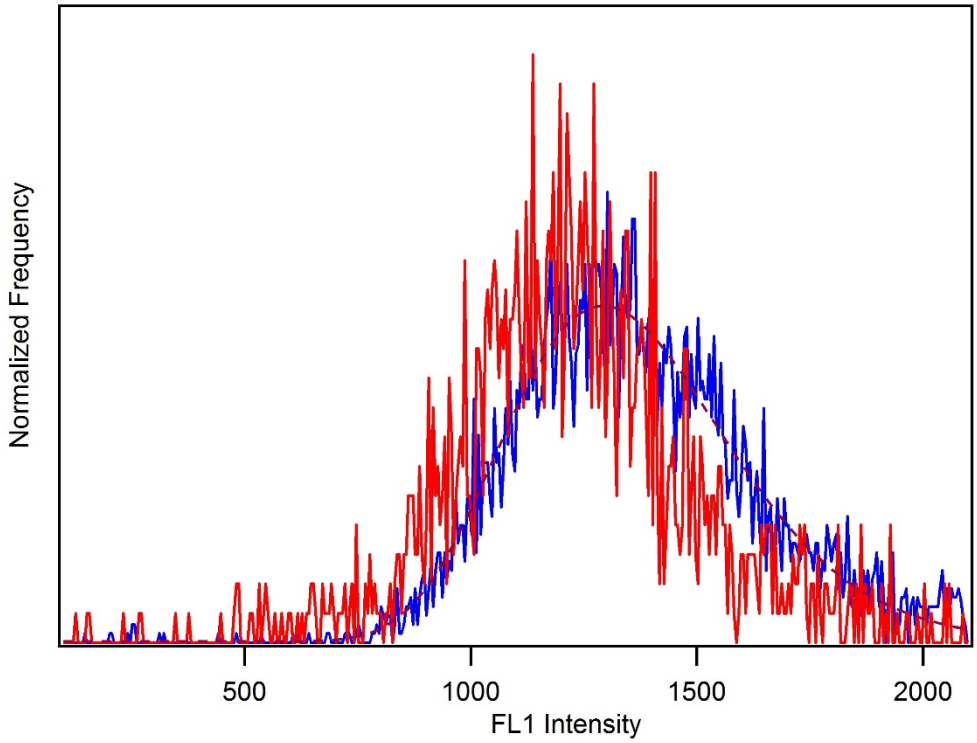

Aspergillus fumigatus (11days), 85%RH, 200ppb Ozone

	Pre O3 (%)	1hr (%)	3hr (%)
Nonfluorescent	0.14	0.17	0.07
Saturated FL1	6.74	1.75	2.64
Channel FL1	99.78	99.81	99.93
Channel FL2	99.38	98.81	99.46
Channel FL3	8.95	9.28	11.59

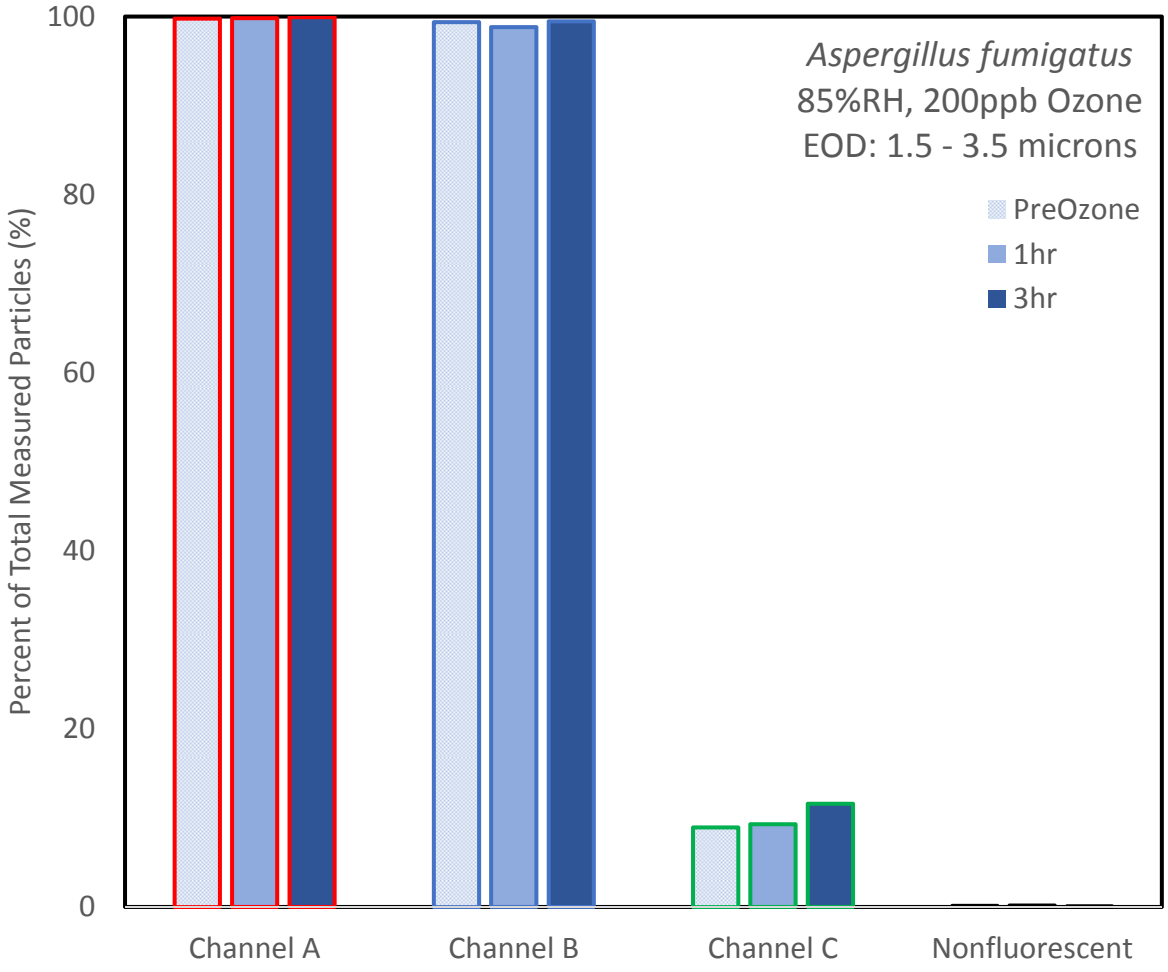

Aspergillus fumigatus, 85%RH, 200ppb Ozone (High Gain)
KS (size, FL1, FL2, FL3)

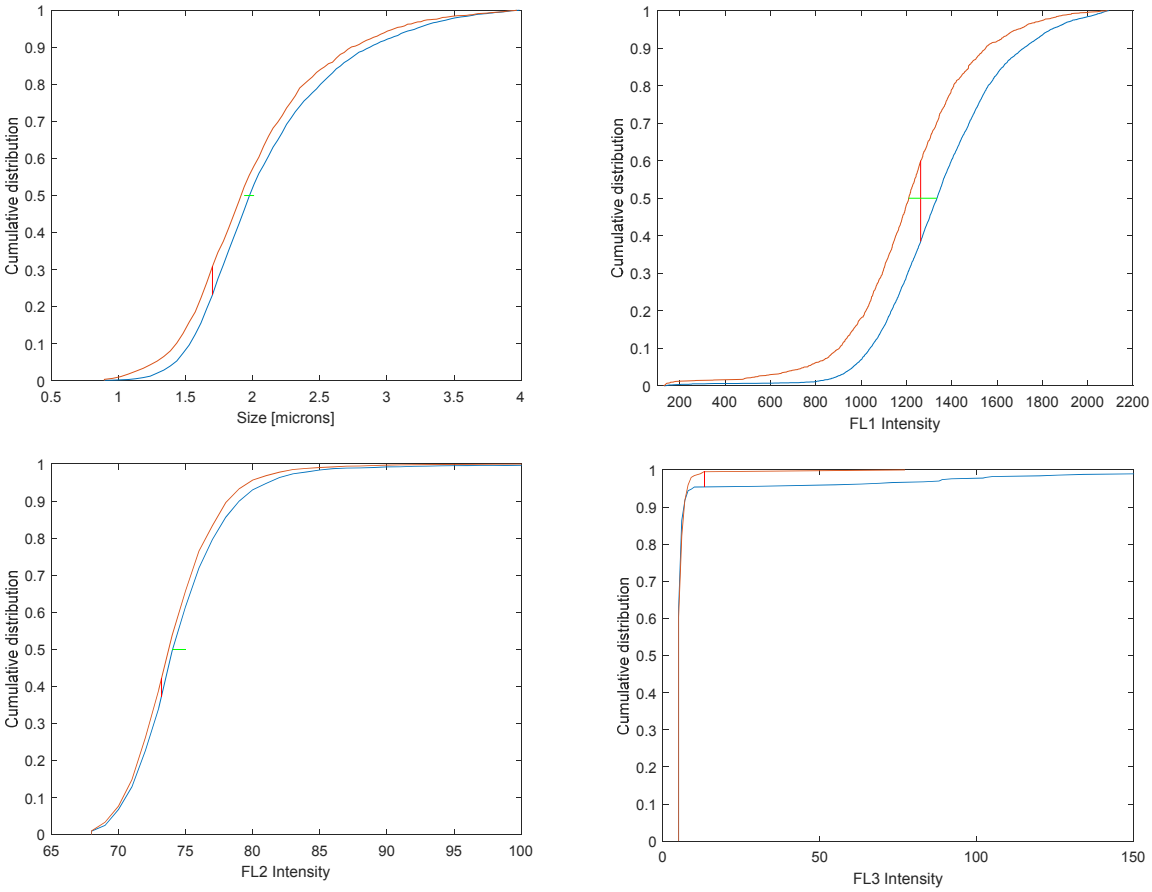

Aspergillus fumigatus (11days), 85%RH, 200ppb Ozone
Peak Stats FL1

Pre

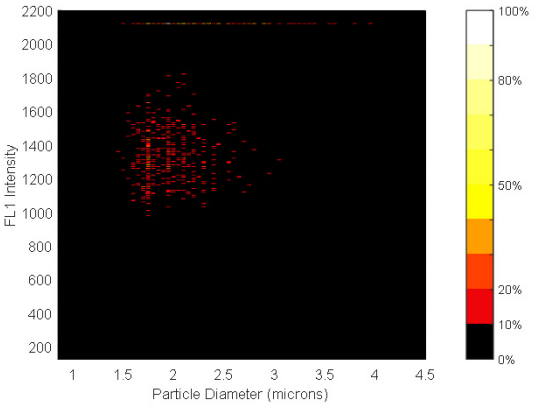

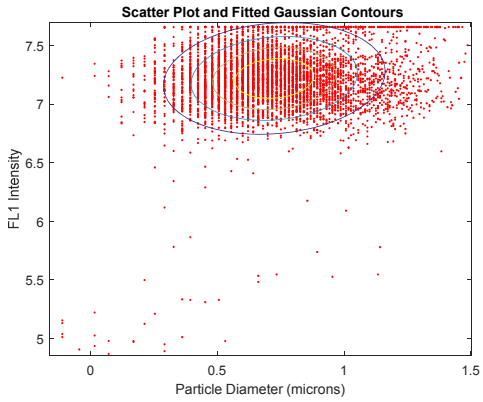

Post

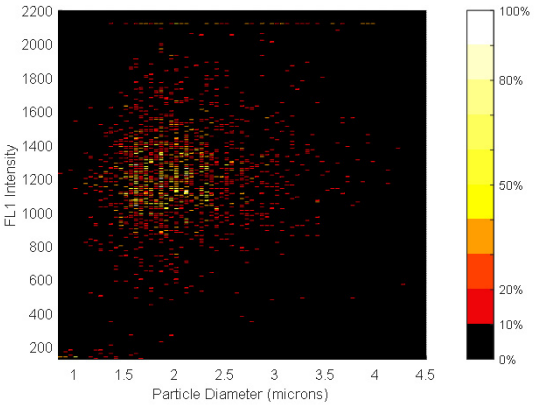

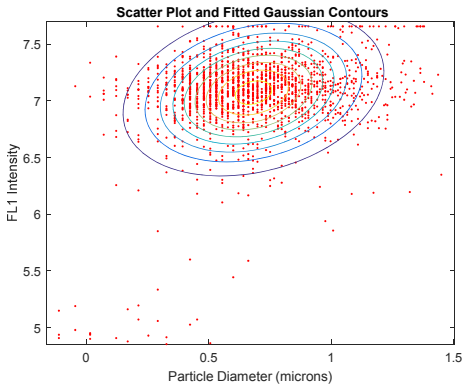

Aspergillus fumigatus

RH (%)	20
Ozone (ppb)/ suspension time (hr)	200 / 3 hours
Chamber Date	09/15/2015
Culture age (days)	18
InstaScope Gain	High
I.S. Files (t=0,1hr,3hr) {points}	0003, 0026, 0032 (Igor points: 1, 24, 32)

Pre Particle Size Distribution

Gauss fit mean	1.7895
SD +/- (width/sqrt(2))	0.5298
Size Range	1.5 – 3.5

Post Particle Size Distribution

Gauss fit mean	1.9051
SD +/- (width/sqrt(2))	0.60293
Size Range	1.5 – 3.5

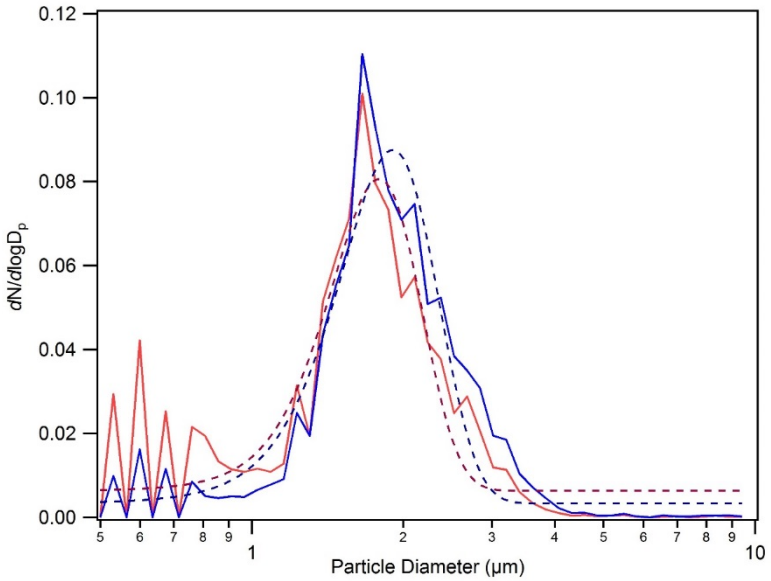

Aspergillus fumigatus (18days), 20%RH, 200ppb Ozone

Pre Particle FL1 Distribution

LogNormalFL1	1631
SD (*,/)	0.310593
Size range	1.5 – 3.5
FL1 Range	128 - 2100

Post Particle FL1 Distribution

LogNormalFL1	1572.9
SD (*,/)	0.326874
Size range	1.5 – 3.5
FL1 Range	128 - 2100

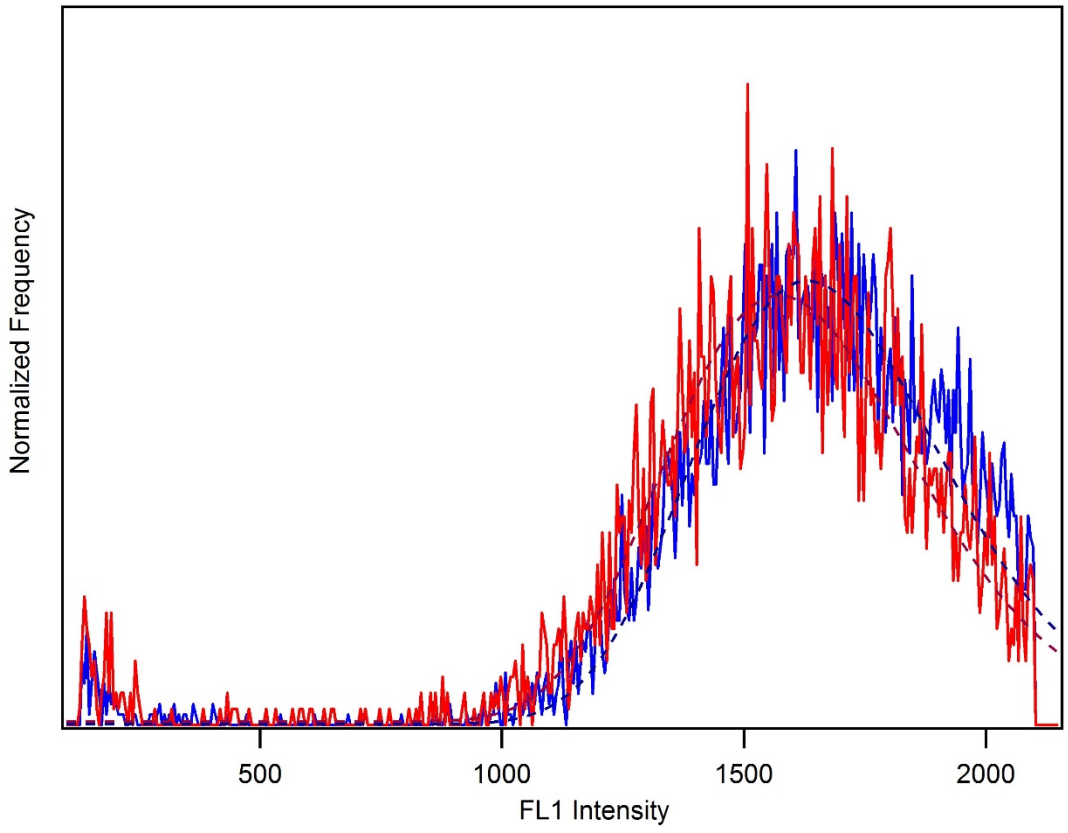

Aspergillus fumigatus (18days), 20%RH, 200ppb Ozone

	Pre O3 (%)	1hr (%)	3hr (%)
Nonfluorescent	0.34	0.27	0.61
Saturated FL1	26.7	18.2	17.4
Channel FL1	99.23	99.25	98.52
Channel FL2	99.36	99.32	98.84
Channel FL3	24.21	19.45	18.60

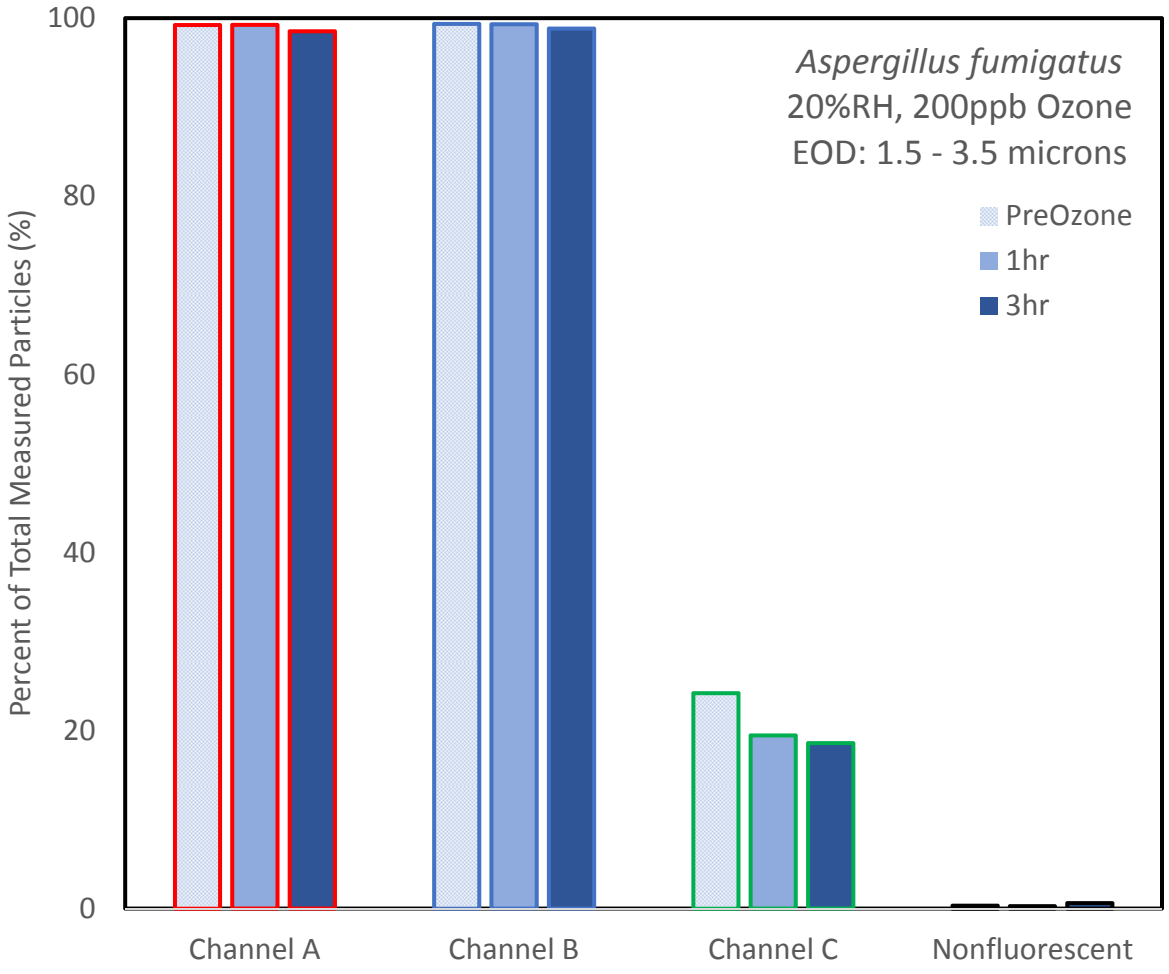

Aspergillus fumigatus, 20%RH, 200ppb Ozone (High Gain)
KS (size, FL1, FL2, FL3)

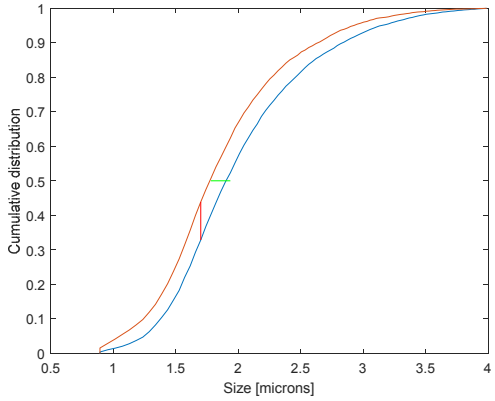

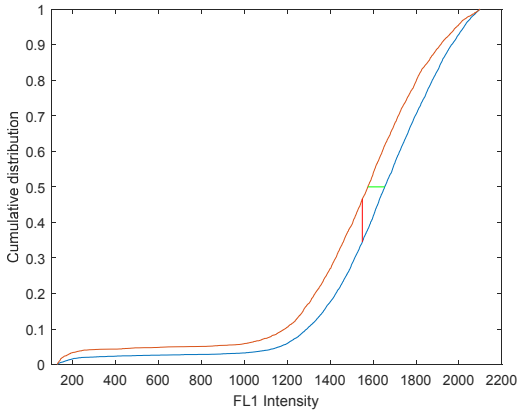

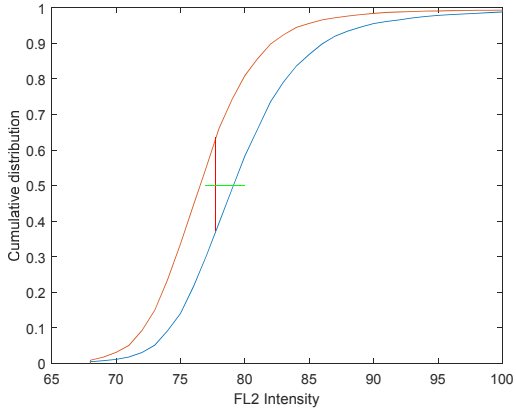

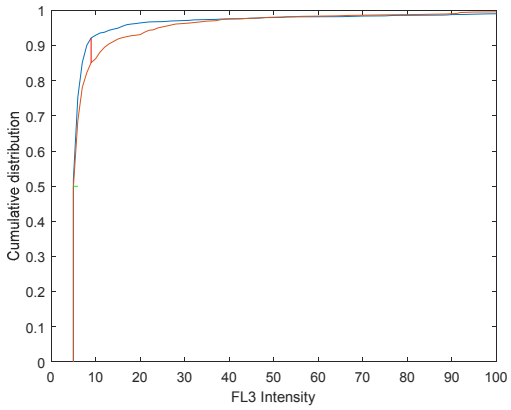

Aspergillus fumigatus, 20%RH, 200ppb Ozone (High Gain)
KS (size, FL1, FL2, FL3)

Ozone

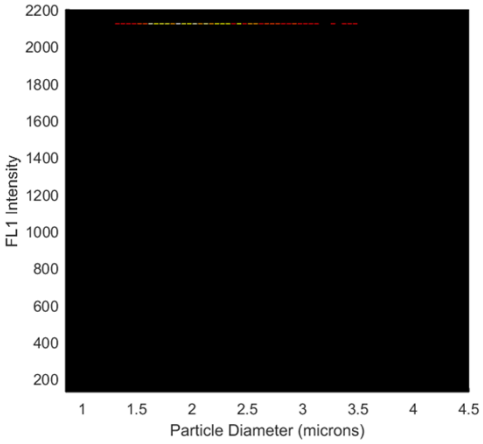

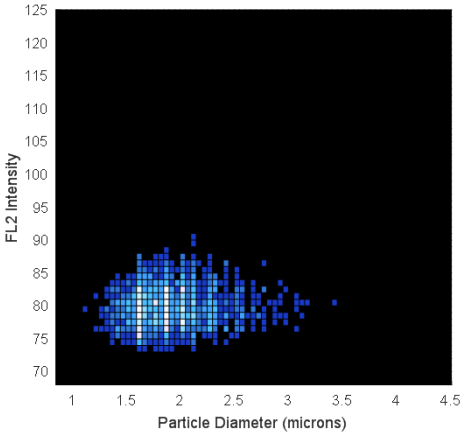

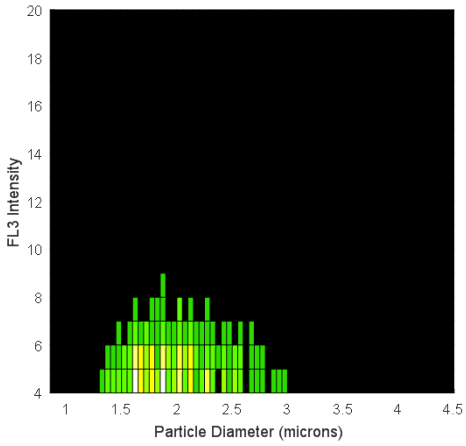

Post Ozone

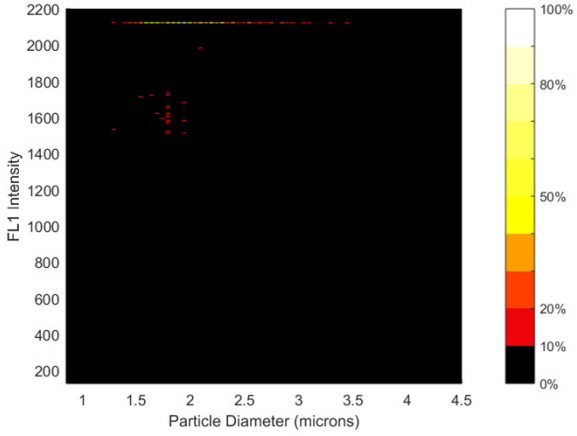

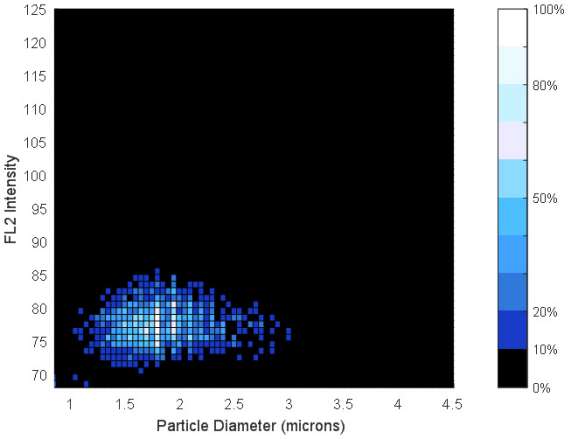

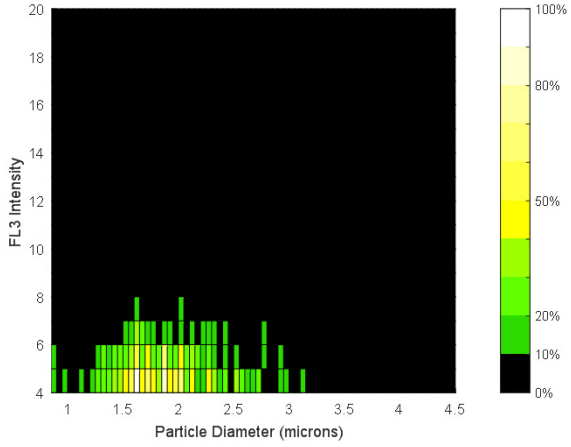

Aspergillus fumigatus

RH (%)	20
Ozone (ppb)/ suspension time (hr)	0 / 3 hours
Chamber Date	09/21/2015
Culture age (days)	24
InstaScope Gain	High
I.S. Files (t=0,1hr,3hr) {points}	0003, 0016, 0030 (Igor points: 1, 14, 28)

Pre Particle Size Distribution

Gauss fit mean	1.8383
SD +/- (width/sqrt(2))	0.46589
Size Range	1.5 – 3.5

Post Particle Size Distribution

Gauss fit mean	1.7376
SD +/- (width/sqrt(2))	0.41022
Size Range	1.5 – 3.5

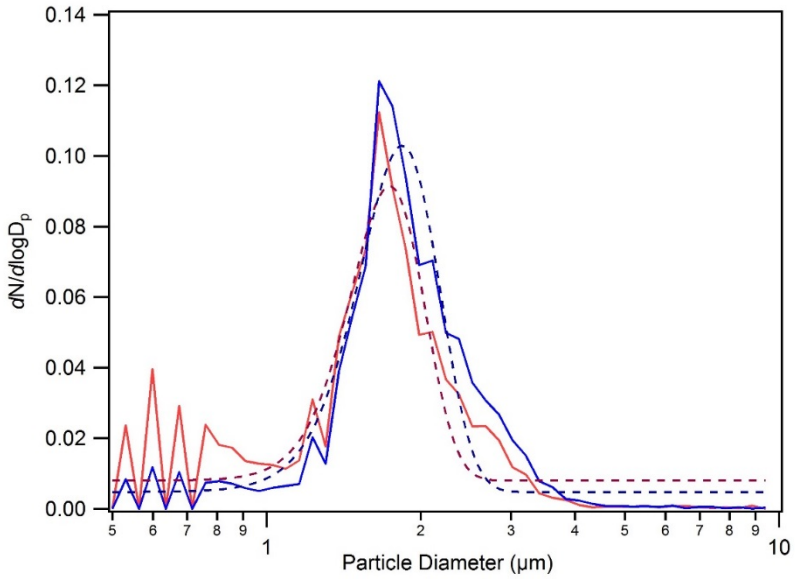

Aspergillus fumigatus (24days), 20%RH, 0ppb Ozone

Pre Particle FL1 Distribution

LogNormalFL1	1527
SD (*,/)	0.329942
Size range	1.5 – 3.5
FL1 Range	128 - 2100

Post Particle FL1 Distribution

LogNormalFL1	1475.6
SD (*,/)	0.328021
Size range	1.5 – 3.5
FL1 Range	128 - 2100

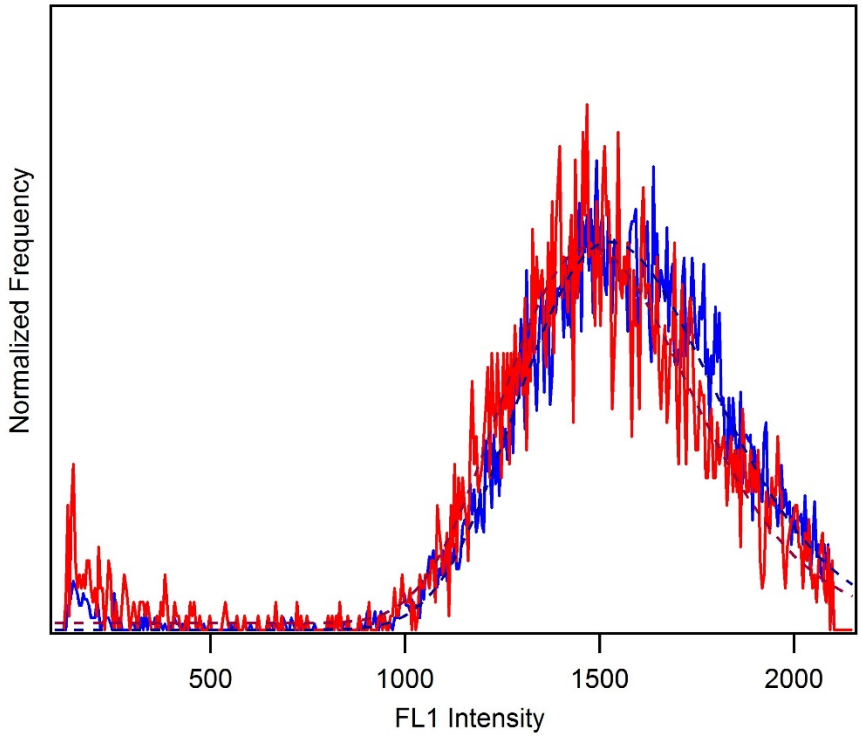

Aspergillus fumigatus (24days), 20%RH, 0ppb Ozone

	Pre O3 (%)	1hr (%)	3hr (%)
Nonfluorescent	0.43	0.42	0.47
Saturated FL1	13.74	12.72	10.87
Channel FL1	99.29	99.29	99.16
Channel FL2	99.12	99.11	98.50
Channel FL3	15.65	14.46	14.22

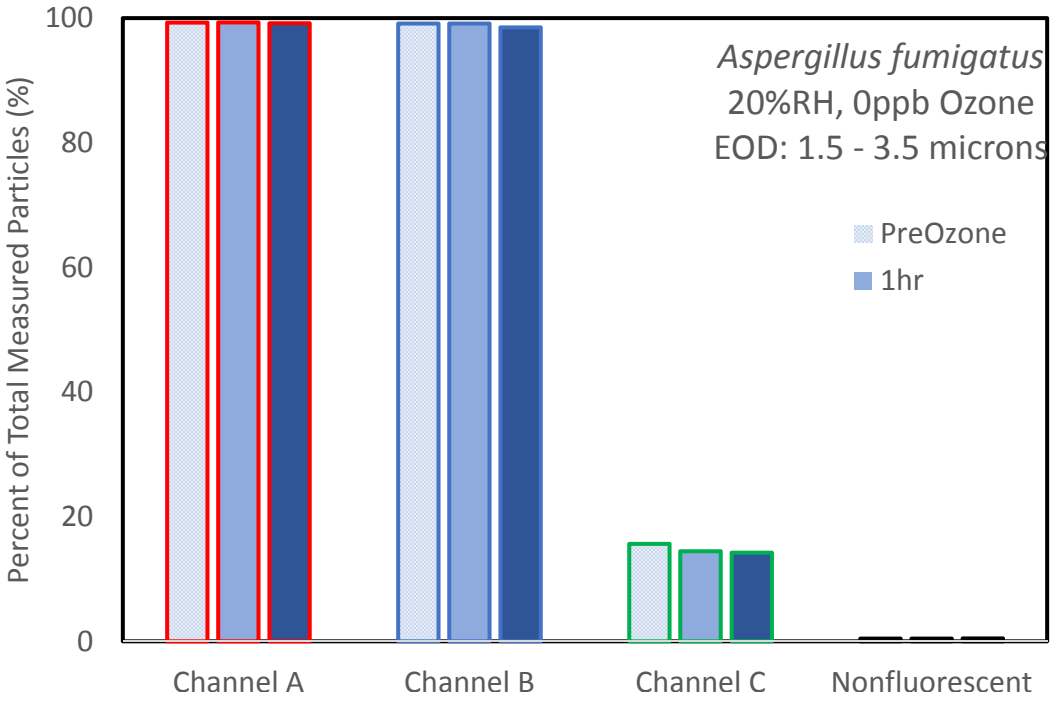

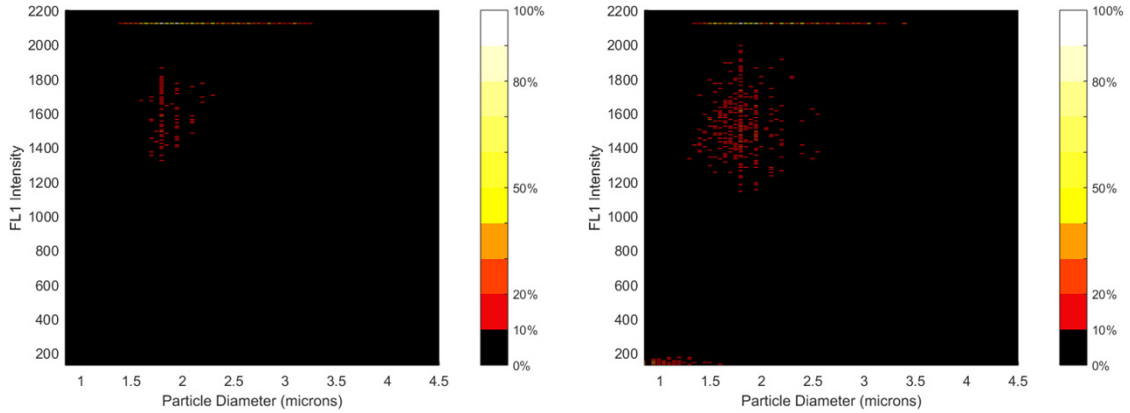

Aspergillus fumigatus, 20%RH, 0ppb Ozone (High Gain)
KS (size, FL1, FL2, FL3)

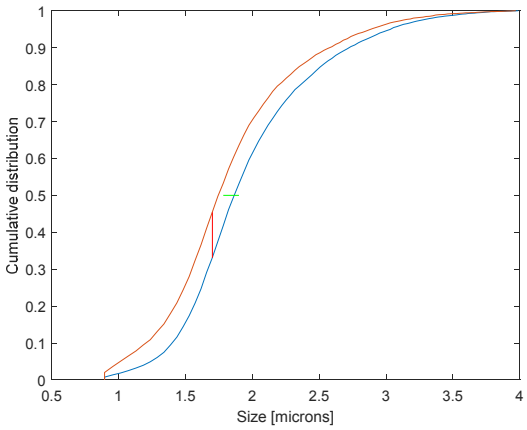

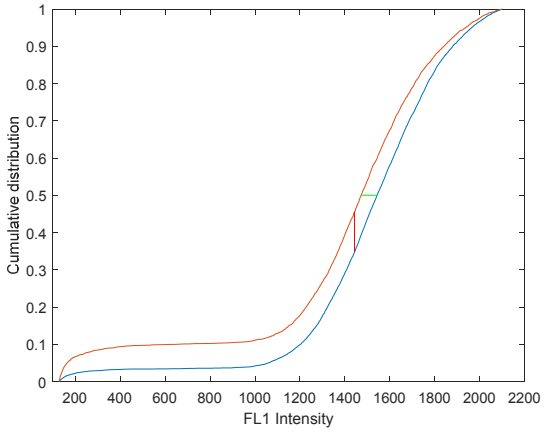

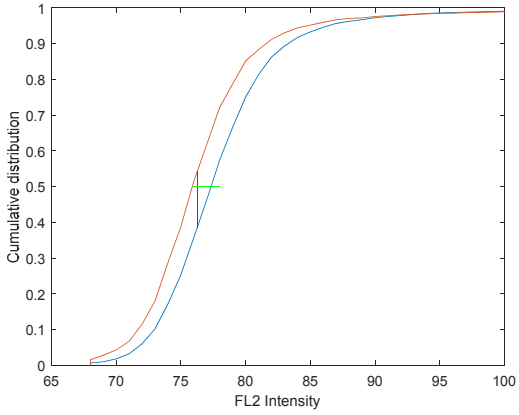

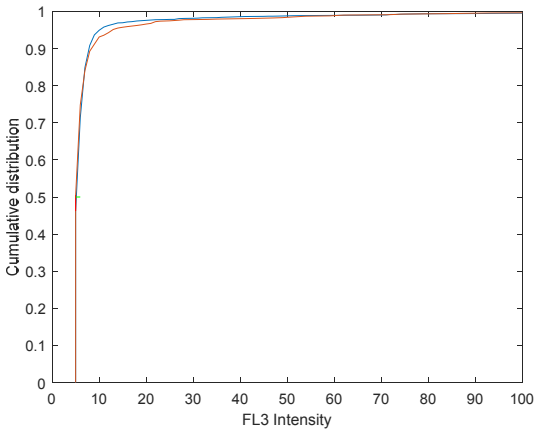

Aspergillus fumigatus

RH (%)	85
Ozone (ppb)/ suspension time (hr)	1000 / 1 hour
Chamber Date	11/18/2015
Culture age (days)	
InstaScope Gain	Low
I.S. Files (t=0,1hr,3hr) {points}	0031, 0047, 0059 (Igor points: 30, 46, 58)

Pre Particle Size Distribution

Gauss fit mean	1.9964
SD +/- (width/sqrt(2))	0.60637
Size Range	1.5 – 3.5

Post Particle Size Distribution

Gauss fit mean	1.9788
SD +/- (width/sqrt(2))	0.56284
Size Range	1.5 – 3.5

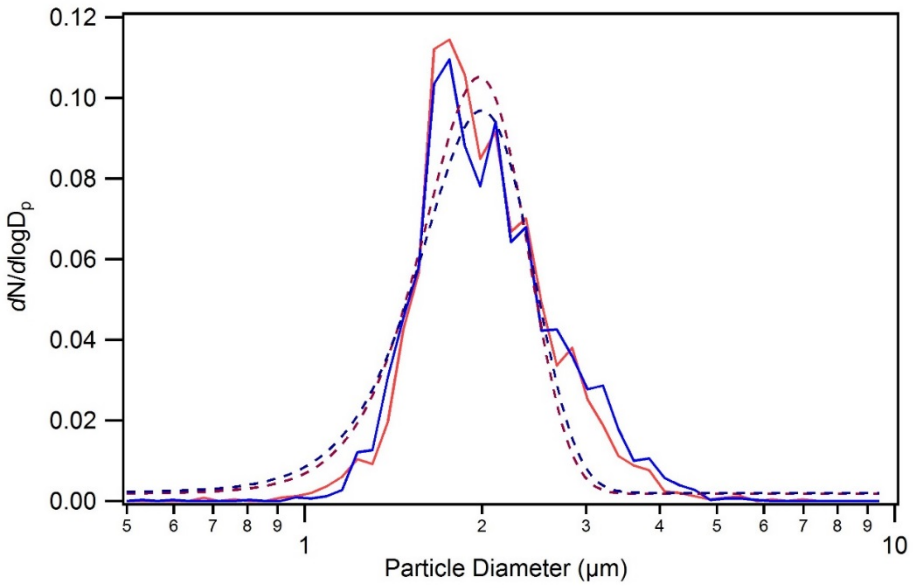

Aspergillus fumigatus (days), 85%RH, 1000ppb Ozone

Pre Particle FL1 Distribution

LogNormalFL1	318.12
SD (*,/)	0.2909
Size range	1.5 – 3.5
FL1 Range	128 - 2100

Post Particle FL1 Distribution

LogNormalFL1	298.39
SD (*,/)	0.289813
Size range	1.5 – 3.5
FL1 Range	128 - 2100

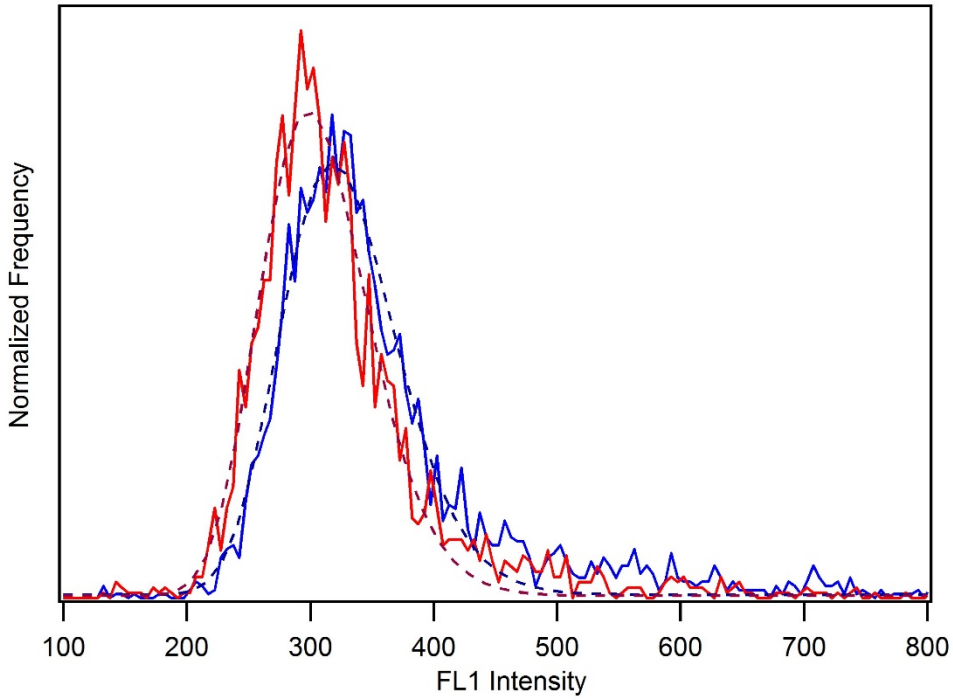

Aspergillus fumigatus (days), 85%RH, 1000ppb Ozone

	Pre O3 (%)	1hr (%)	3hr (%)
Nonfluorescent	0.03	0.23	0.04
Saturated FL1	0	0	0
Channel FL1	99.86	99.53	99.42
Channel FL2	98.86	97.10	97.80
Channel FL3	9.00	6.52	6.81

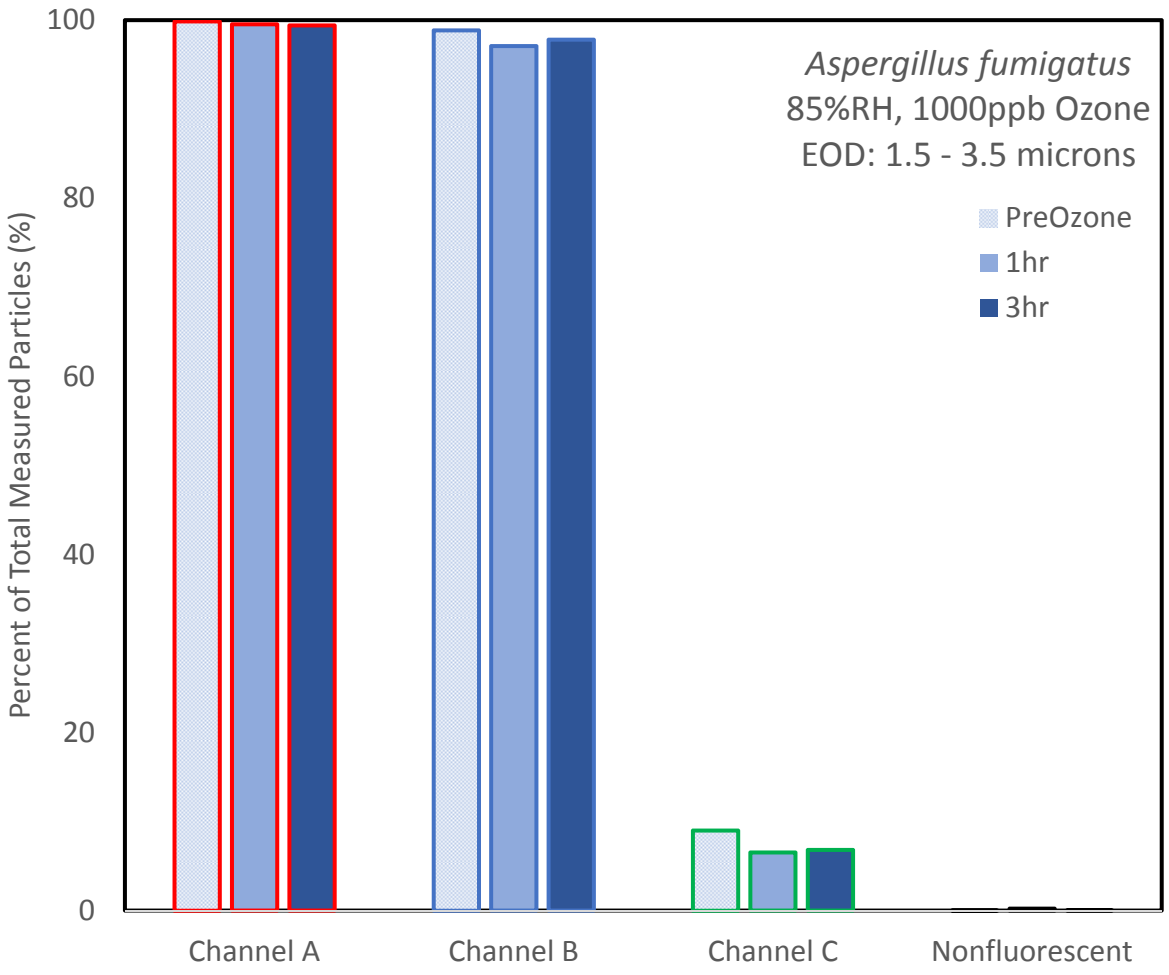

Aspergillus fumigatus, 85%RH, 1000ppb Ozone(Low Gain)
KS (size, FL1, FL2, FL3)

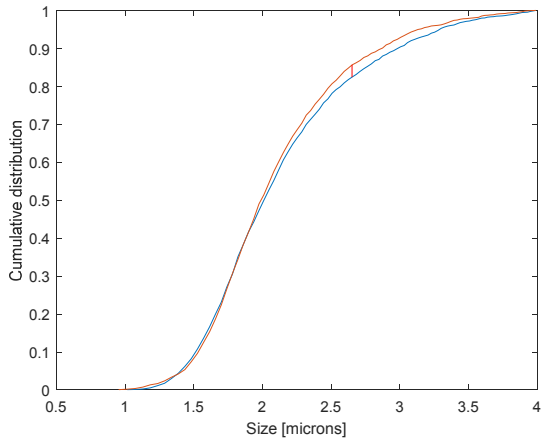

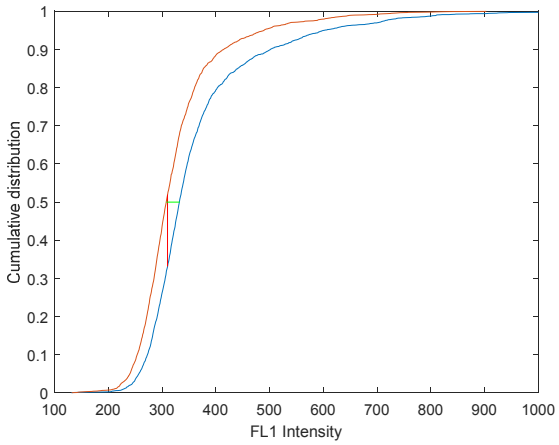

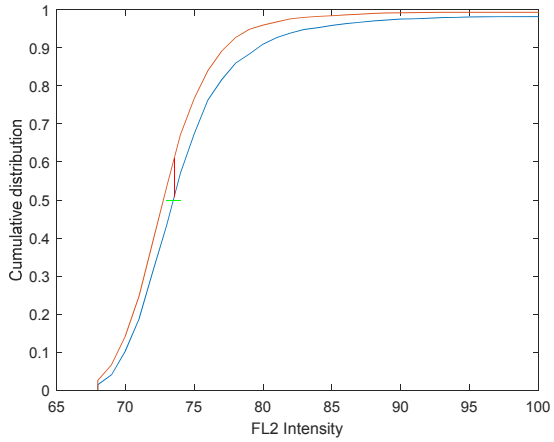

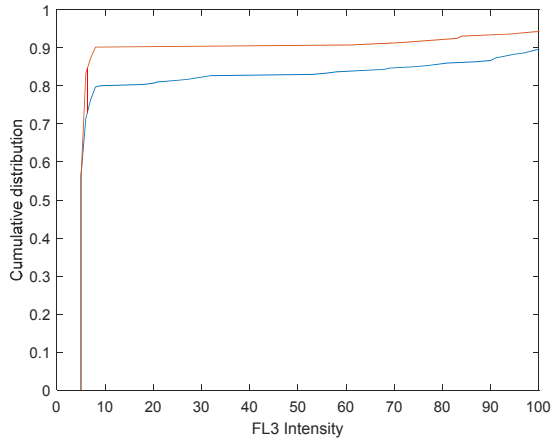

Aspergillus fumigatus,
85%RH, 1000ppb Ozone (Low Gain) FL1

Pre Ozone

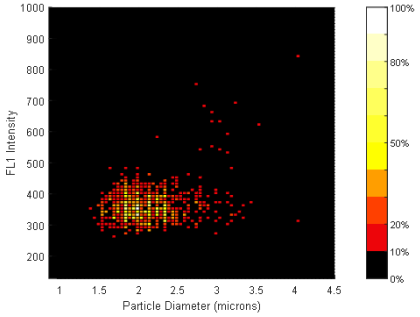

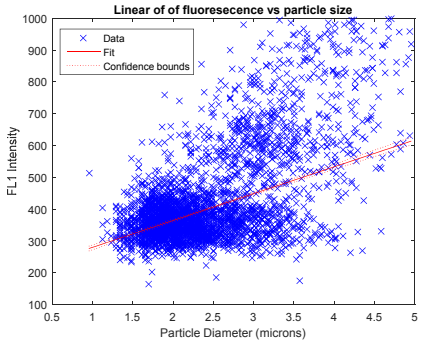

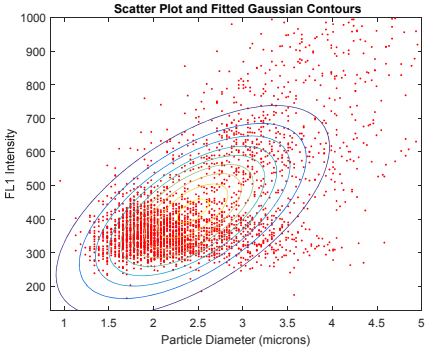

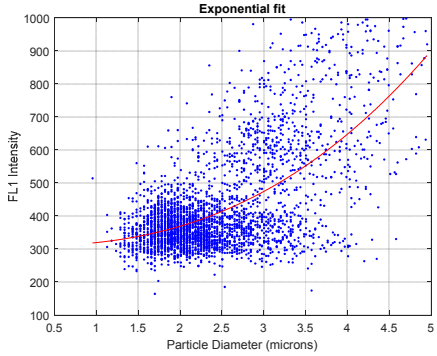

Ozone

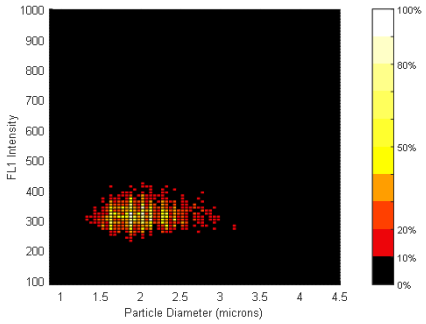

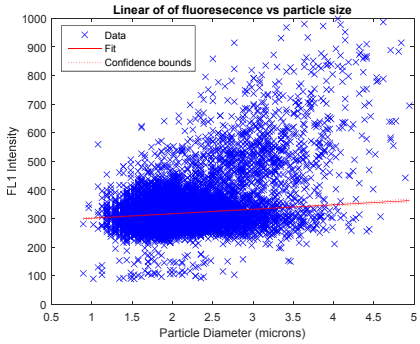

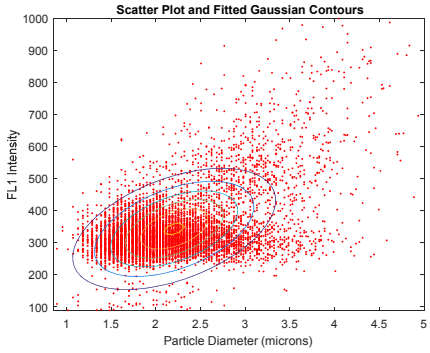

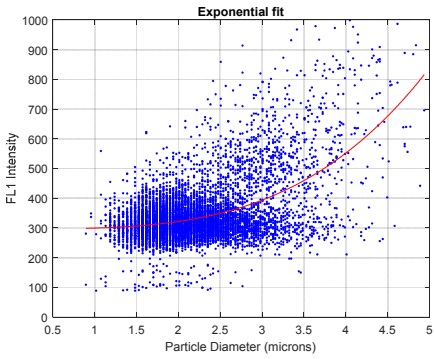

Aspergillus fumigatus,
85%RH, 1000ppb Ozone (Low Gain) FL2

Pre Ozone

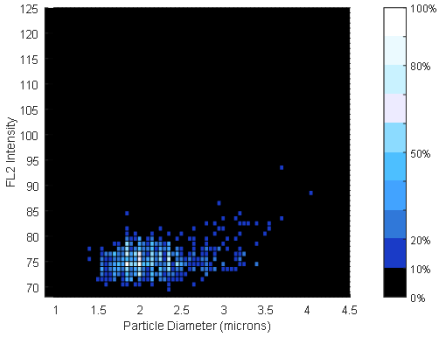

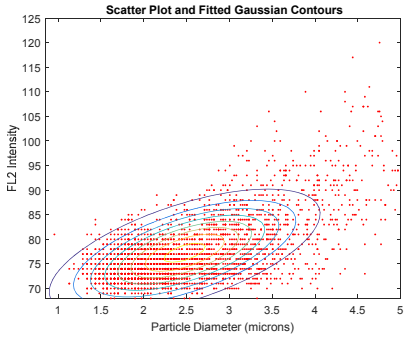

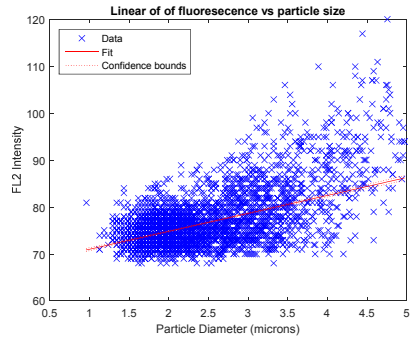

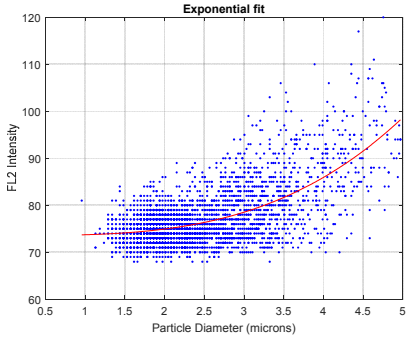

Ozone

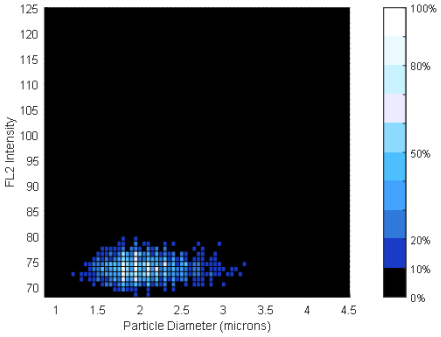

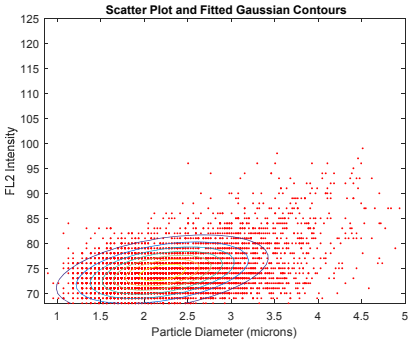

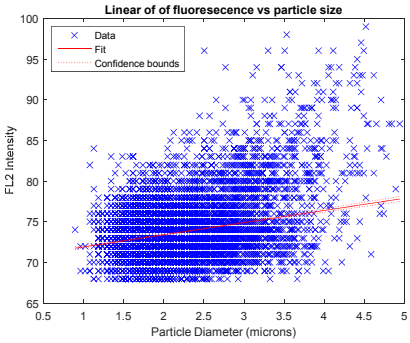

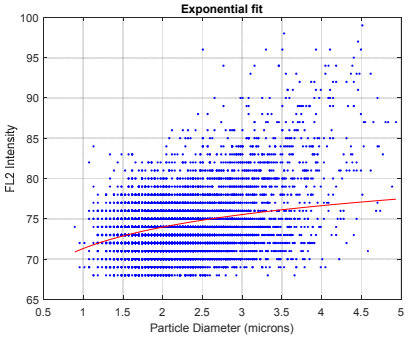

Aspergillus fumigatus

RH (%)	85
Ozone (ppb)/ suspension time (hr)	1200 / 2 hour
Chamber Date	01/25/2016
Culture age (days)	15
InstaScope Gain	Low
I.S. Files (t=0,1hr,3hr) {points}	0016, 0021, 0026 (Igor points: 2, 7, 12)

Pre Particle Size Distribution

Gauss fit mean	1.9298
SD +/- (width/sqrt(2))	0.5255
Size Range	1.5 – 3.5

Post Particle Size Distribution

Gauss fit mean	1.8398
SD +/- (width/sqrt(2))	0.43856
Size Range	1.5 – 3.5

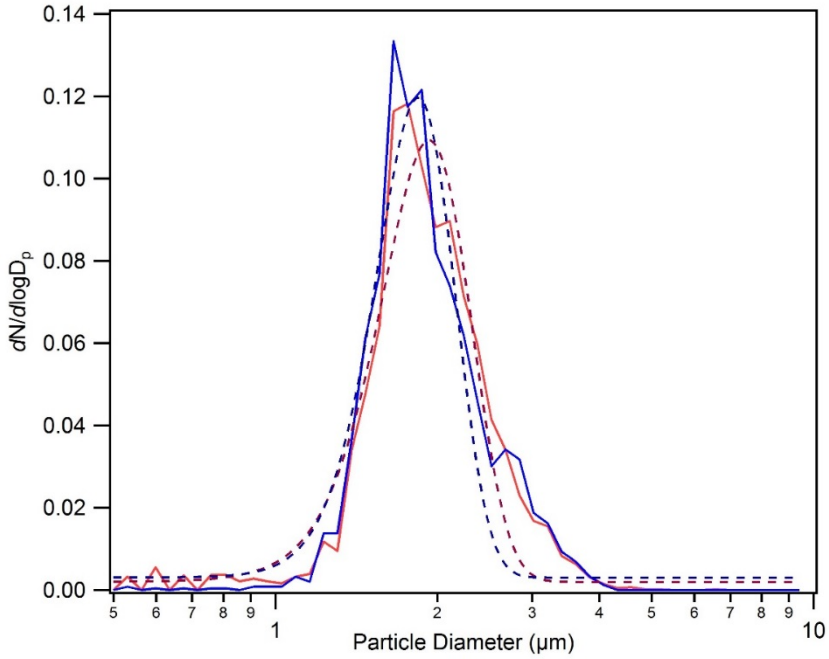

Aspergillus fumigatus (15days), 85%RH, 1200ppb Ozone

Pre Particle FL1 Distribution

LogNormalFL 1	321.09
SD (*,/)	.3169
Size range	1.5 – 3.5
FL1 Range	128 - 2100

Post Particle FL1 Distribution

LogNormalFL1	302.94
SD (*,/)	0.3102
Size range	1.5 – 3.5
FL1 Range	128 - 2100

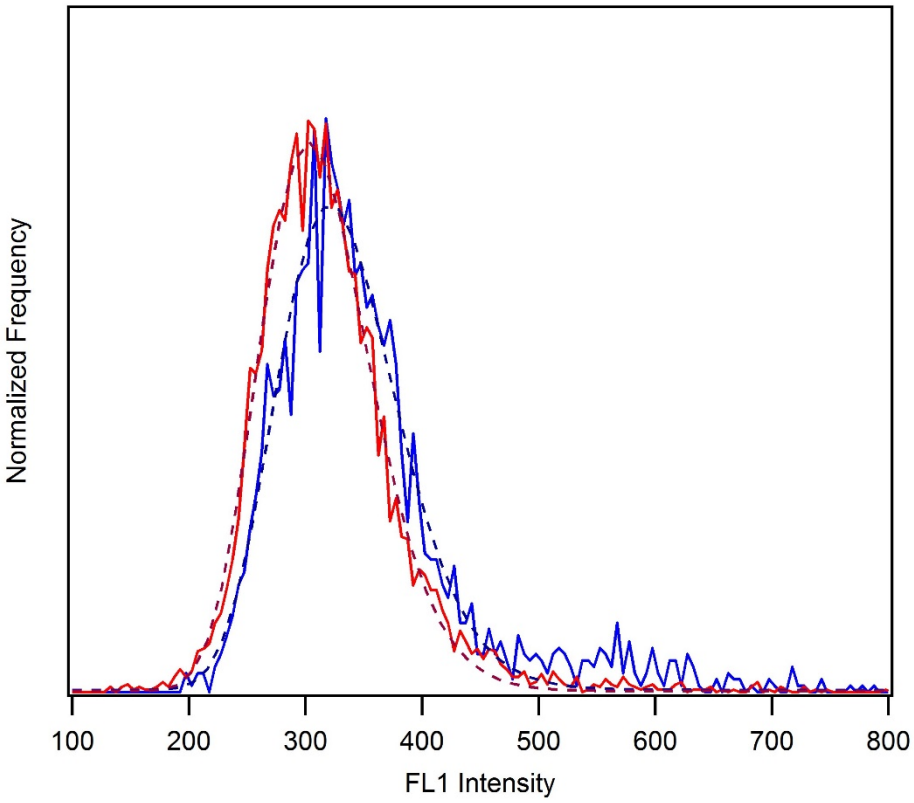

Aspergillus fumigatus (15days), 85%RH, 1200ppb Ozone

	Pre O3 (%)	1hr (%)	3hr (%)
Nonfluorescent	0.05	0.11	0.07
Saturated FL1	0	0	0
Channel FL1	99.72	99.58	99.29
Channel FL2	98.48	96.21	97.42
Channel FL3	7.61	5.90	4.68

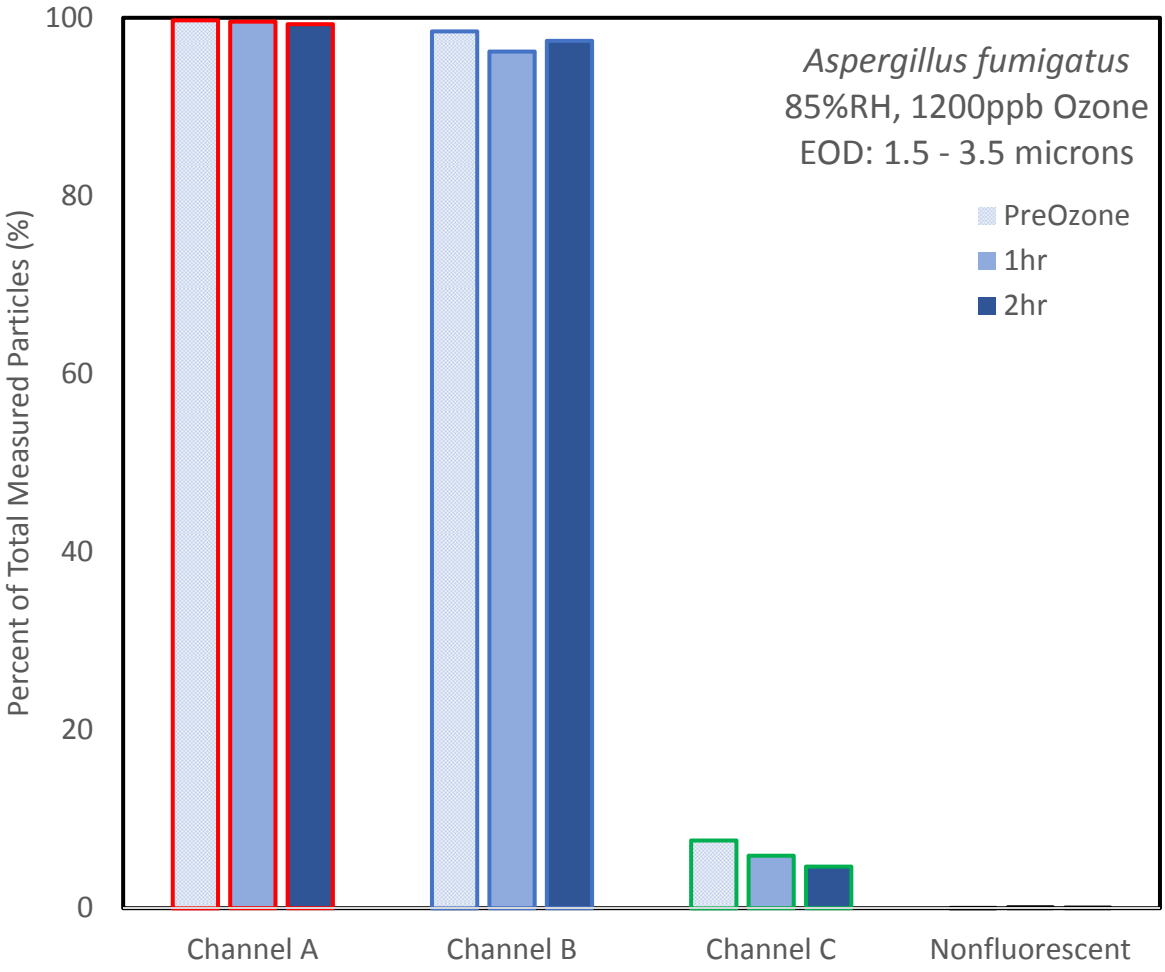

Aspergillus fumigatus,
85%RH, 1200ppb Ozone (Low Gain)
KS (size, FL1, FL2, FL3)

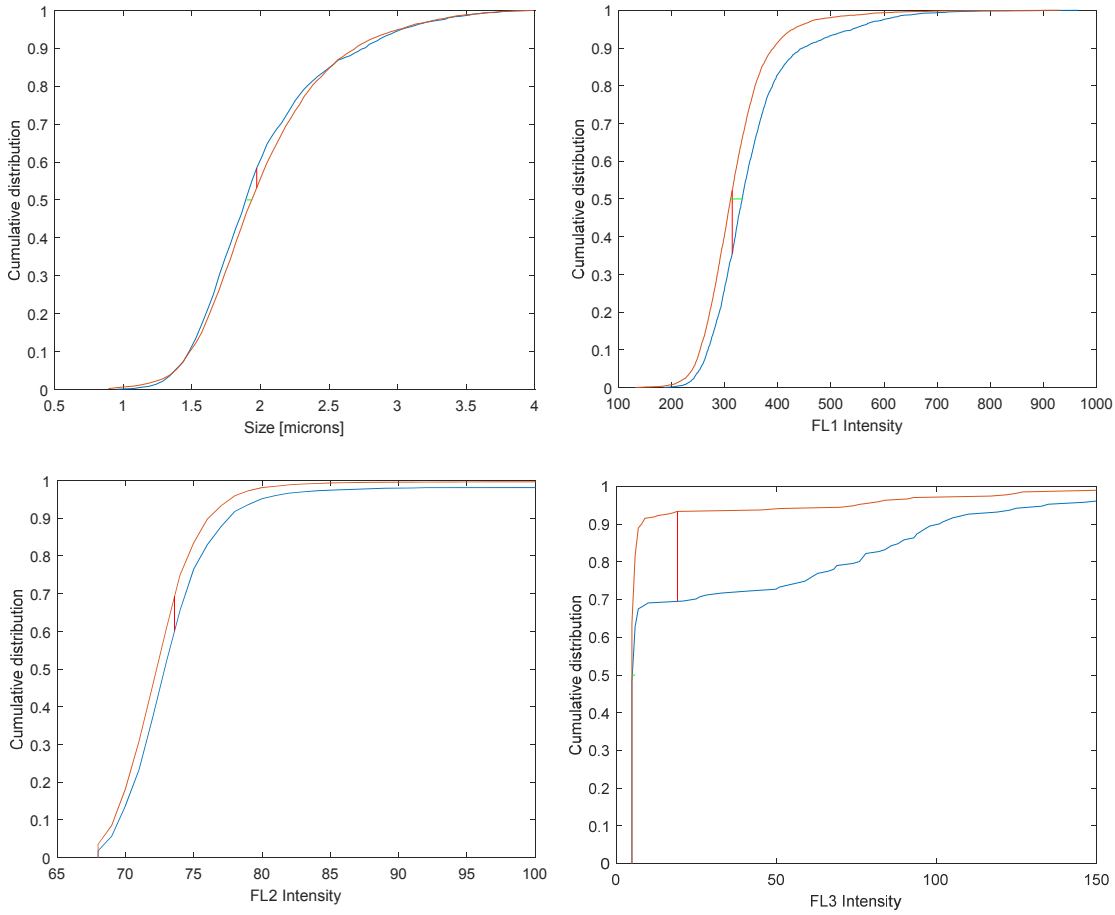

Aspergillus fumigatus,
85%RH, 1200ppb Ozone (Low Gain)
(size, FL1, FL2, FL3)

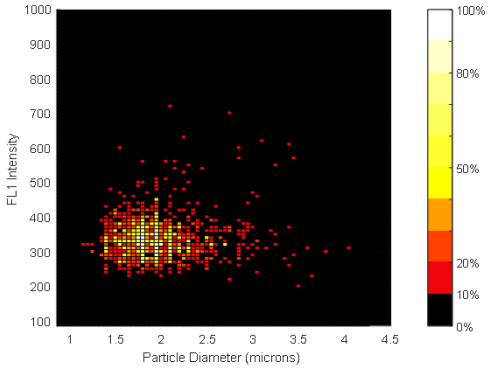

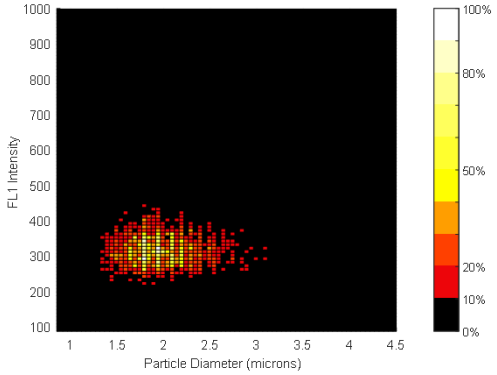

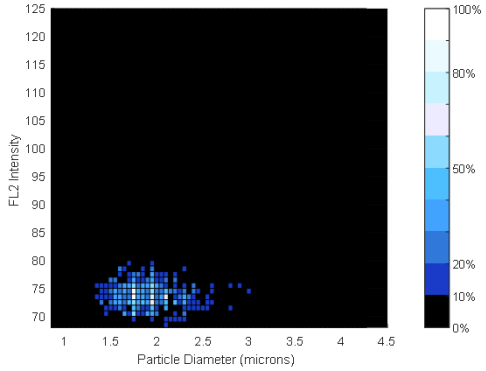

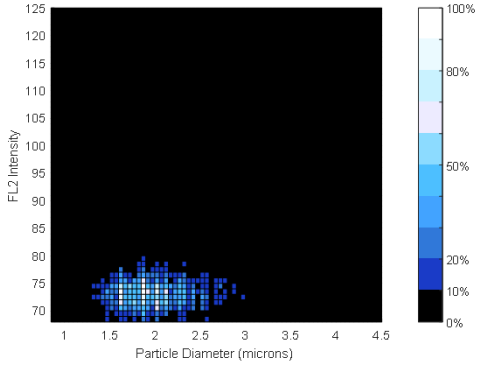

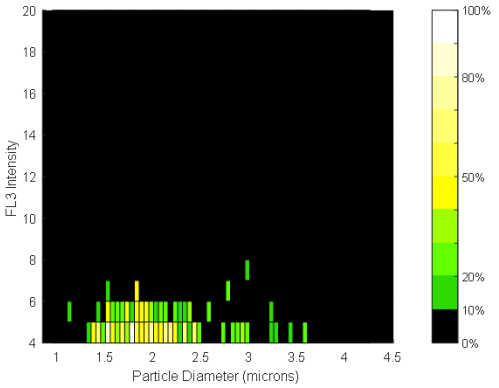

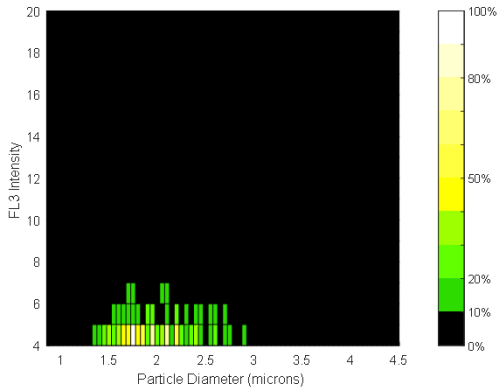

Aspergillus fumigatus

RH (%)	85
Ozone (ppb)/ suspension time (hr)	7500 / 2 hour
Chamber Date	01/26/2016
Culture age (days)	16
InstaScope Gain	Low
I.S. Files (t=0,1hr,3hr) {points}	0002, 0007, 0014 (Igor points: 2, 7, 14)

Pre Particle Size Distribution

Gauss fit mean	1.9677
SD +/- (width/sqrt(2))	0.50882
Size Range	1.5 – 3.5

Post Particle Size Distribution

Gauss fit mean	1.9248
SD +/- (width/sqrt(2))	0.48255
Size Range	1.5 – 3.5

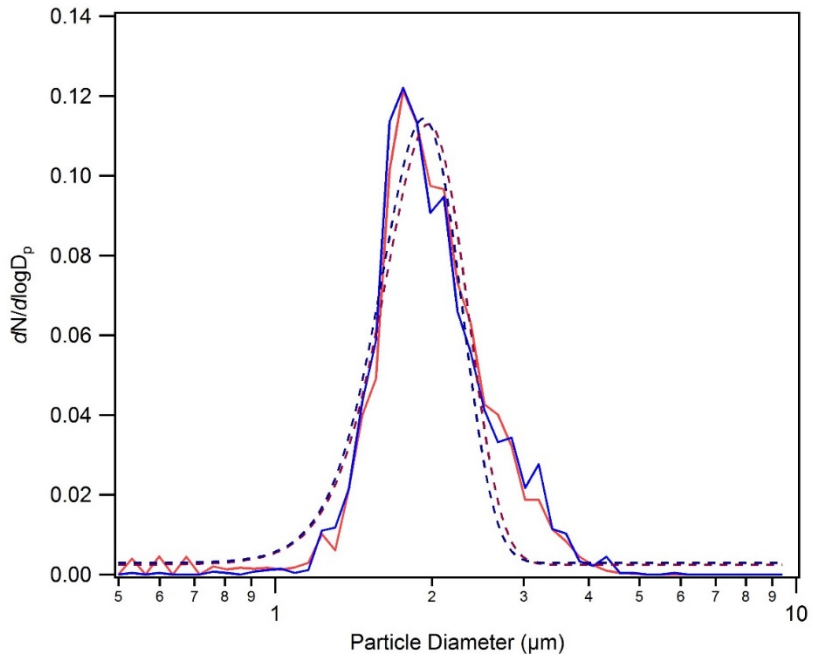

Aspergillus fumigatus (16days), 85%RH, 7500ppb Ozone

Pre Particle FL1 Distribution

LogNormalFL1	339.65
SD (*,/)	.342
Size range	1.5 – 3.5
FL1 Range	128 - 2100

Post Particle FL1 Distribution

LogNormalFL1	280.51
SD (*,/)	.2695
Size range	1.5 – 3.5
FL1 Range	128 - 2100

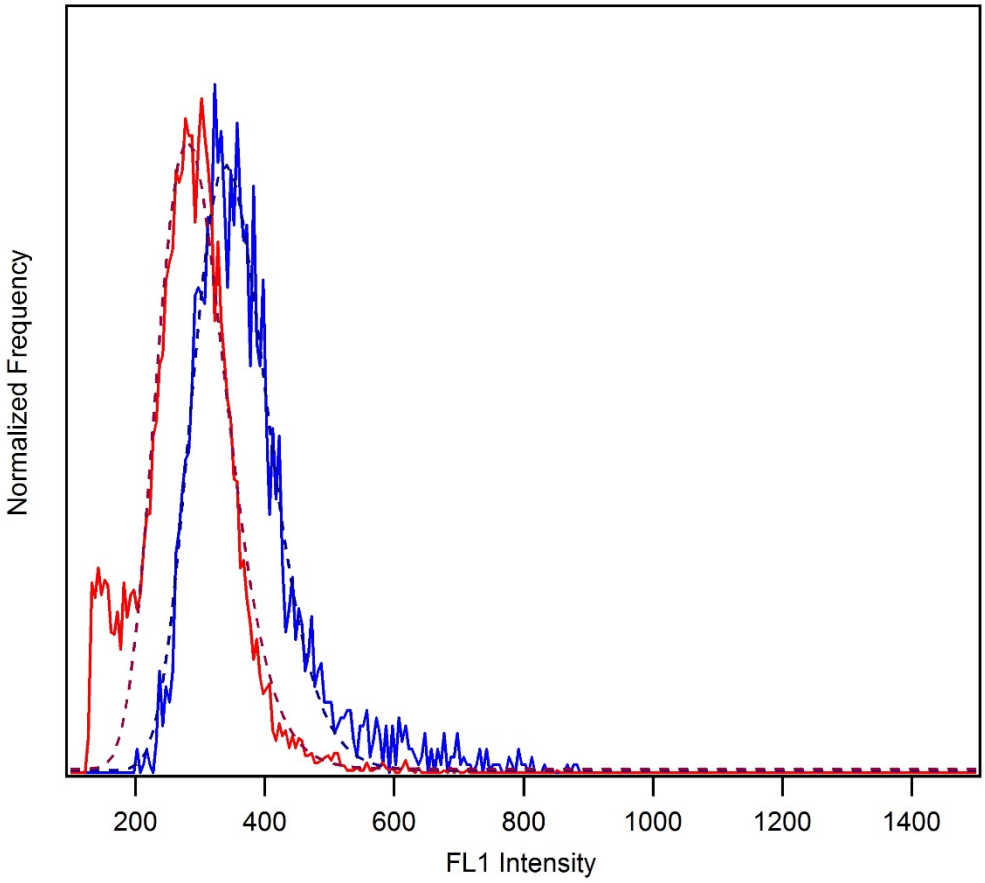

Aspergillus fumigatus (16days), 85%RH, 7500ppb Ozone

	Pre O3 (%)	1hr (%)	3hr (%)
Nonfluorescent	0.08	0.33	0.56
Saturated FL1	0	0	0
Channel FL1	99.84	98.60	96.18
Channel FL2	99.18	93.56	95.08
Channel FL3	7.00	7.75	8.15

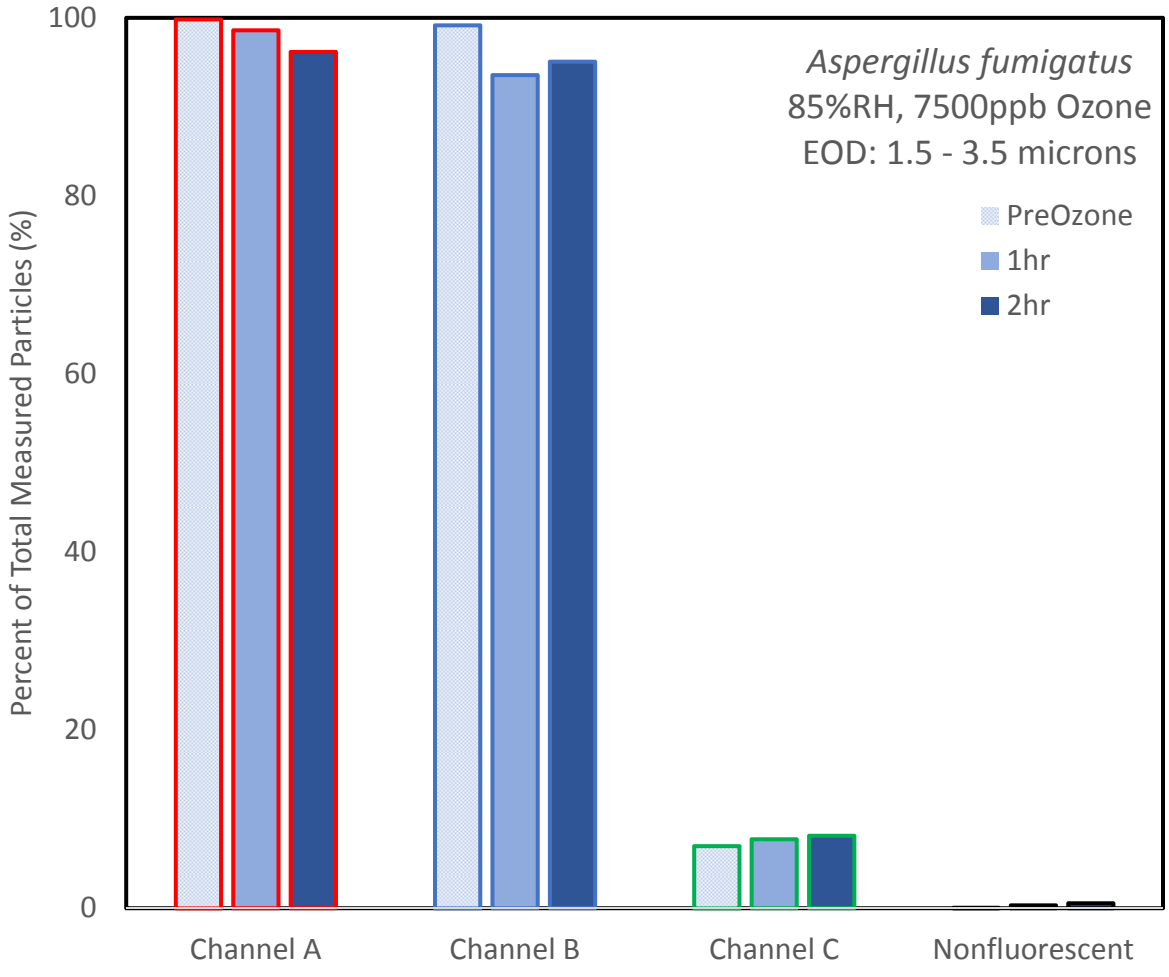

Aspergillus fumigatus,
85%RH, 7500ppb Ozone (Low Gain)
KS (FL1 87 – 1000)

Pre Ozone

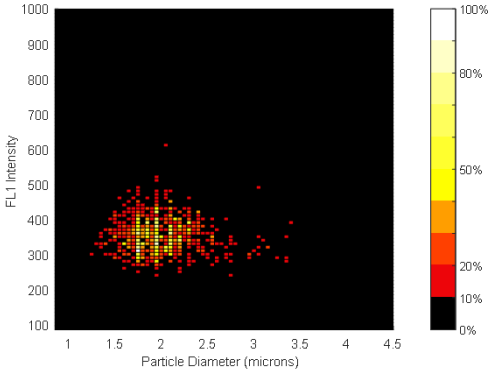

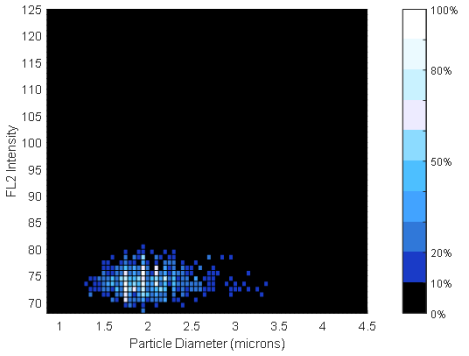

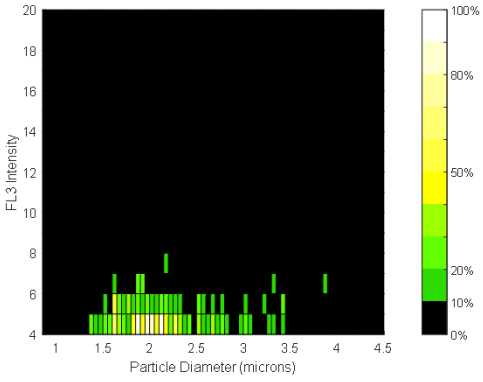

Ozone

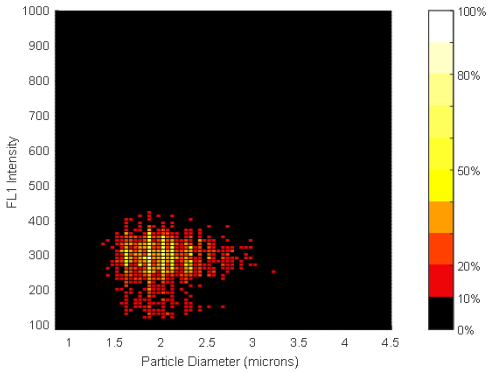

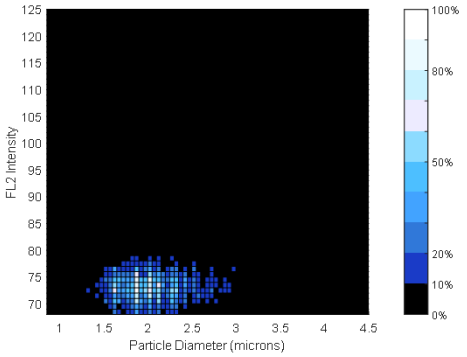

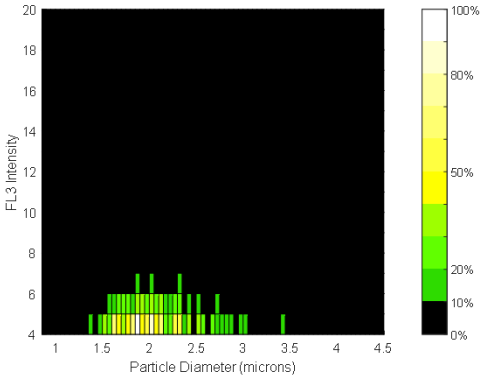

Aspergillus fumigatus,
85%RH, 7500ppb Ozone (Low Gain)
KS (size, FL1, FL2, FL3)

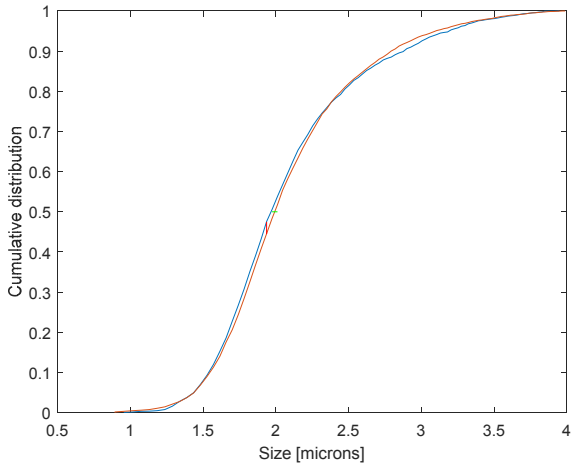

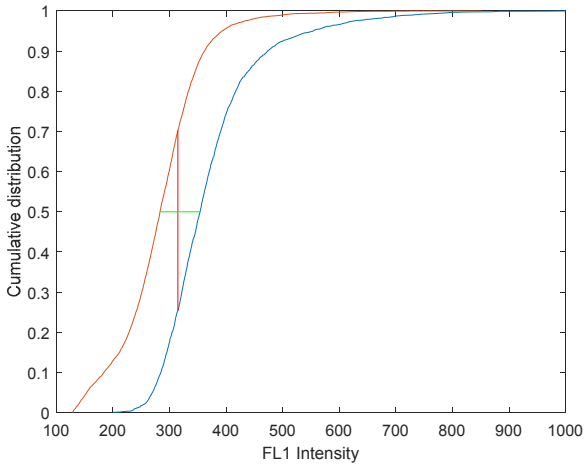

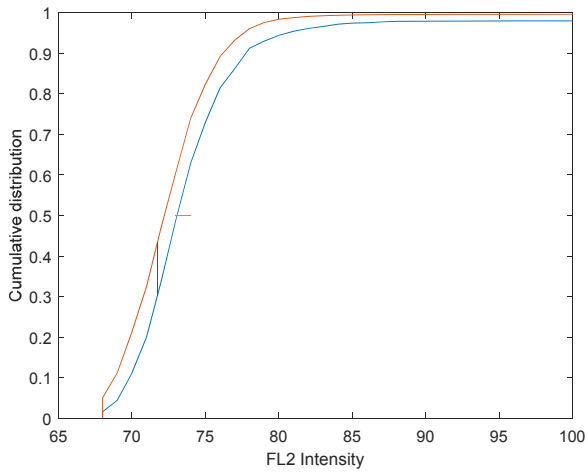

Aspergillus fumigatus

RH (%)	85
Ozone (ppb)/ suspension time (hr)	200 / 3 hour
Chamber Date	06/18/2015
Culture age (days)	28
InstaScope Gain	High
I.S. Files (t=0,1hr,3hr) {points}	0011, 0024, 0037 (Igor points: 0, 13, 28)

Pre Particle Size Distribution

Gauss fit mean	2.08
SD +/- (width/sqrt(2))	0.668
Size Range	1.5 – 3.5

Post Particle Size Distribution

Gauss fit mean	1.993
SD +/- (width/sqrt(2))	0.539
Size Range	1.5 – 3.5

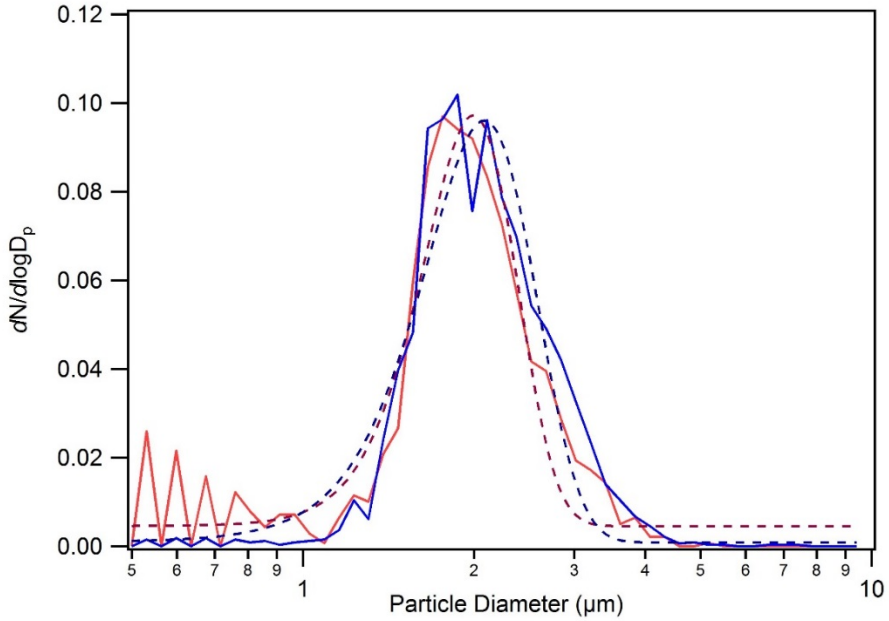

Aspergillus fumigatus (28days), 85%RH, 200ppb Ozone

Pre Particle FL1 Distribution

LogNormalFL1	1238
SD (*,/)	0.361
Size range	1.5 – 3.5
FL1 Range	128 - 2100

Post Particle FL1 Distribution

LogNormalFL1	1179.7
SD (*,/)	0.365
Size range	1.5 – 3.5
FL1 Range	128 - 2100

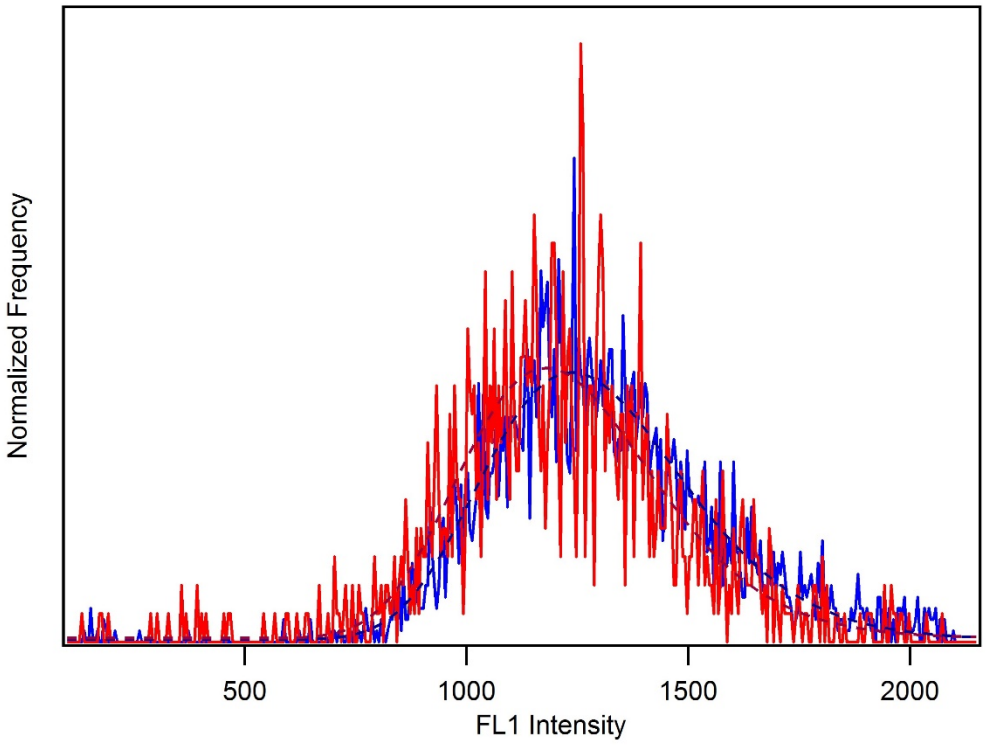

Aspergillus fumigatus (28days), 85%RH, 200ppb Ozone

	Pre O3 (%)	1hr (%)	3hr (%)
Nonfluorescent	0.14	0.26	0.18
Saturated FL1	3.83	2.01	1.15
Channel FL1	99.83	99.74	99.56
Channel FL2	99.11	98.03	99.29
Channel FL3	9.07	5.96	11.81

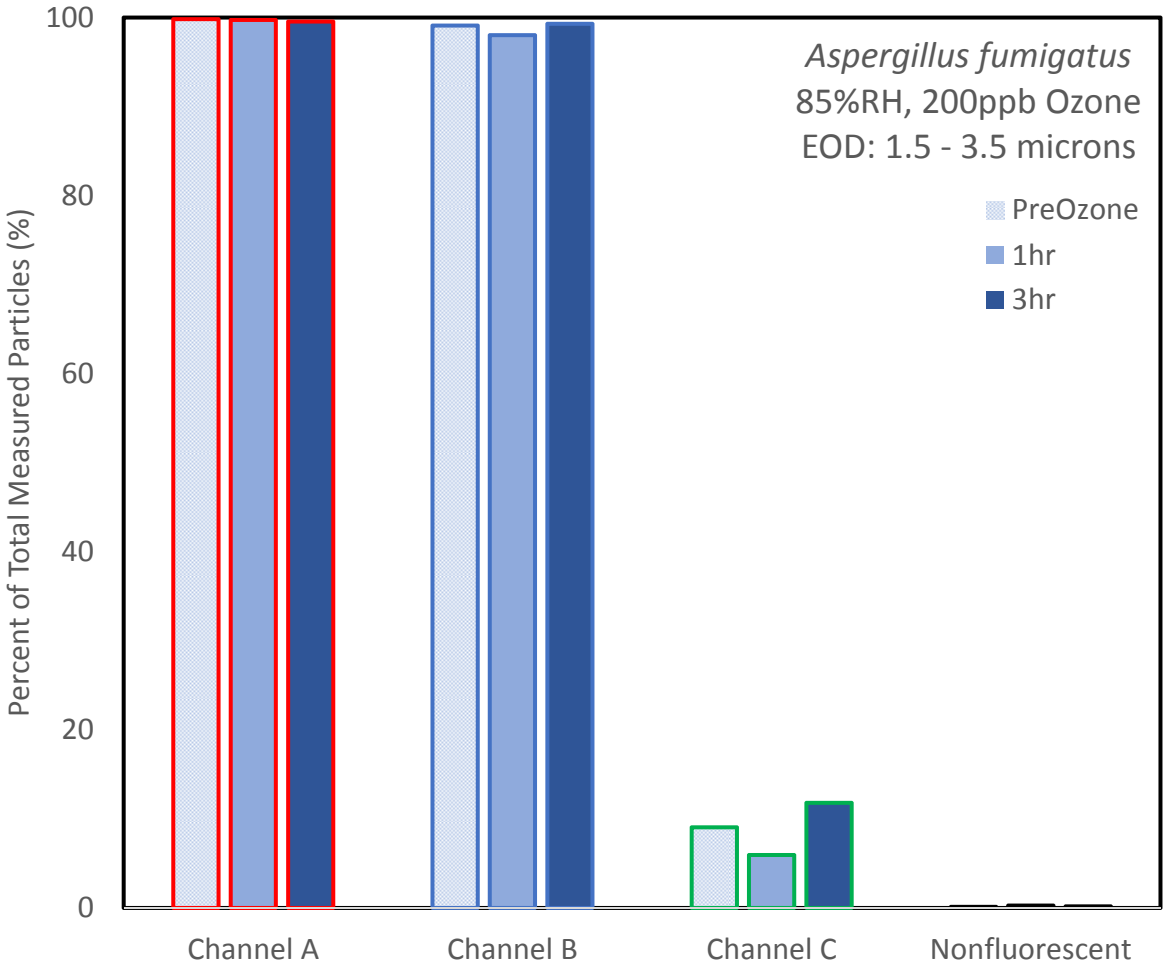

Aspergillus fumigatus (28 days),
85%RH, 200ppb Ozone (Low Gain)
KS (size, FL1, FL2, FL3)

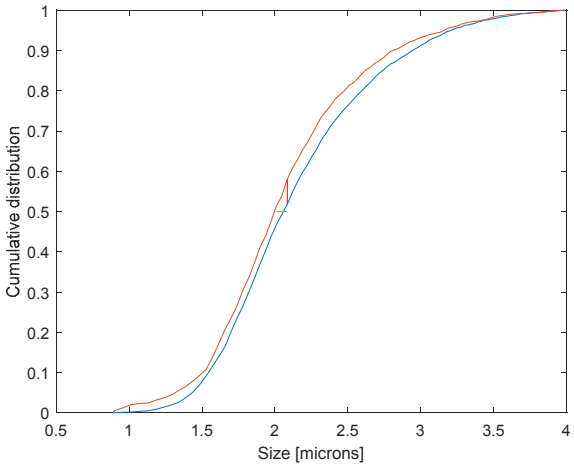

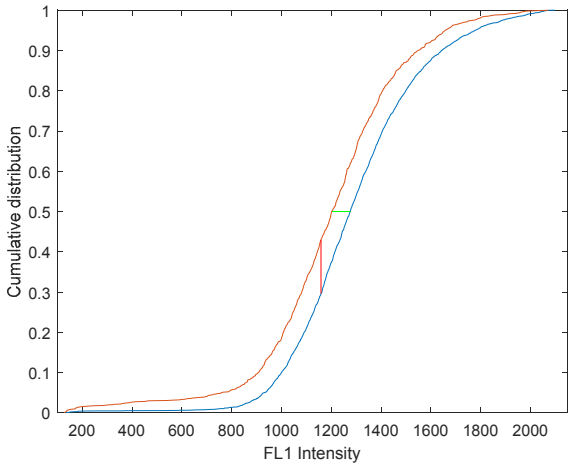

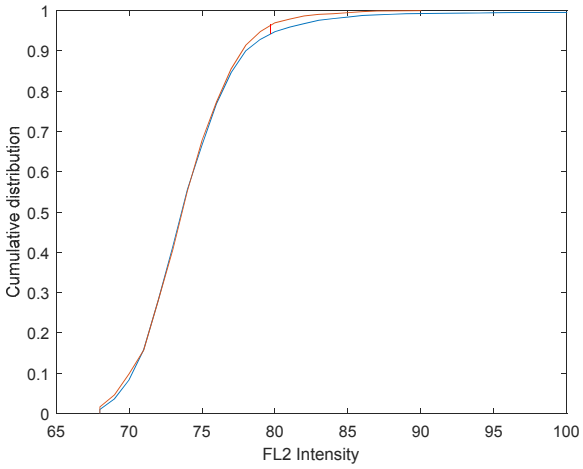

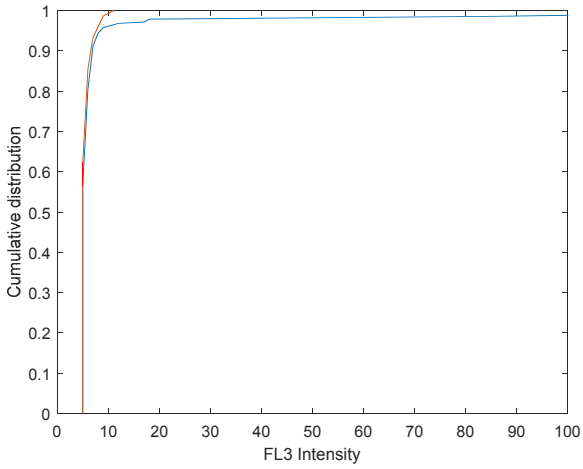

Aspergillus fumigatus (28days), 85%RH, 200ppb Ozone
Peak Stats FL1

Pre

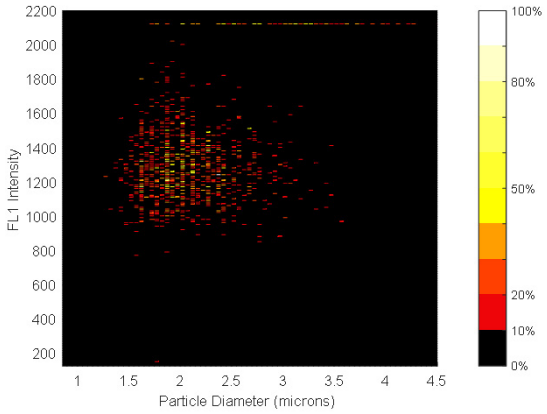

Post

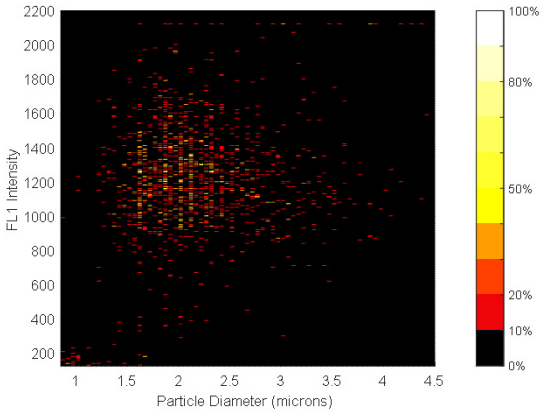

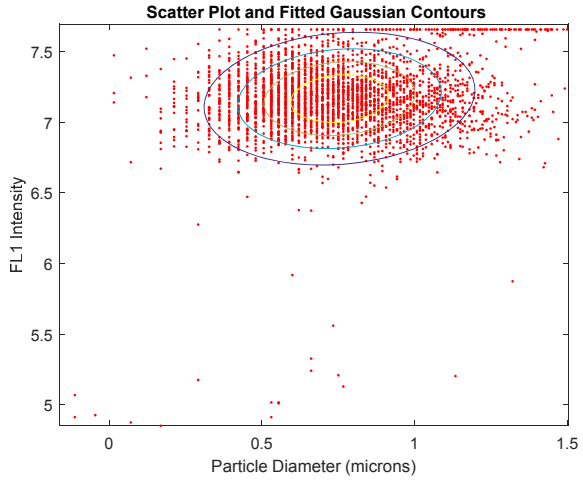

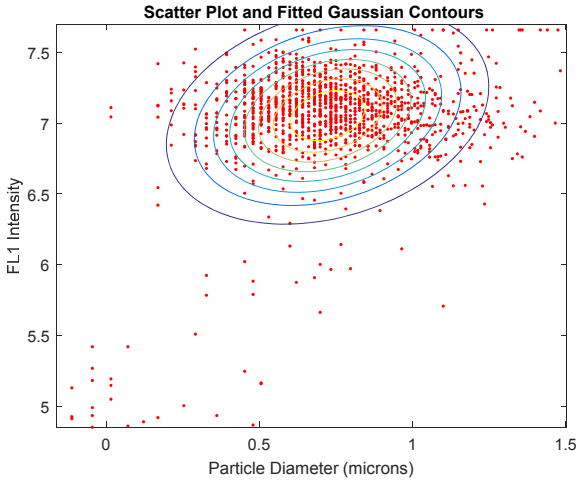

Bacillus subtilis

RH (%)	85
Ozone (ppb)/ suspension time (hr)	200 / 3 hour
Chamber Date	02/04/2016
Culture age (days)	14
InstaScope Gain	High
I.S. Files (t=0,1hr,3hr) {points}	0002, 0008, 0014 (Igor points: 0, 6, 12)

Pre Particle Size Distribution

Gauss fit mean	0.775
SD +/- (width/sqrt(2))	0.454
Size Range	0.5 – 2

Post Particle Size Distribution

Gauss fit mean	0.576
SD +/- (width/sqrt(2))	.0815
Size Range	0.5 - 2

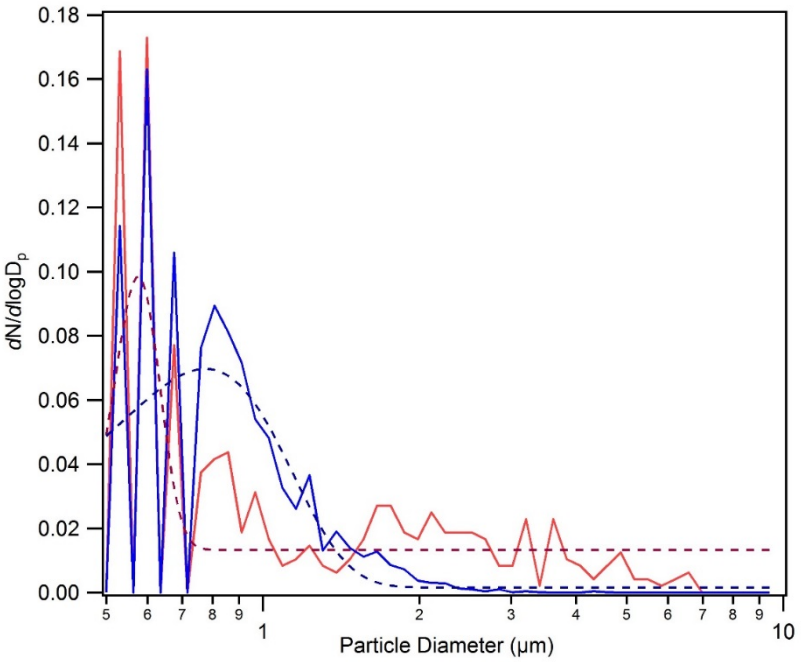

Bacillus subtilis (14days), 85%RH, 200ppb Ozone

Pre Particle FL1 Distribution

LogNormalFL1	132.3
SD (*,/)	0.06
Size range	0.5 - 2
FL1 Range	128 - 2100

Post Particle FL1 Distribution

LogNormalFL1	137.28
SD (*,/)	0.103
Size range	0.5 - 2
FL1 Range	128 - 2100

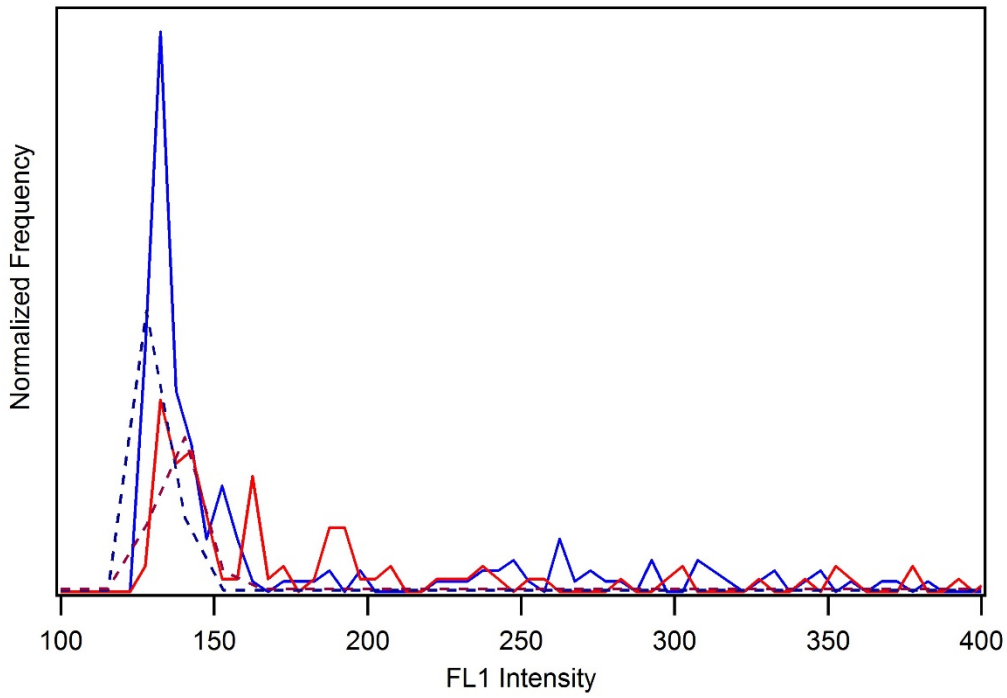

Bacillus subtilis (14days), 85%RH, 200ppb Ozone

	Pre O3 (%)	1hr (%)	3hr (%)
Nonfluorescent	71.32	66.18	66.96
Saturated FL1	0	0	0
Channel FL1	3.24	5.56	5.66
Channel FL2	9.84	10.62	10.17
Channel FL3	3.32	2.44	1.93

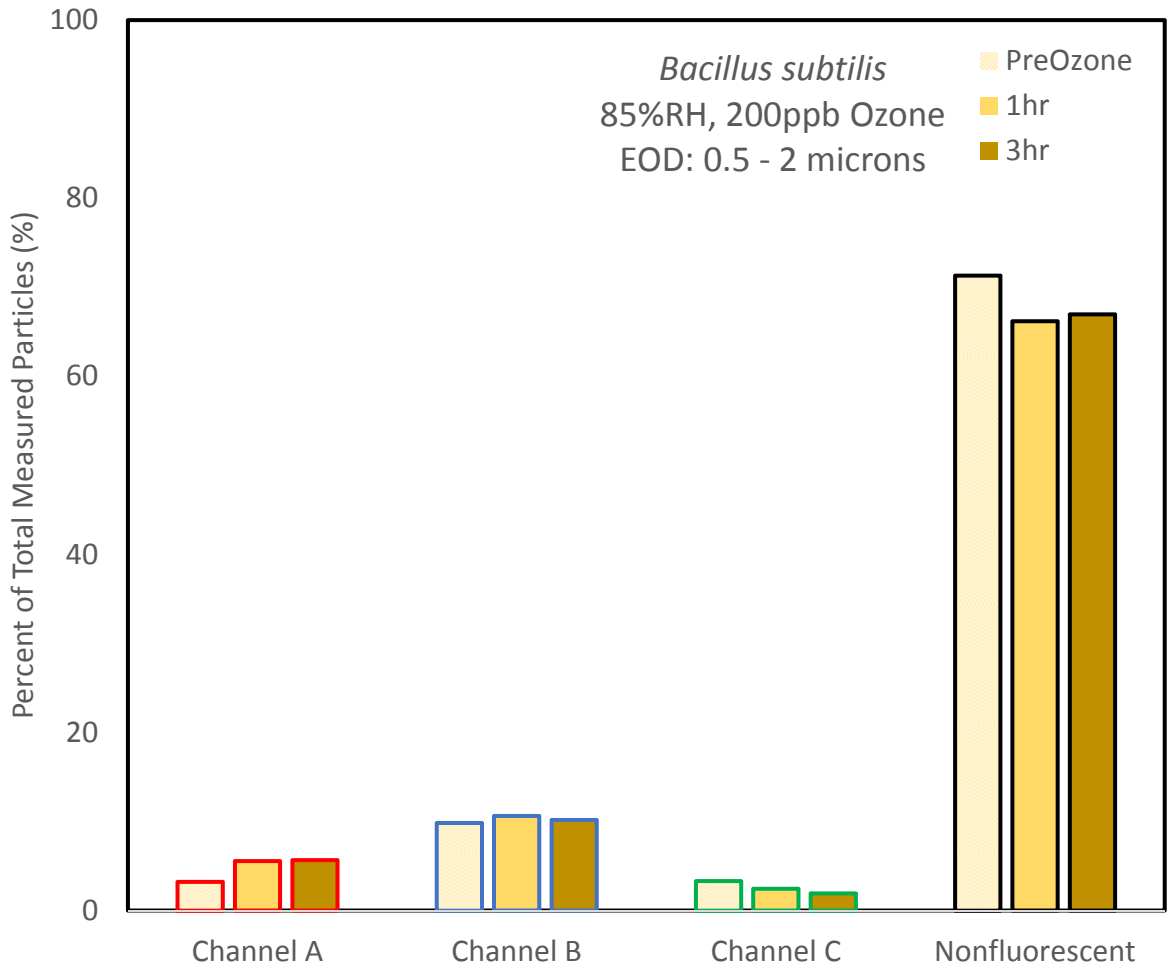

Bacillus subtilis, 85%RH, 200ppb Ozone(High Gain)
KS (size, FL1, FL2, FL3)

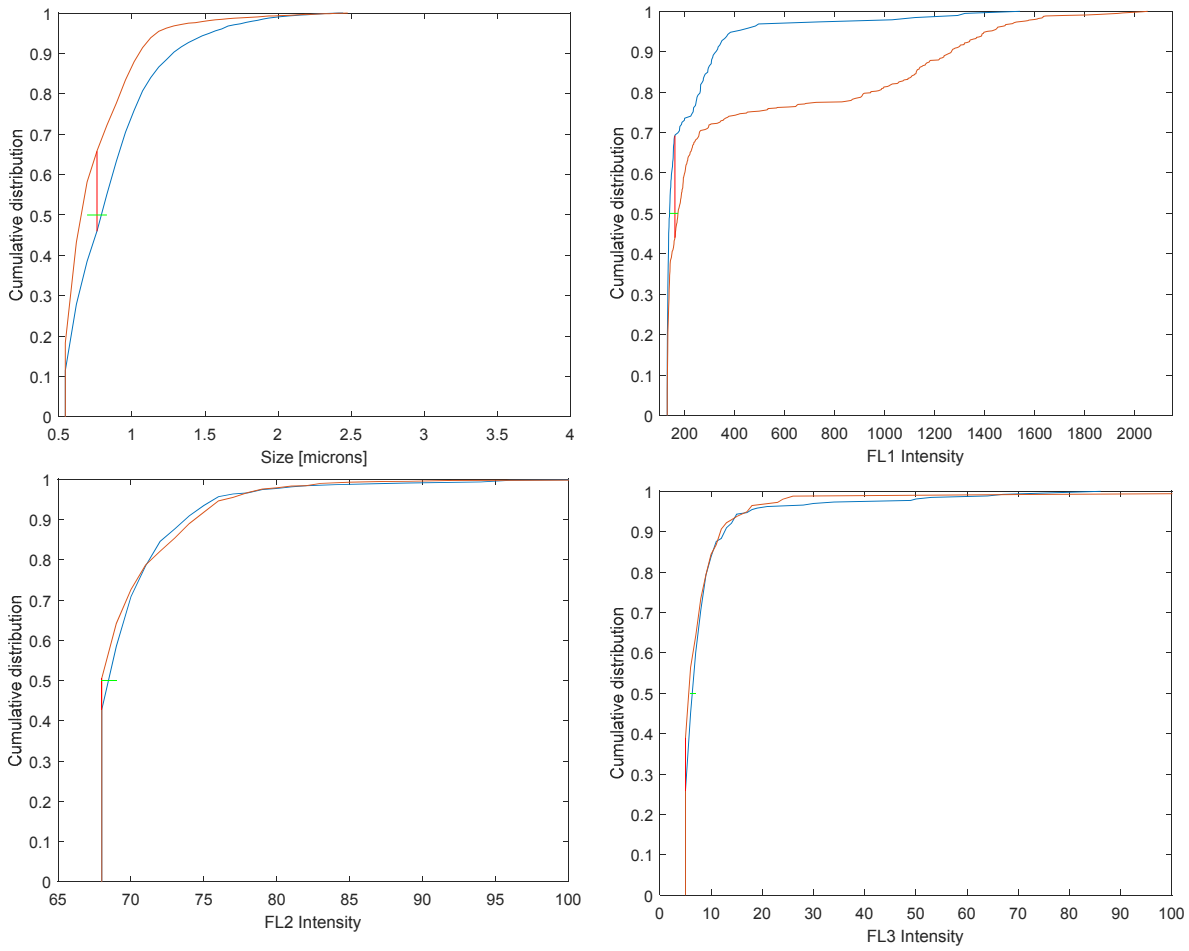

Bacillus subtilis (14days), 85%RH, 200ppb Ozone
Peak Stats FL1

Pre

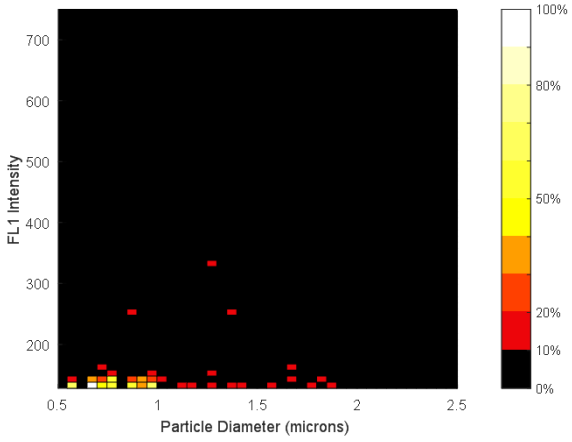

Post

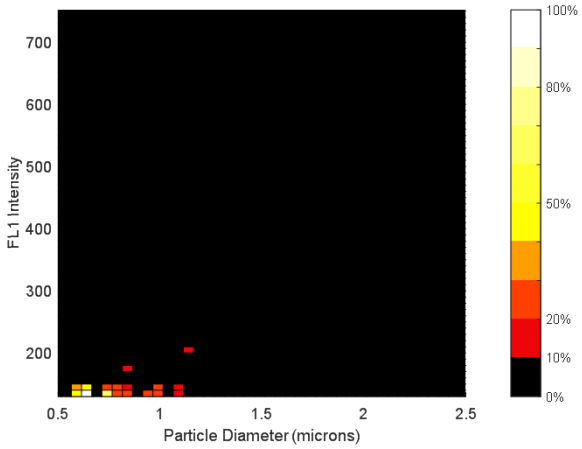

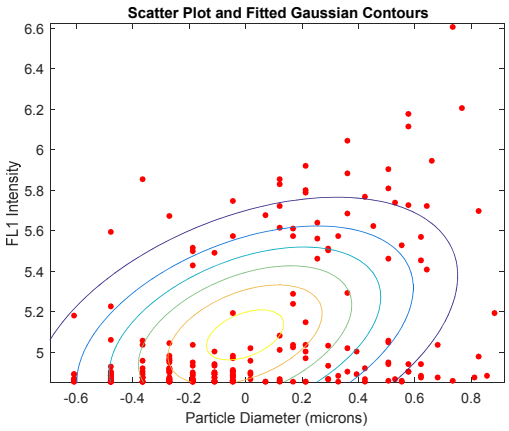

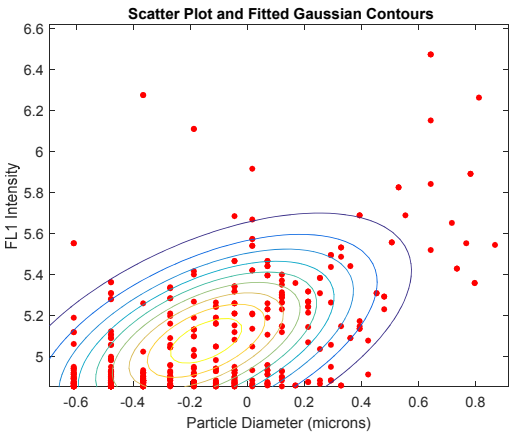

Bacillus subtilis

RH (%)	85
Ozone (ppb)/ suspension time (hr)	0 / 3 hour
Chamber Date	02/04/2016
Culture age (days)	14
InstaScope Gain	High
I.S. Files (t=0,1hr,3hr) {points}	0002, 0004, 0008 (Igor points: 0, 2, 6)

Pre Particle Size Distribution

Gauss fit mean	0.49
SD +/- (width/sqrt(2))	0.64
Size Range	0.5 – 2

Post Particle Size Distribution

Gauss fit mean	0.58
SD +/- (width/sqrt(2))	0.11
Size Range	0.5 - 2

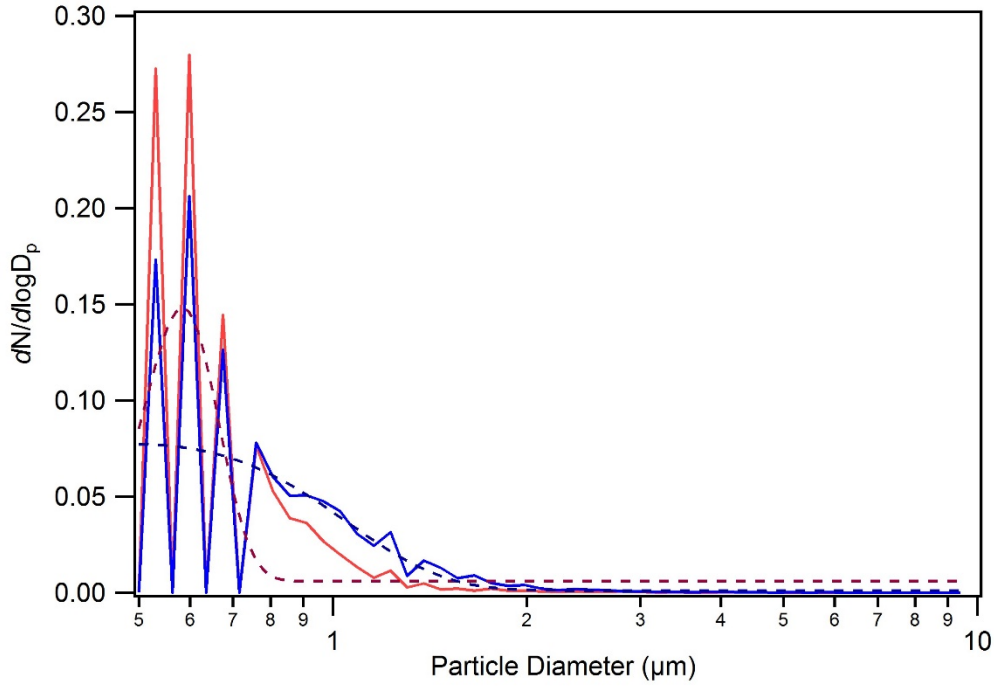

Bacillus subtilis (14days), 85%RH, 0ppb Ozone

Pre Particle FL1 Distribution

LogNormalFL1	133.13
SD (*,/)	0.06
Size range	0.5 - 2
FL1 Range	128 - 2100

Post Particle FL1 Distribution

LogNormalFL1	133.6
SD (*,/)	0.07
Size range	0.5 - 2
FL1 Range	128 - 2100

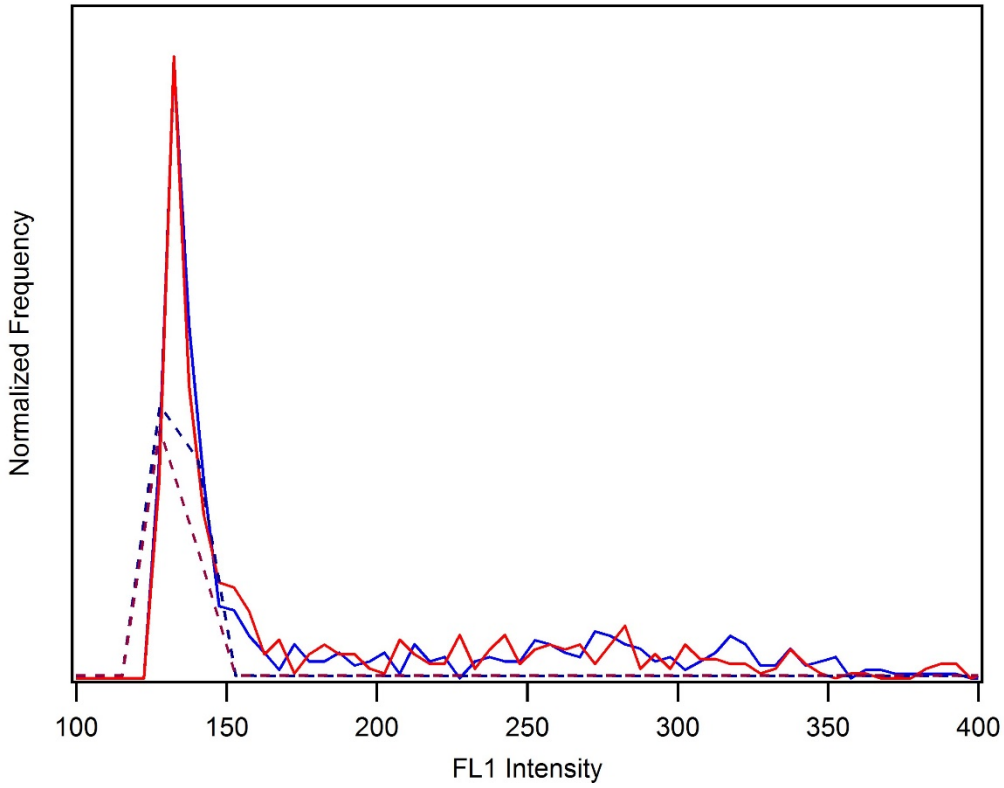

Bacillus subtilis (14days), 85%RH, 0ppb Ozone

	Pre O3 (%)	1hr (%)	3hr (%)
Nonfluorescent	61.70	63.20	61.88
Saturated FL1	0	0	0
Channel FL1	5.78	8.43	8.03
Channel FL2	13.99	12.64	13.03
Channel FL3	4.36	2.81	2.83

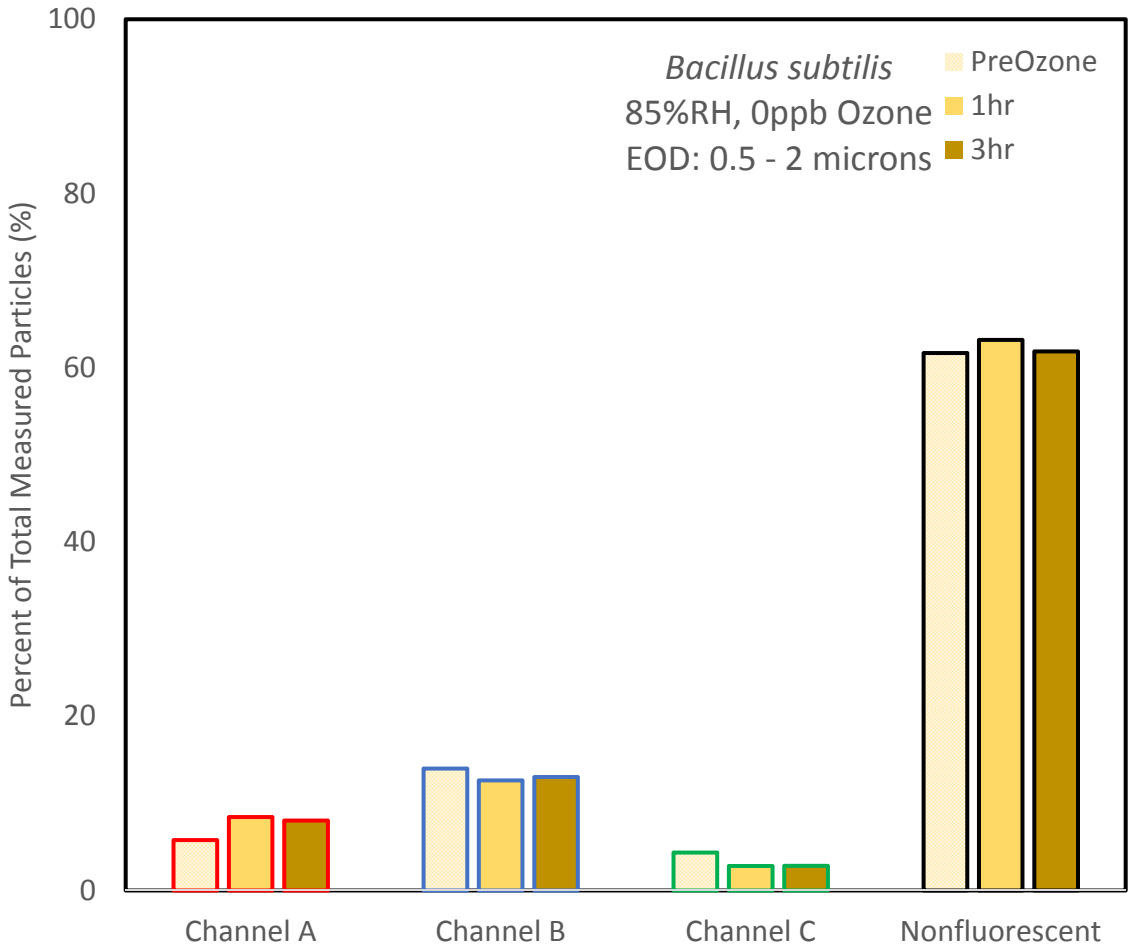

Bacillus subtilis,
85%RH, 0ppb Ozone (High Gain)
KS (size, FL1, FL2, FL3)

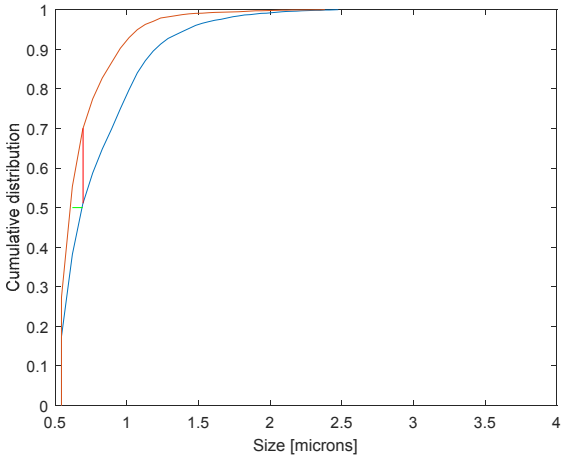

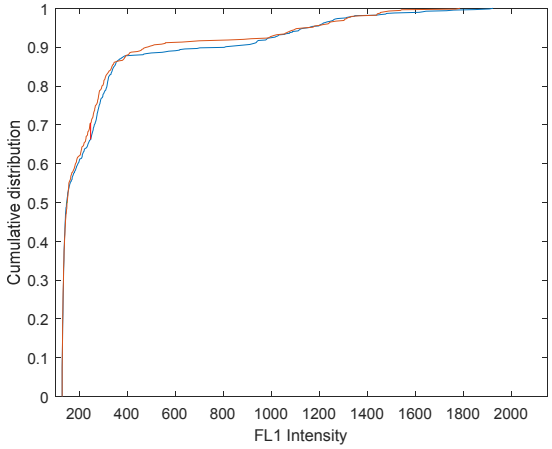

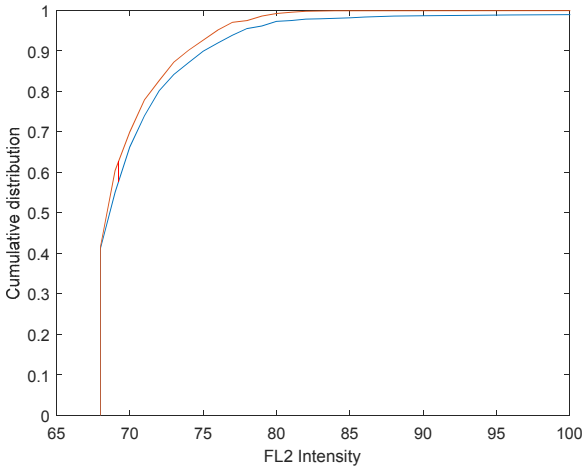

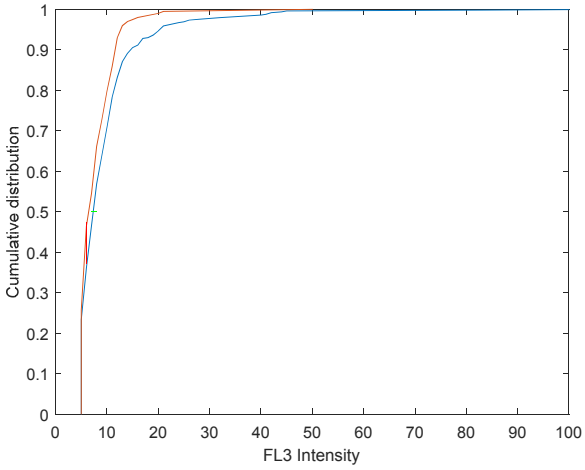

Bacillus subtilis (14days), 85%RH, 0ppb Ozone
Peak Stats FL1

Pre

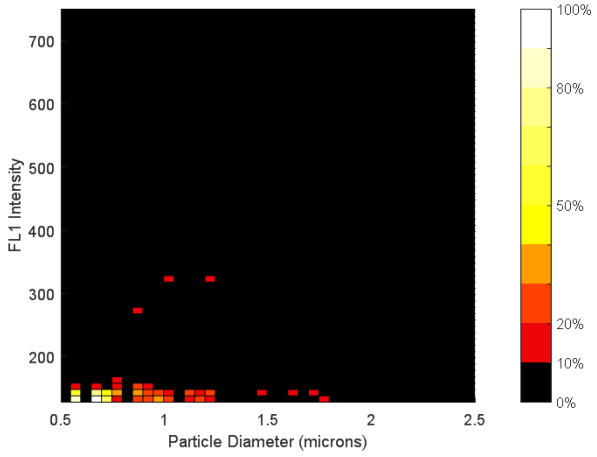

Post

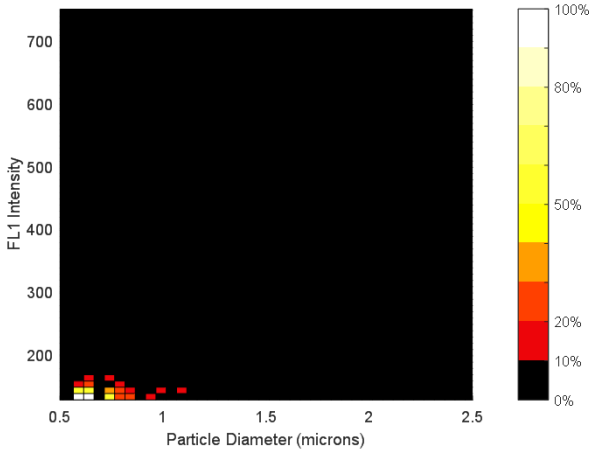

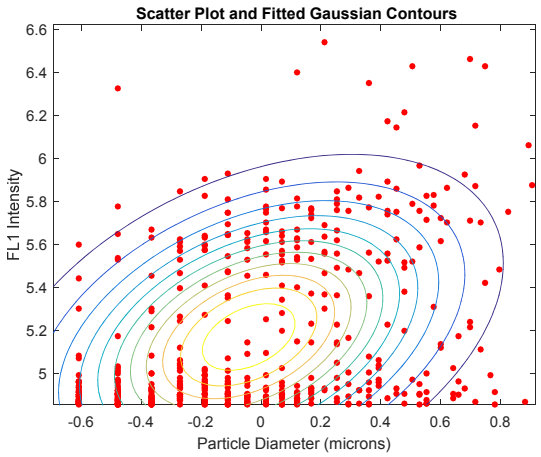

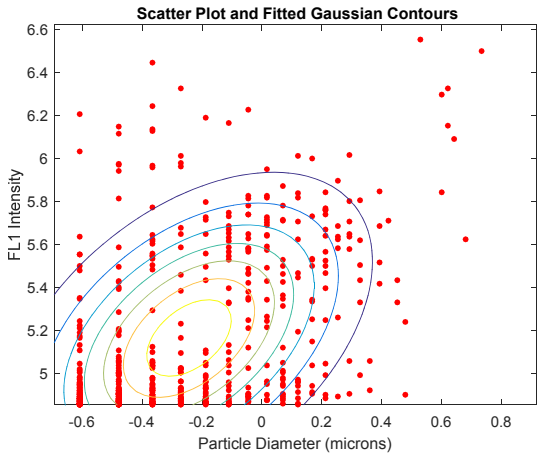

APPENDIX: Bioaerosol EEM Data

Aspergillus fumigatus - 85%RH, 200ppb Ozone

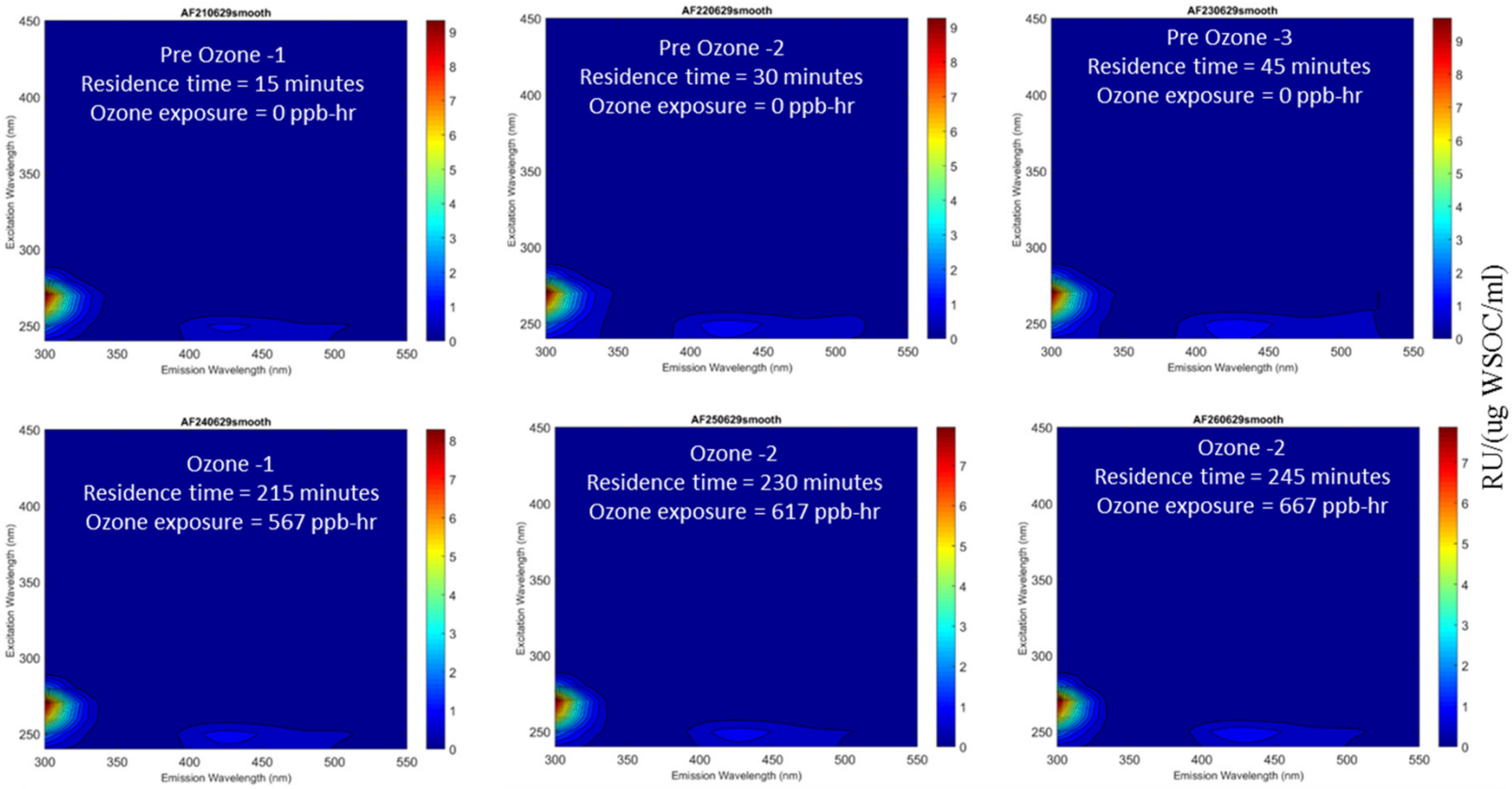

Sample	RH(%)	Ozone (ppb)	SUVA254	FI	HIX	FRI	Tryptophan	Tyrosine	P (Tyr+Tryp)	Tyr/P
A. fumigatus	85	0	0.020	1.78	0.30	0.70	497.23	1961.43	2458.67	0.80
A. fumigatus	85	0	0.023	1.67	0.32	0.71	592.04	1953.69	2545.73	0.77
A. fumigatus	85	0	0.024	1.60	0.34	0.74	557.87	2079.70	2637.57	0.79
A. fumigatus	85	200	0.017	1.90	0.34	0.49	348.34	1735.05	2083.38	0.83
A. fumigatus	85	200	0.018	1.87	0.34	0.58	309.25	1670.84	1980.09	0.84
A. fumigatus	85	200	0.019	1.98	0.37	0.48	269.61	1624.67	1894.28	0.86

Aspergillus fumigatus - 20% RH, 200ppb Ozone

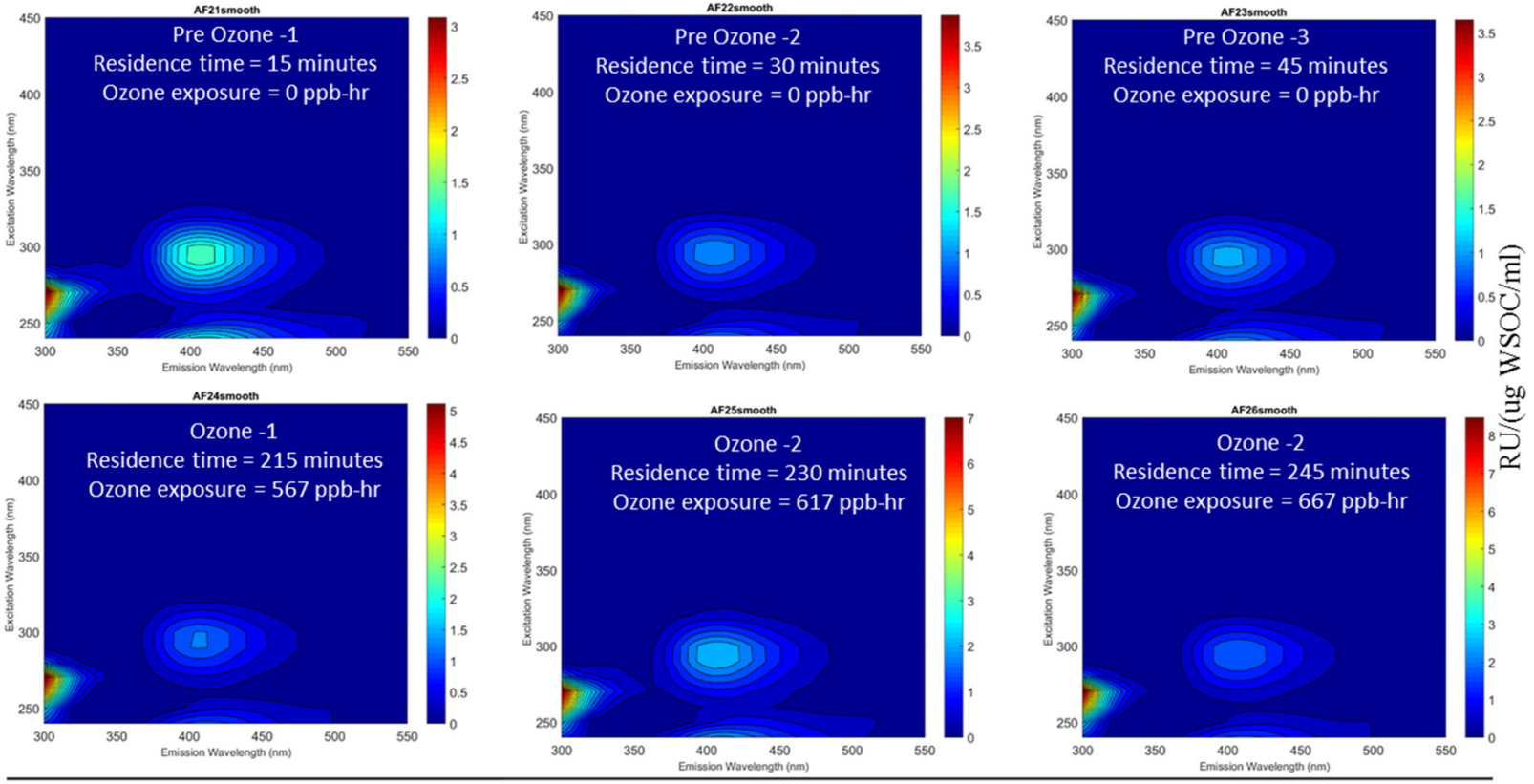

Sample	RH(%)	Ozone (ppb)	SUVA254	FI	HIX	FRI	Tryptophan	Tyrosine	P (Tyr+Tryp)	Tyr/P
A. fumigatus	20	0	0.015	1.63	0.58	0.59	304.49	666.48	970.97	0.69
A. fumigatus	20	0	0.013	1.47	0.44	0.57	178.30	797.86	976.16	0.82
A. fumigatus	20	0	0.014	1.57	0.53	0.59	214.68	749.86	964.54	0.78
A. fumigatus	20	200	0.014	1.55	0.34	0.58	283.56	1065.20	1348.76	0.79
A. fumigatus	20	200	0.017	1.78	0.45	0.57	653.67	1520.32	2173.99	0.70
A. fumigatus	20	200	0.015	1.60	0.32	0.58	526.71	1772.96	2299.66	0.77

Aspergillus fumigatus - 20% RH, 0ppb Ozone

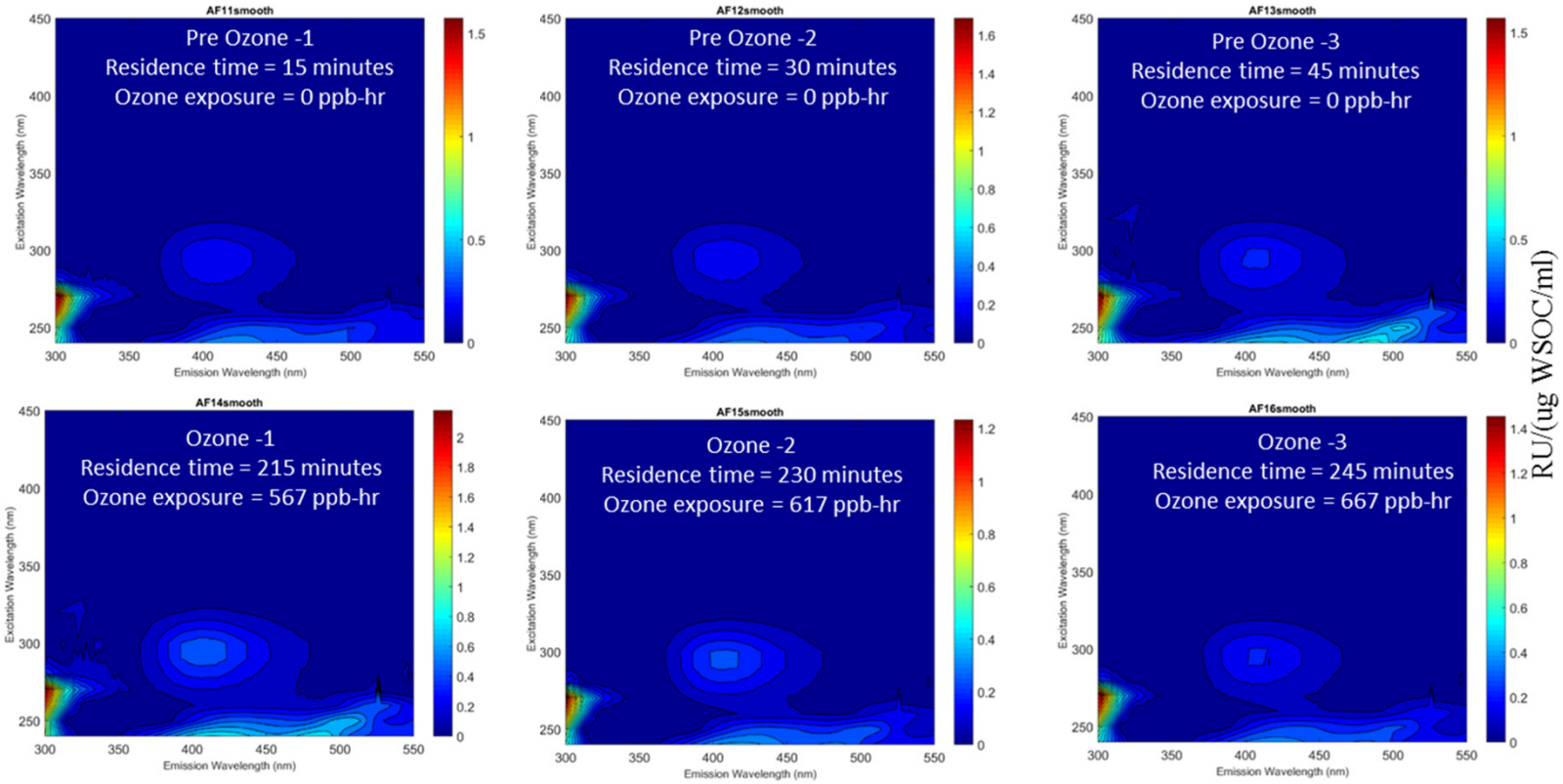

Sample	RH(%)	Ozone (ppb)	SUVA254	FI	HIX	FRI	Tryptophan	Tyrosine	P (Tyr+Tryp)	Tyr/P
A. fumigatus	20	0	0.014	1.49	0.95	0.64	105.84	316.01	421.85	0.75
A. fumigatus	20	0	0.015	1.48	0.90	0.63	84.40	332.07	416.47	0.80
A. fumigatus	20	0	0.014	1.25	0.92	0.65	103.51	318.20	421.71	0.75
A. fumigatus	20	0	0.016	1.29	1.12	0.60	163.04	435.99	599.03	0.73
A. fumigatus	20	0	0.014	1.45	1.18	0.59	46.31	218.51	264.83	0.83
A. fumigatus	20	0	0.015	1.44	0.97	0.60	55.39	281.84	337.23	0.84

Aspergillus versicolor - 85% RH, 200ppb Ozone

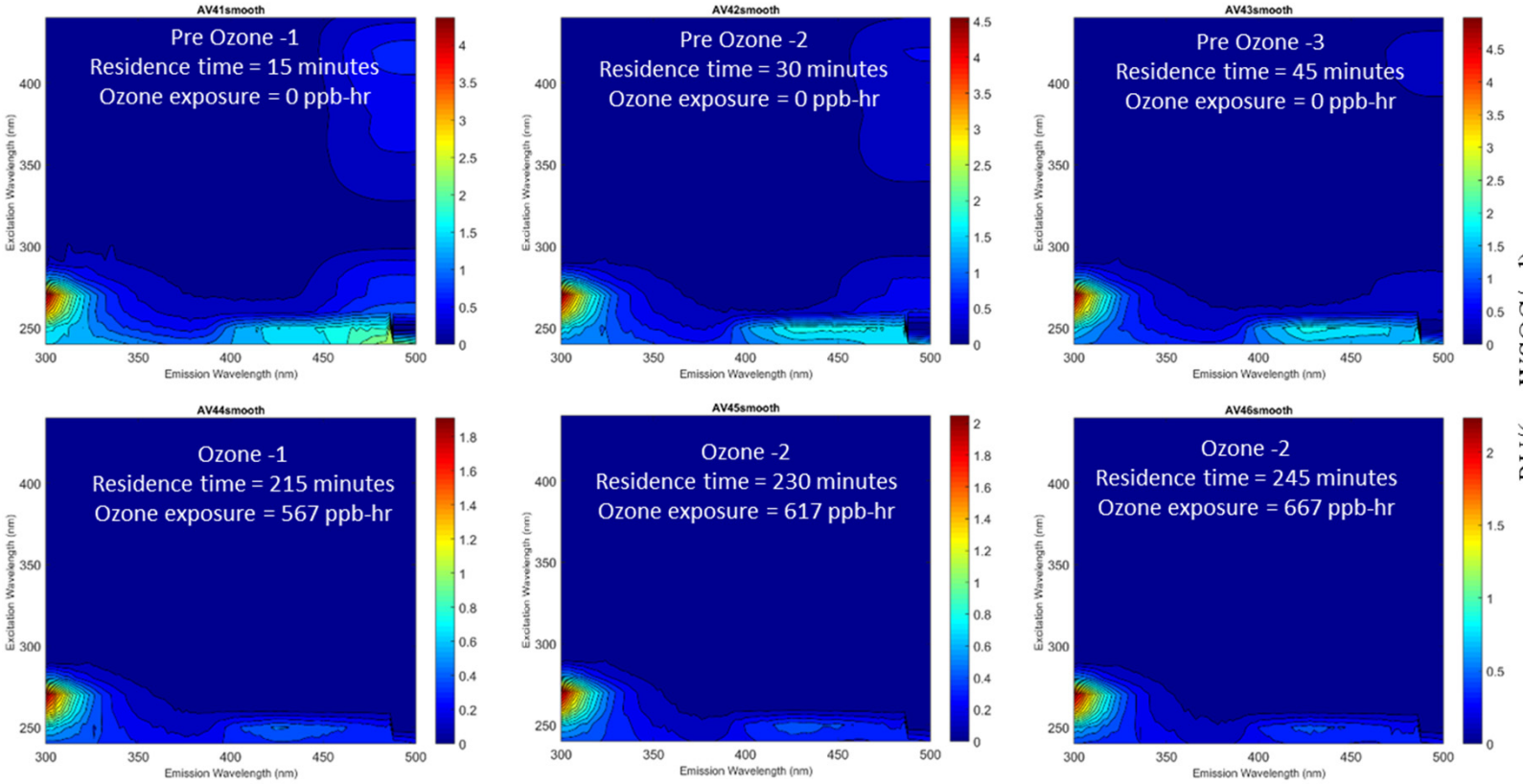

Sample	RH(%)	Ozone (ppb)	SUVA254	FI	HIX	FRI	Tryptophan	Tyrosine	P (Tyr+Tryp)	Tyr/P
A. versicolor	85	0	0.055	0.98	0.98	0.76	266.02	523.65	789.67	0.66
A. versicolor	85	0	0.042	1.00	1.00	0.75	278.91	587.61	866.52	0.68
A. versicolor	85	0	0.040	1.05	0.95	0.69	204.42	468.47	672.89	0.70
A. versicolor	85	200	0.026	1.56	0.49	0.86	375.78	873.70	1249.48	0.70
A. versicolor	85	200	0.023	1.62	0.46	0.86	318.81	783.08	1101.88	0.71
A. versicolor	85	200	0.024	1.59	0.45	0.76	345.45	863.84	1209.29	0.71

Aspergillus versicolor - 85% RH, 0ppb Ozone

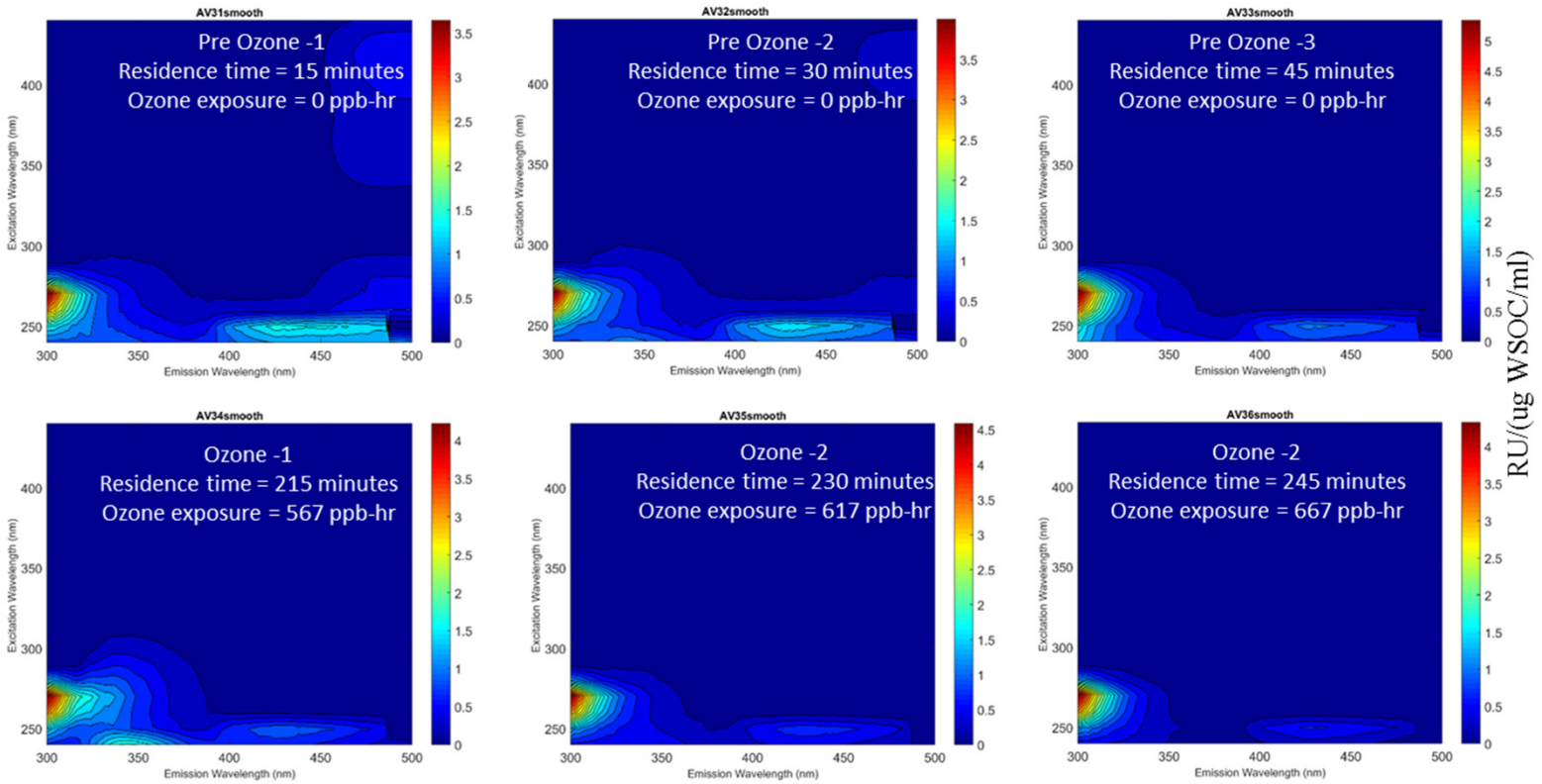

Sample	RH(%)	Ozone (ppb)	SUVA254	FI	HIX	FRI	Tryptophan	Tyrosine	P (Tyr+Tryp)	Tyr/P
A. versicolor	85	0	0.039	1.01	0.96	0.75	347.87	658.56	1006.43	0.65
A. versicolor	85	0	0.035	1.08	0.81	0.74	490.52	762.97	1253.49	0.61
A. versicolor	85	0	0.039	1.09	0.59	0.87	776.29	1745.55	2521.84	0.69
A. versicolor	85	0	0.020	1.50	0.42	1.36	904.24	1060.10	1964.34	0.54
A. versicolor	85	0	0.018	1.40	0.40	0.87	347.84	758.54	1106.38	0.69
A. versicolor	85	0	0.013	1.50	0.34	0.62	261.97	705.31	967.28	0.73

Aspergillus versicolor - 85% RH, 0ppb Ozone

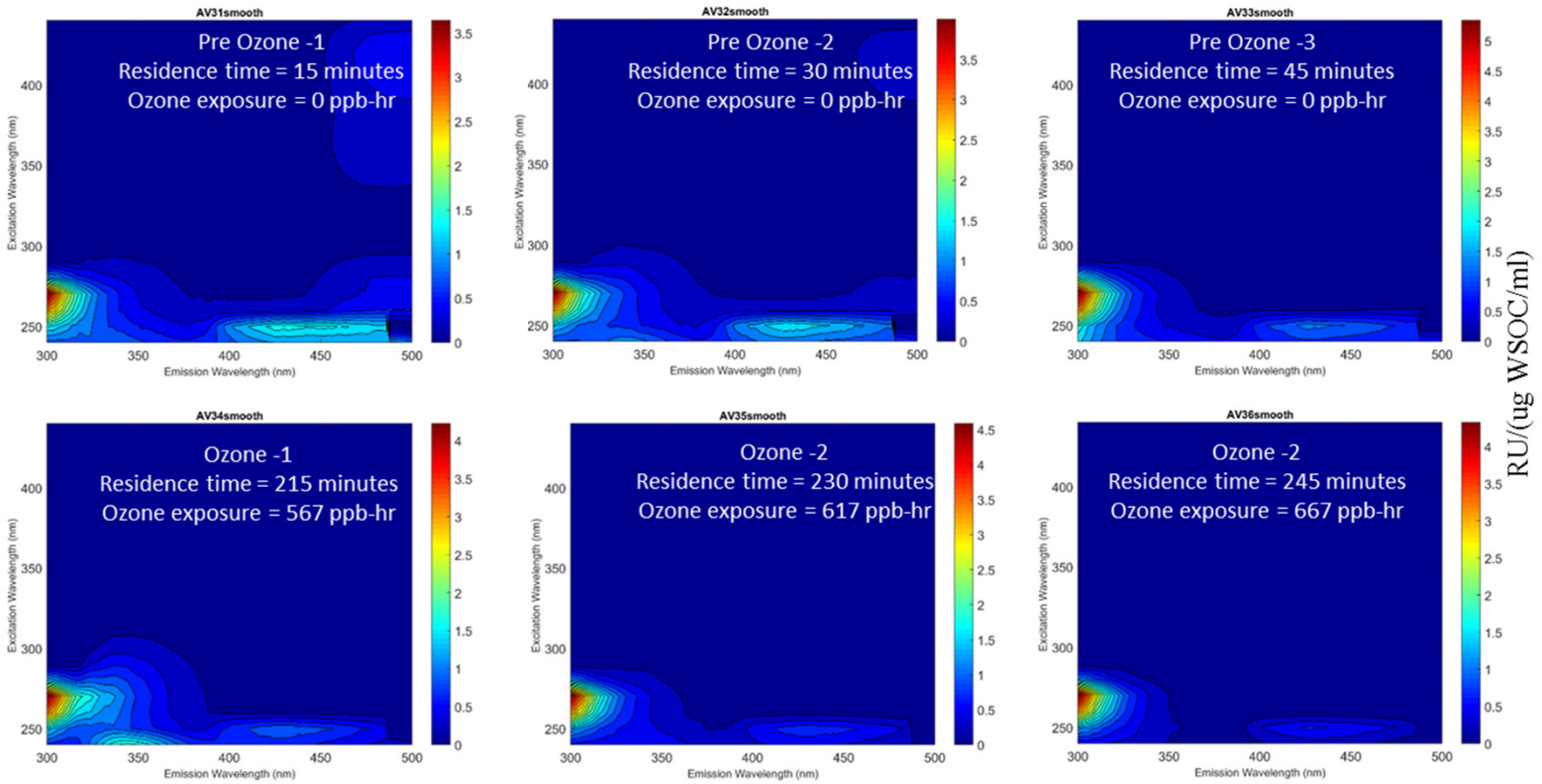

Sample	RH(%)	Ozone (ppb)	SUVA254	FI	HIX	FRI	Tryptophan	Tyrosine	P (Tyr+Tryp)	Tyr/P
A. versicolor	85	0	0.039	1.01	0.96	0.75	347.87	658.56	1006.43	0.65
A. versicolor	85	0	0.035	1.08	0.81	0.74	490.52	762.97	1253.49	0.61
A. versicolor	85	0	0.039	1.09	0.59	0.87	776.29	1745.55	2521.84	0.69
A. versicolor	85	0	0.020	1.50	0.42	1.36	904.24	1060.10	1964.34	0.54
A. versicolor	85	0	0.018	1.40	0.40	0.87	347.84	758.54	1106.38	0.69
A. versicolor	85	0	0.013	1.50	0.34	0.62	261.97	705.31	967.28	0.73

Aspergillus versicolor - 30% RH, 200ppb Ozone

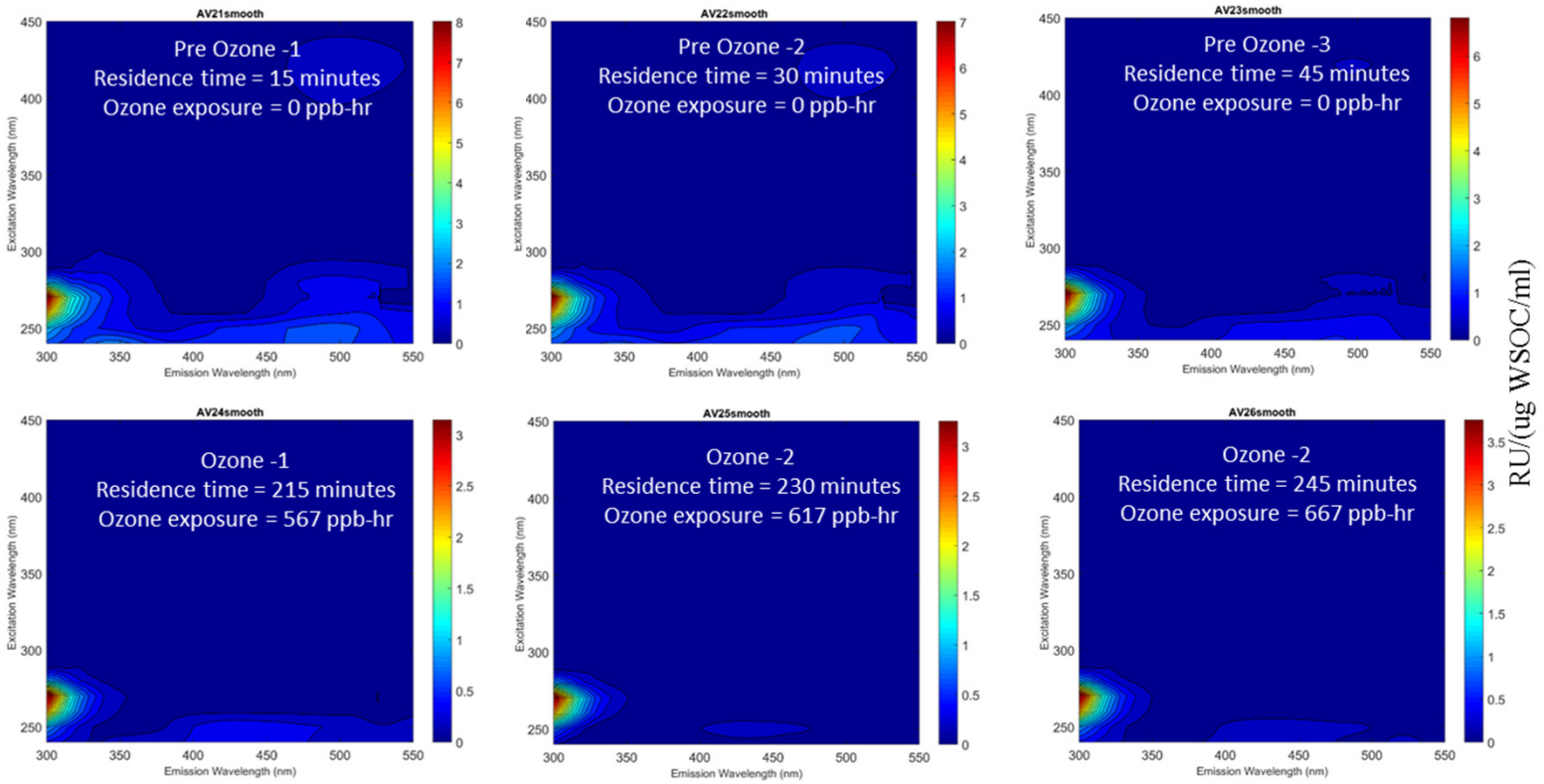

Sample	RH(%)	Ozone (ppb)	SUVA254	FI	HIX	FRI	Tryptophan	Tyrosine	P (Tyr+Tryp)	Tyr/P
A. versicolor	30	0	0.051	0.90	0.59	0.99	1175.11	1905.67	3080.78	0.62
A. versicolor	30	0	0.051	0.91	0.54	1.01	773.00	1626.36	2399.36	0.68
A. versicolor	30	0	0.041	0.92	0.41	0.88	620.89	1565.46	2186.35	0.72
A. versicolor	30	200	0.029	1.31	0.48	0.80	266.03	729.82	995.85	0.73
A. versicolor	30	200	0.018	1.77	0.32	1.14	266.40	740.85	1007.25	0.74
A. versicolor	30	200	0.028	1.33	0.28	0.90	297.96	847.08	1145.04	0.74

Aspergillus versicolor - 30% RH, 0ppb Ozone

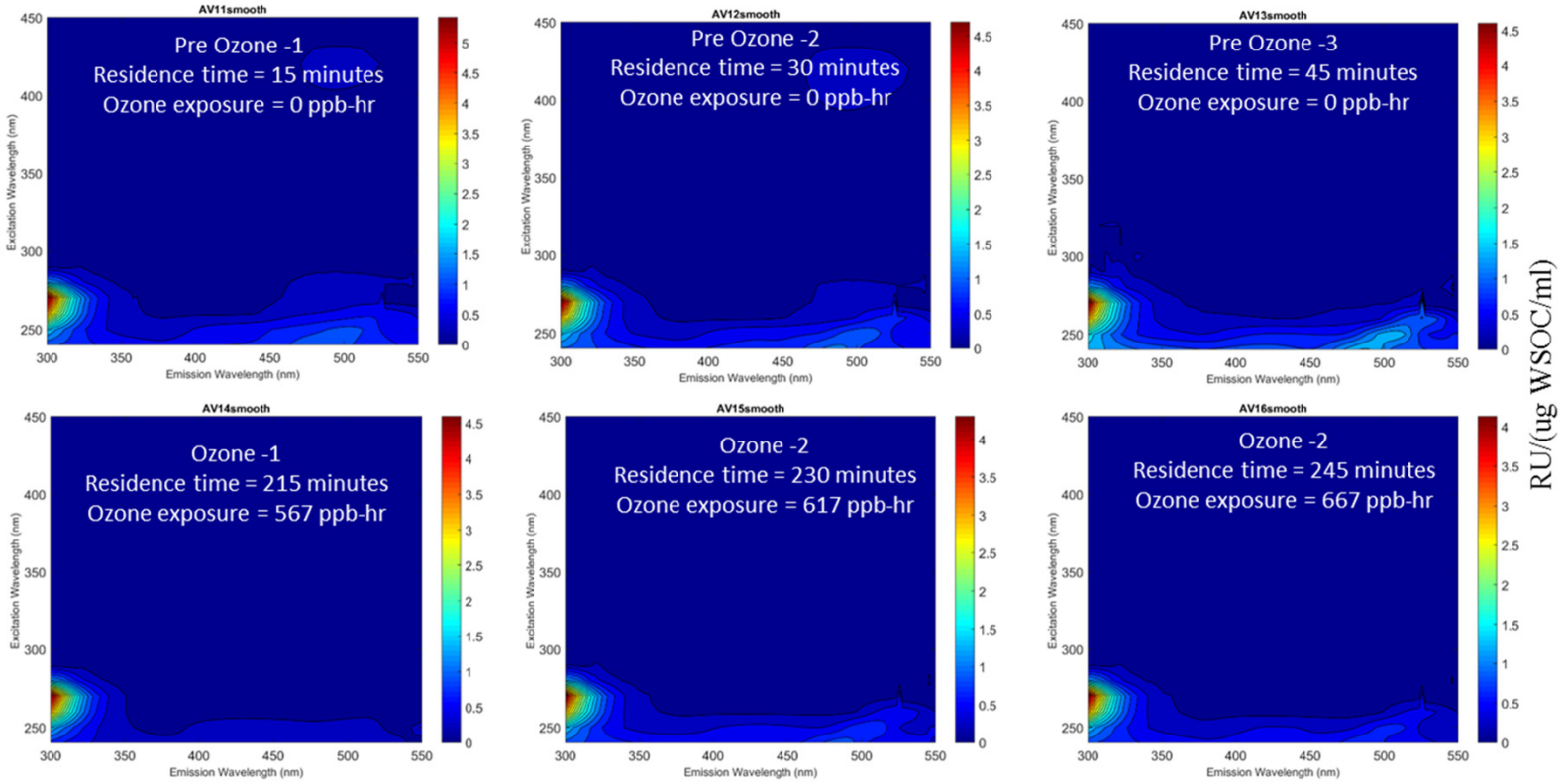

Sample	RH(%)	Ozone (ppb)	SUVA254	FI	HIX	FRI	Tryptophan	Tyrosine	P (Tyr+Tryp)	Tyr/P
A. versicolor	30	0	0.064	0.96	0.52	0.73	522.60	1260.57	1783.17	0.71
A. versicolor	30	0	0.067	0.95	0.43	0.86	465.86	1099.70	1565.56	0.70
A. versicolor	30	0	0.077	0.97	0.43	0.90	470.07	1073.90	1543.97	0.70
A. versicolor	30	0	0.038	1.08	0.25	0.90	389.73	1051.79	1441.52	0.73
A. versicolor	30	0	0.054	1.13	0.33	0.90	382.55	965.10	1347.64	0.72
A. versicolor	30	0	0.048	1.15	0.27	0.96	374.49	951.00	1325.48	0.72